Summer 2015

The role of pharmaceutical excipients in the solid-state degradation of Gabapentin

Radaduen Tinmanee
University of Iowa

THE ROLE OF PHARMACEUTICAL EXCIPIENTS IN THE SOLID-STATE DEGRADATION OF GABAPENTIN

by

Radaduen Tinmanee

A thesis submitted in partial fulfillment
of the requirements for the Doctor of
Philosophy degree in Pharmacy
in the Graduate College of
The University of Iowa

August 2015

Thesis Supervisor: Professor Lee E. Kirsch

Graduate College
The University of Iowa
Iowa City, Iowa

CERTIFICATE OF APPROVAL

_____

PH.D. THESIS

_____

This is to certify that the Ph.D. thesis of

Radaduen Tinmanee

has been approved by the Examining Committee for
the thesis requirement for the Doctor of Philosophy
degree in Pharmacy at the August 2015 graduation.

Thesis Committee: _____
Lee E. Kirsch, Thesis Supervisor

_____
Dale E. Wurster

_____
Maureen D. Donovan

_____
Aliasger K. Salem

_____
Lewis L. Stevens

_____
Kenneth R. Morris

To my parents and my younger sister

ACKNOWLEDGEMENTS

I would like to thank my major advisor, Dr. Lee Kirsch, for his guidance and thoughtful support. His knowledge and insights would be ultimately valuable. This dissertation would not have been completed without his help. Dr. Kirsch is one of the finest mentors I have known.

I would like to thank my committee members: Dr. Dale Wurster, Dr. Maureen Donovan, Dr. Aliasger Salem, Dr. Lewis Stevens and Dr. Kenneth Morris. I would also like to thank Dr. Douglas Flanagan for serving on my comprehensive exam and his feedback on my research throughout the years. I greatly appreciate all professors in Division of Pharmaceutics and Translational Therapeutics.

I would like to acknowledge Dr. Kenneth Morris, Professor and Chair of the Department of Pharmaceutical Sciences at the University of Hawaii-Hilo for his guidance on the use of XRPD and other advanced solids analytical techniques to complete my dissertation objective. I would also like to acknowledge Dr. Sarah Larsen, Professor and Chair of the Department of Chemistry for her guidance on the use of ^{13}C ssNMR to complete my work. Special thanks are given to the University of Iowa Central Nuclear Magnetic Resonance, Department of Chemistry.

Special recognition is given to Dr. Stephen Stamatis for the use of his computer program, the Advanced Modeling and Simulation Took Kit (AMASTK, UI Copyright 2012) for nonlinear optimization, simulation and Bayesian estimation.

I am grateful to my former and current lab mates Zong, Salil, Jiang, Pratak, Hoa, Mo'tasem, and Phawanan. Special recognition is also given to Dr. Eiji Ueyama. He

conducted a series of studies on degradation of gabapentin in parallel with my studies reported herein.

Last, but not least, I would like to thank my father, mother and my younger sister for their support and encouragement.

ABSTRACT

Drug instability in solid dosage forms includes chemical or physical processes involving covalent or polymorphic transformations wherein different polymorphs possess crystal structure differences. Gabapentin chemically degrades by intramolecular cyclization to gabapentin-lactam (lactam) in the solid-state. Additionally, gabapentin undergoes polymorphic solid-state transformations. A kinetic model was developed to describe the environmental and excipient effects on chemical and physical instability associated with milling induced stress and subsequent storage under controlled temperature and humidity conditions.

Reaction mixtures were generated by co-milling gabapentin Form II with various excipients. The effects of environmental conditions were studied by storing reaction mixtures at 40-60 ºC and 5-50 %RH. The chemical and polymorphic compositions of the reaction mixtures were measured as a function of time using a combination of chromatographic method, ^{13}C ssNMR and XRPD. Degradation models that describe the relationship between polymorphs and degradation product in a series of sequential or parallel steps were devised based on analysis of the resultant concentration time profiles. Model parameters were estimated using non-linear regression and Bayesian methods and evaluated in terms of their quantitative relationship to compositional and conditional variations.

In reaction mixtures composed of co-milled gabapentin and excipients, gabapentin was found to exist in three forms: anhydrous polymorph II and III and gabapentin-lactam. A fourth form (II*) was observed based on initial degradation kinetics and was hypothesized to be a crystal-disordered form generated by mechanical stress.

The effect of environment moisture was to decrease the net rate of lactam formation by facilitating polymorphic transformation kinetics and crystal annealing. However, excipient blocked the catalytic moisture effect on polymorphic transformations. The key features of our model are first-order physical state transitions of II* and III to II, first-order degradation of II* to lactam and autocatalytic lactamization of II and III. For chemical transitions, no humidity effect was present but the catalytic effects of excipients on the conversion of II and III➔lactam were observed. For physical transitions, excipient primarily influenced the physical state transitions of II* and III➔II through its ability to interact with humidity and the degree of contact between excipient and substrate.

PUBLIC ABSTRACT

Solid-state drug degradation rates are complicated because drug molecules can exist in multiple states that are capable of undergoing both covalent and/or non-covalent changes at unique rates due in response to their mobility and environment. Systematic studies on the effects of composition (i.e. excipients) and manufacturing stress on drug stability in solid dosage forms are lacking. When drugs degrade to toxic degradants during their shelf-life predictive, quantitative models are needed to ensure drug product safety. The objective of our studies is to build a kinetic model that describes the environmental and excipient effects on chemical and physical instability associated with manufacturing-induced stress and subsequent storage under controlled temperature and humidity conditions using gabapentin as a model compound. Gabapentin chemically degrades to form gabapentin-lactam (lactam) in the solid-state. Lactam is a toxic degradation product, thus the established limit on lactam in gabapentin formulations is less than 0.4 %. Kinetic models that describe the relationship between substrate, intermediate and degradation product were devised based on analysis of the concentration time profiles of gabapentin/excipient reaction mixtures. Model parameters were estimated using non-linear regression and Bayesian methods and evaluated in terms of their quantitative relationship to compositional and conditional variations. The kinetic model was shown to be robust and capable of describing the effects of temperature, humidity and excipient on rate constants associated with kinetics for each physical and chemical transition of gabapentin.

TABLE OF CONTENTS

LIST OF TABLES

LIST OF FIGURES

CHAPTER I

INTRODUCTION

Drug instability involves chemical or physical processes involving covalent or non-covalent structural changes. Solid state reactions include covalent reaction processes and polymorphic transformations wherein different polymorphs possess crystal structure differences based on non-covalent interaction or the loss of drug crystalline structures. (1, 2) The generation of structural disorder can be induced by manufacturing stress associated with various unit operations, including milling, compaction, and freeze drying. The resulting structural disorder may change the chemical reactivity due to high energy and molecular mobility. This disorder is manifested as crystal defects and imperfections that can serve as foci for subsequent covalent and/or non-covalent transformations. Milling-induced polymorphic transformation may involve with the accumulation of lattice defects or transient metastable crystal which is followed by the progressive reorientation of molecules in the crystals to another polymorph. (3, 4) In some cases, physical instability may lead to an increased susceptibility to covalent changes. For example, grinding cefixime trihydrate reduced the integrity of crystal lattice resulting in increases in its chemical instability. (5)

During storage conditions, temperature and humidity may affect physical transformation kinetics of drug substances. Polymorphs with high energy level (less stable) may eventually convert to the most thermodynamically-stable polymorph. Potential energy levels in different polymorphs vary due to the differences in molecular packing. The net effect includes pharmaceutical product performance changes associated

with instability, such as stability and dissolution changes leading to potential changes in bioavailability. (6)

Excipients can influence solid state drug degradation in a variety of ways. Excipients can chemically interact with drug substance, e.g., Maillard reaction whereby reducing sugar excipients, such as lactose, and glucose react with amine-containing drug substances. For example, lactose has been shown to chemically react with fluoxetine HCl in capsule formulation to form colored degradation products. (7)

Excipients can also increase the extent of crystal defect formation during mechanical stress resulting in increased susceptibility to chemical instability. For example, the decrease in crystallinity of aspirin when co-milled with microcrystalline cellulose (10:90 and 20:80 %w/w aspirin/MCC mixtures) as observed by using infrared spectroscopy caused an apparent increase in the degradation rate. (8)

Excipients can induce polymorphic transformations of drug substances. For example, the effect of co-milling with 6.5 %w/w hydroxypropyl cellulose (HPC) on polymorphic transformation of gabapentin Form II was reported. Partial transformation of gabapentin Form II to III was observed when co-milled with HPC, whereas no conversion to Form III was found in the physical mixture of gabapentin and HPC. (9)

Gabapentin has been chosen as a model compound in our studies due to its propensity to undergo both chemical and polymorphic solid-state transformations. (9-11) Gabapentin chemically degrades by intramolecular cyclization to gabapentin-lactam (lactam). (12) This lactam degradation was associated with convulsion activities, including myoclonic twitches and generalized clonic seizures in animal model. (13) An oral LD_{50} of gabapentin-lactam in mice and rats (300 mg/kg and 200-500 mg/kg) is an

order of magnitude lower than gabapentin (8000 mg/kg). Therefore, the United States Pharmacopeia limits for lactam in gabapentin is 0.4 %. (14, 15) The use of gabapentin as a drug model compound for determining the relationship between manufacturing-related stressed and solid-state drug degradation in oral dosage form has been the subject of a US Food and Drug Administration-supported research project. (11) Our group participated in this multi-institutional project by studying the effect of milling on gabapentin and subsequent lactamization kinetics during storage at various controlled-temperature and humidity conditions. A kinetic model (Zong model) was developed to describe a relationship between manufacturing induced-physically transformations and chemical instability of gabapentin in the absence of excipients. (16) The Zong model provided an explanation for the effect of milling and storage stresses on gabapentin. However, these studies did not examine what effect, if any, excipients play in physical and/or chemical transformations during the physical stress induced by milling and storage under various controlled temperature and humidity conditions. Therefore, my project focused on bridging this gap in our understanding of the role of compositional variation and gabapentin instability.

Research Objective

The objective of my research is to build a kinetic model that can quantitatively describe the environmental (temperature and humidity) and compositional (excipient) effects on chemical and polymorphic transformation kinetics of gabapentin.

In order to develop a functional model that describes the chemical and physical transformations of gabapentin and to estimate model parameters with reasonable accuracy, the following steps were taken. Firstly, reaction mixtures were generated by co-

milling gabapentin Form II with various excipients. After milling, the polymorphic composition of the reaction mixtures was measured using ^{13}C solid state nuclear magnetic resonance spectroscopy (^{13}C ssNMR) and X-ray powder diffraction (XRPD). Then, the effects of environmental conditions were studied by storing reaction mixtures at 40-60 ºC and 5-50 %RH. The changes in polymorphic II, III and degradation product concentrations in the reaction mixtures were measured as a function of time using a combination of chromatographic and spectroscopic methods. Thirdly, degradation models that describe the relationship between polymorphs and degradation product in a series of sequential or parallel steps were devised based on analysis of the resultant concentration time profiles. Model parameters (including rate constants and humidity constants for individual pathways) were estimated using non-linear regression and Bayesian methods. Next, various model parameters were evaluated in terms of their quantitative relationship to compositional and conditional variations. The degradation model proposed by Zong (16) to describe lactam formation (in the absence of excipients) was used as a starting point.

Organization

The dissertation is divided into five chapters. This first chapter provides an introduction, objective of this research, organization of this dissertation, and peer collaborated efforts.

Chapter II describes methodologies to quantify polymorphic compositions of gabapentin/excipient mixtures. In this chapter, we develop two analytical methods using ^{13}C ssNMR and XRPD. We investigate capabilities of those techniques for measuring polymorphs. The application of quantitative technique described in this chapter will then

be used in Chapter IV to quantify polymorphic transformation of co-milled gabapentin/excipient mixtures during storage.

Chapter III describes the excipient and environmental (temperature and humidity) effects on chemical transformation kinetics of gabapentin/excipient mixtures during storage at various controlled-temperature and humidity conditions.

Chapter IV describes the excipient and environmental (temperature and humidity) effects on polymorphic transformation kinetics of gabapentin/excipient mixtures during storage at various controlled-temperature and humidity conditions.

Chapter V describes a quantitative kinetic model for describing excipient and environmental (temperature and humidity) effects on chemical and polymorphic transformation kinetics of gabapentin/excipient mixtures during storage. The ability of model to describe data is evaluated. The impact of model parameter variation on model outputs is investigated to determine the reliability of model parameter estimates. The effects of compositional and environmental variations on the kinetics of each pathway are determined.

Peer Collaborated Efforts

The content of Chapter II for the determination of polymorphic compositions involved both ^{13}C ssNMR and XRPD was collaborative efforts with Professor Sarah C. Larsen, Department of Chemistry, The University of Iowa, and Professor Kenneth R. Morris, Department of Pharmaceutical Sciences, The University of Hawaii at Hilo. ^{13}C ssNMR methods were developed using instrumentation available at The University of Iowa Central Nuclear Magnetic Resonance, Department of Chemistry. XRPD methods were developed using facilities generously provided by Professor Kenneth R. Morris,

Department of Pharmaceutical Sciences at the University of Hawaii-Hilo. Professor Morris worked beside me in the laboratory conducting a series of relevant experiment studies of his own design. I have incorporated a few of his studies results and ideas into my dissertation. I also have cited some of his studies in Chapter V.

Chapter I References

1. Morawetz H. Reactivity of Organic Crystals. Science. 1966;152(3723):705-711.
2. Kubicki M. Structural aspects of phase transitions. Diffusion and Defect Data--Solid State Data, Pt B: Solid State Phenomena. 2006;112:1-20.
3. Hu Y, Erxleben A, Hodnett BK, Li B, McArdle P, Rasmuson ÅC, Ryder AG. Solid-State Transformations of Sulfathiazole Polymorphs: The Effects of Milling and Humidity. Crystal Growth & Design. 2013;13(8):3404-3413.
4. Li H, Stowell JG, He X, Morris KR, Byrn SR. Investigations on solid-solid phase transformation of 5-methyl-2-[(4-methyl-2-nitrophenyl)amino]-3-thiophenecarbonitrile. Journal of Pharmaceutical Sciences. 2007;96(5):1079-1089.
5. Satoshi K, Akira M, Shigetaka K, Yukiyoshi M. Effect of grinding on the solid-state stability of cefixime trihydrate. International Journal of Pharmaceutics. 1989;56(2):125-134.
6. Cui Y. A material science perspective of pharmaceutical solids. International Journal of Pharmaceutics. 2007;339(1–2):3-18.
7. Wirth DD, Baertschi SW, Johnson RA, Maple SR, Miller MS, Hallenbeck DK, Gregg SM. Maillard reaction of lactose and fluoxetine hydrochloride, a secondary amine. Journal of Pharmaceutical Sciences. 1998;87(1):31-39.
8. Nakai Y, Nakajima S, Yamamoto K, Terada K, Konno T. Effects of grinding on the physical and chemical properties of crystalline medicinals with microcrystalline cellulose. III. Infrared spectra of medicinals in ground mixtures. Chemical and Pharmaceutical Bulletin. 1978;26(11):3419-3425.
9. Dempah K, Barich D, Kaushal A, Zong Z, Desai S, Suryanarayanan R, Kirsch L, Munson E. Investigating Gabapentin Polymorphism Using Solid-State NMR Spectroscopy. AAPS PharmSciTech. 2013;14(1):19-28.
10. Lin S-Y, Hsu C-H, Ke W-T. Solid-state transformation of different gabapentin polymorphs upon milling and co-milling. International Journal of Pharmaceutics. 2010;396(1–2):83-90.
11. Zong Z, Desai S, Kaushal A, Barich D, Huang H-S, Munson E, Suryanarayanan R, Kirsch L. The Stabilizing Effect of Moisture on the Solid-State Degradation of Gabapentin. AAPS PharmSciTech. 2011;12(3):924-931.
12. Zambon E, Giovanetti R, Cotarca L, Pasquato L. Mechanistic investigation on 2-aza-spiro[4,5]decan-3-one formation from 1-(aminomethyl)cyclohexylacetic acid (gabapentin). Tetrahedron. 2008;64(28):6739-6743.

13. Potschka H, Feuerstein TJ, Löscher W. Gabapentin-lactam, a close analogue of the anticonvulsant gabapentin, exerts convulsant activity in amygdala kindled rats. Naunyn-Schmiedeberg's archives of pharmacology. 2000;361(2):200-205.
14. NDA 20-882 (US. Food and Drug Administration application No. 020882).
15. Pharmacopeia US. The United States Pharmacopeia, USP 30. The National Formulary, NF 25: Official from May 1, 2007. United States Pharmacopeial Convention, Inc.; 2007.
16. Zong Z, Qiu J, Tinmanee R, Kirsch LE. Kinetic model for solid-state degradation of gabapentin. Journal of Pharmaceutical Sciences. 2012;101(6):2123-2133.

CHAPTER II

QUANTIFICATION OF GABAPENTIN POLYMORPHS IN GABAPENTIN/EXCIPIENT MIXTURES USING SOLID STATE 13C NMR SPECTROSCOPY AND POWDER X-RAY DIFFRACTION

Introduction

Different forms of the same active pharmaceutical ingredient (API) may affect the performance properties of the API in a pharmaceutical product. Thus the characterization of solid API forms has become a subject of considerable interest to pharmaceutical scientists, pharmaceutical industries and Food and Drug Administration (FDA). (1) Polymorphs refer to different crystalline forms, including solvate and hydrate of the same drug substance. (2) Polymorphs can have different chemical and physical properties, including chemical reactivity, mechanical properties, dissolution rate, and density. These properties can influence the manufacturing of the drug product, and also its performance such as product stability, dissolution, and bioavailability. Polymorphs can have an impact on quality, safety and efficacy of drug product; thus characterization and quantification of polymorphs in active pharmaceutical ingredient are also important in order to ensure the product quality. (3, 4)

Gabapentin is a ɣ-aminobutyric acid used for the treatment of epilepsy and neuropathic pain. It was chosen as a model compound in our studies due to its polymorphism and propensity to undergo both chemical and physical transformations. (5, 6) In the solid state, gabapentin exists in various forms, including a monohydrate (Form I) and three anhydrous polymorphs: Form II, III and IV [Figure II-1]. (7-9) The structural differences between the anhydrous polymorphs are due to differences in inter- and intra-

molecular hydrogen bonding between amine and carboxylic acid moieties. The similarity of inter-molecular hydrogen bonding distances (N1···O) in Form II and IV are found to be 2.76 and 2.77 Å. Additionally, no intra-molecular hydrogen bonding is observed in both forms. The presence of intra-molecular hydrogen bonding in Form III is unique. The distances (N1 (H15)···O) are reported to be 2.940 Å. A comparison of packing efficiencies of Form II, III, and IV is shown to be 71.3, 70.5, and 68.7 %, respectively. The most efficiently packed is observed in Form II which is the thermodynamically most stable form. (8, 10)

Figure II- 1. Major crystal forms of gabapentin (7-9).

Monohydrate Form I	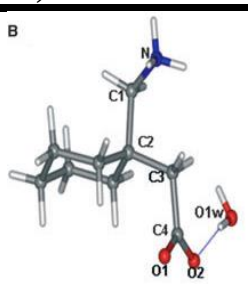
Anhydrate Form II	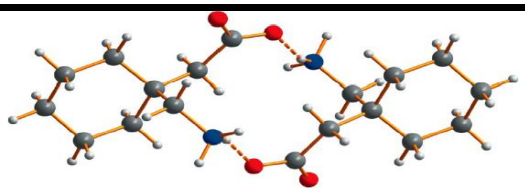
Anhydrate Form III	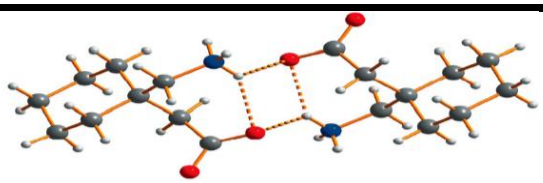
Anhydrate Form IV	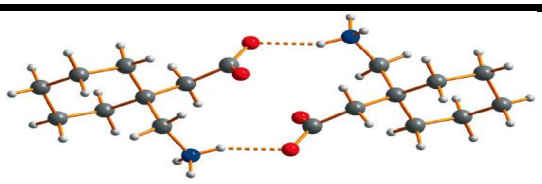

The qualitative effects of excipient and milling on polymorphic transformations of gabapentin Form II have been reported. The effect of milling in the presence and absence of 6.5 %w/w HPC on polymorphic transformation of gabapentin Form II was studied using ^{13}C solid state nuclear magnetic resonance spectroscopy. Partial transformation from gabapentin Form II to III was observed when co-milled with HPC for 45 minutes, whereas no transformation to Form III was found in the absence of HPC or in the physical mixtures of gabapentin and HPC. (11) The effect of co-milling with various excipients on chemical and physical transformations of gabapentin Form II was also investigated using Fourier transform infrared spectroscopy. The polymorphic transformations after milling for 2 hours were dependent on excipient type. For example, no transformation was observed when co-milled with 50 %w/w dicalcium phosphate dihydrate or corn starch; however, partial transformation from Form II to Form IV was found when co-milled with 50 %w/w colloidal silicon dioxide or talc. (12) Although the excipient effect on polymorphic transformation of gabapentin Form II during co-milling was reported using ^{13}C solid state nuclear magnetic resonance spectroscopy and Fourier transform infrared spectroscopy, a required quantitative method for determining polymorphic composition of gabapentin in excipient mixtures has not been systematically investigated. The aim of this work was to develop the methods to determine the polymorphic composition over a range of concentrations. This work also provided quantification of the excipient effect on polymorphic transformation of gabapentin Form II during co-milling. In future studies, these methods will be used to determine the kinetics of polymorphic transformations during storage in the presence of co-milled excipients.

A variety of physical methods used to study polymorphs have been reported, including differential scanning calorimetry (DSC), thermogravimetry (TGA), Raman spectroscopy, Fourier transform infrared spectroscopy (FTIR), microscopy, surface area and density analysis, dynamic vapor sorption, dynamic mechanical analysis, X-ray powder diffraction (XRPD), and solid state nuclear magnetic resonance (ssNMR) spectroscopy. (13, 14) However, some methods have phenomenological or quantification limitations. Gabapentin polymorphs have been characterized by using DSC, TGA, FTIR, XRPD and ^{13}C ssNMR. Thermal analysis by DSC is complicated due to the overlapping endothermic melting peaks of gabapentin and spontaneous decomposition to gabapentin-lactam formation and sublimation. (6, 15) Additionally, FTIR quantitative analysis is complicated because of the overlapping peaks found in polymorphic mixtures especially in the presence of crystalline excipients. (12) Therefore, ^{13}C ssNMR and XRPD were chosen for our studies.

^{13}C ssNMR has been extensively used to characterize polymorphs in API and in the final dosage form. Typically, API peaks are present in different regions of the spectrum than the excipient peaks thus the interference from excipient peaks is minimized. (16, 17) Quantitative results using ^{13}C intensities were demonstrated to be linear with the mass fractions of polymorph mixtures. Thus, the standard curves plotted between the integrated peak areas as a function of mole fraction of carbamazepine polymorph Form I and II and delavirdine mesylate polymorph Form VIII and XI were successfully developed. (18, 19) ^{13}C ssNMR was also used to differentiate small quantities (5 %w/w) of polymorphs Form I and II presented in prednisolone tablets. (20)

Manufacturing conditions and excipients can potentially influence the solid state characteristics of active pharmaceutical ingredients. Highly-ordered drug substances can be qualitatively observed by narrow shape of ssNMR peaks. For example, the effect of lyophilization in the presence of sulfobutylether-β-cyclodextrin on the crystallinity of prednisolone Form II was studied. No evidence of narrow peaks associated with prednisolone polymorph Form II was found, indicating that freeze-drying resulted in disordered state. (21) The effect of ball-milling on peak broadening of gabapentin Form II has been reported. Milled sample maintained the same crystal patterns that corresponded to untreated gabapentin Form II; however, some peak-broadening in ^{13}C spectra were also found. (11, 22) Additionally, the effect of cryo-grinding on ^{13}C ssNMR line width of ibuprofen has been reported. Cryo-ground ibuprofen also maintained the crystal patterns associated with ibuprofen, while the line width of milled sample peaks was significantly broader than those observed in un-milled sample. (23)

XRPD has been routinely used for polymorphic characterization. Quantitative results using relative peak intensities were also demonstrated to be linear with the mass fractions of polymorph mixtures. A quantitative analysis of polymorphic composition in intact tablets was developed. Chlorpropamide Form A and C were prepared and compacted using a Carver single station bench top tablet press at a constant pressure of 7 MPa. Each form was successfully quantified using a linear relationship between integrated intensity and phase composition of Form A and C in intact tablets. (24) Similarly, two synthetic glycine α- and γ-form were prepared and compressed under a pressure of 36200 psi. A peak intensity ratio of two forms (γ/α) in intact compact was plotted against a concentration ratio in the range of 0-100 %w/w. The calibration curves

of glycine compacts showed a linear relationship with high correlation coefficient equaled to one. (25) The standard curves of polymorphic mixtures of neotame Form A and G showed good linearity with the detection limit at 1-2 %w/w. (26, 27) Validation and assay errors associated with quantitative analysis of olanzapine polymorphs Form I and II using XRPD were studied. Assay of six data sets on six different days were reproducible and precise. Relative standard deviation for overall assay error was 5.2 %. (28) The modified XRPD technique using parallel beam X-ray optic combined with a statistical fitting of measured peak intensities and standard reference patterns was investigated. This technique could provide an accurate analysis of amorphous content presented in lactose with a very low limit of detection at 0.37 %. (29)

XRPD is capable of polymorphic fingerprinting. Flufenamic acid Form I and III were prepared using laboratory methods and verified by comparing to theoretical diffractograms based on the reference crystal structure from the Cambridge Crystallographic Data Center (CCDC). (30) To elucidate structural differences of amorphous and nanocrystalline states induced by grinding, model compounds (microcrystalline cellulose, indomethacin and piroxicam) were studied. XRPD patterns of disordered nanocrystalline solids were observed by continuous peak broadening due to loss of long range order symmetry; however, the peak positions of nanocrystalline solid were maintained. For amorphous materials, a diffuse halo in XRPD pattern was observed but neither peak intensity nor position correlated to the parent crystalline polymorph. An analysis of XRPD data was also carried out using a total X-ray diffraction approach (pair distribution functions (PDF)). PDF refers to the probable distance between two atoms. (31)

Both ^{13}C ssNMR and XRPD analyses are capable of characterizing polymorphs in terms of qualitative and quantitative analyses. However, some concerns have been reported regarding the consistency between ^{13}C ssNMR and XRPD. The comparison of ^{13}C ssNMR and XRPD techniques for analyzing neotame polymorphic transformations was reported. The evidence for the transformation of anhydrate form to the stable monohydrate in the presence of moisture under ambient conditions was observed using ^{13}C ssNMR. In contrast, no XRPD peak of monohydrate was observed. (32) Therefore, in this study we anticipate the use of both techniques to quantify the polymorphic transformations of gabapentin and gabapentin/excipient mixtures during co-milling.

Material and Methods

In general, the approach described herein for the determination of polymorphic composition involved both ^{13}C solid state nuclear magnetic resonance spectroscopy (^{13}C ssNMR) and X-ray powder diffraction (XRPD) technologies. ^{13}C ssNMR methods were developed using instrumentation available at The University of Iowa Central Nuclear Magnetic Resonance, Department of Chemistry. XRPD methods were developed using facilities generously provided by Professor Kenneth R. Morris, Department of Pharmaceutical Sciences, The University of Hawaii at Hilo. Synthetic mixtures of two polymorphic forms of gabapentin Form II and III were prepared at The University of Iowa and used to develop calibration curves for each instrument. Additionally, polymorph mixtures were generated at the University of Iowa by co-milling with excipients. These compositional mixtures were measured by each method and the results were compared. Both synthetic and co-milled mixtures were determined firstly using ^{13}C ssNMR at The University of Iowa Central Nuclear Magnetic Resonance, Department of

Chemistry. Then, these samples were shipped on dry ice/Drierite® desiccant and analyzed using XRPD at The University of Hawaii at Hilo. These samples were always stored under Drierite® desiccant and sub-ambient temperature (-80 ºC). Finally, all mixtures were shipped back to the University of Iowa and re-analyzed by ^{13}C ssNMR. Experimental details were provided below.

Materials

Gabapentin Form II was obtained from Hangzhou Starshine Pharmaceutical Co., Ltd. (Hangzhou, China). Gabapentin Form III was crystallized by dissolving gabapentin Form II in 95 %v/v ethanol until the solution was saturated and then heated at 60 ˚C for 24 hours. The crystal is formed during cooling of the supersaturated solution. (8) Both polymorphic forms were then verified by comparing to the theoretical XRPD diffractograms based on the reference crystal structure from CCDC. Four excipients, including colloidal silicon dioxide (SiO_2, CAB-O-SIL® TS-530, Billerica, MA), hydroxy propyl cellulose (HPC, given by FDA, FDA-sponsored contract number HHSF2232008199292C), pregelatinized corn starch (starch, UNI-PURE™ DW, Bridgewater, NJ), and dibasic calcium phosphate dihydrate ($CaHPO_4$, Emcompress®, Patterson, NY) were used as received.

Milling Stress

The effect of co-milling gabapentin Form II in the presence of excipients was studied by placing a two gram aliquot of 6.5 or 50 %w/w mixture gabapentin Form II/excipient (SiO_2, HPC, starch, and $CaHPO_4$) into 45 ml milling chamber with four stainless steel balls (25 mm) and milling in a planetary mill (Pulviserette7, Planetary Micro Mill, FRITSCH GmbH, Idar-Oberstein, Germany) for 60 minutes with speed

setting 7. At this speed, the motor and grinding bowl speeds were 2400 and 1000 rpm, respectively. All milling operations were conducted at ambient conditions.

^{13}C Solid State Nuclear Magnetic Resonance Spectroscopy (^{13}C ssNMR)

ssNMR spectroscopy is an inherently quantitatively method because the amount of signal observed is proportional to the number of nuclei that resonate at a given frequency. In order to perform a ^{13}C ssNMR experiment, cross-polarization and magic angle spinning (CP/MAS) are generally used to improve sensitivity of the ^{13}C signal; however, a magnetization transfer occurs during the cross-polarization period which depends on two characteristic parameters: the cross-polarization rate constant (T_{CH}) and the proton spin-relaxation time in the rotating frame ($T_{1\rho H}$). (17) These two parameters must be experimentally determined in order to obtain quantitatively reliable ^{13}C CP/MAS NMR spectra. T_{CH} was used for determining the optimal contact time (τ) range for the CP/MAS experiment. The shortest contact time was chosen to be approximately ten times greater than the T_{CH} value. (19) To determine T_{CH} and $T_{1\rho H}$, the contact time for gabapentin polymorph Form II and III was varied from 0.025 to 6 ms to determine the peak intensity versus contact time profile. Two model parameters (T_{CH} and $T_{1\rho H}$) describing the cross-polarization kinetics given by Mehring were estimated [Equation II-1]. $I_{(\tau)}$ is the peak area for each contact time (τ). M_0 is the thermal equilibrium magnetization. γ_H and γ_C are the magnetogyric ratios for proton and carbon, respectively. T_{CH} is the cross-polarization rate constant, and $T_{1\rho H}$ is the proton spin-relaxation time in the rotating frame. (33, 34)

$$I_{(\tau)} = \frac{M_0 \frac{\gamma_H}{\gamma_C}\left[\frac{\exp(-\tau)}{T_{1\rho H}} - \frac{\exp(-\tau)}{T_{CH}}\right]}{1-\left(\frac{T_{CH}}{T_{1\rho H}}\right)} \qquad \text{Equation II-1}$$

All ^{13}C spectra were obtained using a Bruker Avance 500 MHz. An 80 mg sample was packed under ambient conditions in a 4 mm zirconia rotor. Duplicate runs were measured for each sample. Spectra were obtained at a ^{13}C frequency of 125 MHz and a 500 MHz ^{1}H frequency. The spectra were acquired using ramp cross-polarization and magic angle spinning (CP/MAS). A SPINAL-64 decoupling pulse sequence was used and the spinning was done at rate 12 kHz. Spectra were collected using a 32 decoupling pulse sequence. Acquisition parameter for ^{1}H 90° pulse was set to be 4.8 μs. The optimal contact times were chosen as described previously. Proton relaxation time in laboratory frame (^{1}H T_1) was measured by inversion recovery. (35) To ensure a full return of magnetization to equilibrium between CP/MAS NMR transients, the recycle delay is considered to be approximately five times of ^{1}H T_1 value for each sample. (36, 37) Data acquisition and processing were operated using Bruker TopSpin 3.0 software. A total of 2048 data points were acquired for each experiment. All data were collected at ambient probe temperature.

The method for quantifying polymorphic form concentration using ^{13}C intensity was adapted from the work of Offerdahl et al. (38) The synthetic mixtures of known concentrations of Form II and III were prepared to contain 3, 6, 10, 15, 30, and 50 %w/w Form III. Mixtures were briefly blended with a Vortex® mixer for 1 minute. To improve spectra sensitivity, mixtures were gently ground by hand with a pestle in a mortar prior to packing.

Specific chemical shifts of Form II and III as described in Table II-1 were identified (11) and calibrated indirectly to the adamantane peak (29.5 ppm relative to tetramethysilane). (19)

Table II- 1. Chemical shifts of carbon peaks of gabapentin Form II and III (11).

Compound	Chemical Shifts (ppm)							
Gabapentin Form II	47.6	39.1	36.2	35.3	34.5	28.2	22.4	21.6
Gabapentin Form III	51.4 51.0	41.0	37.6	36.3	33.8	27.0	22.1	

The representative ^{13}C ssNMR spectra for the aliphatic region of gabapentin Form II and Form III are shown in Figure II-2.

Figure II- 2. Representative ^{13}C ssNMR spectra for the aliphatic region of gabapentin Form II (A) and gabapentin Form III (B). The ^{13}C ssNMR was operated under ambient conditions.

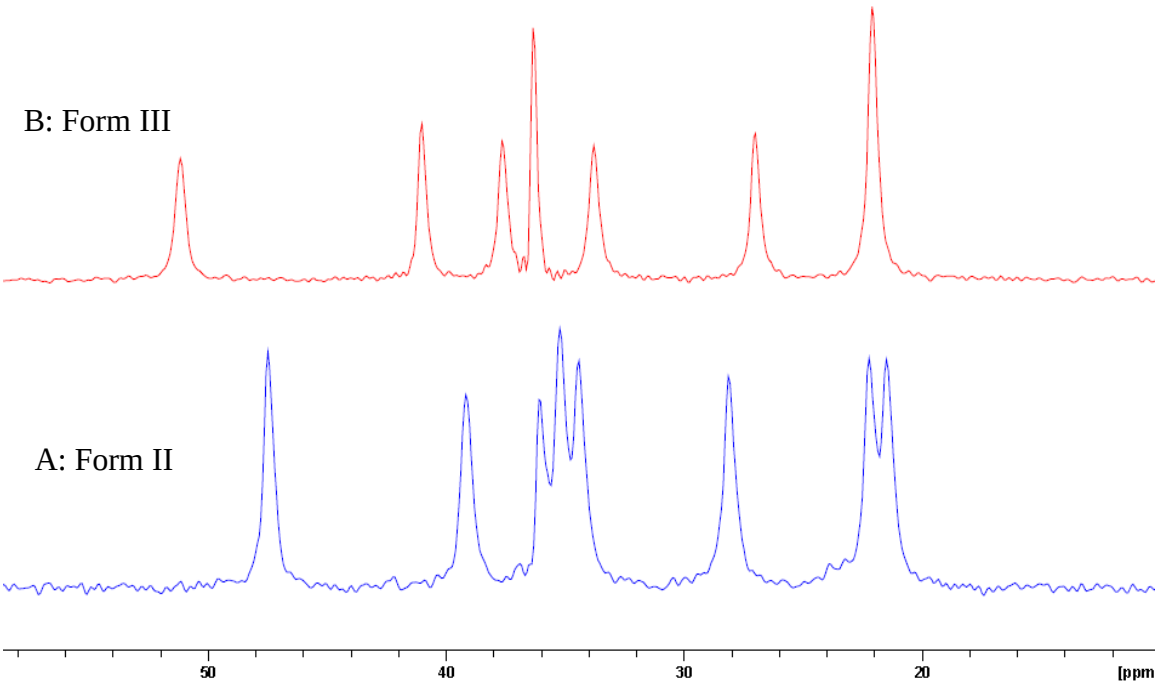

The peak areas for chemical shifts at 28.2 and 39.1 ppm were selected to quantify Form II, and the peak areas for chemical shifts at 37.6 and 41.0 ppm were used for Form III measurement. The natural log of the peak areas for each form was plotted against contact times (τ). The extrapolated peak areas at $\tau = 0$ were estimated for each form. The standard curves were drawn based on natural log of peak areas (Form II and III) at $\tau = 0$ against the percentage of Form II and III, respectively. Three groups of standard mixture samples were prepared and analyzed on three different days to test the robustness of

analytical technique using an external standard curve. The mean slope value and standard deviation were calculated from the resulting standard curves. The limit of detection (LOD) and quantitation (LOQ) were estimated by following equations [Equation II-2 and II-3] where σ is a standard deviation of y-intercepts of regression lines and S is a slope of calibration curve. (39)

$$LOD = \frac{3.3\,\sigma}{S}$$ Equation II-2

$$LOQ = \frac{10\,\sigma}{S}$$ Equation II-3

The ^{13}C ssNMR spectra of gabapentin Form II and Form III and the gabapentin/excipient mixtures were recorded under identical experimental conditions. The chemical shifts of gabapentin Form II and III in neat sample and in gabapentin/excipient mixtures were the same. To ensure the lack of excipient peak interference, ^{13}C ssNMR spectra of excipients and co-milled gabapentin/excipient mixtures were compared to synthetic mixtures of Form II and III. No peak associated with excipient was found in the aliphatic region of ^{13}C ssNMR spectra (0-60 ppm), thereby demonstrating the absence of excipient interference.

X-ray Powder Diffraction (XRPD)

XRPD patterns were determined at ambient conditions using an X-ray diffractometer with Cu Kα radiation at 40 mA, 40 kV (Bruker, model D8-Discover, Madison, WI). The scanning conditions were from 5 to 40° 2Θ by a Cu Kα radiation source with 0.1 mm divergence slit. The step side was 0.01˚ and the scan speed was 0.5 second/step. A Ni-plated copper sample holder with sample area (L X W): 14 X 10 mm and groove: 0.8 mm was used, and an approximately 100 mg aliquot sample was loaded into the sample holder. Duplicate runs were measured for each sample. A quantitative

method using relative peak areas was developed using synthetic mixtures of Form II and III. Synthetic mixtures of known polymorphic concentration were prepared to contain 3, 6, 10, 15, 30, and 50 %w/w Form III by weighing Forms II and III and mixing briefly with a Vortex® mixer for 1 minute. To avoid preferred orientation, mixtures were gently ground by hand with a pestle in a mortar for 1 minute to reduce the non-spherical geometry to approximately spherical particles. The experimentally-obtained diffraction patterns were compared to the theoretical diffractograms based on the crystal structure from the Cambridge Crystallographic Data Center (CCDC). Forms II and III had distinctive XRPD patterns, in which the strongest peaks for distinguishing and quantitating the two polymorphs were 6.1° 2Θ for Form III and 7.8° 2Θ for Form II [Figure II-3]. The peak area of two peaks, 6.1° 2Θ for Form III and 7.8° 2Θ for Form II, were obtained by using a profile function of JADE software (Version 9.0, Materials Data Inc., Livermore, CA). In addition, the 2Θ values of both polymorphic Form II and III compared well with those of calculated XRPD diffractograms published from CCDC, thereby demonstrating the pure crystalline forms of gabapentin Form II and III. The standard curves were drawn based on relatively peak area of Form II and III ($\frac{P_{III}}{P_{II}+P_{III}}$) against the percentage of Form III, where P_{II} and P_{III} were the peak area of Form II and Form III. (27) Three groups of standard mixture samples were prepared and analyzed on three different days to test the robustness of analytical technique using an external standard curve. The mean slope value and standard deviation were calculated from the resulting standard curves. The limit of detection (LOD) and quantitation (LOQ) were estimated by equation II-2 and II-3 as described previously. (39) The diffractograms of gabapentin Form II and Form III and the gabapentin/excipient mixtures were recorded

under identical experimental conditions. To ensure the lack of excipient peak interference, XRPD patterns of excipients and co-milled gabapentin/excipient mixtures were compared to synthetic mixtures of Form II and III. No peak associated with excipient hindered the selected peaks (6.1° 2Θ for Form III and 7.8° 2Θ for Form II) for quantitative analysis, thereby demonstrating the absence of excipient interference.

Figure II- 3. Representative XRPD patterns of gabapentin Form II and III. The XRPD was operated under ambient conditions.

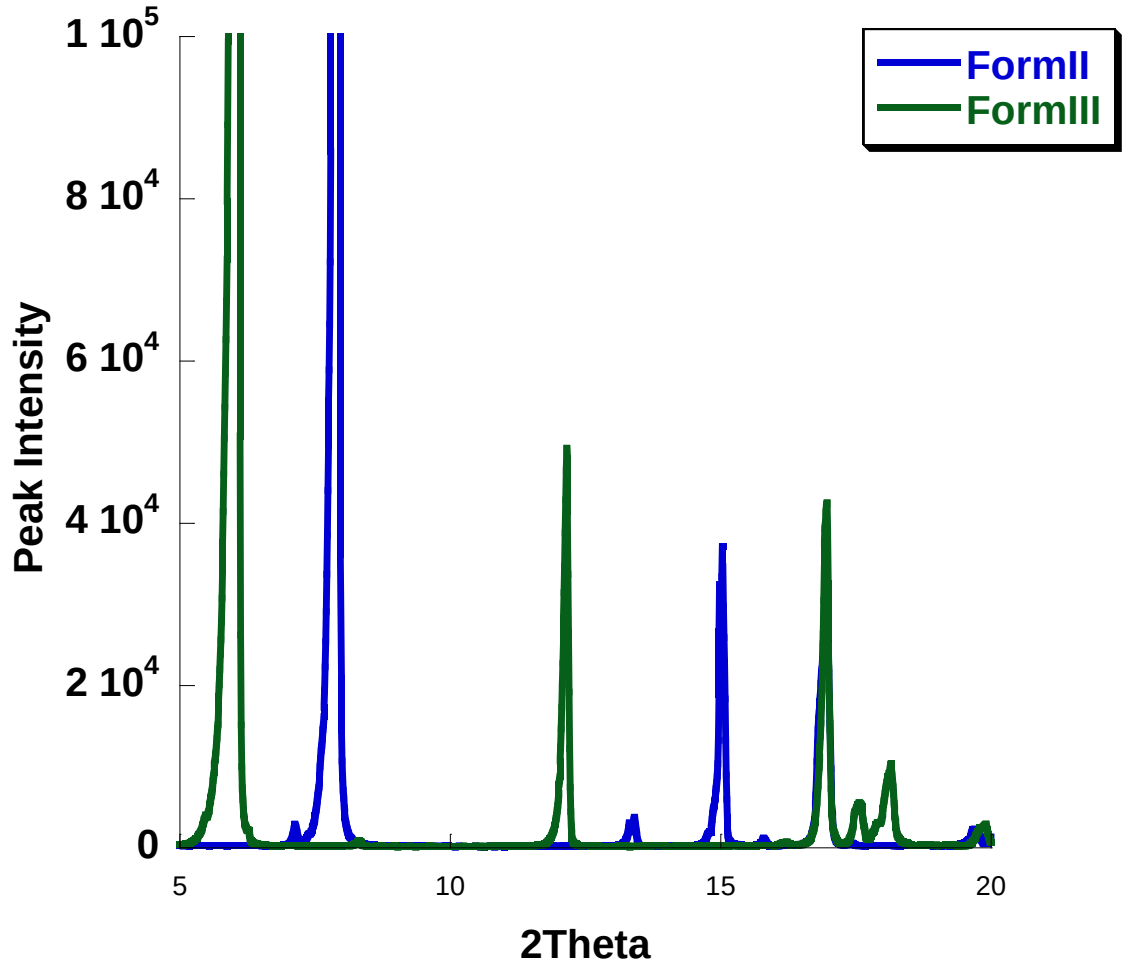

Since the analysis by ^{13}C ssNMR and XRPD techniques was used in quantify polymorphic transformation kinetics of environmentally-stressed mixtures (as described in Chapter IV), stability of the sample prior and during analysis and the consistency of results from both ^{13}C ssNMR and environmentally-controlled XRPD (VT-XRPD) were investigated. Aliquots of each excipient mixtures (SiO_2, $CaHPO_4$, starch and HPC) were placed into three groups and treated as described below.

Samples in group 1 were placed in a 20 ml Type II scintillation glass vial and stored in desiccators at 50 °C and 47.5 %RH. At 0, 4, 8, 12, and 24 hours, aliquots were removed from the stability chambers and immediately subjected to ^{13}C ssNMR analysis.

Samples in group 2 were stored and sampled as described for group 1. At 0, 4, 8, 12, and 24 hours, aliquots were removed from the 50 °C/47.5 %RH chamber and placed in a storage chamber containing Drierite® desiccant and maintained at -80 °C for 24 hours prior to ^{13}C ssNMR analysis.

Samples in group 3 were analyzed by environmentally-controlled XRPD (VT-XRPD) at reaction conditions (50 °C and 47.5 %RH). Analysis was carried out using VT-XRPD with Cu Kα radiation at 40 mA, 40 kV (Bruker, model D8-Discover, Madison, WI and Anton-Paar TTK 450 temperature chamber, Anton Paar, Austria). The temperature unit was controlled at 50 ˚C by TCU 100 Eurotherm® controller and the heating rate was 0.2˚C/second. Saturated salt solution reservoir ($Mg(NO_3)_2$) was prepared and connected to the TTK 450 temperature unit to supply humidity (47.5 %RH) through the chamber. During study, the temperature was controlled and monitored automatically by the TCU 100 unit and the humidity was recorded continuously using EL-USB-2 Temperature and Humidity Data Logger recorder (DATAQ Instruments, Inc., Akron, OH) with ± 3.0 %RH

accuracy. The diffraction patterns of co-milled excipient samples were automatically recorded at 0, 2, 4, 8, 12, 16, and 24 hours.

Form III concentration time profiles in reaction mixtures containing SiO_2 and starch (50 °C and 47.5 %RH) were determined for each group using both ^{13}C ssNMR and VT-XRPD [Figure II-4 to II-5]. These concentration time profiles were indistinguishable. Thus the samples from reaction mixtures containing either of these two excipients were stable during analysis and the results from either ^{13}C ssNMR or VT-XRPD were consistent.

Form III concentration time profiles in reaction mixtures containing $CaHPO_4$ and HPC (50 °C and 47.5 %RH) were determined for each group by ^{13}C ssNMR and VT-XRPD [Figure II-6 to II-7]. For these mixtures, the Form III concentration in group 2 and 3 were the same and thereby demonstrating consistency between ^{13}C ssNMR and VT-XRPD methods of analysis. However, the Form III concentration in group 1 was less than those obtained from group 2 or 3. These observed differences suggest that the reaction mixture samples were not quenched by simply removing them from thermal and humidity stress but continued to degrade during ^{13}C ssNMR analysis. The results also demonstrate that the reactions were quenched by cold temperature (-80 °C) and dry condition (Drierite® desiccant) and were stable during ^{13}C ssNMR analysis. These results established a sample handling procedure for all subsequent solid-state degradation studies as reported in Chapter IV.

Figure II- 4. Form III concentration time profiles of reaction mixtures in the presence of SiO_2 stored at 50 ºC and 47.5 %RH. Samples in group 1 were removed from stability chambers and immediately subjected to ^{13}C ssNMR analysis (●). Samples in group 2 were stored under Drierite® desiccant and -80 °C for 24 hours prior subjecting to ^{13}C ssNMR analysis (■). Samples in groups 3 were analyzed using VT-XRPD (♦).

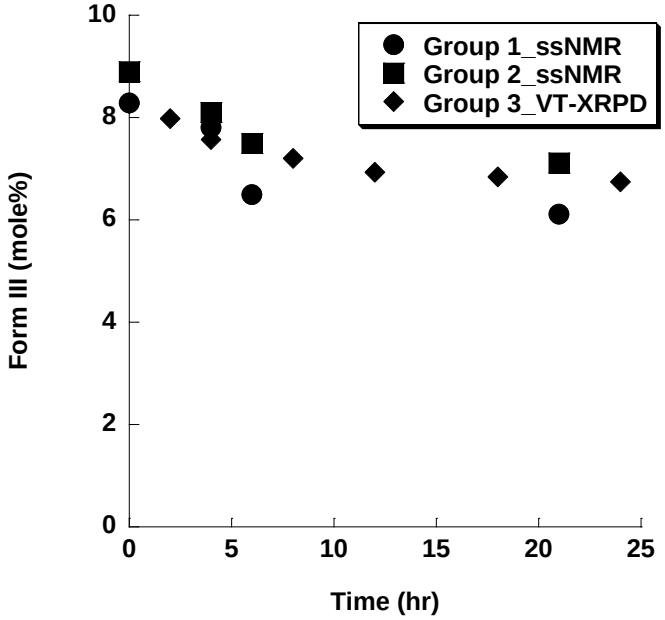

Figure II- 5. Form III concentration time profiles of reaction mixtures in the presence of starch stored at 50 ºC and 47.5 %RH. Samples in group 1 were removed from stability chambers and immediately subjected to ^{13}C ssNMR analysis (●). Samples in group 2 were stored under Drierite® desiccant and -80 °C for 24 hours prior subjecting to ^{13}C ssNMR analysis (■). Samples in groups 3 were analyzed using VT-XRPD (♦).

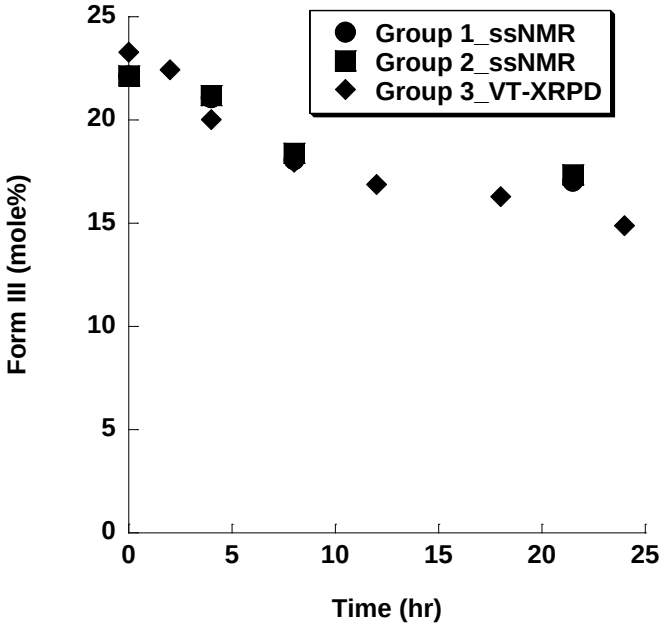

Figure II- 6. Form III concentration time profiles of reaction mixtures in the presence of $CaHPO_4$ stored at 50 ºC and 47.5 %RH. Samples in group 1 were removed from stability chambers and immediately subjected to ^{13}C ssNMR analysis (●). Samples in group 2 were stored under Drierite® desiccant and -80 °C for 24 hours prior subjecting to ^{13}C ssNMR analysis (■). Samples in groups 3 were analyzed using VT-XRPD (♦).

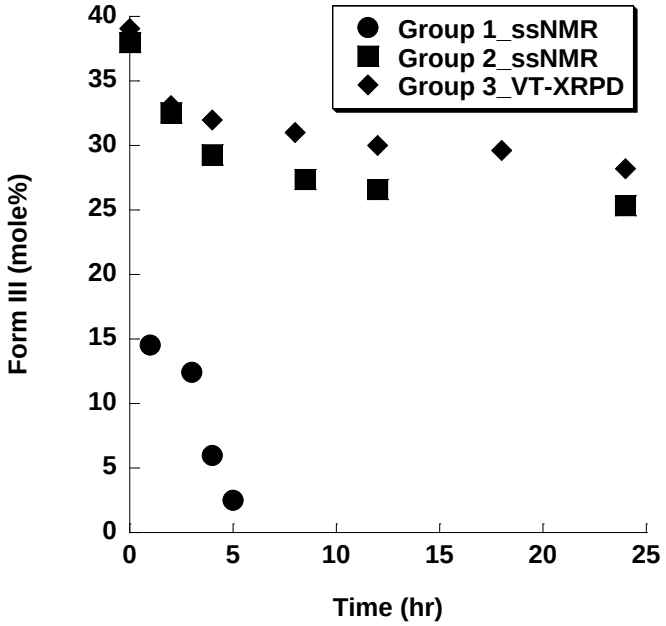

Figure II- 7. Form III concentration time profiles of reaction mixtures in the presence of HPC stored at 50 ºC and 47.5 %RH. Samples in group 1 were removed from stability chambers and immediately subjected to ^{13}C ssNMR analysis (●). Samples in group 2 were stored under Drierite® desiccant and -80 °C for 24 hours prior subjecting to ^{13}C ssNMR analysis (■). Samples in groups 3 were analyzed using VT-XRPD (♦).

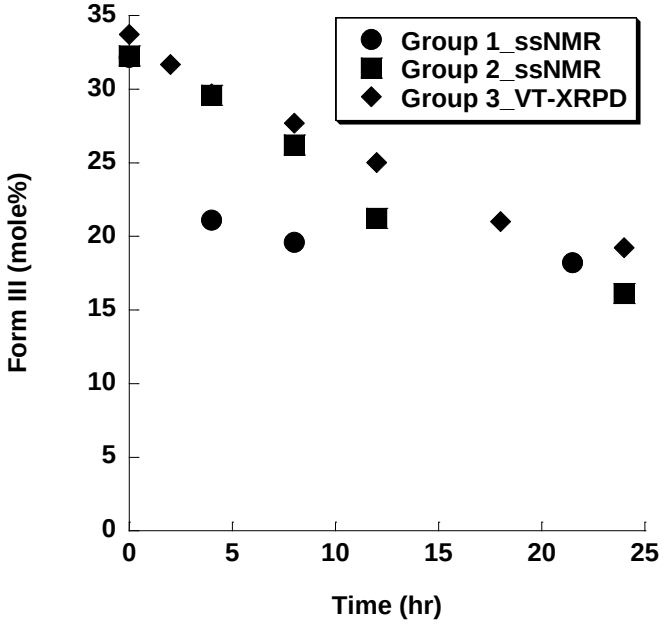

Results and Discussion

Determination of ^{13}C ssNMR Relaxation Behavior of Gabapentin Form II and III

Cross-polarization is used to transfer the magnetization from ^{1}H to ^{13}C, but the signal areas are not directly proportional to the number of ^{13}C nuclei. As a result, it is impractical to obtain quantitative information from a single spectrum acquired at a given contact time value. (17, 40) Therefore, the ^{13}C ssNMR relaxation behavior profiles of gabapentin Form II and III were determined in order to optimize the contact time ranges in this study. The ^{13}C ssNMR spectra of Form II and III were recorded as a function of contact times. During cross polarization, T_{CH} and $T_{1\rho H}$ reflect how quickly the ^{13}C magnetization grows and decays, respectively. The magnetization initially increased owing to cross polarization time (T_{CH}) effect, whereas the decrease in terminal phase was due to the proton spin lattice relaxation time in the rotating frame ($T_{1\rho H}$) effect. A natural log of peak area ($I_{(\tau)}$) for each polymorph was plotted against contact times (τ). The theoretical model [Equation II-1] described previously was fitted and then $T_{1\rho H}$ and T_{CH} were simultaneously determined. Both Form II and III showed similar cross-polarization profiles [Figure II-8].

Figure II- 8. ^{13}C CP/MAS NMR contact time profiles for gabapentin Form II at carbon chemical shift 28.2 ppm (A), 39.1 ppm (B) and gabapentin Form III at carbon chemical shift 37.6 ppm (C), 41.0 ppm (D). The ^{13}C ssNMR was operated under ambient conditions.

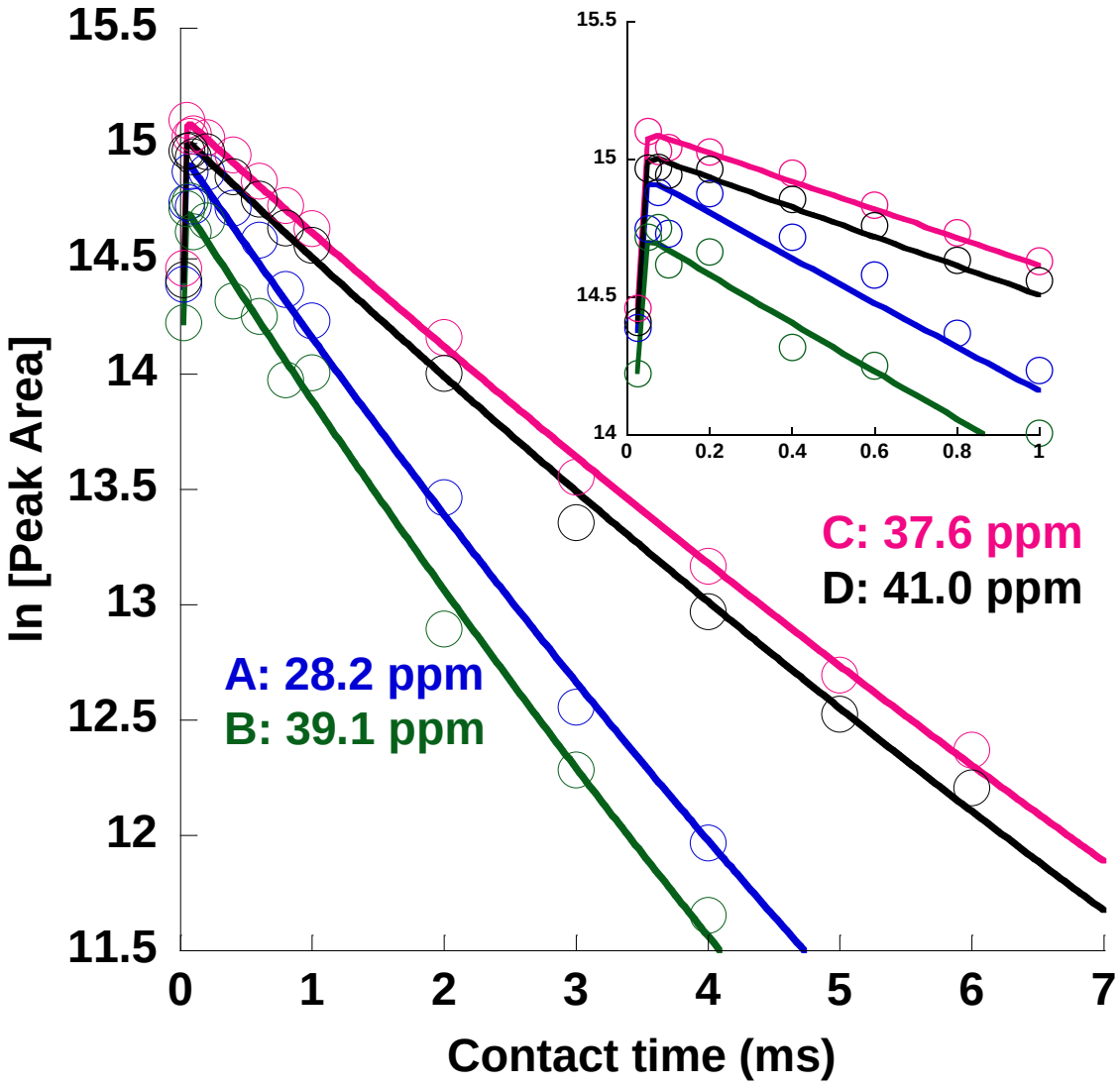

The T_{CH} values of gabapentin Form II and III were similar (0.0074 and 0.0079 ms, respectively). These T_{CH} values were considered to be short as a result of rapid magnetization build-up. This fast rate could indicate high crystallinity of the organic compound. The rapid rise of magnetization was also observed in glycine crystals (T_{CH} = 0.022 ms). (41) The T_{CH} values at 0.0074-0.0079 ms suggested that for the contact times greater than 0.1 ms (approximately 10 times greater than T_{CH} value), 99% of the maximum magnetization has been fully transferred to the ^{13}C nuclei. Therefore to ensure the complete transfer to ^{13}C nuclei in this study, the amount of each polymorph presented in pure forms and in gabapentin/excipient mixtures was acquired at the following series of contact times: 0.2, 0.4, 0.6, 0.8, and 1 ms.

The $T_{1\rho H}$ values of gabapentin Form II and III were comparable (16.78 and 28.07 ms, respectively). $T_{1\rho H}$ relaxation time is presumably sensitive to inter-molecular interaction which is dependent on the neighboring hydrogen atoms. (42) Extensive hydrogen bonding between NH_3^+ and COO^- groups of neighboring molecules was found in gabapentin Form III; therefore, this probably facilitated the proton spin diffusion. (8)

Based on the similarity of $T_{1\rho H}$ and T_{CH} values for both polymorphs, their peak intensities were equivalent to their molar ratio in mixtures between two forms. The contact time series (0.2, 0.4, 0.6, 0.8, and 1 ms) was shown to be appropriate, since these selected measurement time points were greater than T_{CH} values and smaller than $T_{1\rho H}$ values. Therefore, the signal intensity only depended on a number of nuclei giving rise to the signal. (43) For each sample, the peak area at $\tau = 0$ was determined by measuring the peak area over a series of contact times (0.2, 0.4, 0.6, 0.8, and 1 ms) and back

extrapolation to $\tau = 0$. Then the calibration curve for each polymorph was built by plotting the peak area at $\tau = 0$ against known polymorph concentration.

Reliability of ^{13}C ssNMR and XRPD Techniques for Polymorphic Quantitation

Using ^{13}C ssNMR, typical standard plots for the quantitative analysis of Form III in synthetic mixtures of Form II and III were linear at the range of 3-50 mole% [Figure II-9]. Measured concentrations of Form III in synthetic mixtures of Form II and III were within 1 mole% of known concentrations [Table II-2]. The limit of detection and quantitation (LOD and LOQ) of Form III were 0.58 mole% and 1.76 mole%, respectively. Comparable results were obtained using XRPD. The standard curves for the quantitative analysis of Form III in synthetic mixtures of Form II and III were linear at the range of 3-50 mole% [Figure II-10]. Measured concentrations of Form III in synthetic mixtures of Form II and III were within 1 mole% of known concentrations [Table II-3]. The limit of detection and quantitation (LOD and LOQ) of Form III were 0.77 mole% and 2.34 mole%, respectively. Therefore, both techniques were capable of measuring polymorphs in synthetic mixtures with reasonable accuracy. Moreover, both methods were capable of measuring polymorphic composition in excipient mixtures without excipient peak interference.

Figure II- 9. Representative standard plot for the quantitative analysis of Form III in synthetic mixtures of Form II and III using ^{13}C ssNMR. The natural log of peak areas for Form III were plotted against the contact times (τ): 0.2, 0.4, 0.6, 0.8 and 1 ms then the extrapolated peak areas at $\tau = 0$ for Form III were estimated. The standard plot was drawn based on natural log of peak area of Form III at $\tau = 0$ against the percentage of Form III.

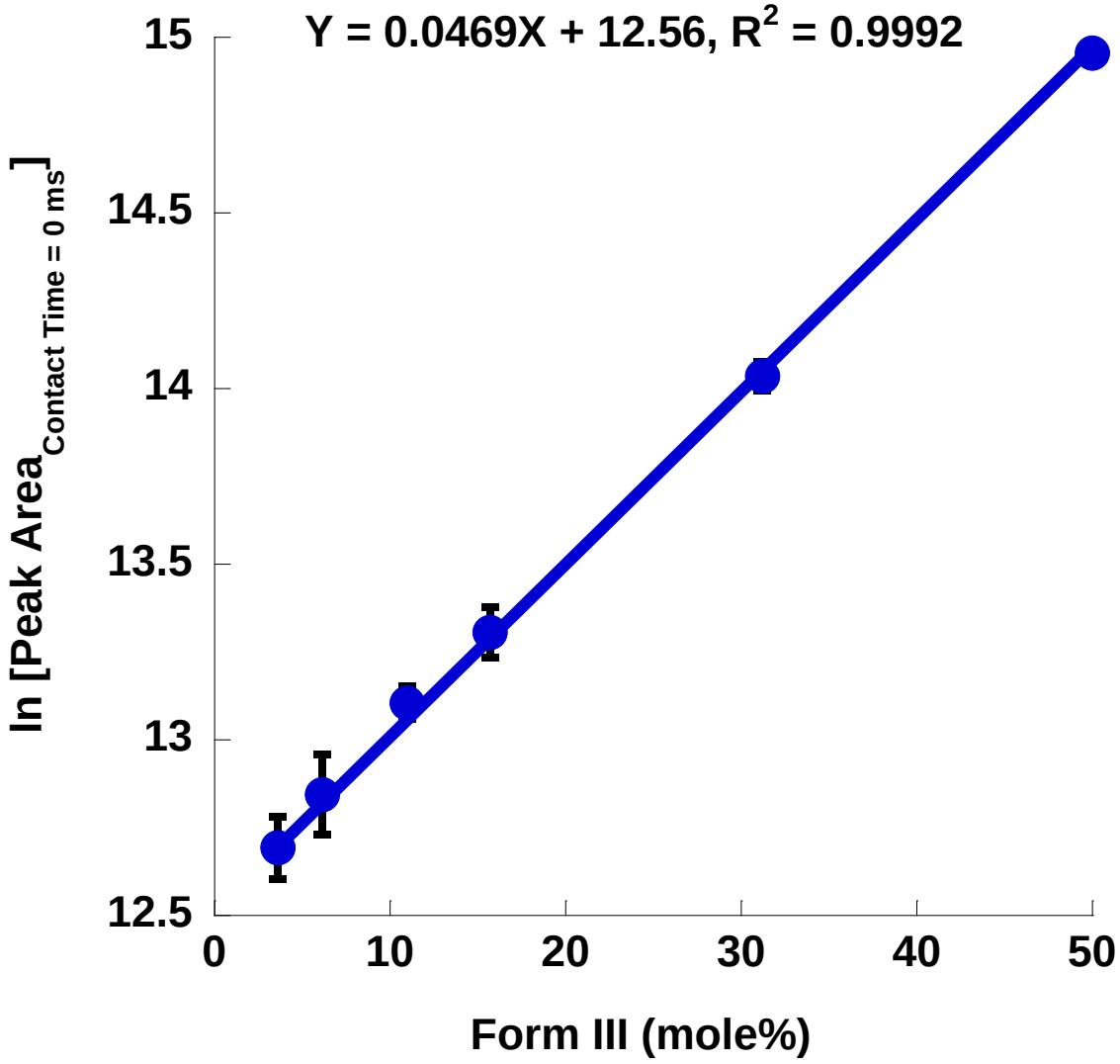

Figure II- 10. Representative standard plot for the quantitative analysis of Form III in synthetic mixtures of Form II and III using XRPD. The standard curves were drawn based on relatively peak area of Form II and III ($\frac{P_{III}}{P_{II}+P_{III}}$) against the percentage of Form III, where P_{II} and P_{III} were the peak area of Form II and Form III.

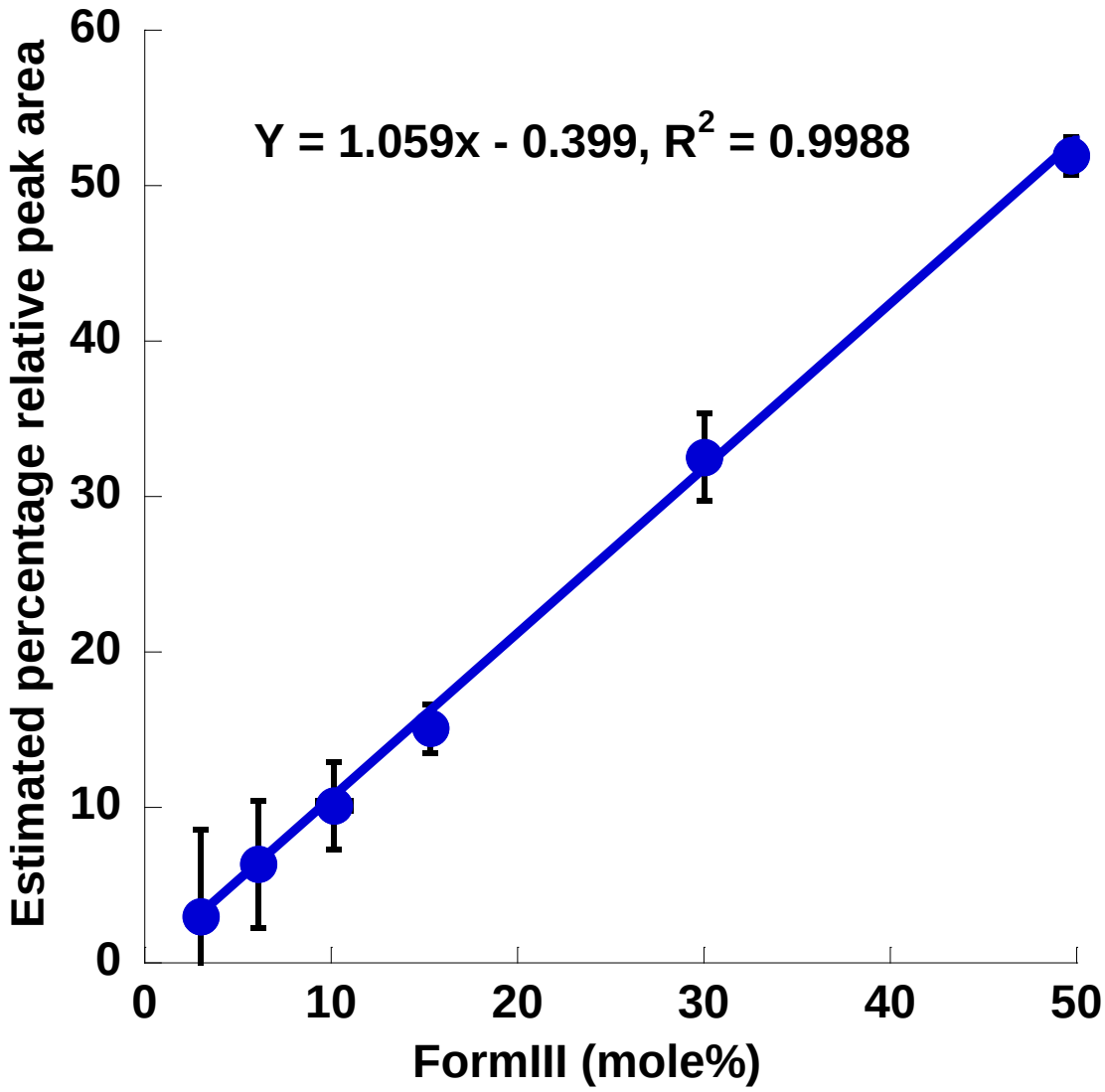

Table II- 2. Comparison of known and measured amount of Form III in synthetic mixtures of Form II and III. These results were analyzed using ^{13}C ssNMR on three different days under ambient conditions.

Form III mole (%)	Average Measured Form III mole (%)	SD (n=3)
3.63	3.50	0.26
6.15	6.20	0.10
11.0	11.1	0.15
15.7	15.8	0.14
31.2	31.0	0.41
50.9	51.1	0.15

Table II- 3. Comparison of known and measured amount of Form III in synthetic mixtures of Form II and III. These results were analyzed using XRPD on three different days under ambient conditions.

Form III mole (%)	Average Measured Form III mole (%)	SD (n=3)
3.03	2.95	0.65
6.11	6.34	0.53
10.2	10.1	0.23
15.4	15.1	0.63
31.1	31.2	0.16
50.7	50.9	0.15

Physical Composition of Co-Milled Gabapentin/Excipient Mixtures

The effects of selected inorganic (SiO_2 and $CaHPO_4$) and organic (starch and HPC) excipients on physical transformation of gabapentin Form II were determined by measuring the polymorphic conversion after milling using ^{13}C ssNMR and XRPD. Although no polymorphic conversion has been previously reported in the absence of excipients under the described milling conditions (22), partial conversion of gabapentin from Form II (more stable) to Form III (less stable) caused by milling was observed in the presence of excipients. (11) The extent of polymorphic transformations during milling depended on the type of excipient. In the presence of $CaHPO_4$, 39 mole% Form III was generated, whereas only 8.7 mole% was found in the presence of SiO_2. For organic excipients, 21 and 33 mole% of Form III were generated in the presence of starch and HPC, respectively. No other detectable polymorphs were found.

To demonstrate the reproducibility of the milling results, two batches (Milling #1 and 2) of co-milled mixtures were prepared and analyzed as freshly prepared using ^{13}C ssNMR. The results varied within 1 mole% [Table II-4], thus demonstrating the differences observed with different excipient batches could be attributed to compositional difference and not to batch variation.

Since the co-milled gabapentin/excipient mixtures were firstly prepared at the University of Iowa (UI), then shipped to the University of Hawaii at Hilo (UHH), and shipped back to UI two months later, the stability of co-milled samples during storage and shipping were determined. The temperature and humidity conditions of co-milled samples were recorded continuously by using EL-USB-2 Temperature and Humidity Data Logger recorder (DATAQ Instruments, Inc., Akron, OH) with ± 3.0 %RH accuracy. The records of temperature and humidity conditions of co-milled samples during shipping from UI to UHH (June 19-20, 2012) and UHH to UI (August 27-28, 2012) are shown in Figure II-11 and II-12. The co-milled mixtures (Milling #2) were analyzed as freshly prepared using ^{13}C ssNMR at UI. The same batch of samples was re-analyzed a week later using XRPD at UHH. Two months later, the same samples were shipped back to UI and re-analyzed using ^{13}C ssNMR. The results showed consistency and varied within 1 mole% [Table II-4]. The differences observed with different excipients could be attributed to the properties of the co-milled batches and not to stability issues.

The consistency in results obtained with either ^{13}C ssNMR or XRPD supported the ability of either method to accurately quantify polymorphic composition. For example, the results (Milling #2) obtained from both ^{13}C ssNMR and XRPD analyses varied within 1 mole%, thereby demonstrating inter-method consistency [Table II-4].

Table II- 4. The polymorphic compositions of gabapentin Form II/excipient mixtures. The analyses were conducted under ambient conditions by using ^{13}C ssNMR at the University of Iowa Central Nuclear Magnetic Resonance, and XRPD at the University of Hawaii at Hilo. The ^{13}C ssNMR analyses (A) were determined as freshly prepared. The XRPD analyses (B) were determined one week after preparation. The ^{13}C ssNMR analyses (C) were determined two months after preparation. Standard deviation values are shown parenthetically (n=3).

	^{13}C ssNMR Analyses (A)				XRPD Analyses (B)		^{13}C ssNMR Analyses (C)	
	Milling #1		Milling #2		Milling #2		Milling #2	
Excipient (50 %w/w)	Form III (mole %)	Form II (mole %)	Form III (mole %)	Form II (mole %)	Form III (mole %)	Form II (mole %)	Form III (mole %)	Form II (mole %)
SiO_2	8.4 (0.12)	90 (0.15)	8.6 (0.21)	90 (0.36)	8.7 (0.32)	90 (0.25)	8.7 (0.25)	90 (0.50)
HPC (6.5%)	33 (0.31)	65 (0.40)	33 (0.10)	66 (0.45)	34 (0.15)	65 (0.20)	33 (0.20)	66 (0.32)
starch	22 (0.50)	77 (0.40)	21 (0.56)	77 (0.67)	22 (0.21)	76 (0.21)	21 (0.45)	76 (0.35)
$CaHPO_4$	40 (0.40)	58 (0.65)	39 (0.25)	59 (0.20)	39 (0.36)	59 (0.30)	39 (0.26)	59 (0.36)

Figure II- 11. Representative record showing temperature and humidity conditions of co-milled samples during shipping from the University of Iowa to the University of Hawaii at Hilo (June 19-20, 2012). The conditions were monitored by using EL-USB-2 Temperature and Humidity Data Logger recorder (DATAQ Instruments, Inc., Akron, OH) with ± 3.0 %RH accuracy.

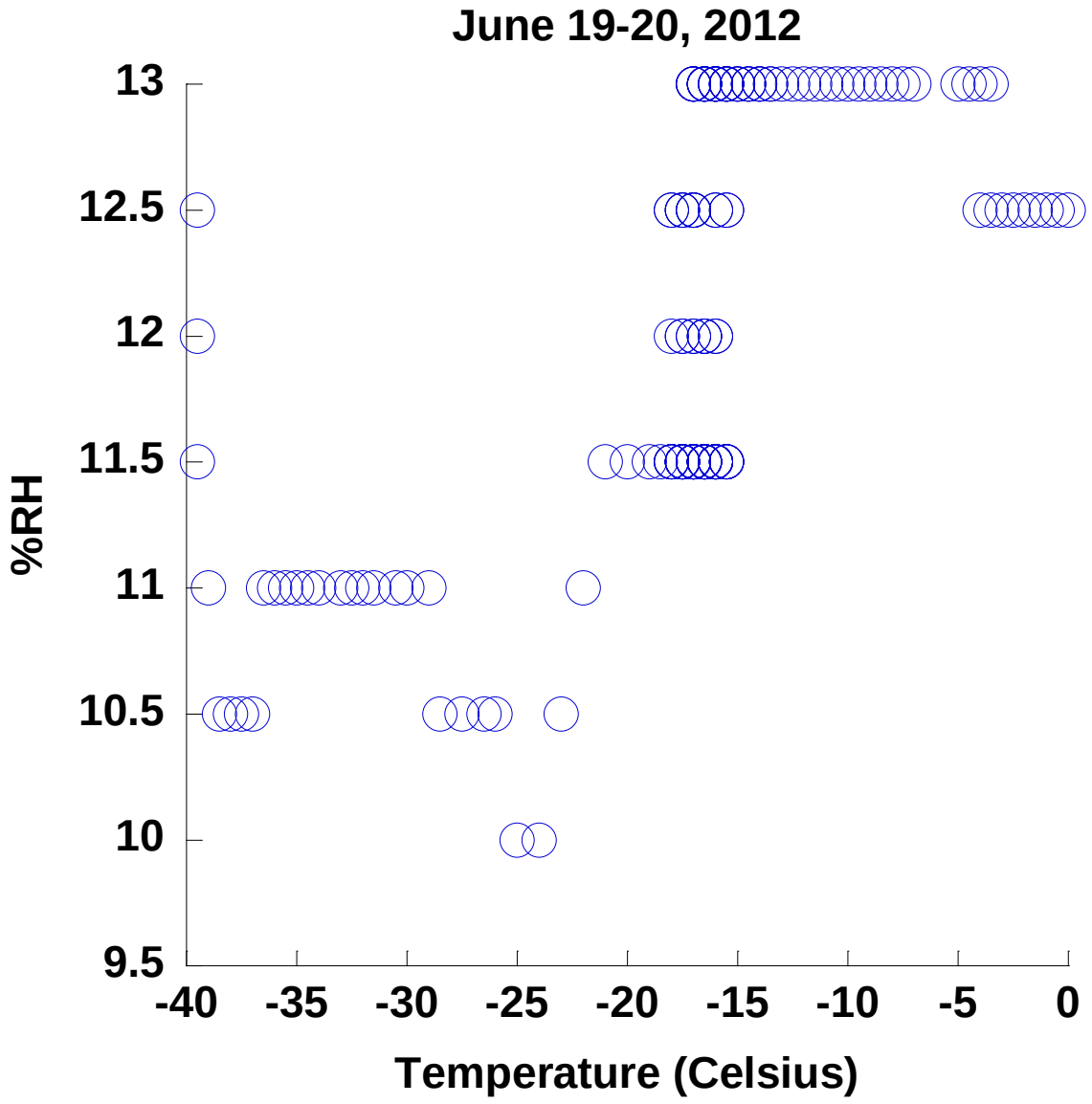

Figure II- 12. Representative record showing temperature and humidity conditions of co-milled samples during shipping from the the University of Hawaii at Hilo to the University of Iowa (August 27-28, 2012). The conditions were monitored by using EL-USB-2 Temperature and Humidity Data Logger recorder (DATAQ Instruments, Inc., Akron, OH) with ± 3.0 %RH accuracy.

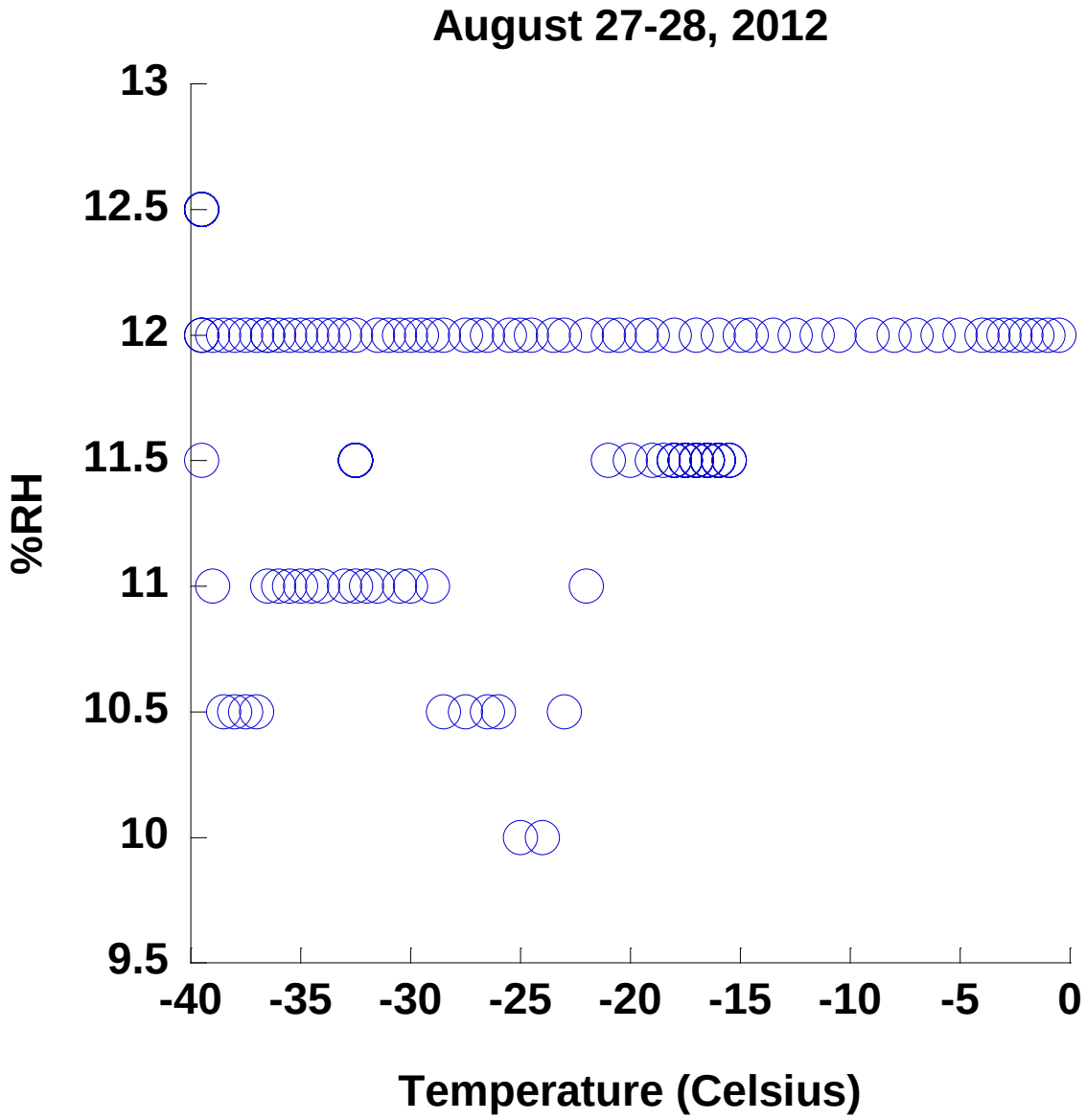

Qualitative Characteristic of Co-Milled Gabapentin/Excipient Mixtures

The excipient effects on characteristic of ^{13}C ssNMR spectra and XRPD patterns were investigated. The representative ^{13}C ssNMR spectra for the aliphatic region and XRPD patterns of co-milled samples are shown in Figure II-13 and II-14. These were well resolved from the excipient signals. Co-milled samples maintained the same crystal patterns that corresponded to gabapentin Form II and Form III; however, some peak-broadening in ^{13}C spectra were also found. The decrease in intensity of XRPD peaks was observed in co-milled excipient samples, but the diffraction profiles showed no halo pattern associated with amorphous content. ^{13}C ssNMR peak-broadening and decrease in intensity of XRPD peaks might be due to the formation of some increased levels of crystal defects. Increased chemical instability associated with milling stress in the presence of 6.5 %w/w HPC has been previously attributed to crystal disorder or defects. (11)

Figure II- 13. Representative ^{13}C ssNMR spectra for the aliphatic region of gabapentin Form II (A), co-milled gabapentin Form II with HPC (B), co-milled gabapentin Form II with $CaHPO_4$ (C), co-milled gabapentin Form II with starch (D), co-milled gabapentin Form II with SiO_2 (E), and gabapentin Form III (F). The ^{13}C ssNMR was operated under ambient conditions.

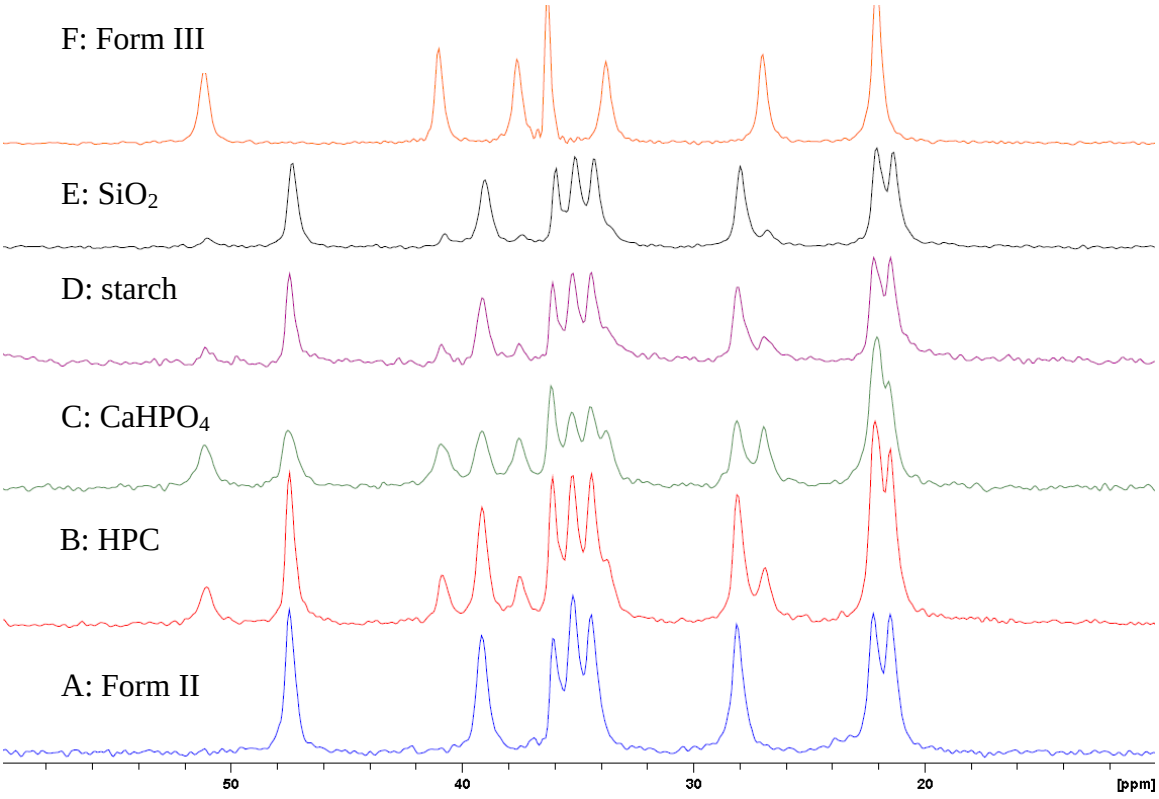

Figure II- 14. Representative overlaid XRPD patterns of gabapentin Form II, III and co-milled mixtures of gabapentin Form II with various excipients: HPC (A), starch (B), $CaHPO_4$ (C), and SiO_2 (D). The XRPD was operated under ambient conditions.

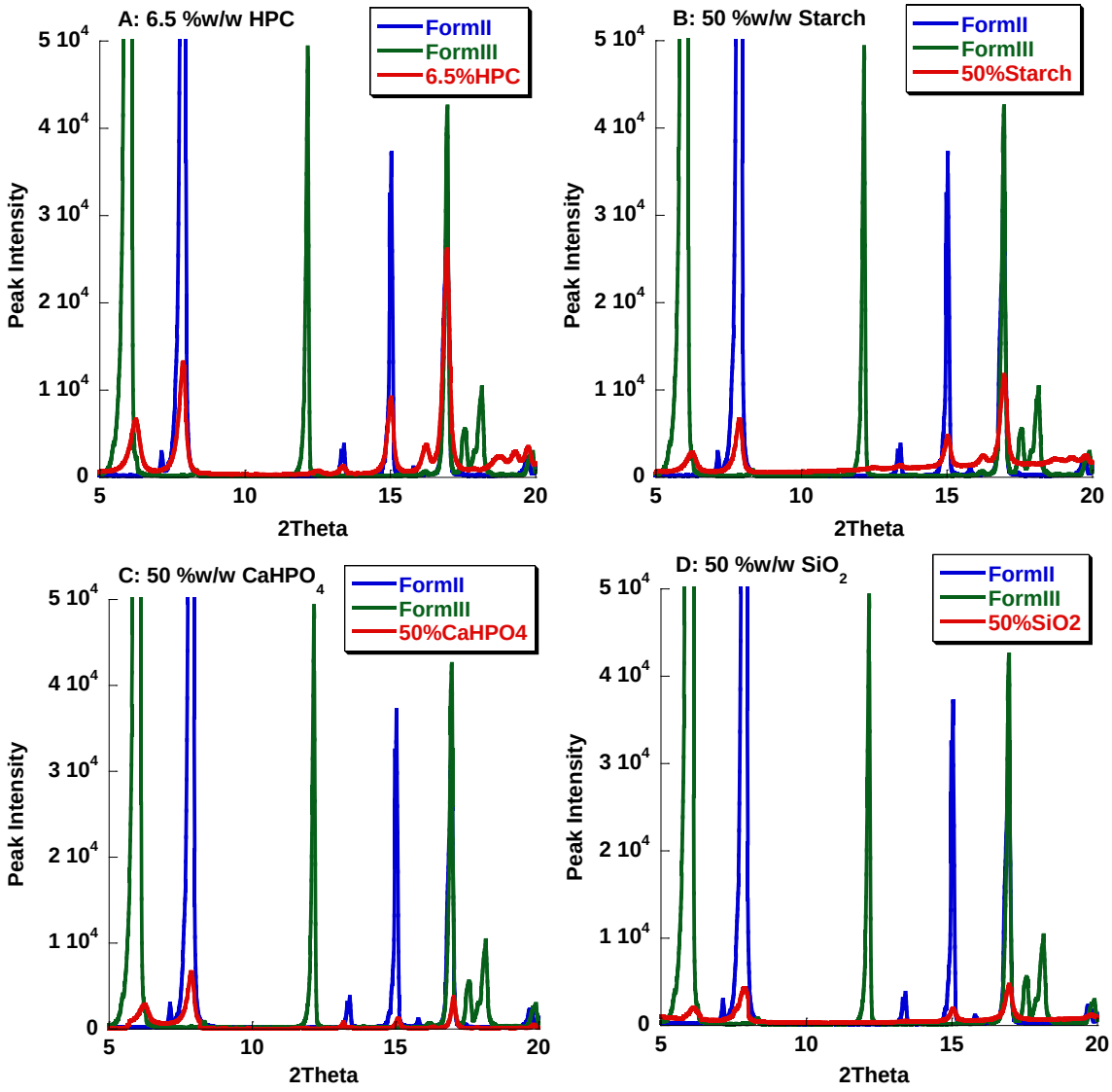

In addition to differences in the amount of gabapentin Form III generated during co-milling, the proton relaxation time in laboratory frame ($^1H\ T_1$) of each sample was varied. In the absence of excipient, no change in polymorphic transformation was observed after ball-milling gabapentin Form II for 45 minutes; however, the decrease in proton relaxation time of gabapentin Form II was observed. $^1H\ T_1$ values of un-processed gabapentin Form II and III were reported to be 134 and 63 s, respectively. After ball-milling gabapentin Form II, $^1H\ T_1$ value reduced to 41 s. This value was noticeably shorter than that observed in un-processed gabapentin Form II. (11) This decrease in proton relaxation time could be due to the particle size reduction as well as the generation of crystal defects and decrease in long-range order. (44) In the presence of excipient, all co-milled gabapentin Form II/excipient mixtures had shorter proton relaxation time than that observed in the neat gabapentin Form II milled for 45 minutes. $^1H\ T_1$ values of gabapentin Form II co-milled with HPC, starch, $CaHPO_4$, and SiO_2 for 60 minutes were found to be 7.6, 3, 1.5, and 0.6 s, respectively. Similar $^1H\ T_1$ value was reported to be 11 s when co-milling gabapentin Form II with 6.5 %w/w HPC for 45 minutes. (11) When cryo-milling aspirin with 50 %w/w starch 1500 for 30 minutes, a similar result has been reported. The relaxation time of cryo-ground aspirin/starch 1500 was shortened from 14 s (neat aspirin cryo-ground for 60 minutes) to 7.6 s. Cryo-grinding with starch 1500 could create more high energy sites as a result of reducing crystal integrity and increasing mobility in the lattice, thereby causing the reduction of overall proton relaxation time for the entire mixture. (44-46)

Conclusion

^{13}C ssNMR and XRPD provided unique peaks for each polymorphic forms of gabapentin Form II and III. No excipient peak interference occurred. Both techniques were capable of measuring polymorphic composition in synthetic mixtures and gabapentin Form II/excipient mixtures with reasonable accuracy. The application of those techniques to quantify excipient effects on polymorphic transformation kinetics of gabapentin are discussed in Chapter IV.

Chapter II References

1. Brittain HG. Polymorphism in Pharmaceutical Solids. New York: Informa Healthcare; 2009. p. 1-3.
2. Guidance for Industry, ANDAs: Pharmaceutical Solid Polymorphism Chemistry, Manufacturing, and Controls Information. Food and Drug Administration: Silver Spring; 2007.
3. Byrn S, Pfeiffer R, Ganey M, Hoiberg C, Poochikian G. Pharmaceutical Solids: A Strategic Approach to Regulatory Considerations. Pharmaceutical Research. 1995;12(7):945-954.
4. Aitipamula S, Banerjee R, Bansal AK, Biradha K, Cheney ML, Choudhury AR, Desiraju GR, Dikundwar AG, Dubey R, Duggirala N, Ghogale PP, Ghosh S, Goswami PK, Goud NR, Jetti RRKR, Karpinski P, Kaushik P, Kumar D, Kumar V, Moulton B, Mukherjee A, Mukherjee G, Myerson AS, Puri V, Ramanan A, Rajamannar T, Reddy CM, Rodriguez-Hornedo N, Rogers RD, Row TNG, Sanphui P, Shan N, Shete G, Singh A, Sun CC, Swift JA, Thaimattam R, Thakur TS, Kumar Thaper R, Thomas SP, Tothadi S, Vangala VR, Variankaval N, Vishweshwar P, Weyna DR, Zaworotko MJ. Polymorphs, Salts, and Cocrystals: What's in a Name? Crystal Growth & Design. 2012;12(5):2147-2152.
5. Pharmacopeia US. The United States Pharmacopeia, USP 30. The National Formulary, NF 25: Official from May 1, 2007. United States Pharmacopeial Convention, Inc.; 2007.
6. Braga D, Grepioni F, Maini L, Rubini K, Polito M, Brescello R, Cotarca L, Duarte MT, Andre V, Piedade MFM. Polymorphic gabapentin: thermal behaviour, reactivity and interconversion of forms in solution and solid-state. New Journal of Chemistry. 2008;32(10):1788-1795.
7. Ibers J. Gabapentin and gabapentin monohydrate. Acta Crystallographica Section C. 2001;57(5):641-643.
8. Reece HA, Levendis DC. Polymorphs of gabapentin. Acta Crystallographica Section C. 2008;64(3):o105-o108.
9. Vasudev PG, Aravinda S, Ananda K, Veena SD, Nagarajan K, Shamala N, Balaram P. Crystal Structures of a New Polymorphic Form of Gabapentin

Monohydrate and the E and Z Isomers of 4-Tertiarybutylgabapentin. Chemical Biology & Drug Design. 2009;73(1):83-96.
10. Delaney SP, Smith TM, Korter TM. Conformation versus cohesion in the relative stabilities of gabapentin polymorphs. Royal Society of Chemistry Advances. 2014;4(2):855-864.
11. Dempah K, Barich D, Kaushal A, Zong Z, Desai S, Suryanarayanan R, Kirsch L, Munson E. Investigating Gabapentin Polymorphism Using Solid-State NMR Spectroscopy. AAPS PharmSciTech. 2013;14(1):19-28.
12. Lin S-Y, Hsu C-H, Ke W-T. Solid-state transformation of different gabapentin polymorphs upon milling and co-milling. International Journal of Pharmaceutics. 2010;396(1–2):83-90.
13. Byrn SR, Pfeiffer RR, Stowell JG. Solid State Chemistry of Drugs. West Lafayette; 1999. p. 3.
14. Shah B, Kakumanu VK, Bansal AK. Analytical techniques for quantification of amorphous/crystalline phases in pharmaceutical solids. Journal of Pharmaceutical Sciences. 2006;95(8):1641-1665.
15. Hsu C-H, Ke W-T, Lin S-Y. Progressive steps of polymorphic transformation of gabapentin polymorphs studied by hot-stage FTIR microspectroscopy. Journal of Pharmacy and Pharmaceutical Sciences. 2010;13(1):67-77.
16. VanderHart DL. Magnetic Susceptibility and High Resolution NMR of Liquids and Solids. Encyclopedia of Magnetic Resonance: John Wiley & Sons, Ltd; 2007.
17. Geppi M, Mollica G, Borsacchi S, Veracini CA. Solid-State NMR Studies of Pharmaceutical Systems. Applied Spectroscopy Reviews. 2008;43(3):202-302.
18. Suryanarayanan R, Wiedmann TS. Quantitation of the Relative Amounts of Anhydrous Carbamazepine ($C_{15}H_{12}N_2O$) and Carbamazepine Dihydrate ($C_{15}H_{12}N_2O.2H_2O$) in a Mixture by Solid-State Nuclear Magnetic Resonance (NMR). Pharmaceutical Research. 1990;7(2):184-187.
19. Gao P. Determination of the Composition of Delavirdine Mesylate Polymorph and Pseudopolymorph Mixtures Using 13C CP/MAS NMR. Pharmaceutical Research. 1996;13(7):1095-1104.
20. Saindon PJ, Cauchon NS, Sutton PA, Chang Cj, Peck GE, Byrn SR. Solid-State Nuclear Magnetic Resonance (NMR) Spectra of Pharmaceutical Dosage Forms. Pharmaceutical Research. 1993;10(2):197-203.
21. Sotthivirat S, Lubach JW, Haslam JL, Munson EJ, Stella VJ. Characterization of prednisolone in controlled porosity osmotic pump pellets using solid-state NMR spectroscopy. Journal of Pharmaceutical Sciences. 2007;96(5):1008-1017.
22. Zong Z, Desai S, Kaushal A, Barich D, Huang H-S, Munson E, Suryanarayanan R, Kirsch L. The Stabilizing Effect of Moisture on the Solid-State Degradation of Gabapentin. AAPS PharmSciTech. 2011;12(3):924-931.
23. Barich DH, Davis JM, Schieber LJ, Zell MT, Munson EJ. Investigation of solid-state NMR line widths of ibuprofen in drug formulations. Journal of Pharmaceutical Sciences. 2006;95(7):1586-1594.
24. Wildfong PLD, Morley NA, Moore MD, Morris KR. Quantitative determination of polymorphic composition in intact compacts by parallel-beam X-ray powder diffractometry II: Data correction for analysis of phase transformations as a

function of pressure. Journal of Pharmaceutical and Biomedical Analysis. 2005;39(1–2):1-7.
25. Cao W, Bates S, Peck GE, Wildfong PLD, Qiu Z, Morris KR. Quantitative determination of polymorphic composition in intact compacts by parallel-beam X-ray powder diffractometry. Journal of Pharmaceutical and Biomedical Analysis. 2002;30(4):1111-1119.
26. Dong Z, Padden BE, Salsbury JS, Munson EJ, Schroeder SA, Prakash I, Grant DJW. Neotame Anhydrate Polymorphs I: Preparation and Characterization. Pharmaceutical Research. 2002;19(3):330-336.
27. Dong Z, Munson E, Schroeder S, Prakash I, Grant D. Neotame Anhydrate Polymorphs II: Quantitation and Relative Physical Stability. Pharmaceutical Research. 2002;19(9):1259-1264.
28. Tiwari M, Chawla G, Bansal AK. Quantification of olanzapine polymorphs using powder X-ray diffraction technique. Journal of Pharmaceutical and Biomedical Analysis. 2007;43(3):865-872.
29. Chen X, Bates S, Morris KR. Quantifying amorphous content of lactose using parallel beam X-ray powder diffraction and whole pattern fitting. Journal of Pharmaceutical and Biomedical Analysis. 2001;26(1):63-72.
30. Chen X, Stowell JG, Morris KR, Byrn SR. Quantitative study of solid-state acid–base reactions between polymorphs of flufenamic acid and magnesium oxide using X-ray powder diffraction. Journal of Pharmaceutical and Biomedical Analysis. 2010;51(4):866-874.
31. Bates S, Zografi G, Engers D, Morris K, Crowley K, Newman A. Analysis of Amorphous and Nanocrystalline Solids from Their X-Ray Diffraction Patterns. Pharmaceutical Research. 2006;23(10):2333-2349.
32. Padden BE, Zell MT, Dong Z, Schroeder SA, Grant DJW, Munson EJ. Comparison of Solid-State 13C NMR Spectroscopy and Powder X-ray Diffraction for Analyzing Mixtures of Polymorphs of Neotame. Analytical Chemistry. 1999;71(16):3325-3331.
33. Mehring M. Principles of High Resolution NMR in Solids. New York: Springer-Verlag; 1983. p. 129-185 (Chapter 124).
34. Alemany LB, Grant DM, Pugmire RJ, Alger TD, Zilm KW. Cross polarization and magic angle sample spinning NMR spectra of model organic compounds. 1. Highly protonated molecules. Journal of the American Chemical Society. 1983;105(8):2133-2141.
35. Knicker H. Solid state CPMAS 13C and 15N NMR spectroscopy in organic geochemistry and how spin dynamics can either aggravate or improve spectra interpretation. Organic Geochemistry. 2011;42(8):867-890.
36. Virtanen T, Maunu SL. Quantitation of a polymorphic mixture of an active pharmaceutical ingredient with solid state 13C CPMAS NMR spectroscopy. International Journal of Pharmaceutics. 2010;394(1–2):18-25.
37. Sanchez S, Ziarelli F, Viel S, Delaurent C, Caldarelli S. Improved solid-state NMR quantifications of active principles in pharmaceutical formulations. Journal of Pharmaceutical and Biomedical Analysis. 2008;47(4–5):683-687.
38. Offerdahl TJ, Salsbury JS, Dong Z, Grant DJW, Schroeder SA, Prakash I, Gorman EM, Barich DH, Munson EJ. Quantitation of crystalline and amorphous

forms of anhydrous neotame using 13C CPMAS NMR spectroscopy. Journal of Pharmaceutical Sciences. 2005;94(12):2591-2605.
39. International Conference on Harmonization (ICH) Harmonized Tripartite Guideline, Notes for Guidance On Validation of Analytical Procedures: Methodology. CPMP/ICH/281/95. 1996.
40. Tishmack PA, Bugay DE, Byrn SR. Solid-state nuclear magnetic resonance spectroscopy—pharmaceutical applications. Journal of Pharmaceutical Sciences. 2003;92(3):441-474.
41. Knicker H, Totsche KU, Almendros G, Gonzalez-Vila FJ. Condensation degree of burnt peat and plant residues and the reliability of solid-state VACP MAS 13C NMR spectra obtained from pyrogenic humic material. Organic Geochemistry. 2005;36(10):1359-1377.
42. Gaou P. Characterization of Three Crystalline Forms (VIII, XI, and XII) and the Amorphous Form (V) of Delavirdine Mesylate Using 13C CP/MAS NMR. Pharmaceutical Research. 1998;15(9):1425-1433.
43. Smernik RJ, Oades JM. The use of spin counting for determining quantitation in solid state 13C NMR spectra of natural organic matter 1. Model systems and the effects of paramagnetic impurities. Geoderma. 2000;96(1-2):101-129.
44. Lubach JW, Xu D, Segmuller BE, Munson EJ. Investigation of the effects of pharmaceutical processing upon solid-state NMR relaxation times and implications to solid-state formulation stability. Journal of Pharmaceutical Sciences. 2007;96(4):777-787.
45. Lubach JW. Applications of nuclear magnetic resonance spectroscopy to pharmaceutical solids. Ann Arbor: University of Kansas; 2007. p. 376.
46. Nishiyama Y, Frey MH, Mukasa S, Utsumi H. 13C solid-state NMR chromatography by magic angle spinning 1H T1 relaxation ordered spectroscopy. Journal of Magnetic Resonance. 2010;202(2):135-139.

CHAPTER III

THE TEMPERATURE AND MOISTURE STABILIZING EFFECTS ON SOLID-STATE DEGRADATION OF GABAPENTIN/EXCIPIENT MIXTURES

Introduction

Gabapentin is a ɣ-aminobutyric acid used for the treatment of epilepsy and neuropathic pain. In aqueous solution, gabapentin can exist as cationic, anionic, zwitterionic, and neutral species. The carboxylate and amine pKa have been reported to be 3.7 and 9.4, respectively. At elevated temperatures, gabapentin chemically undergoes degradation by intramolecular cyclization to gabapentin-lactam (lactam) [Figure III-1]. (1) Unlike gabapentin, lactam has shown a neuro-protective activity and effect on neural dendrites. (2, 3) Lactam (10-50 mg/kg) caused convulsion activities including myoclonic twitches and generalized clonic seizures in animal models. (4) An oral LD_{50} of lactam in mice and rats (300 mg/kg and 200-500 mg/kg) is an order of magnitude lower than gabapentin (8000 mg/kg). (5) The United States Pharmacopeia limit for lactam in gabapentin is 0.4%. (6) In solution, lactamization is pH-dependent with minimum rate at 5.5-6.2 and is buffer catalyzed. The Arrhenius activation energy for lactamization in solution (pH 6) was estimated to be 140-160 kJ/mol. (7)

Figure III- 1. Lactamization scheme for gabapentin. (1)

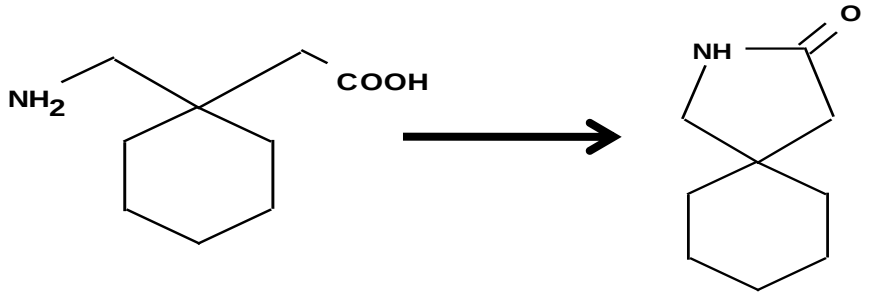

Gabapentin **Gabapentin-lactam (Lactam)**

In the solid state, gabapentin exists as a zwitterion and as different polymorphs, including a monohydrate (Form I) and three anhydrous polymorphs: Form II, III and IV. The packing efficiencies of Form II, III, and IV are 71.3, 70.5, and 68.7 %, respectively. The most efficiently packed form is Form II which is the thermodynamically most stable form. (8, 9) The thermal-induced lactamization of gabapentin in solid state has been reported. (10, 11)

The effect of milling on the chemical transformation of gabapentin Form II has been reported. Milled samples remained crystalline, but decreases in the intensity of X-ray powder diffraction peaks were observed. No other polymorphic forms were present. Milling significantly increased lactam concentrations from 0.007 mole% (un-milled) to 0.23 mole%. (12)

The relationship between specific surface area and initial lactamization rate of un-milled and milled gabapentin was investigated. Aliquots of un-milled and milled gabapentin were divided into different sized particles using sieve fractions and then thermally stressed to induce lactamization at 50 ºC and 5 %RH. For sieved fractions of un-milled samples, the specific surface area varied from 0.1-0.9 m^2/g and the rate increased 2-fold after thermal stress. For sieved fractions of 10-minute milled samples, the specific surface area varied within the range between 4.2-5.4 m^2/g, while the rates remained unchanged. These results were compared to milled samples for different durations without sieving and subsequently subjected to thermal stress (50 ºC and 5 %RH). The lactamization rates of milled samples without sieving increased as a function of specific surface area. The increased rates for the samples generated by varying the durations of milling were much greater than the samples separated by sieving. These

results suggested that the increase in lactamization rate could not be explained solely by increasing specific surface area but were due to the combination effects of changes in specific surface area, initial crystal defects, and initial lactam concentration. (12)

The effect of cyclodextrin on lactamization rate of gabapentin in aqueous solution has been reported. The lactamization rate was catalyzed by α-, γ-, β-, and hydroxyl propyl-β-cyclodextrins in the pH range of 5.9-7.1. Michaelis-Menten-type kinetic was used to estimate the rate of gabapentin-cyclodextrin complex formation. The lactamization rate of complexed gabapentin was higher than un-complexed drug, and the rate was dependent on type of cyclodextrin. (13)

The effect of co-milling in the absence and presence of various excipients on chemical and polymorphic transformations of gabapentin Form II was qualitatively investigated using Fourier transform infrared spectroscopy (FTIR). In the absence of excipient, the FTIR bands associated with lactam and Form III were observed after milling gabapentin for 105 minutes. In the presence of excipient, the lactam and polymorphic transformations after co-milling for 2 hours varied depending upon excipient type. For example, neither lactam nor polymorphic transformation was observed when co-milled with 50 %w/w dicalcium phosphate dihydrate or corn starch. However, the FTIR bands that corresponded to lactam and Form IV were found when co-milled with 50 %w/w colloidal silicon dioxide or talc. (14)

The effect of milling in the presence and absence of 6.5 %w/w HPC on chemical and polymorphic transformations of gabapentin Form II was studied using high performance liquid chromatography and ^{13}C solid state nuclear magnetic resonance spectroscopy. No polymorphic transformation was observed when gabapentin was milled

without excipient, whereas partial transformation to Form III was observed when gabapentin (Form II) was co-milled with HPC. Additionally, significant increases in lactam formation (4-fold) were observed in the mixtures containing HPC. (15)

The lactamization kinetics of freeze-dried gabapentin Form II with various excipients were studied under storage conditions at 50 ºC and different relative humidity levels (0, 45 and 75 %RH). The physical state change of lyophilized samples was investigated as freshly prepared and after storage for 4 weeks using differential scanning calorimetry. As prepared, the physical state of lyophilized samples with hydroxypropyl-β-cyclodextrin (HP-β-CD), sulfobutylether-β-cyclodextrin sodium salt (SBE-β-CD), and polyvinylpyrrolidone (PVP)-K30 was amorphous. However, the physical state of lyophilized samples with lactose, raffinose, trehalose, and mannitol remained crystalline. No physical state change was observed in any samples after conditions of storage. Zero-order kinetics was used to describe the apparent rates of lactamization. The rates varied depending upon excipient type and storage conditions. The highest rate was observed in sample containing HP-β-CD. The lactamization rates of samples containing raffinose, trehalose and mannitol decreased with increased humidity, whereas the opposite effects were observed in samples containing HP-β-CD, SBE-β-CD, PVP-K30 and lactose. (16)

Although excipients are known to affect gabapentin instability, the systematic quantification of excipient effects on both chemical and physical instability of gabapentin has not been reported. Additionally, few detailed studies on the quantitation of environmental and compositional effects on drug instability have been published. (17-21) Therefore, the overall objective of this research is to build a kinetic model that can quantitatively describe the environmental and excipient effects on chemical and physical

instability associated with milling induced stress and subsequent storage under controlled temperature and humidity conditions using gabapentin as a model compound. The chemical transformation of gabapentin during milling and subsequent storage is presented in this chapter. The polymorphic transformation of gabapentin during milling and subsequent storage is presented in the next chapter. Kinetic models that describe the environmental and excipient effects on chemical and physical transformations of gabapentin are presented in the last chapter.

Material and Methods

Gabapentin Form II was obtained from Hangzhou Starshine Pharmaceutical Co., Ltd. (Hangzhou, China). Seven excipients, including colloidal silicon dioxide (SiO_2, CAB-O-SIL® TS-530, Billerica, MA), hydroxy propyl cellulose (HPC, given by FDA, FDA-sponsored contract number HHSF2232008199292C), pregelatinized corn starch (starch, UNI-PURE™ DW, Bridgewater, NJ), dibasic calcium phosphate dihydrate ($CaHPO_4$, Emcompress®, Patterson, NY), microcrystalline cellulose (MCC, Avicel® PH-101, FMC BioPolymer, PA), hydroxypropyl methylcellulose (HPMC, Methocel™ E50 PRM LV, Dow Chemical Company, MI), and hydrous magnesium silicate (talc, City Chemical LLC, CT) were used as received. Those excipients were chosen based on the preliminary studies of excipient effects on chemical and physical transformations of gabapentin Form II during co-milling. (14, 15)

Milling Stress

The effect of co-milling gabapentin Form II in the presence of excipients was studied by placing a two gram aliquots of 6.5 or 50 %w/w mixture gabapentin Form II/excipient (SiO_2, HPC, starch, $CaHPO_4$, MCC, HPMC, and talc) into a 45 ml milling

chamber with four stainless steel balls (25 mm) and milling in a planetary mill (Pulviserette7, Planetary Micro Mill, FRITSCH GmbH, Idar-Oberstein, Germany) for 60 minutes with speed setting 7. At this speed, the motor and grinding bowl speeds were 2400 and 1000 rpm, respectively. All milling operations were conducted at ambient conditions.

High Performance Liquid Chromatographic Methods (HPLC)

HPLC method was adapted from previously reported studies. (12, 22) The analysis was conducted using a Thermo Separations HPLC consisting of a P4000 Quaternary pump (Fisher Scientific, Pittsburg, PA), UV 6000LP diode array detector, AS 3000 auto injector, and an online degasser. Data was analyzed using Chromquest, version 4.0, software. Separation was carried out on a µBondapak Cyano (3.9x30 cm, 10µm) column (Water Corp. Milford, MA). Isocratic analysis was conducted using mobile phase (5% Acetonitrile: 95% 10mM KH_2PO_4/10 mM K_2HPO_4) at a flow rate of 1 ml/min. The mobile phase was filtered through 0.2 µm nylon filter before using. The effluent was monitored at 210 nm, and the run time was 12 minutes. All components of the system were maintained at room temperature and the injection volume was 20 µl. A representative chromatogram of aliquots of co-milled gabapentin Form II with 6.5 % w/w HPC stored at 50 ˚C and 30 %RH for 335 hours is shown in Figure III-2. The retention time of gabapentin and lactam was 4.1 and 7.6 minutes, respectively. Gabapentin and lactam peaks in all chromatograms were well resolved, and no interference from the excipients was observed. Mass balance was 100 % (±2%) of the initial amounts of gabapentin and lactam. Calibration plots for gabapentin and lactam were linear at the range of 0.4-10 mg/ml and 0.008-1 mg/ml, respectively [Figure III-3]. The method was

capable of measuring lactam concentrations with limit of quantitation at 0.5 µg/ml. (12) Duplicate runs were used for each sample and random injection schemes were used to avoid assay sequence effect.

Figure III- 2. Representative HPLC chromatogram showing peaks of gabapentin and lactam found in aliquots of 60 minutes co-milled gabapentin Form II with 6.5 %w/w HPC stored at 50 ˚C and 30 %RH for 335 hours.

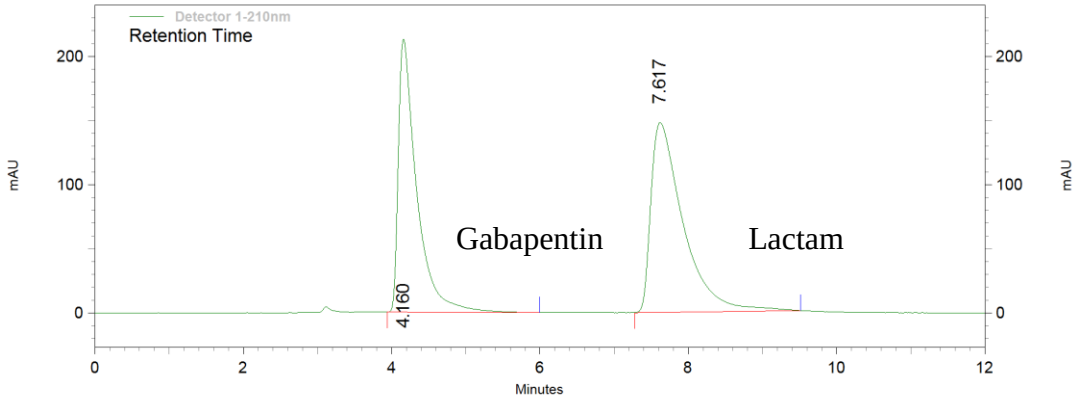

Figure III- 3. Representative calibration plots of gabapentin and lactam. Samples of gabapentin and lactam were prepared using aqueous solution in concentration ranges of 0.4-10 mg/ml and 0.008-1.0 mg/ml (8-1,000 µg/ml), respectively.

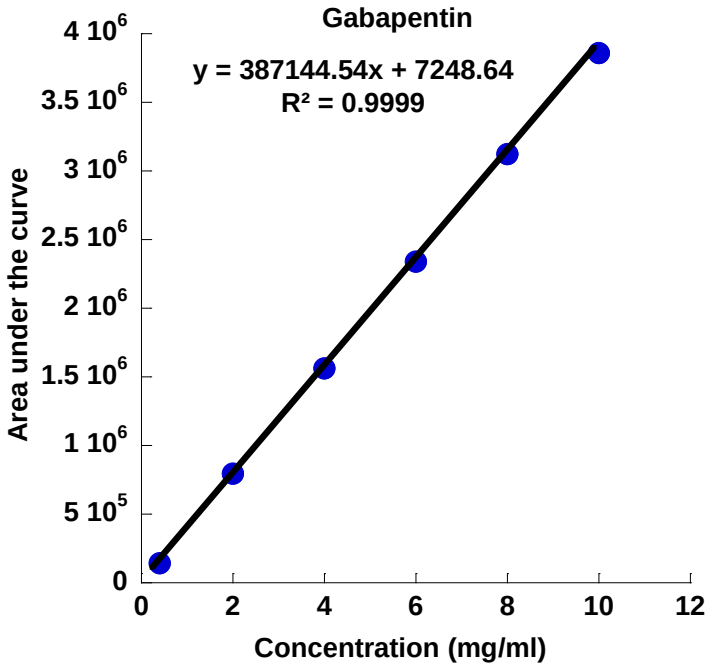

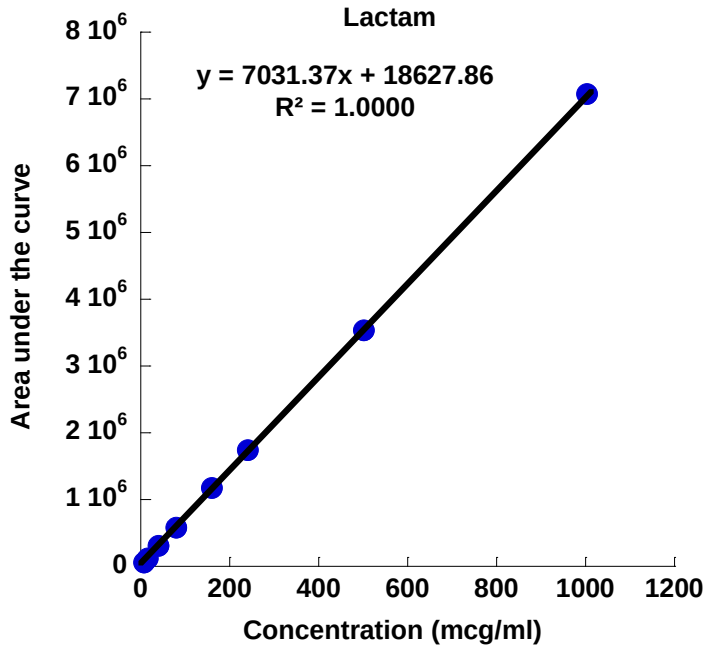

Solid State Degradation Studies

As previously reported in Chapter II, reaction mixture samples containing $CaHPO_4$ and HPC required a special reaction quenching procedure prior to ^{13}C ssNMR analysis to measure polymorphic kinetics. The following study was conducted to determine the stability of reaction mixture samples with respect to covalent changes prior to HPLC analysis. In this experiment, 10 mg reaction mixture samples (containing gabapentin and each of the four excipients) were placed in a 20 ml Type II scintillation glass vial and then stored in desiccators containing anhydrous calcium sulfate (Drierite®) (5 %RH), LiCl (11 %RH), $MgCl_2$ (30 %RH), and $Mg(NO_3)_2$ (50 %RH) at various thermal conditions: 40, 50, and 60 ˚C. Drierite® was used as received to prepare a controlled 5 %RH chamber. For other controlled humidity chambers, saturated salt solutions of LiCl, $MgCl_2$, and $Mg(NO_3)_2$ were prepared by dissolving each salt in Nanopure water with equilibration under controlled temperature ovens for 24 hours prior experiment. The humidity was measured by using an EL-USB-2 Temperature and Humidity Data Logger recorder (DATAQ Instruments, Inc., Akron, OH) with ± 3.0 %RH accuracy. The humidity chambers were measured to be 5, 12, 32, and 48 %RH (40 ºC), 5, 11, 29, 47.5 %RH (50 ºC), and 5, 10, 27, 44 %RH (60 ºC), respectively.

Reaction mixture aliquots were periodically removed from the reaction chambers (0, 24, 48, 96, 144, 240, 336, 386, 434, and 576 hours), and either assayed immediately or placed in a storage chamber containing Drierite® desiccant and maintained at -80 °C for 24 hours prior subjecting to HPLC analysis.

Samples were prepared for HPLC analysis by suspending them in 1 mL of water, mixing briefly using a Vortex® mixer and then filtering through a 0.45 μm nylon filter. HPLC analysis was carried out as described previously.

The lactam concentration time profiles were indistinguishable for both the samples stored at dry/sub-ambient conditions (Treatment) and those immediately prepared for HPLC analysis (No treatment). Representative lactamization profiles of excipient mixtures stored at 50 ºC/47.5 %RH are presented in Figure III-4 (A-D). These results demonstrated that the quenching procedure used for measuring polymorphic kinetics with ^{13}C ssNMR analysis were not necessary for measuring covalent transition kinetics by HPLC.

Figure III- 4. Lactamization profiles of co-milled gabapentin Form II with SiO_2 (A), $CaHPO_4$ (B), starch (C) and HPC (D) stored at 50 ºC and 47.5 %RH.

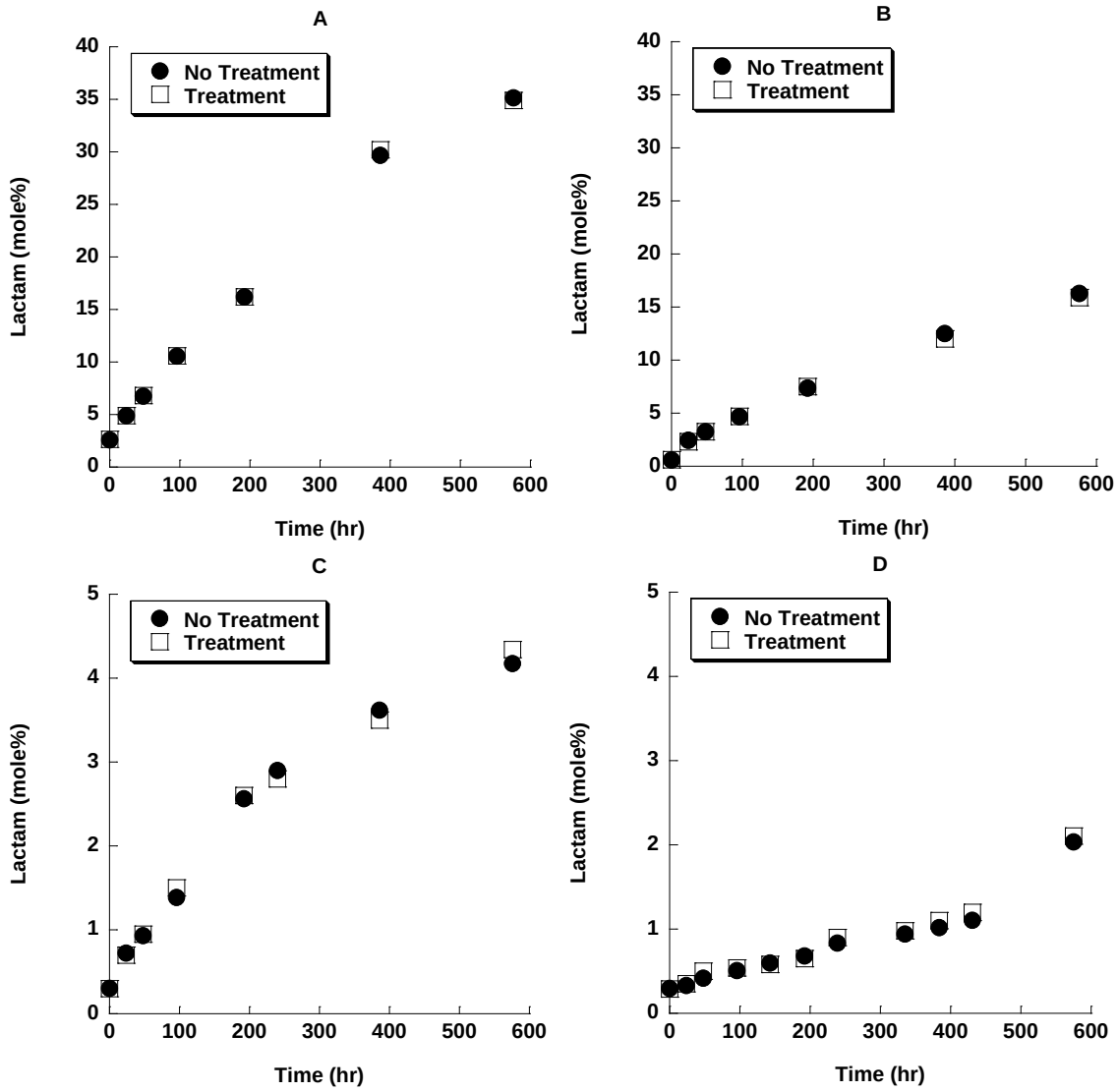

Results and Discussion

Lactam Formation of Co-Milled Gabapentin during Milling

The effects of inorganic (SiO_2, $CaHPO_4$, and talc) and organic (starch, MCC, HPMC and HPC) excipients on covalent transformation of gabapentin were determined by measuring lactam concentrations during milling [Table III-1]. In the absence of excipients, the concentration of lactam in milled sample was found to be 0.24 mole %. Lactam concentrations in co-milled excipient mixtures were varied depending upon excipient type. In the presence of inorganic excipients, the concentrations of lactam increased 3-fold for $CaHPO_4$, 4-fold for talc, and 11-fold for SiO_2. However, the lactam concentrations in co-milled mixtures containing organic excipients were in the same range (0.27-0.32 mole %) as the milled sample without excipient (0.24 mole %).

To demonstrate the reproducibility of the milling results, three batches (Milling #1, 2, and 3) of co-milled gabapentin/excipient mixtures were prepared and freshly analyzed using HPLC [Table III-1]. The resulting lactam formation varied within the range of 0.008-0.1 mole %, thereby demonstrating that the differences observed between different excipients could be attributed to compositional differences and not to batch variation.

Table III- 1. The effect of excipients on lactamization in three different batches of co-milled gabapentin Form II/excipient mixtures.

Excipient (50 %w/w)	Initial Lactam (mole %)			Mean	SD (n=3)
	Milling #1	Milling #2	Milling #3		
None	0.250	0.230	0.240	0.240	0.010
HPC (6.5%)	0.290	0.258	0.269	0.272	0.016
MCC	0.281	0.272	0.294	0.282	0.011
Starch	0.305	0.315	0.285	0.302	0.015
HPMC	0.322	0.310	0.329	0.320	0.010
$CaHPO_4$	0.605	0.610	0.587	0.601	0.012
Talc	0.925	0.931	0.940	0.932	0.008
SiO_2	2.60	2.49	2.69	2.59	0.100

The effects of low and high levels of excipient compositions (6.5 and 50 %w/w) on covalent transformation of gabapentin were determined by measuring lactam concentration during milling [Table III-2]. The representative inorganic (SiO_2 and $CaHPO_4$) and organic (starch and HPC) excipients were chosen. Generally, the lactam concentrations in samples containing high levels of excipients were greater than at low level of excipients. However, the opposite effect was observed when substrate was co-milled with HPC [Table III-2].

The effects of co-milled excipients on substrate degradation were not the focus of our investigations; rather the effects of excipients on the subsequent physical and chemical transitions during storage were the primary subject of our studies. Nonetheless, we can speculate the co-milled excipients are likely to have a variety of effects on in-process gabapentin degradation including potential catalysis, alteration in heat transfer during mixing, inducement of crystal defects and surface area generation. The complexity of excipient-substrate interactions during milling has been the subject of some reported studies. (20, 23)

The susceptibility of co-milled gabapentin/excipient mixtures to further lactamization was investigated by measuring the initial lactamization rate of mixture aliquots at 50 °C/50 %RH for 24 hours [Table III-2]. In the absence of excipients, the rate was found to be 0.42 mole%/day. Generally, the susceptibility to further lactamization was greater in the samples containing high levels of excipients than those with low levels of excipients. However, the opposite effect was observed when co-milled with HPC. Among excipients, the highest susceptibility to further lactamization was observed for SiO_2 mixtures.

Table III- 2. The effect of excipient compositions on lactamization of co-milled gabapentin Form II/excipient mixtures.

Excipient	%w/w	Initial Lactam (mole %)	Lactamization rate at 50 ºC/5%RH (mole%/day)
None	0	0.240	0.420
HPC	6.5	0.272	2.42
	50	0.060	0.999
Starch	6.5	0.185	0.542
	50	0.302	1.48
$CaHPO_4$	6.5	0.327	0.178
	50	0.601	4.18
SiO_2	6.5	0.456	0.632
	50	2.59	7.40

Lactamization Kinetic Profiles

For reaction mixtures stored for 24 days, a sigmoid-shaped degradation product concentration-time profile was typically observed. This profile is explained by a kinetic model that relates the growth of the degradation product to an autocatalytic crystallization model. (24) A typical lactamization kinetic profile of milled gabapentin Form II stored under 40 ºC/5 %RH has been previously observed to follow the sigmoid-shaped kinetic profile which can be described in two stages [Figure III-5]. Initially, the lactamization rate was due to the rapid conversion of structurally-disordered crystals caused by milling. Toward the completion of disordered crystal conversion to lactam, the lactamization rate decreased and then increased according to autocatalytic degradation involving disorder propagation and chemical conversion to lactam. (25, 26)

Figure III- 5. Typical lactamization profile of milled gabapentin Form II stored at 40 ºC and 5 %RH. (26)

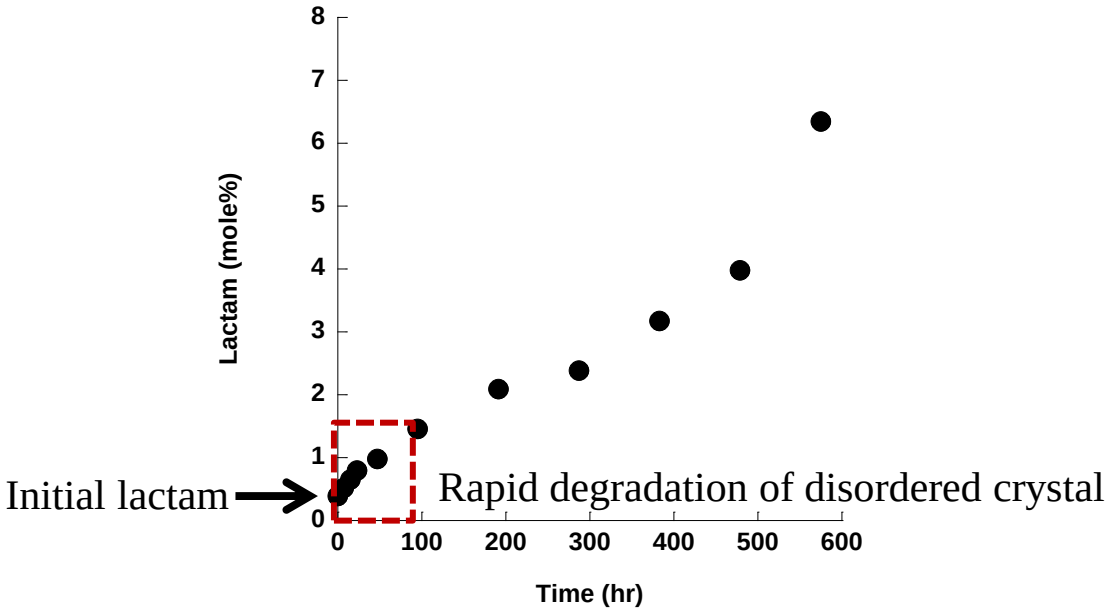

The representative lactamization kinetic profiles of co-milled gabapentin/ excipient mixtures stored at 40 ºC/5 %RH are presented in Figure III-6 (A-D). The profile of mixtures containing SiO_2 [Figure III-6A] noticeably followed the sigmoid-shaped behavior; however the sigmoid appearance was less noticeable in other excipient mixtures [Figure III-6 (B-D)].

Figure III- 6. Lactamization profiles of co-milled gabapentin Form II with SiO_2 (A), $CaHPO_4$ (B), starch (C) and HPC (D) stored at 40 ºC and 5 %RH.

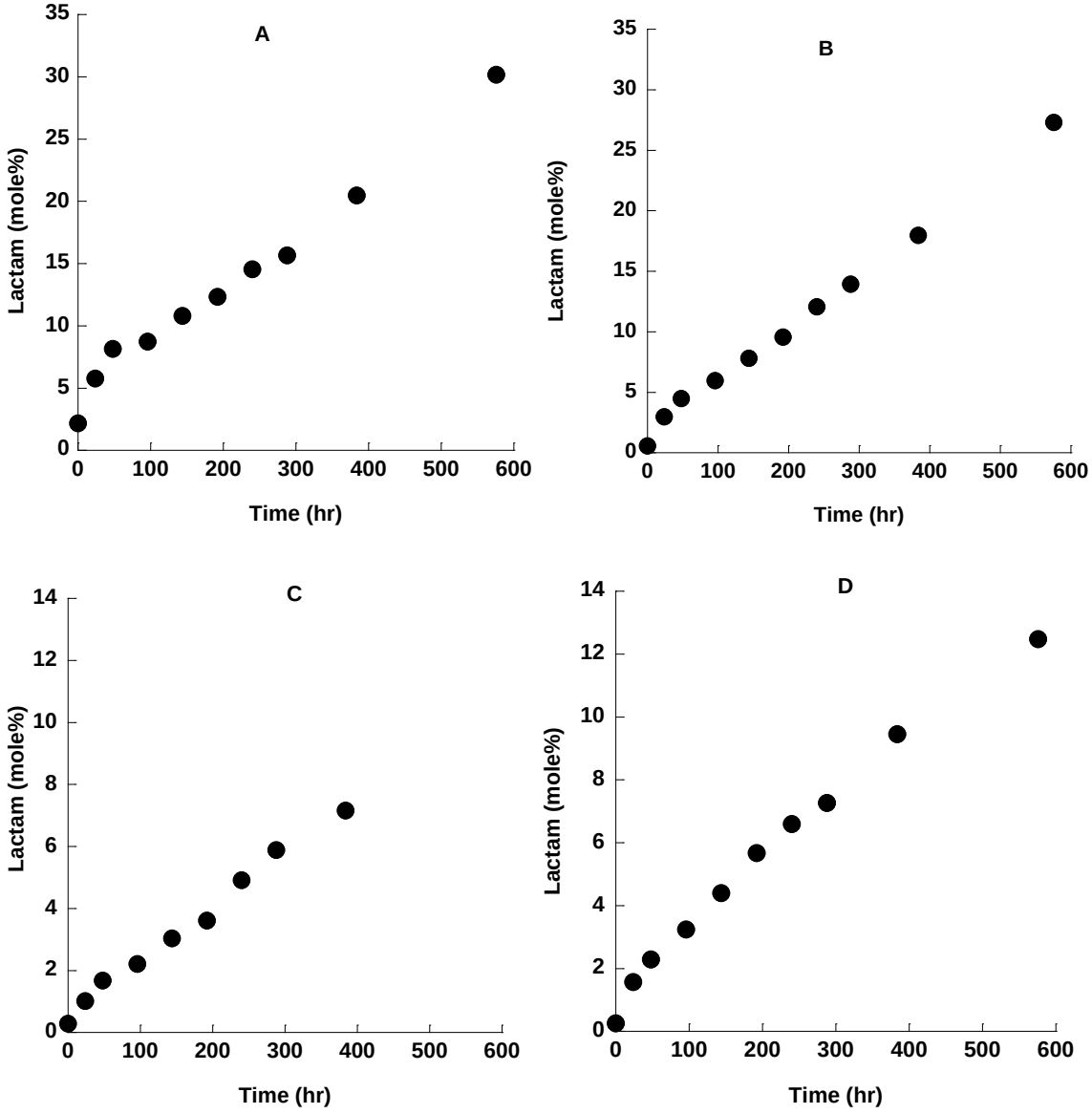

According to literature reports, milling may reduce the induction period resulting in an initial rate increase. This initial rate increase may be prominent when substrate is co-milled with excipients. (27, 28) For example, aspirin and MCC mixtures (10:90 and 20:80 %w/w) were co-milled for 30 and 240 minutes. Increased initial degradation rate was observed with samples subjected to higher levels of MCC and longer milling times. (29)

After the initial rapid lactam increase, the lactamization rate decreased although this decrease was less apparent in mixtures containing $CaHPO_4$ [Figure III-6B], starch [Figure III-6C] and HPC [Figure III-6D]. This may be due to the sizable amounts of gabapentin III generated during co-milling as reported in Chapter II. In the absence of excipient, no polymorphic transformation was observed. However, gabapentin III was generated when co-milled with various excipients, and the amounts of III varied depending upon excipient type. For example, concentrations of III were found to be 39, 33, 21, and 8.7 mole% in mixtures containing $CaHPO_4$, HPC, starch, and SiO_2, respectively.

Moisture Effect

The effects of inorganic (SiO_2, $CaHPO_4$, and talc) [Figure III-7 (A-C)] and organic excipients (starch, HPC, MCC and HPMC) [Figure III-8 (A-D)] on lactamization kinetics during storage at 50 °C and various humidity conditions; 5, 11, 29, and 47.5 %RH were investigated. Overall, lactamization rate decreased when humidity increased. Moisture decreased both initial and autocatalytic lactamization rates, but the magnitude of the moisture stabilizing effect varied depending upon the excipient type.

The magnitude of moisture stabilization effect was evaluated by comparing lactamization rates at conditions of storage at 5 and 47.5 %RH. The highest moisture stabilizing effect was observed for the samples containing HPC where the rate decreased 12-fold [Figure III-8B]. The least effect was observed for the samples containing SiO_2 where the rate decreased 1.5 fold [Figure III-7A]. Moderate stabilizing effects were observed for the samples containing HPMC [Figure III-8D], MCC [Figure III-8C], $CaHPO_4$ [Figure III-7B], talc [Figure III-7C] and starch [Figure III-8A] where the rates

decreased 4.5, 4, 4, 3.5, and 3-fold, respectively. Due to the similar kinetic profiles of co-milled gabapentin containing MCC [Figure III-8C], HPMC [Figure III-8D], and talc [Figure III-7C], two inorganic (SiO_2 and $CaHPO_4$) and organic (starch and HPC) excipients were chosen for further studies in this chapter and the subsequent chapters.

In all co-milled gabapentin/excipient mixtures, mass balance was 100 % (±2%) based on the initial amounts of gabapentin and lactam. A physical state change of co-milled gabapentin/excipient mixtures was investigated as freshly prepared, and periodically determined during storage using ^{13}C solid state nuclear magnetic resonance spectroscopy. Gabapentin monohydrate was not detected in any excipient mixtures stored at any experimental conditions.

Figure III- 7. Lactamization profiles of co-milled gabapentin Form II with SiO_2 (A), $CaHPO_4$ (B), and talc (C) stored at 50 ºC and various humidity levels (●: 5 %RH, ■: 11 %RH, ♦: 29 %RH, and ▲: 47.5 %RH).

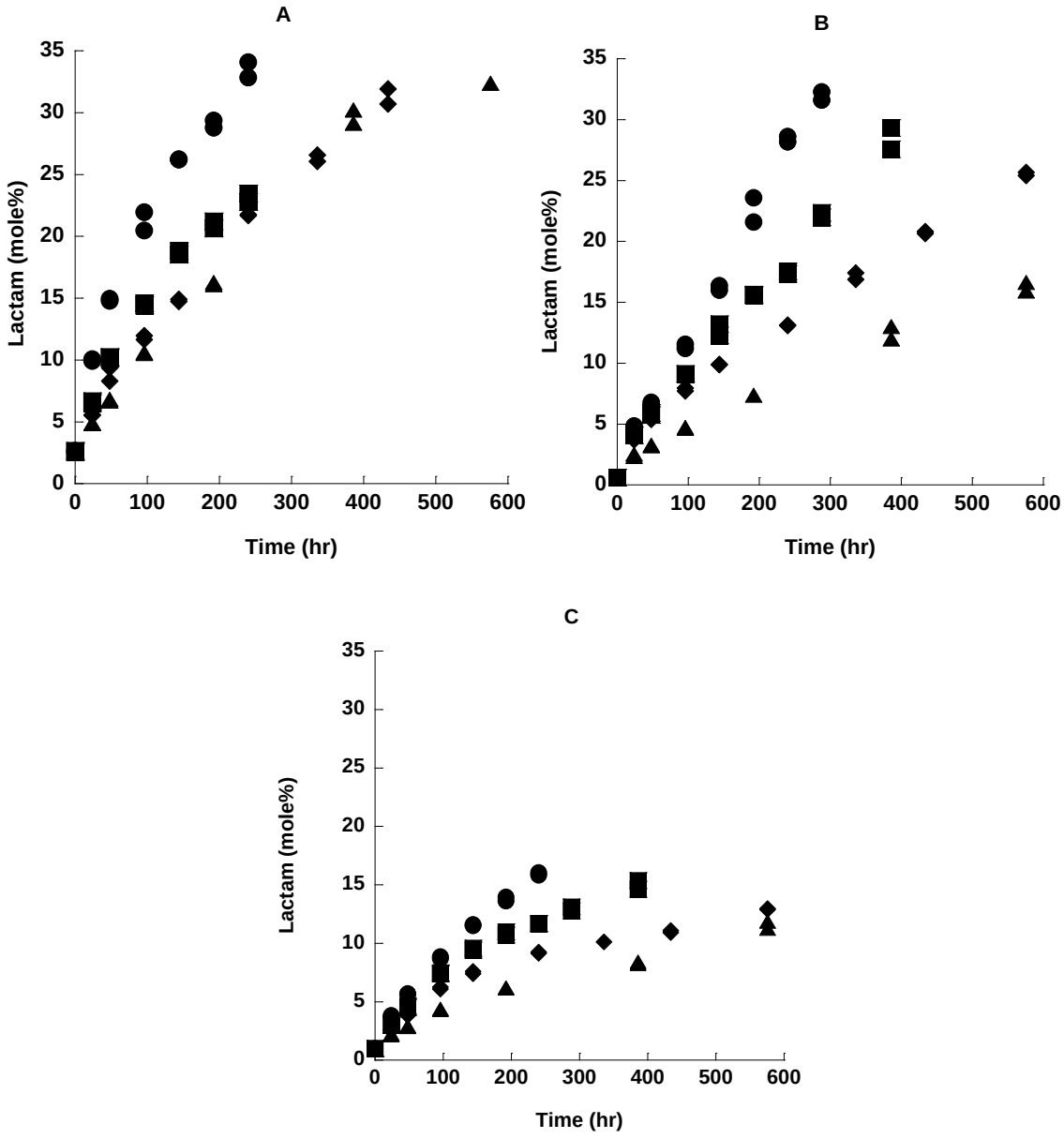

Figure III- 8. Lactamization profiles of co-milled gabapentin Form II with starch (A), HPC (B), MCC (C), and HPMC (D) stored at 50 ºC and various humidity levels (●: 5 %RH, ■: 11 %RH, ♦: 29 %RH, and ▲: 47.5 %RH).

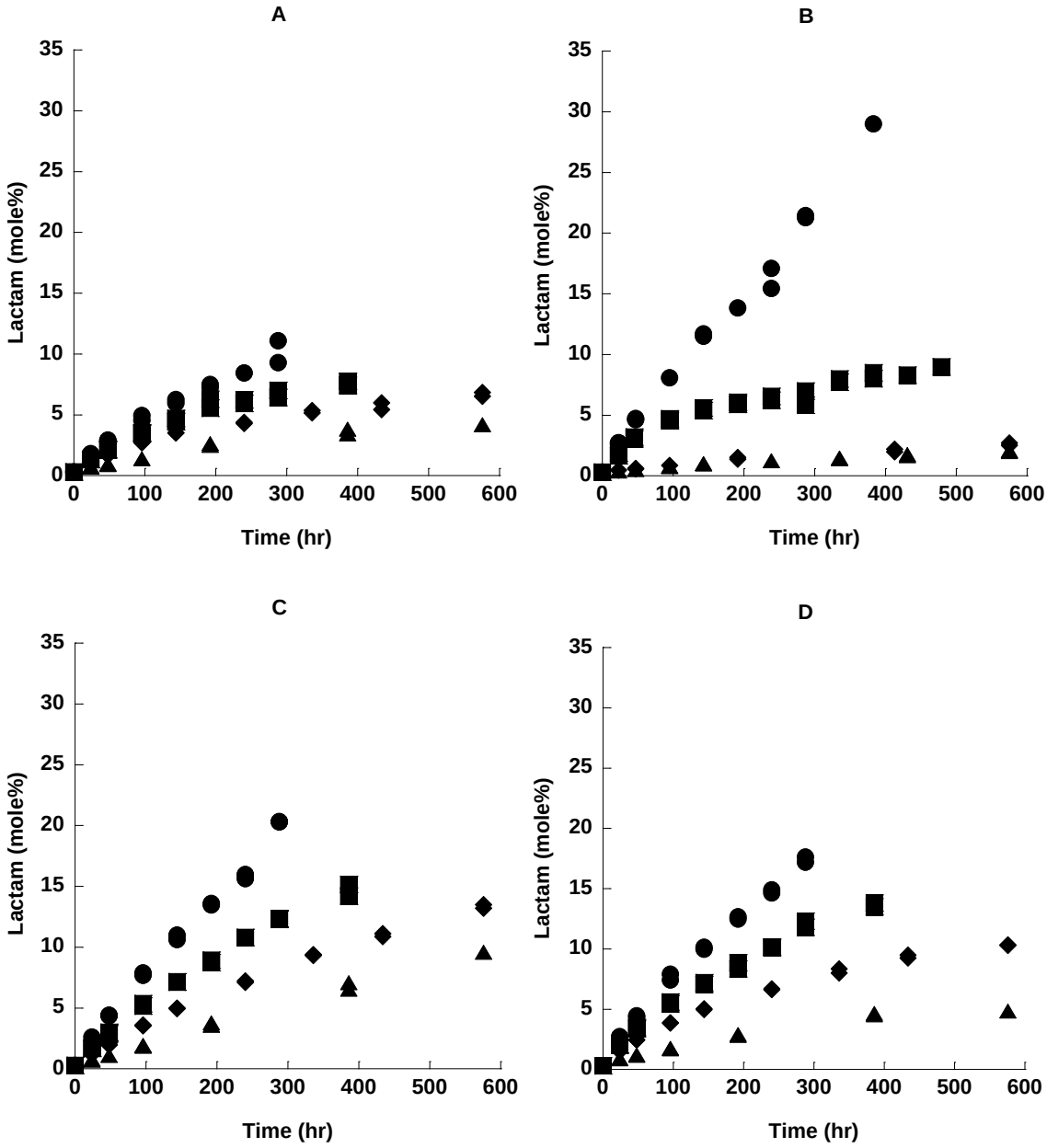

The stabilizing effect of moisture on the degradation of milled gabapentin in the absence of excipients has been previously reported. Both the initial and autocatalytic lactamization rates were decreased in the presence of humidity [Figure III-9]. Lactamization appeared to be nearly shut down at 30 %RH. (26) It has been proposed that high humid conditions may facilitate the annealing of crystal defects (caused by milling) to stabilize gabapentin. The annealing process was hypothesized to be kinetically competitive with lactamization. (12)

A similar kinetic model has been proposed by Waterman wherein crystalline substrate degrades through the formation of a reactive intermediate (crystal defects) which can reversibly revert to intact crystalline or competitively degrade to product. This model has been used to describe the solid state degradation kinetics of ascorbic acid and aspirin tablets. (30)

Figure III- 9. Lactamization profiles of milled gabapentin Form II stored at 50 ºC and various humidity levels (●: 5 %RH, ■: 11 %RH, ♦: 31 %RH, and ▲: 50 %RH). (26)

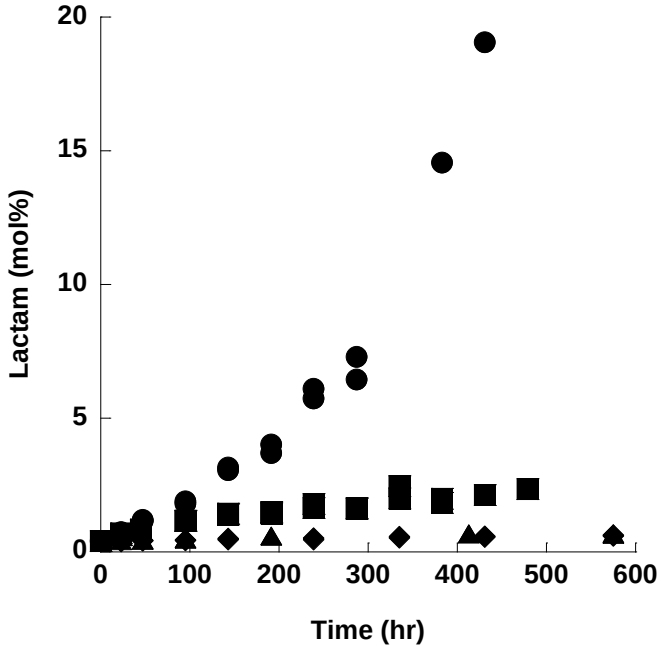

In another example, the effect of moisture on decreased degradation rate of milled sodium prasterone sulfate dihydrate was investigated at 40 ºC/50-80 %RH. The degradation rate at 80 %RH was less than that observed at 50 %RH. The decrease in degradation rates at high humidity was described by increasing crystallinity (from 51.6 % to 77.4 %) as a result of strong hydrogen bond formation between hydrate crystal and sodium prasterone sulfate. (31)

Temperature Effect

The effects of inorganic (SiO_2 and $CaHPO_4$) [Figure III-10 (A-B)] and organic excipients (starch and HPC) [Figure III-10 (C-D)] on lactamization kinetics during storage at 5 %RH and various temperature conditions; 40, 50, and 60 ˚C were investigated. Generally, lactamization rate increased with increased temperature. At any temperature, the lactamization rates of co-milled mixtures containing inorganic excipients [Figure III-10 (A-B)] were two times greater than that observed in the mixtures containing organic excipients [Figure III-10 (C-D)].

The temperature effects on increased lactamization rates of mixtures containing inorganic excipients stored at other humidity conditions; 10, 30 and 50 %RH were observed. Lactamization profiles of mixtures containing SiO_2 stored at 10 %RH, 30 %RH, and 50 %RH are illustrated in [Figure III-11 (A-C)]. Similar profiles were observed for the mixtures containing $CaHPO_4$ stored at identical conditions of storage [Figure III-12 (A-C)].

Figure III- 10. Lactamization profiles of co-milled gabapentin Form II with SiO_2 (A), $CaHPO_4$ (B), starch (C), and HPC (D) stored at 5 %RH and various temperature conditions (●: 40 ºC, ■: 50 ºC, and ♦: 60 ºC).

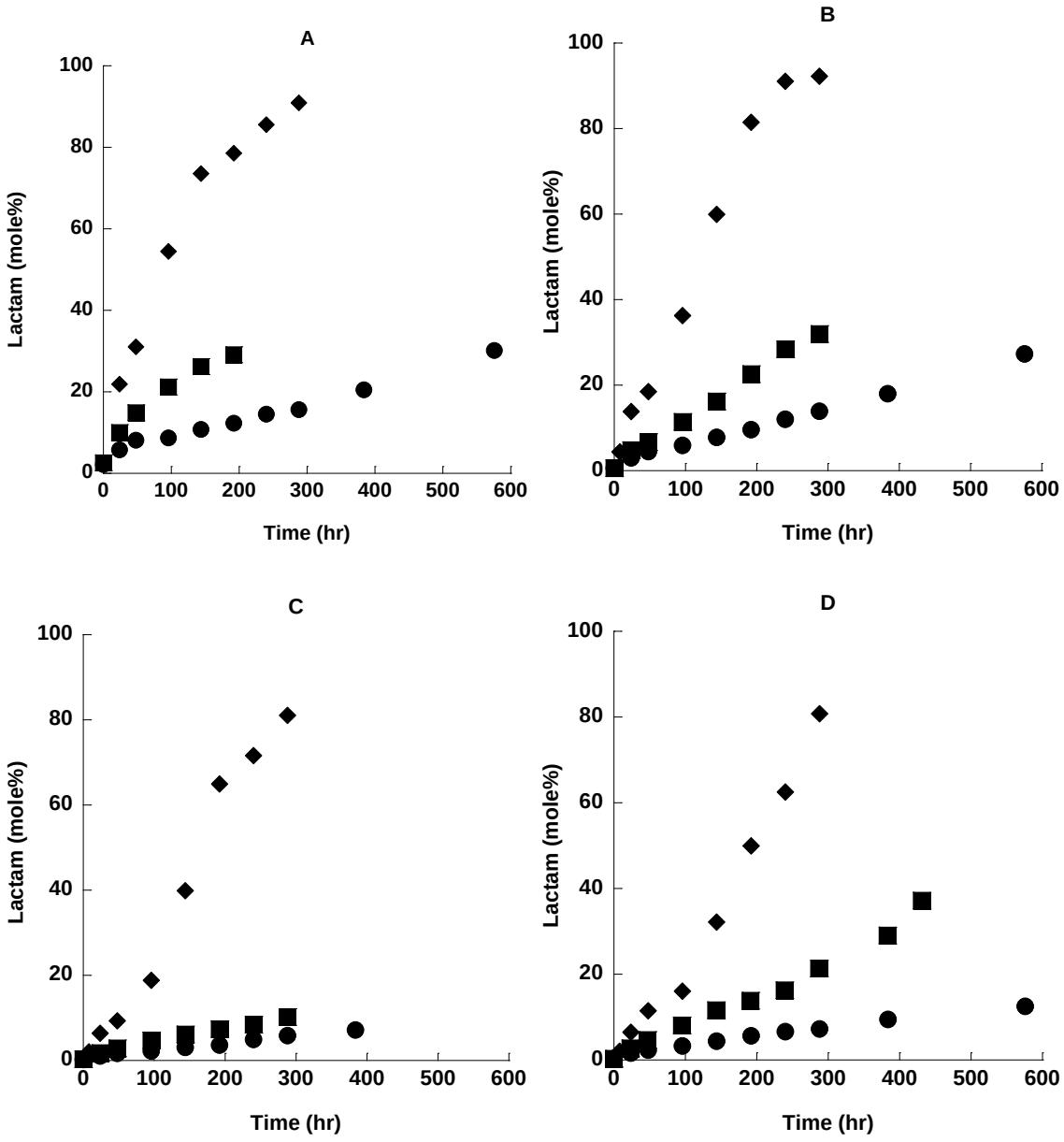

Figure III- 11. Lactamization profiles of co-milled gabapentin Form II with SiO_2 stored under various temperature (●: 40 ºC, ■: 50 ºC, and ♦: 60 ºC) and humidity conditions: 10 %RH (A), 30 %RH (B), and 50 %RH (C).

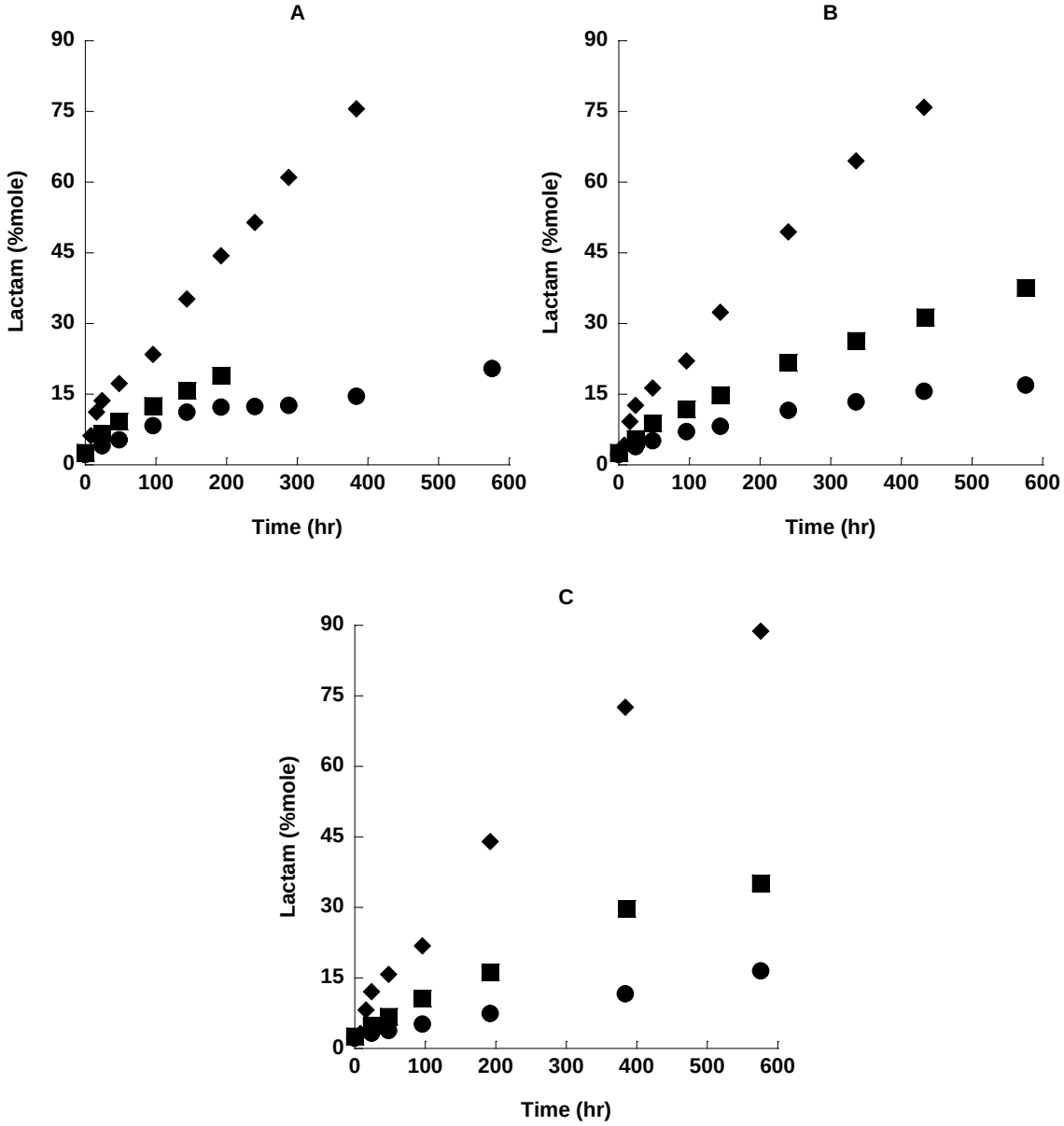

Figure III- 12. Lactamization profiles of co-milled gabapentin Form II with $CaHPO_4$ stored under various temperature (●: 40 ºC, ■: 50 ºC, and ♦: 60 ºC) and humidity conditions: 10 %RH (A), 30 %RH (B), and 50 %RH (C).

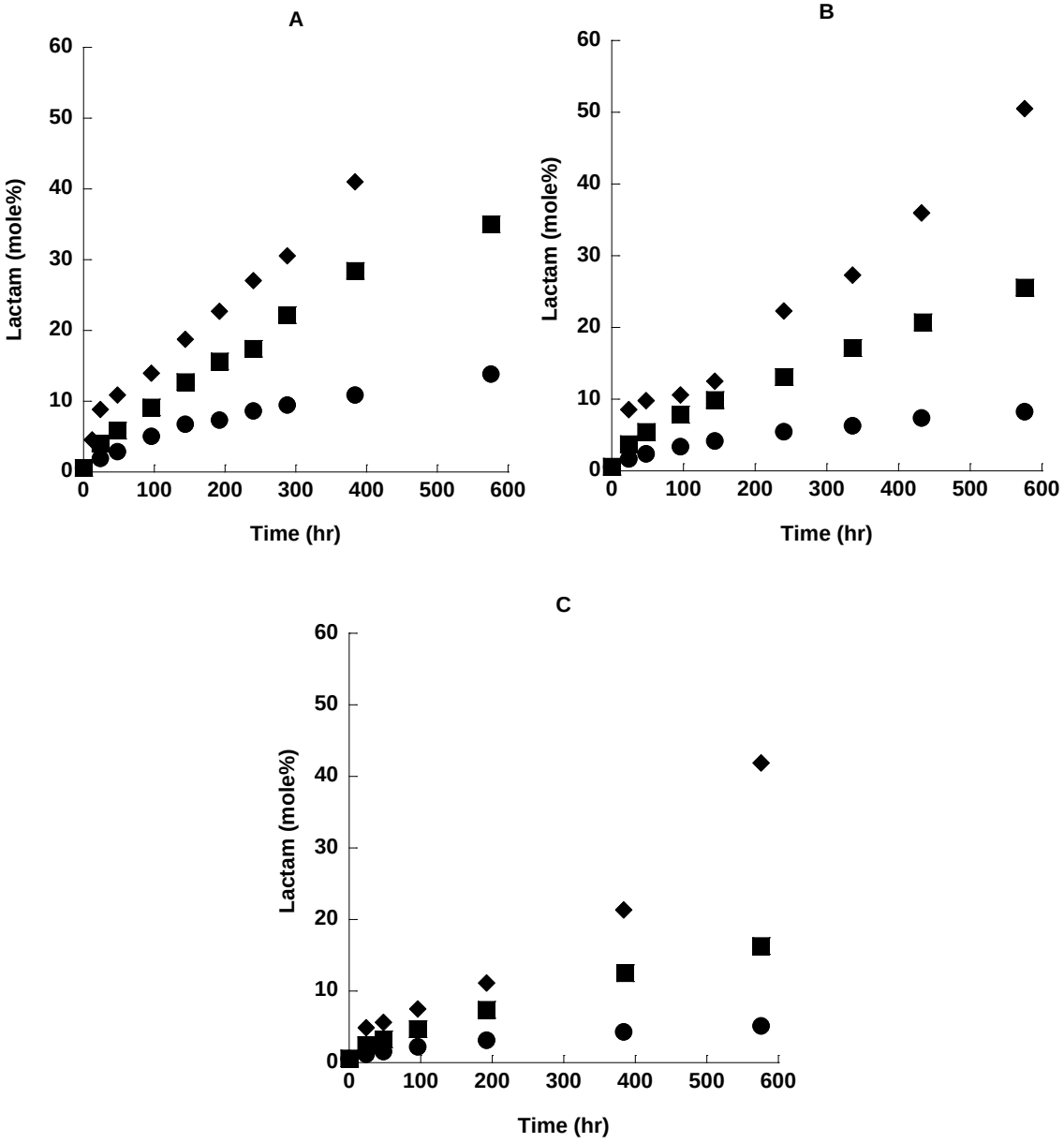

The temperature effects on increased lactamization rates of mixtures containing organic excipients stored at 10, 30 and 50 %RH were less apparent. Lactamization profiles of mixtures containing starch stored at 10 %RH, 30 %RH, and 50 %RH are illustrated in [Figure III-13 (A-C)]. Similar profiles were observed for the mixtures containing HPC stored at identical conditions of storage [Figure III-14 (A-C)]. These results suggest that the humidity effect was more prominent for organic excipients than for inorganic excipient reaction mixtures.

Suppressed temperature effects on lactamization rates of milled gabapentin without excipient stored at 10-50 %RH was also observed [Figure III-15 (A-C)]. (25) A likely explanation involves the relative susceptibility of the organic and inorganic excipients to moisture dependent polymorphic transformations or crystal defect annealing. The relative sensitivity of physical transformations to moisture and temperature variation is the subject of Chapter IV.

Figure III- 13. Lactamization profiles of co-milled gabapentin Form II with starch stored under various temperature (●: 40 ºC, ■: 50 ºC, and ♦: 60 ºC) and humidity conditions: 10 %RH (A), 30 %RH (B), and 50 %RH (C).

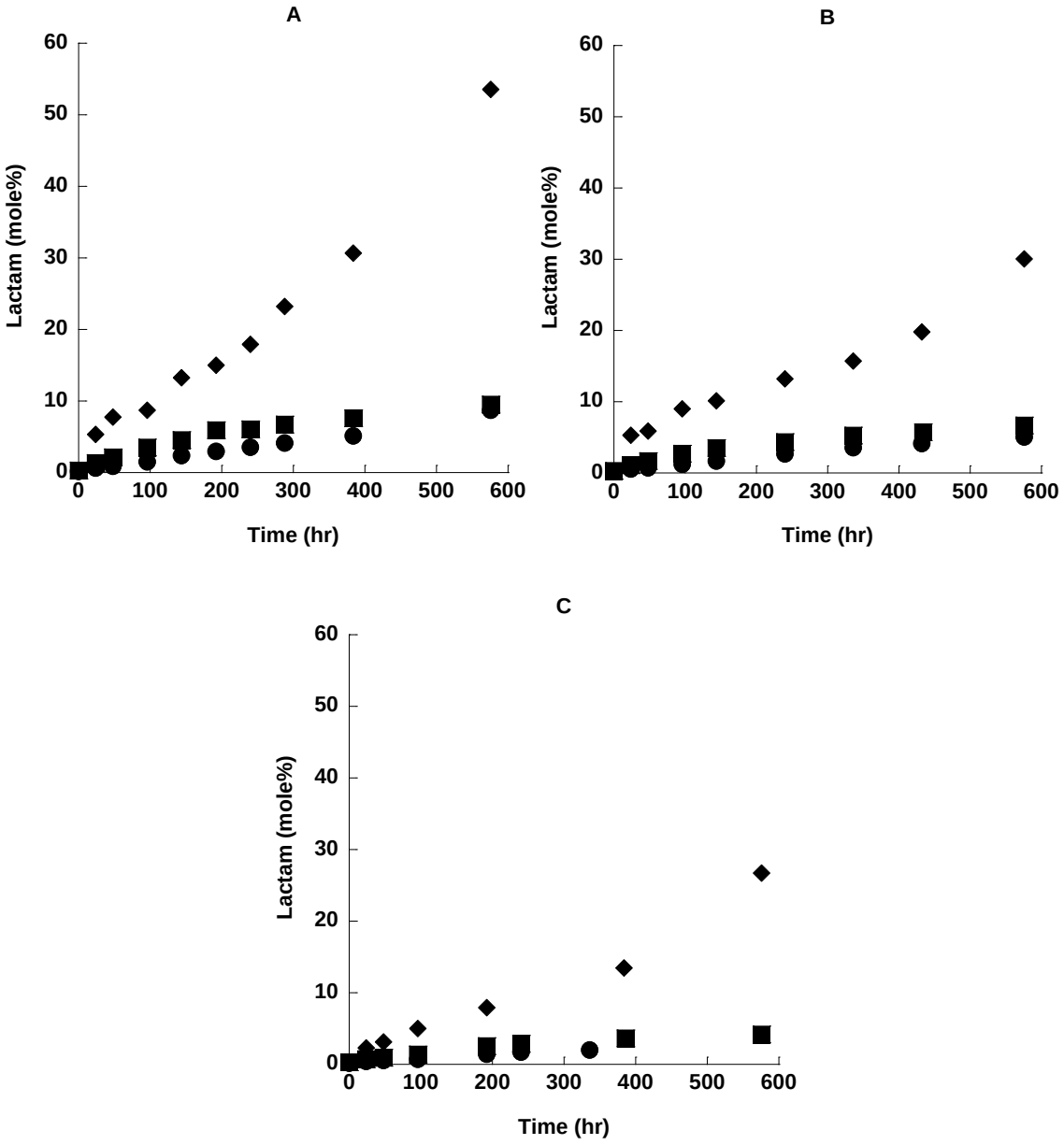

Figure III- 14. Lactamization profiles of co-milled gabapentin Form II with HPC stored under various temperature (●: 40 ºC, ■: 50 ºC, and ♦: 60 ºC) and humidity conditions: 10 %RH (A), 30 %RH (B), and 50 %RH (C).

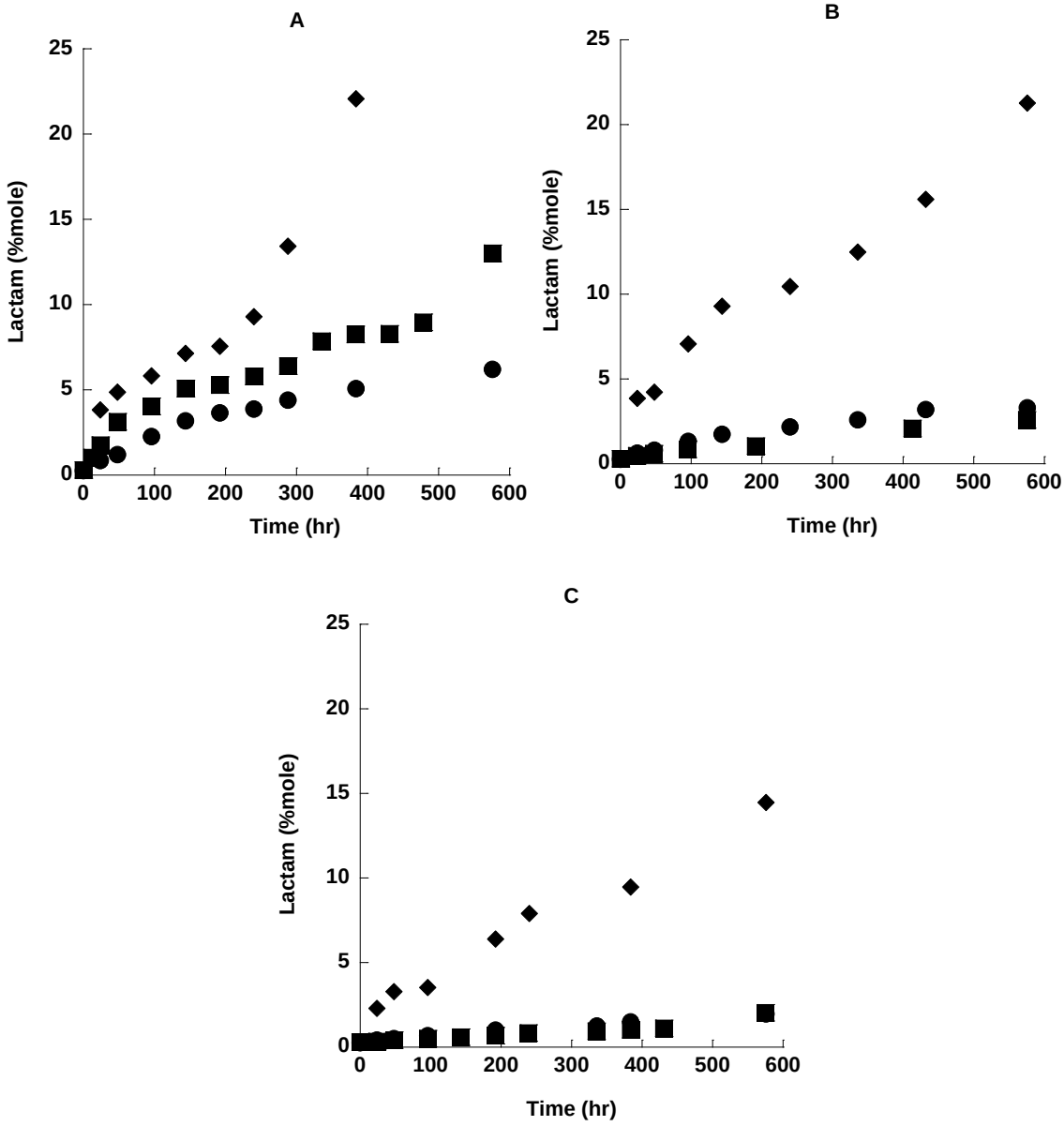

Figure III- 15. Lactamization profiles of milled gabapentin Form II stored under various temperature (●: 40 ºC, ■: 50 ºC, and ♦: 60 ºC) and humidity conditions: 10 %RH (A), 31 %RH (B), and 50 %RH (C). (25)

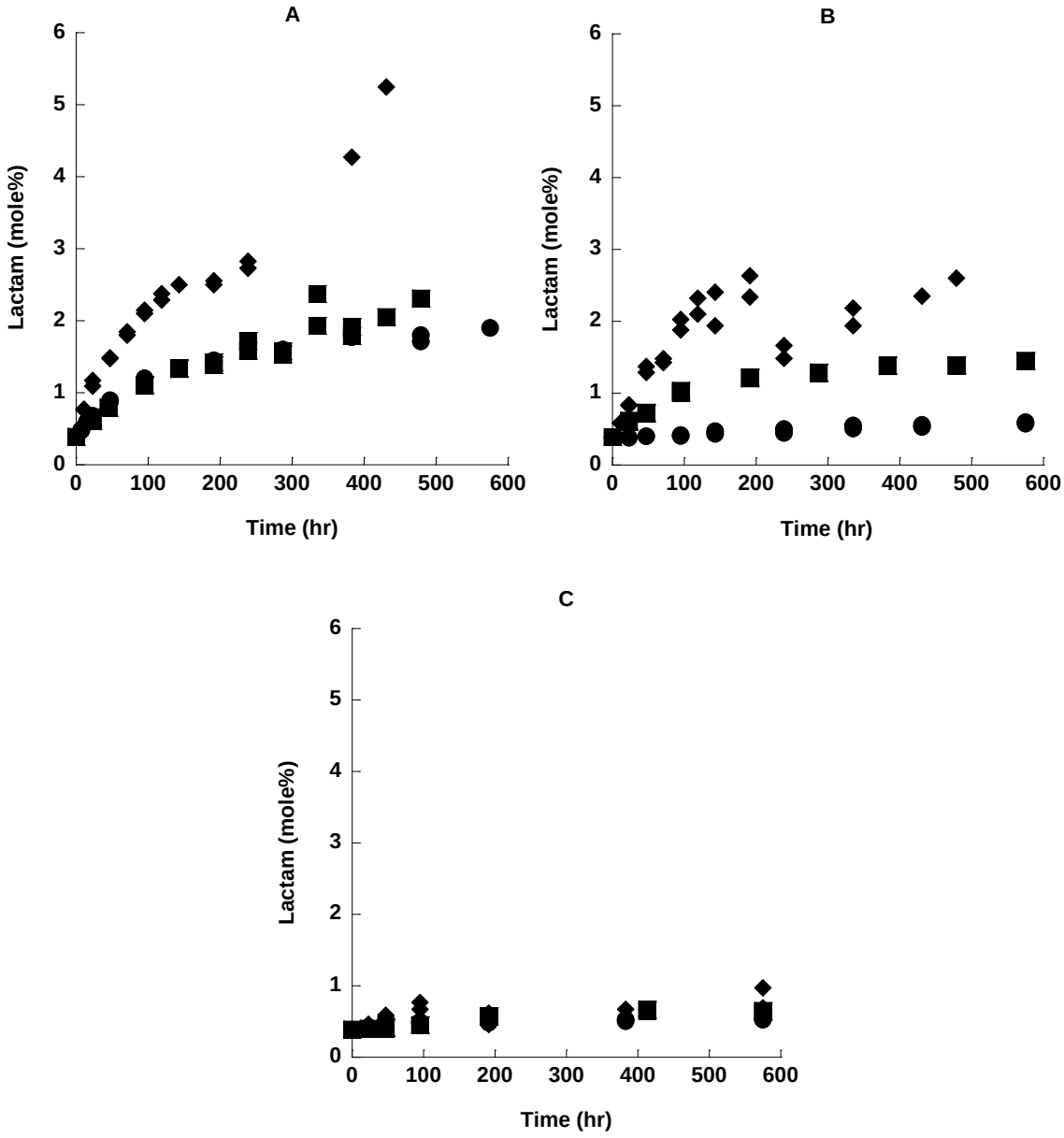

Conclusion

Lactamization kinetic profiles of co-milled gabapentin/excipient mixtures showed less sigmoid-shaped behavior than previously observed in the reaction mixtures without excipients. The initial rate of lactamization was increased in the presence of excipient and therefore the transitional phase between initial and subsequent autocatalytic phases was less obvious. Our interpretation is further complicated by the presence of Form III. Therefore, a complete explanation awaits the development and application of a suitable kinetic model to describe simultaneous physical and chemical transformations. The moisture stabilizing effect was observed in all co-milled excipient mixtures. However, the magnitude of the humidity effect was profound and influenced by excipient type.

Chapter III References

1. Zambon E, Giovanetti R, Cotarca L, Pasquato L. Mechanistic investigation on 2-aza-spiro[4,5]decan-3-one formation from 1-(aminomethyl)cyclohexylacetic acid (gabapentin). Tetrahedron. 2008;64(28):6739-6743.
2. Jehle T, Lagrèze WA, Blauth E, Knörle R, Schnierle P, Lücking CH, Feuerstein TJ. Gabapentin-lactam (8-aza-spiro[5,4]decan-9-on; GBP-L) inhibits oxygen glucose deprivation-induced [3H]glutamate release and is a neuroprotective agent in a model of acute retinal ischemia. Naunyn-Schmiedeberg's Archives of Pharmacology. 2000;362(1):74-81.
3. Henle F, Leemhuis J, Fischer C, Bock HH, Lindemeyer K, Feuerstein TJ, Meyer DK. Gabapentin-Lactam Induces Dendritic Filopodia and Motility in Cultured Hippocampal Neurons. Journal of Pharmacology and Experimental Therapeutics. 2006;319(1):181-191.
4. Potschka H, Feuerstein TJ, Löscher W. Gabapentin-lactam, a close analogue of the anticonvulsant gabapentin, exerts convulsant activity in amygdala kindled rats. Naunyn-Schmiedeberg's archives of pharmacology. 2000;361(2):200-205.
5. NDA 20-882 (US. Food and Drug Administration application No. 020882).
6. Pharmacopeia US. The United States Pharmacopeia, USP 30. The National Formulary, NF 25: Official from May 1, 2007. United States Pharmacopeial Convention, Inc.; 2007.
7. Zour E, Lodhi S, Nesbitt R, Silbering S, Chaturvedi P. Stability Studies of Gabapentin in Aqueous Solutions. Pharmaceutical Research. 1992;9(5):595-600.
8. Reece HA, Levendis DC. Polymorphs of gabapentin. Acta Crystallographica Section C. 2008;64(3):o105-o108.

9. Delaney SP, Smith TM, Korter TM. Conformation versus cohesion in the relative stabilities of gabapentin polymorphs. Royal Society of Chemistry Advances. 2014;4(2):855-864.
10. Braga D, Grepioni F, Maini L, Rubini K, Polito M, Brescello R, Cotarca L, Duarte MT, Andre V, Piedade MFM. Polymorphic gabapentin: thermal behaviour, reactivity and interconversion of forms in solution and solid-state. New Journal of Chemistry. 2008;32(10):1788-1795.
11. Hsu C-H, Lin S-Y. Rapid examination of the kinetic process of intramolecular lactamization of gabapentin using DSC–FTIR. Thermochimica Acta. 2009;486(1–2):5-10.
12. Zong Z, Desai S, Kaushal A, Barich D, Huang H-S, Munson E, Suryanarayanan R, Kirsch L. The Stabilizing Effect of Moisture on the Solid-State Degradation of Gabapentin. AAPS PharmSciTech. 2011;12(3):924-931.
13. Kearney AS, Mehta SC, Radebaugh GW. The effect of cyclodextrins on the rate of intramolecular lactamization of gabapentin in aqueous solution. International Journal of Pharmaceutics. 1992;78(1–3):25-34.
14. Lin S-Y, Hsu C-H, Ke W-T. Solid-state transformation of different gabapentin polymorphs upon milling and co-milling. International Journal of Pharmaceutics. 2010;396(1–2):83-90.
15. Dempah K, Barich D, Kaushal A, Zong Z, Desai S, Suryanarayanan R, Kirsch L, Munson E. Investigating Gabapentin Polymorphism Using Solid-State NMR Spectroscopy. AAPS PharmSciTech. 2013;14(1):19-28.
16. Cutrignelli A, Denora N, Lopedota A, Trapani A, Laquintana V, Latrofa A, Trapani G, Liso G. Comparative effects of some hydrophilic excipients on the rate of gabapentin and baclofen lactamization in lyophilized formulations. International Journal of Pharmaceutics. 2007;332(1–2):98-106.
17. Carstensen JT, Osadca M, Rubin SH. Degradation mechanisms for water-soluble drugs in solid dosage forms. Journal of Pharmaceutical Sciences. 1969;58(5):549-553.
18. Genton D, Kesselring UW. Effect of temperature and relative humidity on nitrazepam stability in solid state. Journal of Pharmaceutical Sciences. 1977;66(5):676-680.
19. Mroso PV, Wan Po AL, Irwin WJ. Solid-state stability of aspirin in the presence of excipients: Kinetic interpretation, modeling, and prediction. Journal of Pharmaceutical Sciences. 1982;71(10):1096-1101.
20. Waterman KC, Gerst P, Dai Z. A generalized relation for solid-state drug stability as a function of excipient dilution: Temperature-independent behavior. Journal of Pharmaceutical Sciences. 2012;101:4170-4177.
21. Waterman KC, Gerst P, MacDonald BC. Relative humidity hysteresis in solid-state chemical reactivity: A pharmaceutical case study. Journal of Pharmaceutical Sciences. 2012;101(2):610-615.
22. Ciavarella AB, Gupta A, Sayeed VA, Khan MA, Faustino PJ. Development and application of a validated HPLC method for the determination of gabapentin and its major degradation impurity in drug products. Journal of Pharmaceutical and Biomedical Analysis. 2007;43(5):1647-1653.

23. Ahlneck C, Zografi G. The molecular basis of moisture effects on the physical and chemical stability of drugs in the solid state. International Journal of Pharmaceutics. 1990;62(2–3):87-95.
24. Skwierczynski RD. Disorder, molecular mobility, and solid-state kinetics: The two-environment model. Journal of Pharmaceutical Sciences. 1999;88(11):1234-1236.
25. Zong Z. Studies on the mechanisms of solid state and solution instability of drugs. The University of Iowa; 2011. p. 135.
26. Zong Z, Qiu J, Tinmanee R, Kirsch LE. Kinetic model for solid-state degradation of gabapentin. Journal of Pharmaceutical Sciences. 2012;101(6):2123-2133.
27. Garner WE. Chemistry of the solid state. London: Butterworths Scientific publications; 1955. p. 254-267.
28. Carstensen JT. Stability of solids and solid dosage forms. Journal of Pharmaceutical Sciences. 1974;63(1):1-14.
29. Nakai Y, Nakajima S, Yamamoto K, Terada K, Konno T. Effects of grinding on the physical and chemical properties of crystalline medicinals with microcrystalline cellulose. III. Infrared spectra of medicinals in ground mixtures. Chemical and Pharmaceutical Bulletin. 1978;26(11):3419-3425.
30. Waterman K, Carella A, Gumkowski M, Lukulay P, MacDonald B, Roy M, Shamblin S. Improved Protocol and Data Analysis for Accelerated Shelf-Life Estimation of Solid Dosage Forms. Pharmaceutical Research. 2007;24(4):780-790.
31. Nakagawa H, Takahashi Y, Sugimoto I. The effects of grinding and drying on the solid state stability of sodium prasterone sulfate. Chemical and Pharmaceutical Bulletin. 1982;30(1):242-248.

CHAPTER IV

THE TEMPERATURE AND MOISTURE EFFECTS ON POLYMORPHIC TRANSFORMATION OF GABAPENTIN/EXCIPIENT MIXTURES

Introduction

During the manufacturing process, drug substances are subjected to mechanical stresses such as milling, blending and compression. Milling may decrease the lattice energy of crystal drug leading to structural defects. Crystal defects are thermodynamically unstable and serve as foci for chemical and physical instability. (1-3) Milling-induced polymorphic transformations of pharmaceutical compounds have been reported. For example, fostedil, chloramphenicol palmitate, indomethacin, cimetidine, sulfamerazine, fananserine, glycine, sulfathiazole and gabapentin have been reported to undergo polymorphic transformations during milling. (4-14) Milling-induced polymorphic transformations may involve the accumulation of lattice defects or transient metastable crystals which is followed by the progressive reorientation of molecules in the crystals to another polymorph. (12, 15, 16)

The effects of humidity on polymorphic transformation kinetics of milled pharmaceutical compounds have been studied. For example, the polymorphic transformation kinetics of milled sulfathiazole (FI➔FII or FIV) was studied at 22 °C/10-98 %RH. The transformations involved the collapse of low density-FI and simultaneous growth of either FII or FIV in the presence of humidity greater than 75 %RH. (12) Similar humidity effects on polymorphic transformation of milled fostedil (II➔I) has been observed. The transformation rates at 40 °C/80 %RH were significantly greater than those observed at 40 °C/0 %RH. This was attributed to the interaction between water

molecules and crystal lattice, thereby facilitating the transformation of II➔I. (4) In another example, the polymorphic transformation kinetics of milled-5-methyl-2-[(4-methyl-2-nitrophenyl) amino]-3-thiophenecarbonitrile (4´-Me DR➔R) were studied under storage conditions at 85 °C/0, 58 and 95 %RH. The polymorphic transformation rates were increased after exposure to humidity conditions at 58 and 95 %RH. Water molecules participate in the polymorphic transformation by binding to the defect sites on the crystal surface and serving as a nucleation catalyst, thereby increasing the molecular mobility and promoting the transformation of 4´-Me DR➔R. (15)

In our studies, gabapentin has been chosen as a model compound due to its propensity to undergo both chemical and physical transformations. We conducted a series of experiments to investigate the environmental (temperature and humidity) effects on chemical and physical transformations of gabapentin/excipient mixtures during storage conditions. In the previous chapter, we demonstrated the effects of environment and excipient on lactam formation kinetics of gabapentin during storage at 40-60 °C and 5-50 %RH. In this chapter, we present the results of our investigation into the effects of environment and excipient on polymorphic transformation kinetics of gabapentin during storage conditions at 40-60 °C and 10-50 %RH. Finally, a kinetic model to describe the environmental and excipient effects on chemical and physical transformations of gabapentin are presented in the last chapter which bring together all transitions in a holistic model.

Material and Methods

Materials (gabapentin Form II, SiO_2, HPC, starch, and $CaHPO_4$) and milling protocol used to prepare co-milled gabapentin/excipient mixtures for our studies in this chapter were identical to those described in Chapter III.

Polymorphic Transformation Kinetic Studies

The polymorphic transformation (Form II and III) kinetics were determined using aliquots of co-milled gabapentin Form II/excipient mixtures. Approximately 80 mg of sample was weighed and placed in a 20 ml Type II scintillation glass vial and then stored unsealed in desiccators containing LiCl (11 %RH), and $Mg(NO_3)_2$ (50 %RH) at various thermal conditions: 40, 50, and 60 ˚C. For controlled humidity chambers, the saturated salt solutions: LiCl, and $Mg(NO_3)_2$ were prepared by dissolving each salt in Nanopure water and equilibration in controlled temperature ovens for 24 hours prior experiment. The humidity was measured by using EL-USB-2 Temperature and Humidity Data Logger recorder (DATAQ Instruments, Inc., Akron, OH) with ± 3.0 %RH accuracy. The humidity levels in chambers were determined to be 12 and 48 %RH (40 ºC), 11 and 47.5 %RH (50 ºC), and 10 and 44 %RH (60 ºC), respectively. At 0, 24, 48, 96, 144, 240, 336, 386, 434, and 576 hours, samples were then removed from the stability chambers and stored under Drierite® desiccant and sub-ambient temperature (-80 °C) prior to ^{13}C ssNMR analysis as described in Chapter II for determining gabapentin Form II and III concentrations.

Results and Discussion

Polymorphic Compositions of Co-Milled Gabapentin Form II/Excipient Mixtures

The effect of selected inorganic ($CaHPO_4$ and SiO_2) and organic (starch and HPC) excipients on polymorphic transformation of gabapentin Form II were determined by measuring polymorphic compositions during co-milling using ^{13}C ssNMR [Figure IV-1]. The extent of polymorphic transformations (II➔III) during milling depended on the type of excipient. In the presence of $CaHPO_4$, 39 mole% Form III was generated, whereas only 8.7 mole% was found in the presence of SiO_2. For organic excipients, 21 and 33 mole% of Form III were generated in the presence of starch and HPC, respectively. No other detectable polymorphs were found. A similar result regarding the effect of excipient type on the polymorphic transformation (II➔III) during milling has been reported. (13)

Figure IV- 1. Polymorphic compositions of co-milled gabapentin/excipient mixtures after co-milling. The analyses were conducted under ambient condition by using ^{13}C ssNMR. Error bars represent the standard deviation (n=6).

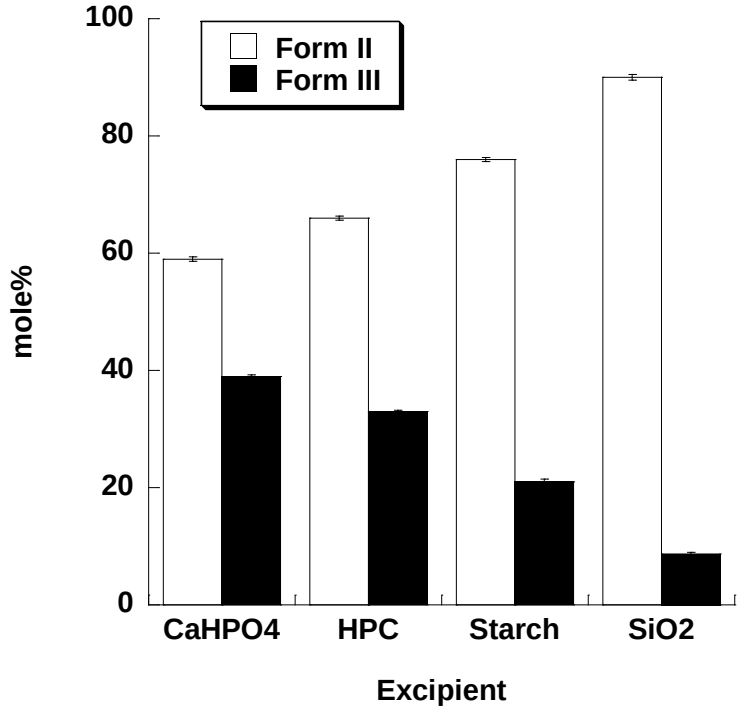

Polymorphic Transformation Kinetic Profiles

Solid-state polymorphic transformations typically involve surface phenomenon. The solid-solid transformation of the polymorph may require a long period of time under mild stress conditions of storage. (16) Therefore, polymorphic transformation kinetics are typically studied under thermal stress and/or elevated humidity conditions. For example, the polymorphic transformation kinetics of milled phenylbutazone (β➔δ) was studied under various thermal (40, 50 and 60 °C) and humidity (30-80 %RH) conditions. (17)

For consistency with the series of experiments described in Chapter III (chemical transformation kinetics), polymorphic transformation kinetics of co-milled gabapentin/excipient mixtures were studied by measuring changes in II and III concentrations over time at various thermal (40, 50 and 60 °C) and humidity (10 and 50 %RH) conditions. The representative ^{13}C ssNMR spectra for the aliphatic region of co-milled gabapentin with $CaHPO_4$, SiO_2, starch and HPC stored at 40 °C/ 48 %RH in a given period of time are shown in Figure IV-2 to IV-5. Gabapentin III (generated by milling) converted to II under the conditions of storage, but II did not generate III during storage. Additionally, no other detectable polymorphs were found. The polymorphic transformation of III➔II has been previously reported (18) and the lack of transformation of II➔III under identical storage conditions was confirmed in previous studies in our laboratory. (19)

Figure IV- 2. The representative 13C ssNMR spectra for the aliphatic region of co-milled gabapentin Form II with CaHPO4 stored under 40 °C/48 %RH at 0, 24, 96, and 192 hours. The 13C ssNMR was operated under ambient conditions.

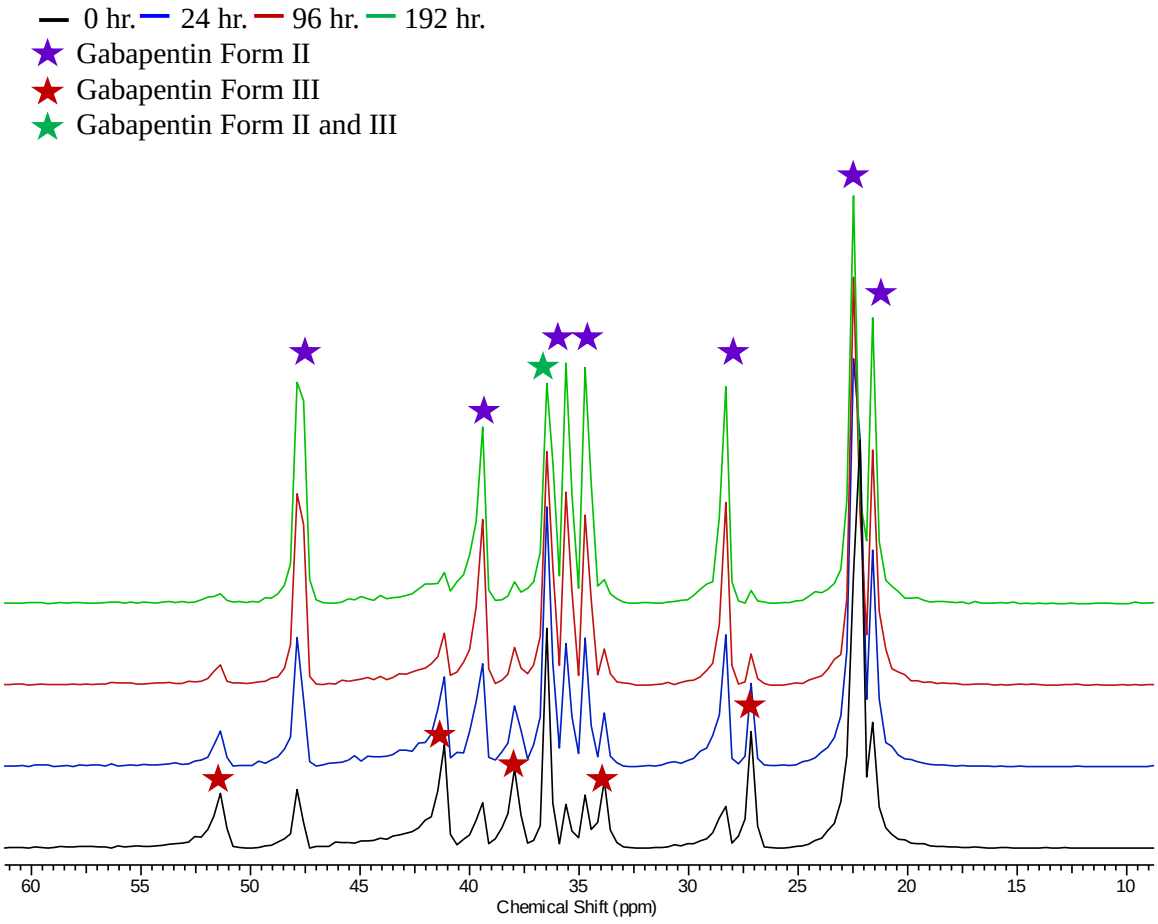

Figure IV- 3. The representative ^{13}C ssNMR spectra for the aliphatic region of co-milled gabapentin Form II with SiO_2 stored under 40 °C/48 %RH at 0, 96, and 192 hours. The ^{13}C ssNMR was operated under ambient conditions.

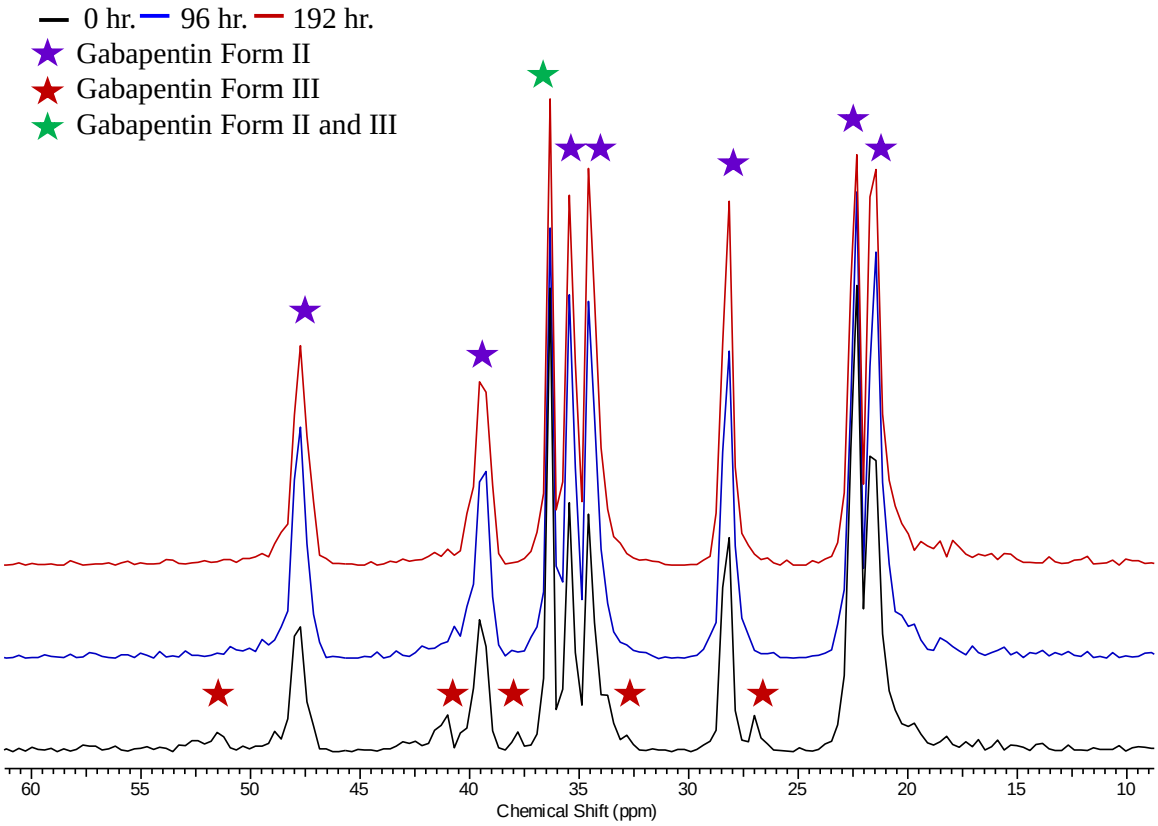

Figure IV- 4. The representative ^{13}C ssNMR spectra for the aliphatic region of co-milled gabapentin Form II with starch stored under 40 °C/48 %RH at 0, 24, 96, and 192 hours. The ^{13}C ssNMR was operated under ambient conditions.

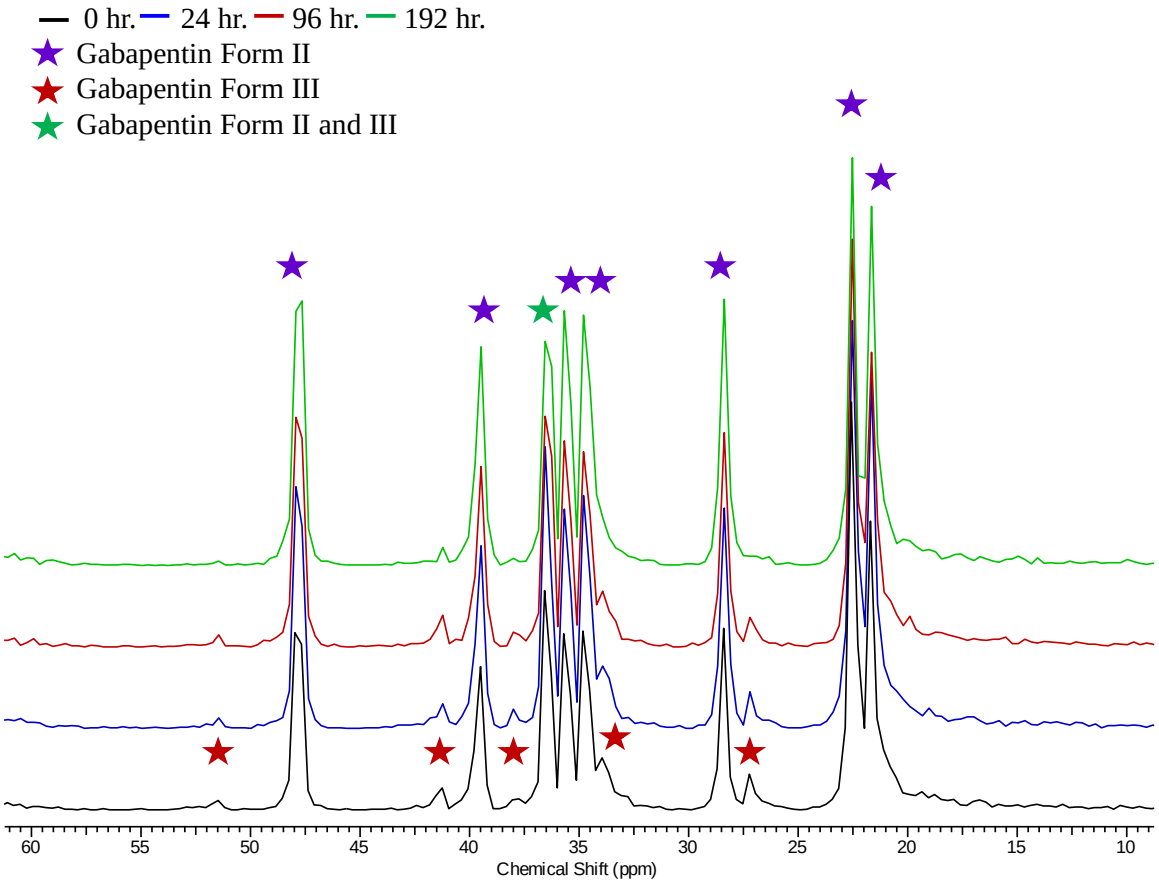

Figure IV- 5. The representative ^{13}C ssNMR spectra for the aliphatic region of co-milled gabapentin Form II with HPC stored under 40 °C/48 %RH at 0, 96, 192, 336, and 384 hours. The ^{13}C ssNMR was operated under ambient conditions.

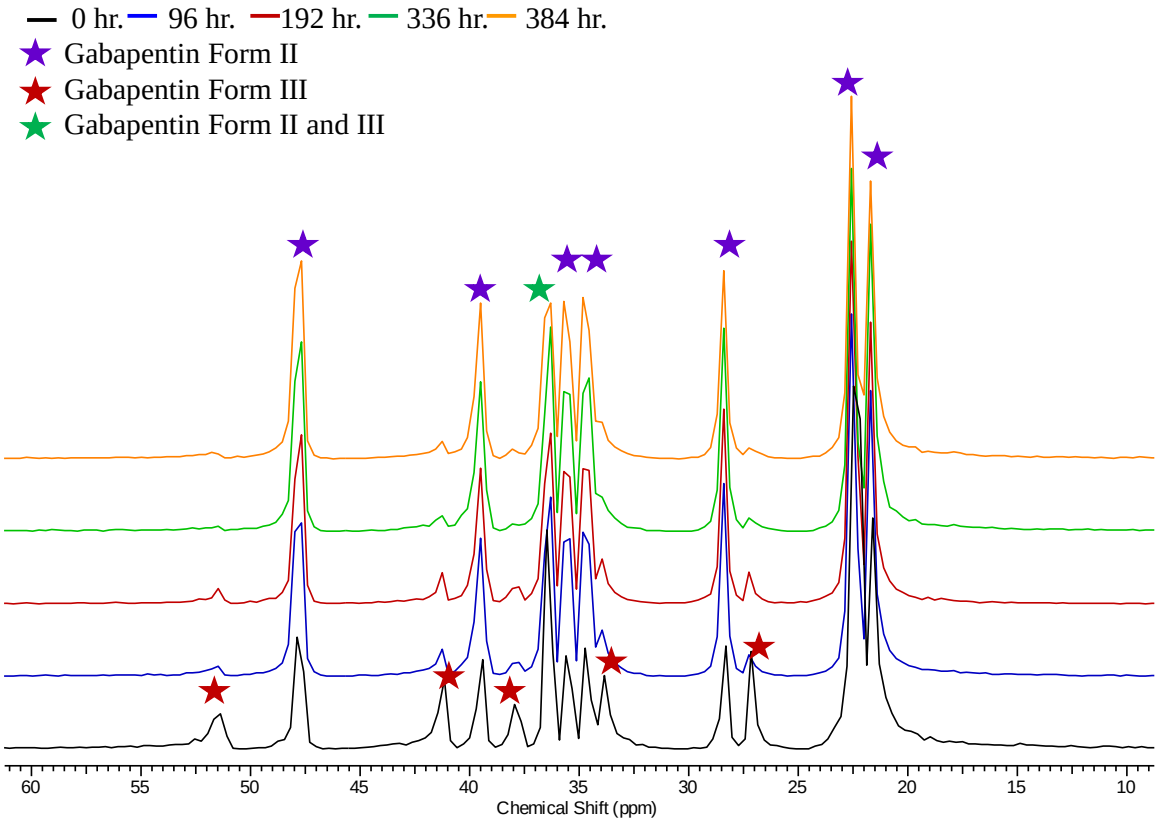

Typical concentration time profiles for polymorph II and III in reaction mixtures containing $CaHPO_4$, SiO_2, starch and HPC stored at 40 °C/48 %RH are illustrated [Figure IV-6 to IV-9]. For reaction mixtures containing $CaHPO_4$ [Figure IV-6], starch [Figure IV-8] and HPC [Figure IV-9], the concentrations of III decreased over time with commensurate increases in II concentrations. Form III loss appeared to follow first-order kinetics, and the rates of III loss were reflected in the appearance of II. For SiO_2 mixtures; however, both concentrations of II and III decreased over time [Figure IV-7].

Figure IV- 6. Form II and III concentration time profiles of co-milled gabapentin Form II with $CaHPO_4$ stored at 40 ºC/48 %RH.

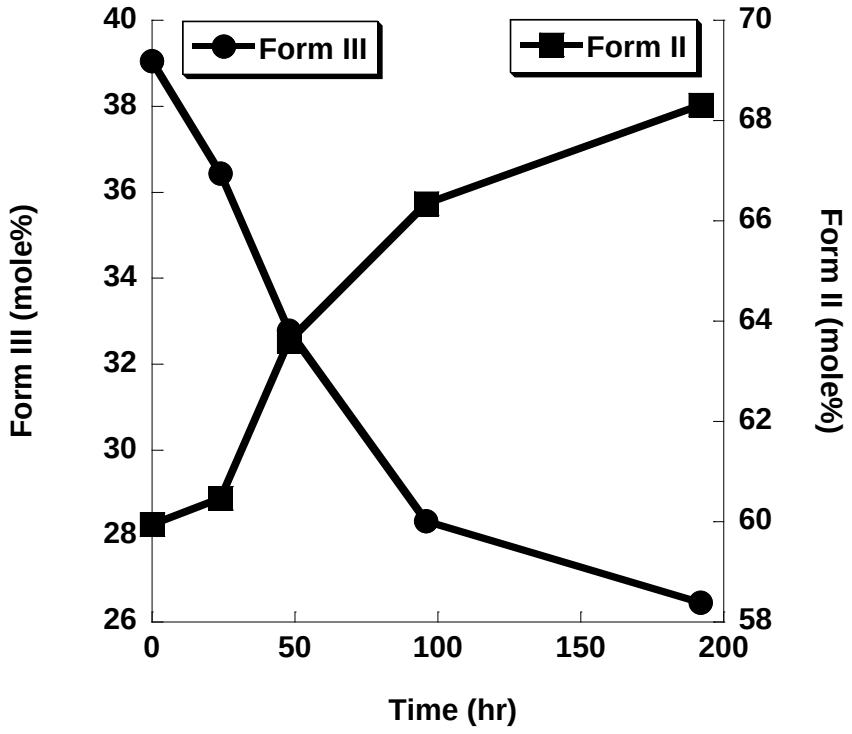

Figure IV- 7. Form II and III concentration time profiles of co-milled gabapentin Form II with SiO_2 stored at 40 ºC/48 %RH.

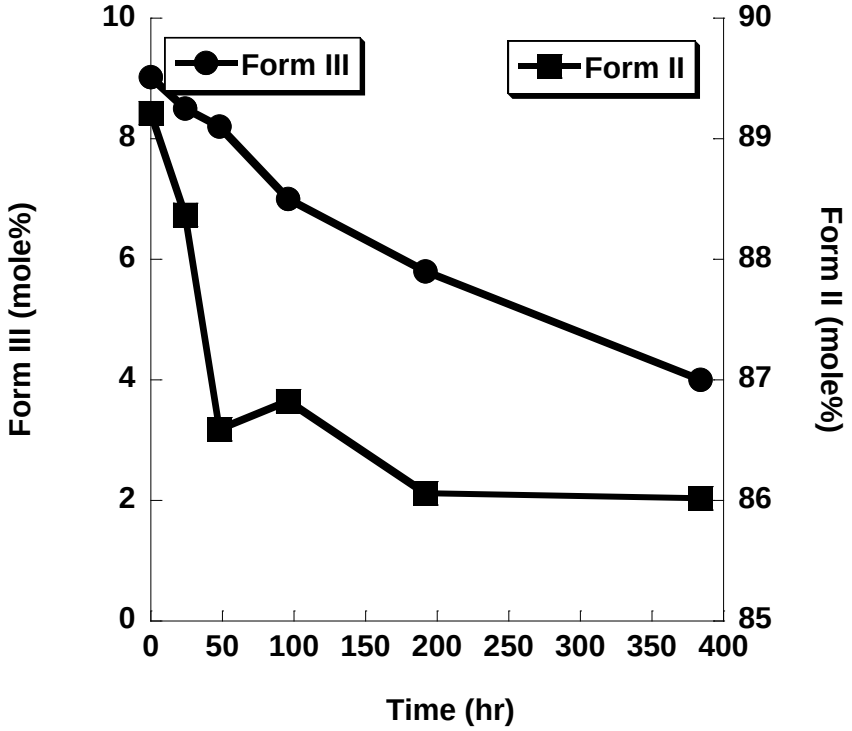

Figure IV- 8. Form II and III concentration time profiles of co-milled gabapentin Form II with starch stored at 40 ºC/48 %RH.

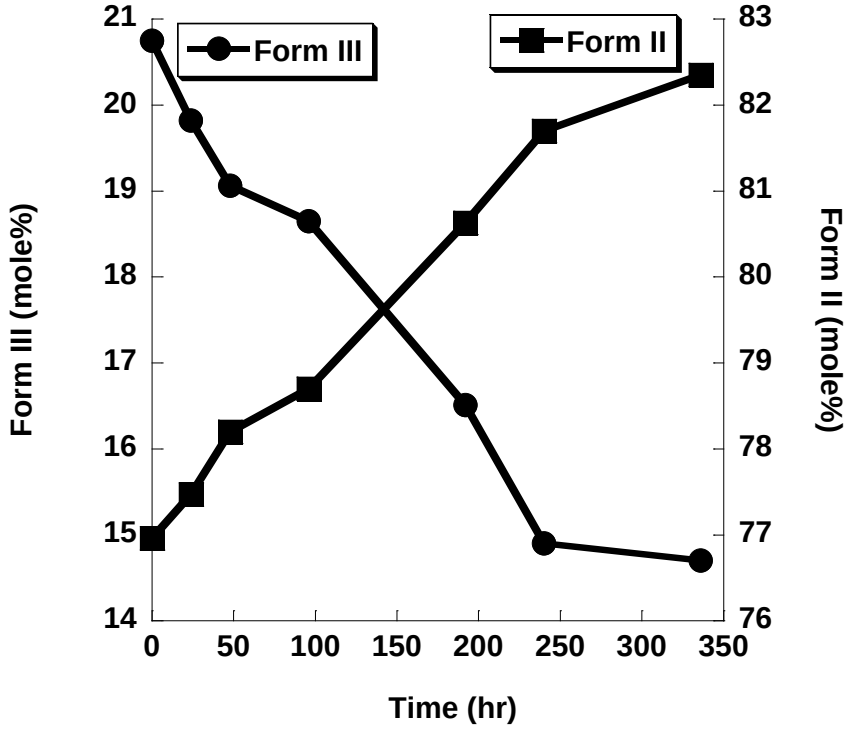

Figure IV- 9. Form II and III concentration time profiles of co-milled gabapentin Form II with HPC stored at 40 ºC/48 %RH.

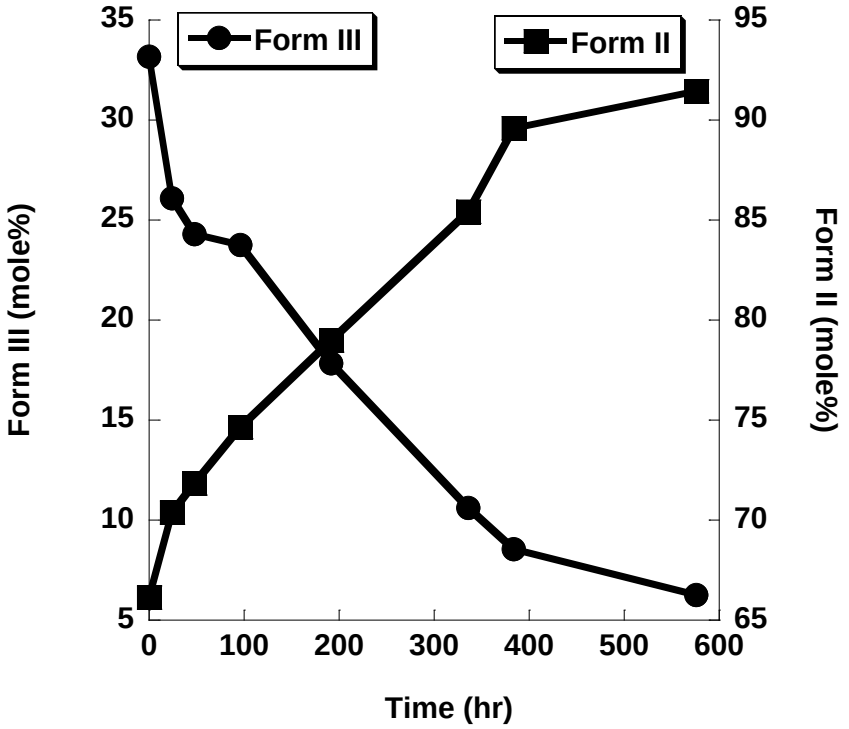

The Environmental Effects on Polymorphic Transformation Kinetics

The effects of temperature and humidity on polymorphic transformation of reaction mixtures containing inorganic ($CaHPO_4$ and SiO_2) and organic (starch and HPC) excipients were investigated by measuring changes in II and III concentrations over time at various thermal (40, 50 and 60 °C) and humidity (10 and 50 %RH) conditions.

Concentrations of III in reaction mixtures containing $CaHPO_4$ stored at 10 %RH decreased with increased storage temperature [Figure IV-10A]. Similar effects on III loss profiles at 50 %RH were observed [Figure IV-10B]. At every storage temperature, rates of III loss at 50 %RH [Figure IV-10B] were 2-fold greater than those observed at 10 %RH [Figure IV-10A]. At 10 %RH and at any temperature, the rate of II formation as a consequence of III➔II was greater than the rate of II loss [Figure IV-11 (A-C)]. However, eventually the rate of II formation became competitive or less than the rate of

II loss due to chemical instability [Figure IV-11 (B-C)]. In contrast at 50 %RH, concentrations of II in reaction mixtures stored at various temperatures increased with commensurate decreases in III concentrations [Figure IV-12 (A-C)].

Figure IV- 10. Form III concentration time profiles of co-milled gabapentin Form II with $CaHPO_4$ stored under various temperatures (●: 40 ºC, ■: 50 ºC, and ♦: 60 ºC) and humidity conditions; 10 %RH (A) and 50 %RH (B).

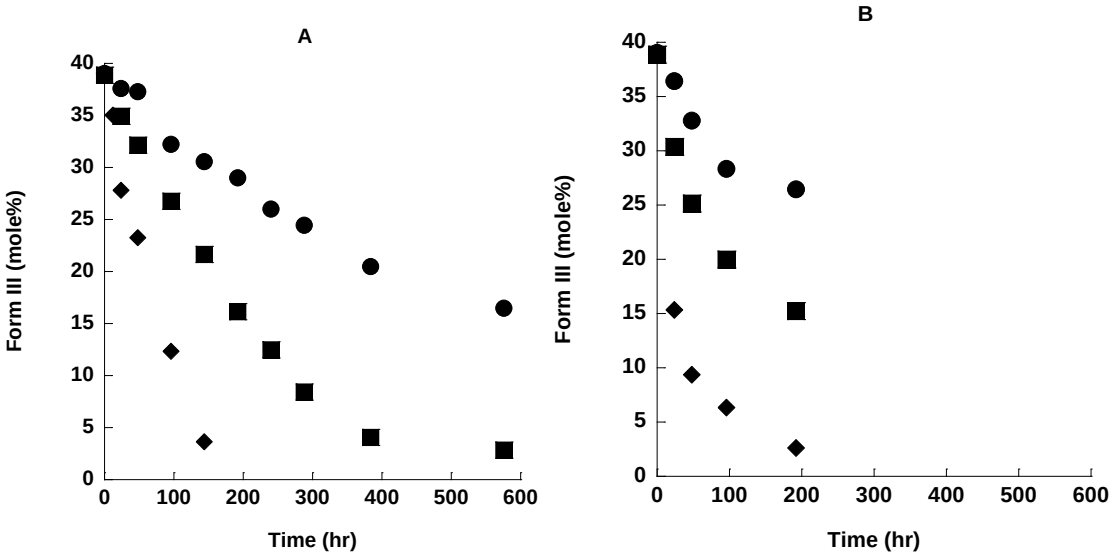

Figure IV- 11. Form II and III concentration time profiles of co-milled gabapentin Form II with $CaHPO_4$ stored at 10 %RH/40 ºC (A), 50 ºC (B) and 60 ºC (C).

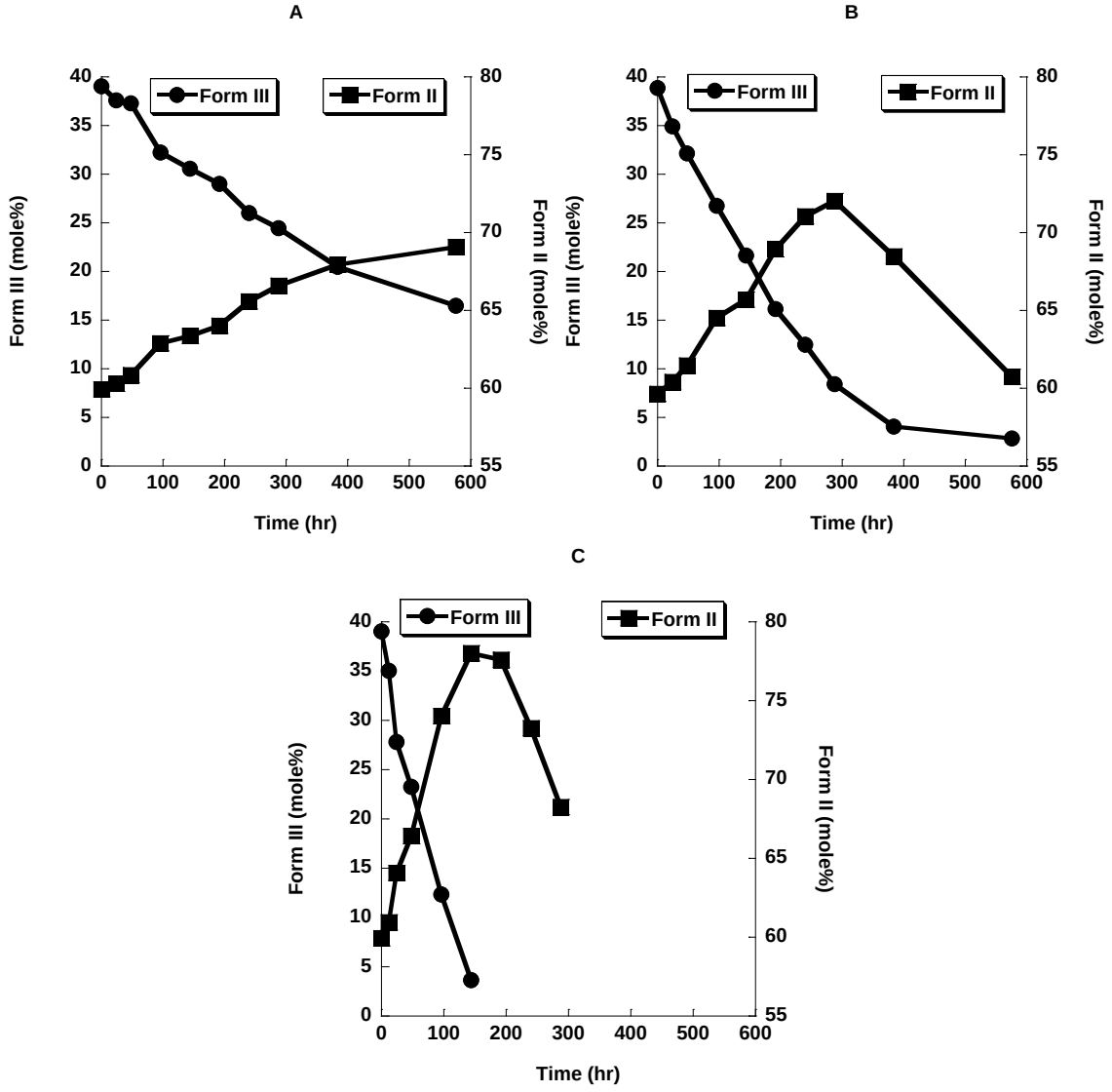

Figure IV- 12. Form II and III concentration time profiles of co-milled gabapentin Form II with $CaHPO_4$ stored at 50 %RH/40 ºC (A), 50 ºC (B) and 60 ºC (C).

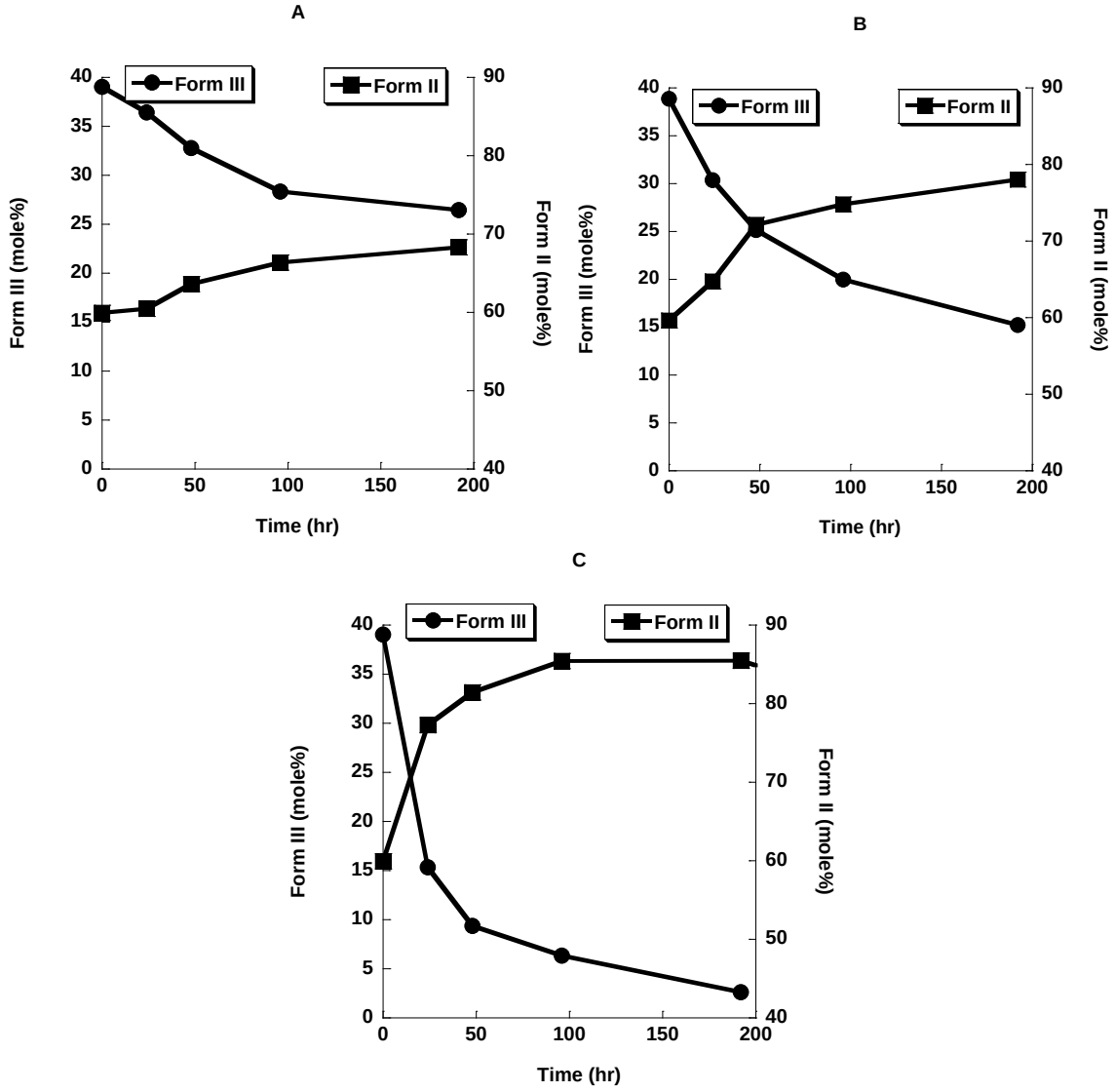

For reaction mixtures containing SiO_2, temperature facilitated the loss of III more markedly than did humidity [Figure IV-13A and 13B]. At every storage temperature, rates of III loss at 10 %RH [Figure IV-13A] and 50 %RH [Figure IV-13B] were indistinguishable. Rate of II loss in reaction mixtures stored at 10 %RH [Figure IV-14 (A-C)] and 50 %RH [Figure IV-15 (A-C)] increased with increased temperature. Additionally, the rates of II loss at 10 and 50 %RH were indistinguishable, thereby indicating less humidity effect on the decreased amounts of II and III in the mixtures containing SiO_2. Since the initial levels of III in SiO_2 reaction mixtures were low (< 10 mole %), these results suggest that the predominant substrate loss pathway (i.e., lactamization) is not very sensitive to moisture.

Figure IV- 13. Form III concentration time profiles of co-milled gabapentin Form II with SiO_2 stored under various temperatures (●: 40 ºC, ■: 50 ºC, and ♦: 60 ºC) and humidity conditions; 10 %RH (A) and 50 %RH (B).

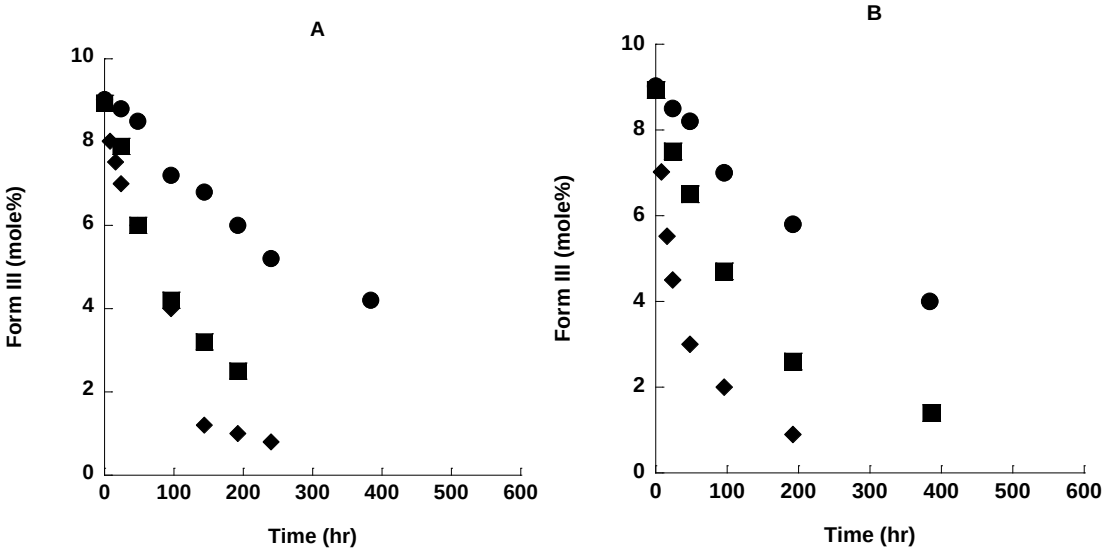

Figure IV- 14. Form II and III concentration time profiles of co-milled gabapentin Form II with SiO_2 stored at 10 %RH/40 ºC (A), 50 ºC (B) and 60 ºC (C).

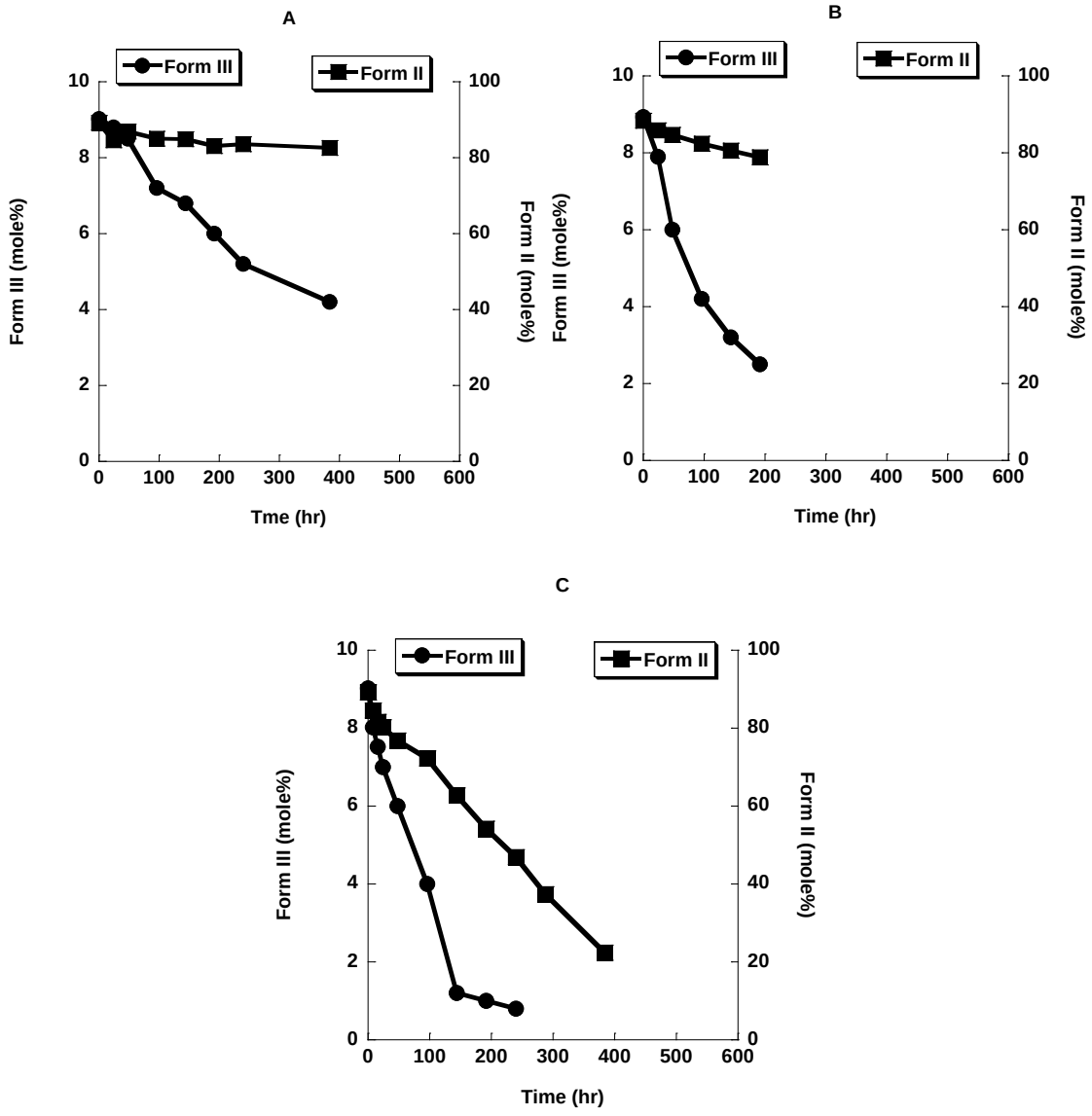

Figure IV- 15. Form II and III concentration time profiles of co-milled gabapentin Form II with SiO_2 stored at 50 %RH/40 ºC (A), 50 ºC (B) and 60 ºC (C).

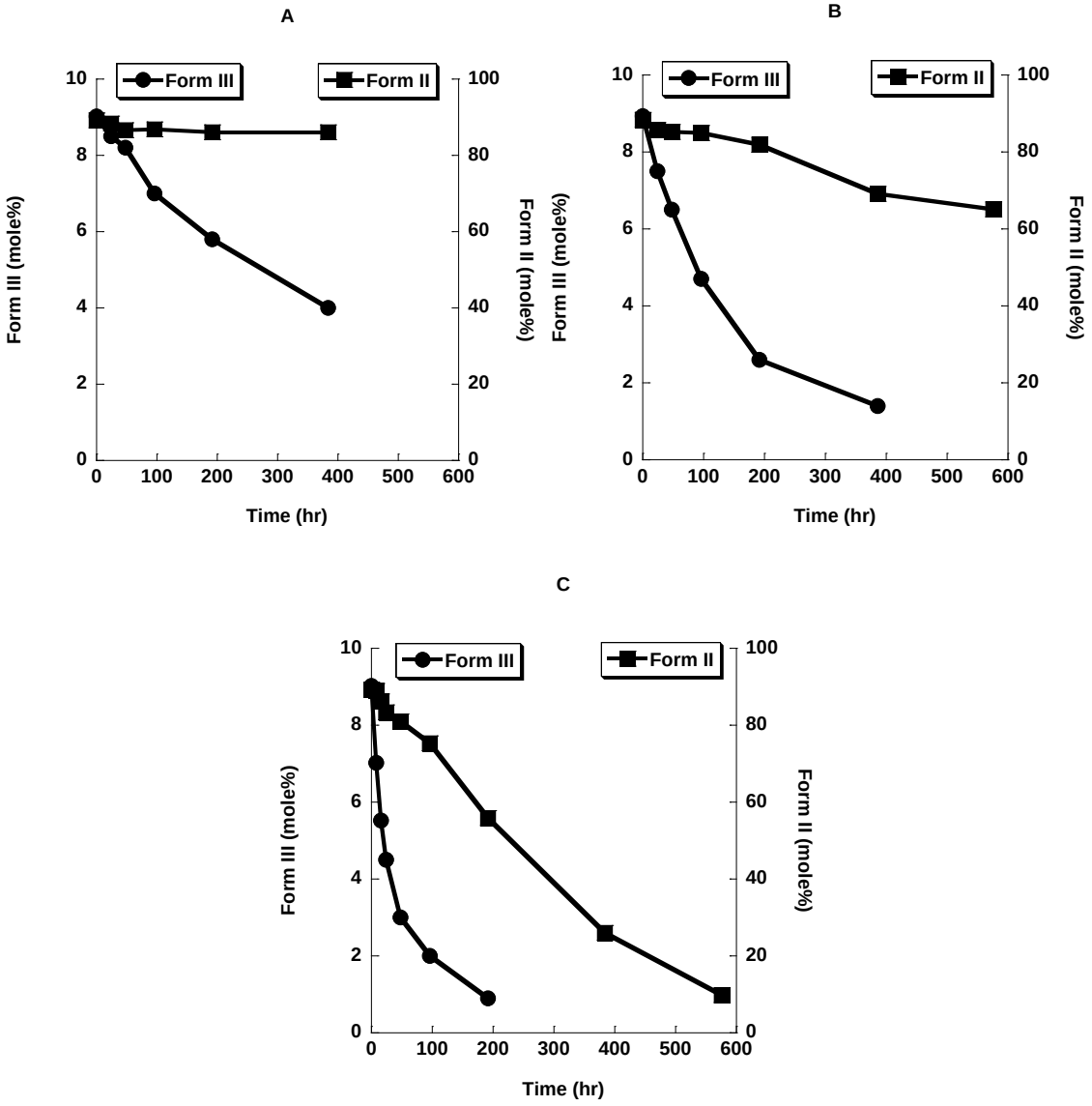

The rate of III loss in the presence of starch at 10 %RH increased noticeably with increased storage temperature [Figure IV-16A]. Similar temperature effects for III loss kinetics were observed at 50 %RH [Figure IV-16B]. At every storage temperature, the rates of III loss at 50 %RH [Figure IV-16B] were 2.5-fold greater than at 10 %RH [Figure IV-16A]. Some of the concentration time profiles for polymorph II in the presence of starch were similar in shape to those associated with $CaHPO_4$ reaction mixtures [Figure IV-17 and IV-18 (A-C)]. At 10 %RH and 60 °C, the concentration of II initially increased and then decreased [Figure IV-17C]. At 10 %RH and storage temperatures at 40 and 50 °C, the concentration of II was largely at steady state wherein its rate of formation from polymorph III was essentially equal to its rate of covalent transformation to lactam [Figure IV-17A and 17B]. Similar behavior was observed at 50 %RH, although the rates of III loss (and consequently, II formation) were greater than at 10 %RH [Figure IV-18 (A-C)].

Figure IV- 16. Form III concentration time profiles of co-milled gabapentin Form II with starch stored under various temperatures (●: 40 ºC, ■: 50 ºC, and ♦: 60 ºC) and humidity conditions; 10 %RH (A) and 50 %RH (B).

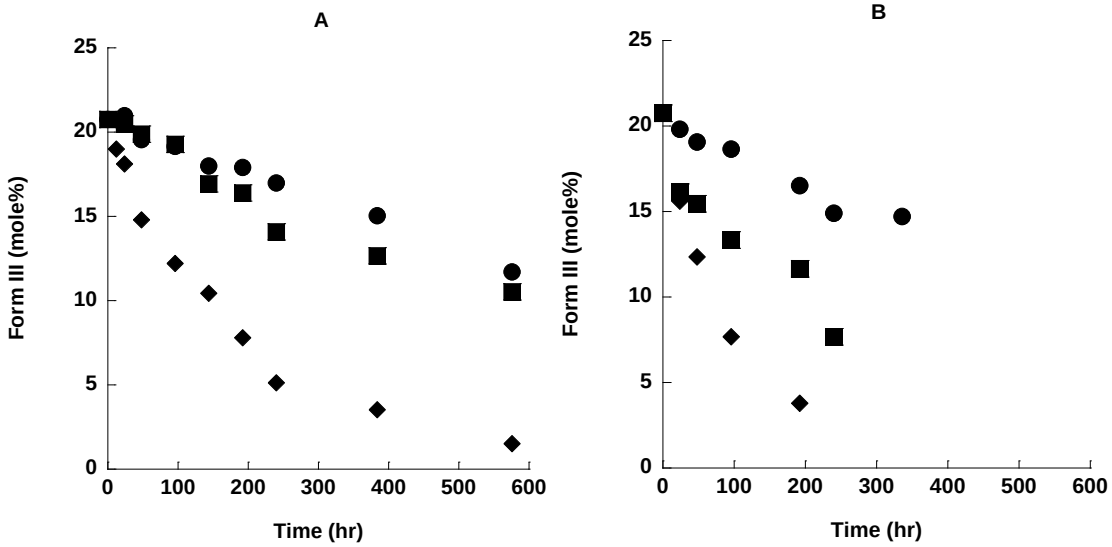

Figure IV- 17. Form II and III concentration time profiles of co-milled gabapentin Form II with starch stored at 10 %RH/40 ºC (A), 50 ºC (B) and 60 ºC (C).

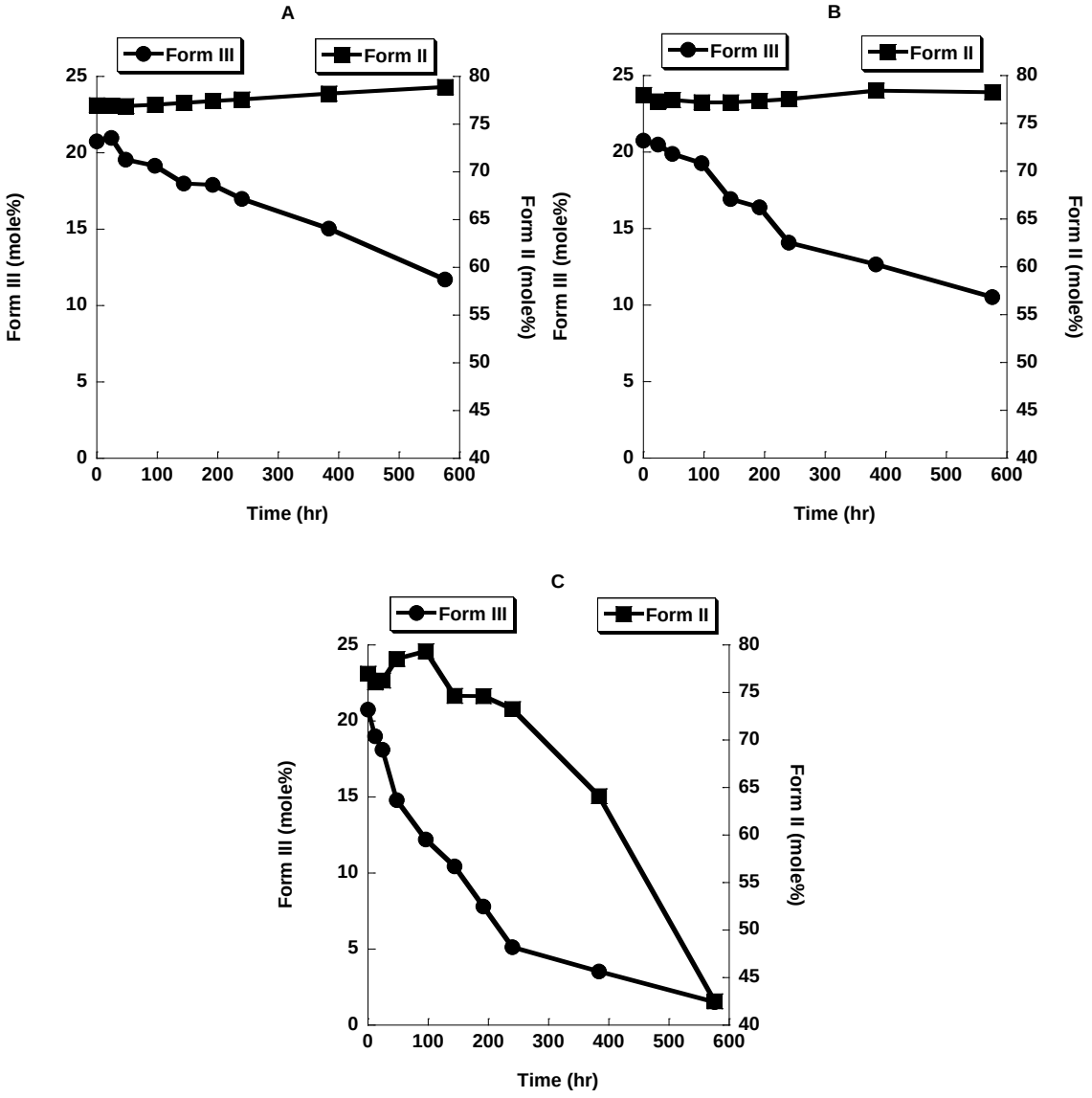

Figure IV- 18. Form II and III concentration time profiles of co-milled gabapentin Form II with starch stored at 50 %RH/40 ºC (A), 50 ºC (B) and 60 ºC (C).

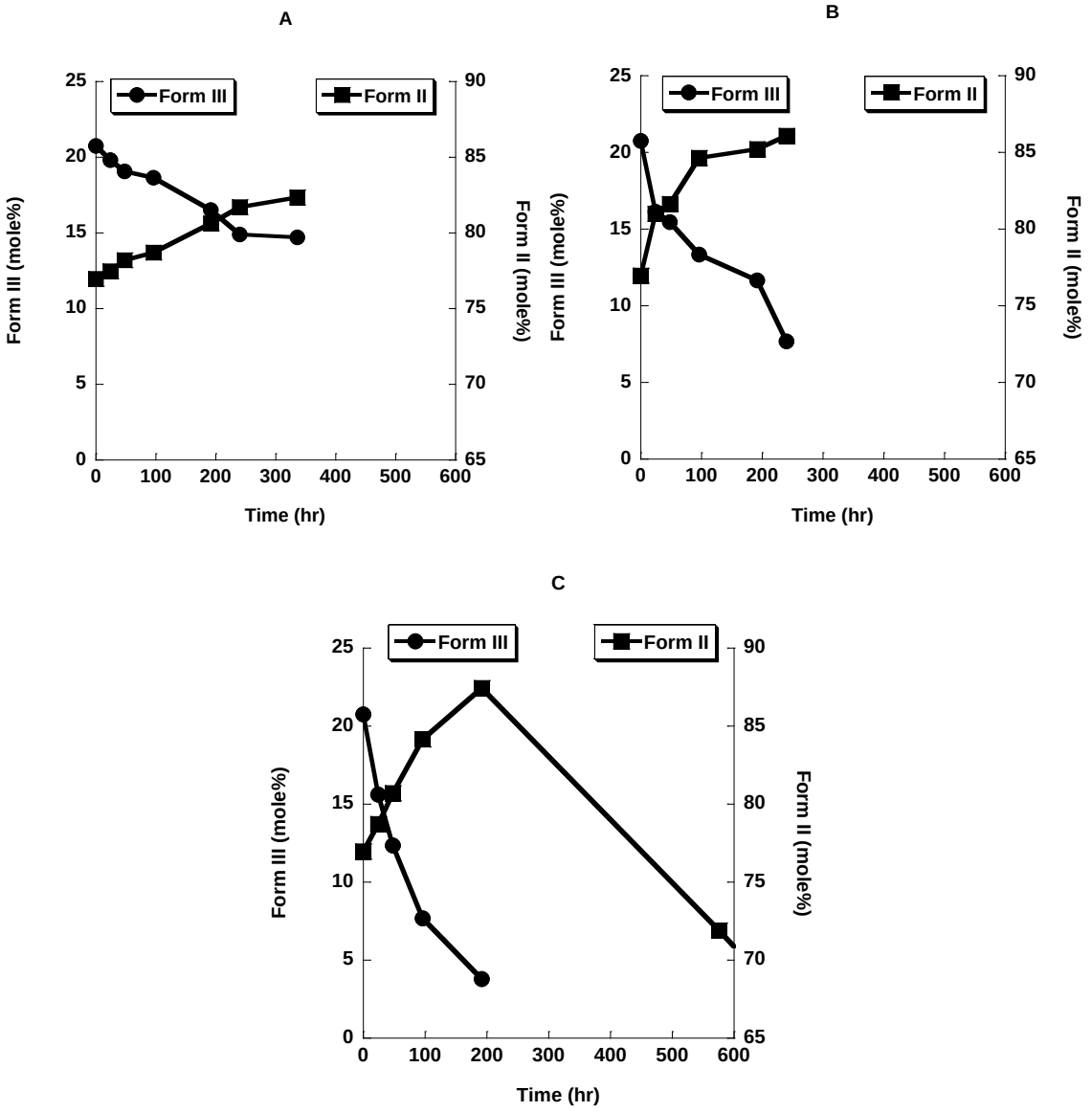

As was observed with other excipient mixtures ($CaHPO_4$, SiO_2 and starch), the rate of III loss in the presence of HPC at 10 %RH increased with storage temperature [Figure IV-19A]. Similar storage temperature effects on III loss profiles at 50 %RH were observed [Figure IV-19B]. At every storage temperature, rates of III loss at 50 %RH [Figure IV-19B] were 10-fold greater than at 10 %RH [Figure IV-19A]. Once again, the polymorph II concentration time profiles were consistent with the net effects of III➔II and II lactamization rates [Figure IV-20 and IV-21 (A-C)].

Figure IV- 19. Form III concentration time profiles of co-milled gabapentin Form II with HPC stored under various temperatures (●: 40 ºC, ■: 50 ºC, and ♦: 60 ºC) and humidity conditions; 10 %RH (A) and 50 %RH (B).

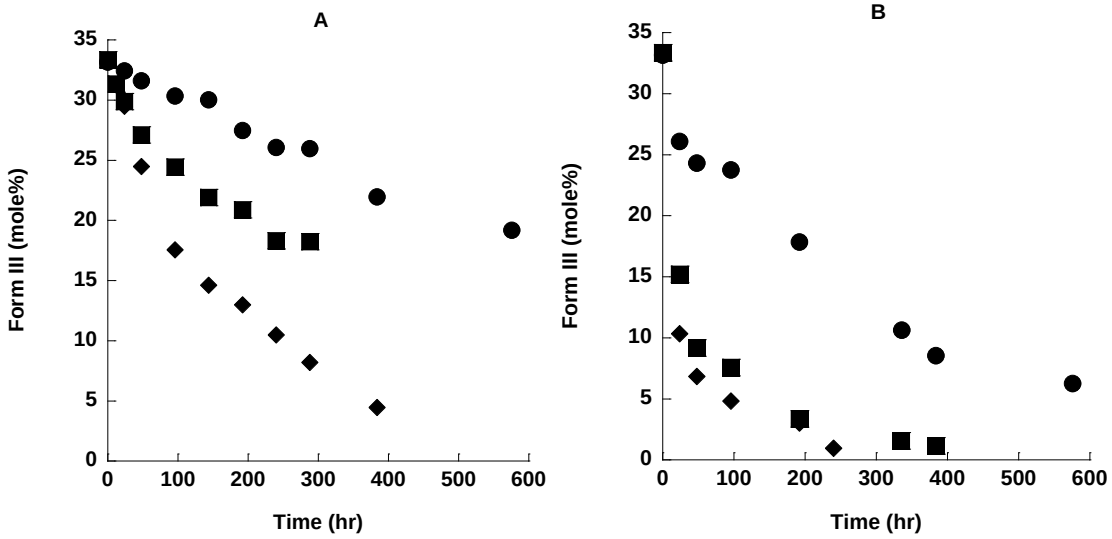

Figure IV- 20. Form II and III concentration time profiles of co-milled gabapentin Form II with HPC stored at 10 %RH/40 ºC (A), 50 ºC (B) and 60 ºC (C).

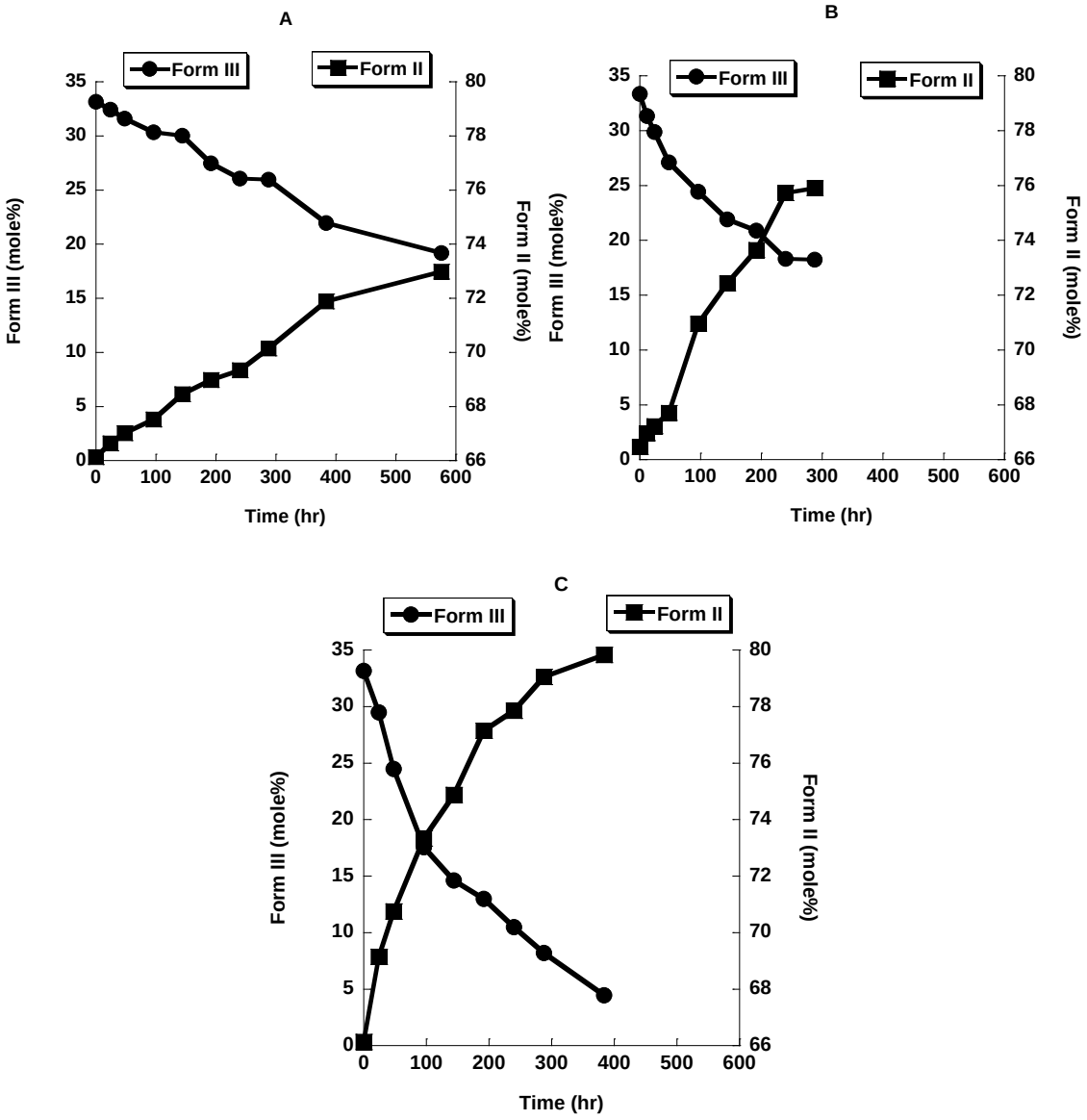

Figure IV- 21. Form II and III concentration time profiles of co-milled gabapentin Form II with HPC stored at 50 %RH/40 ºC (A), 50 ºC (B) and 60 ºC (C).

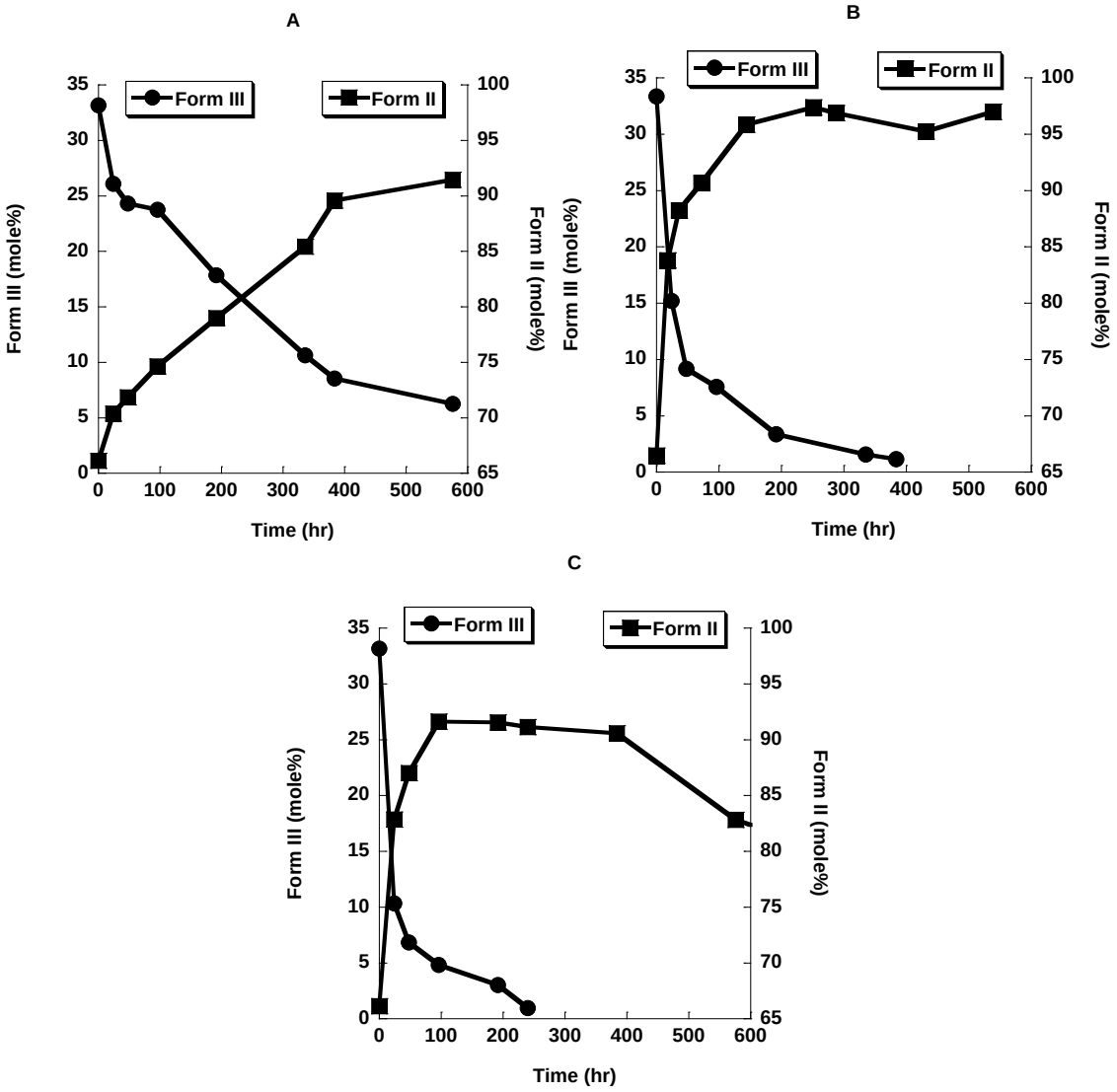

The magnitude of the humidity effect on the rate of III➔II in reaction mixtures containing organic (starch and HPC) was greater than inorganic ($CaHPO_4$ and SiO_2) excipients. Rates of III loss of reaction mixtures containing HPC, starch and $CaHPO_4$ stored at 50 %RH, were 10, 2.5 and 2-fold greater than that observed at 10 %RH. For SiO_2 mixtures, no difference was observed.

The rates of III loss varied depending upon excipient type. For example, although the initial concentration of III after milling in $CaHPO_4$ mixtures (39 mole %) was present to the same extent as HPC (33 mole %), the rate of III loss of HPC mixtures was much greater (3-fold) than the mixtures containing $CaHPO_4$ [Figure IV-22].

The polymorph II concentration time profiles of HPC, $CaHPO_4$ and starch at 10 and 50 %RH were consistent with the net effects of II formation (III➔II) and loss rates. For SiO_2 mixtures, the rates of II loss at 10 and 50 %RH were not different.

Figure IV- 22. Form III concentration time profiles of co-milled gabapentin Form II with $CaHPO_4$ and HPC stored at 50 ºC/47.5 %RH.

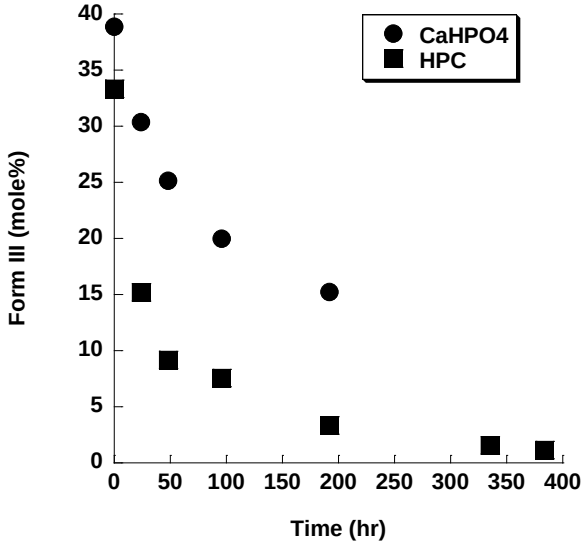

According to literature reports, polymorphic transformation may start at crystal defects and continue by a progressive propagation of the reaction interface. (15) The transformation rates may depend on the mobility of molecules in the solid; therefore, the rates vary considerably with humidity. Water may serve as a nucleation catalyst, thereby facilitating the transformation. For example, the effects of humidity on polymorphic transformation kinetics of milled phenylbutazone (β➔δ) were studied under storage conditions at 60 °C/0, 50, 70 and 80 %RH. The transformation appeared to follow first-order kinetics during storage in the presence of moisture. The transformation at crystal defects was facilitated by water molecules acting as a nucleation catalyst. (17) Similar humidity effect on polymorphic transformation (II➔I) of milled fostedil was observed during storage at 40 °C/80 %RH. (4)

In the presence of excipients, the humidity effect may be altered by the ability of excipients to interfere with hydrogen bonding between substrate and water at the surface and to alter the degree of contact between drug, excipient and water vapor. (20) The influence of excipient-water interactions on solid state transformation of pharmaceutical compounds has been reported. Mixtures of amorphous nifedipine and microcrystalline cellulose (MCC), methylcellulose (MC) and starch were used to determine the crystallization rates upon storage at 50 °C/13-60 %RH. The crystallization rates of mixtures with excipients were slower than those observed in the absence of excipient due to the decreases in water mobility in contact with nifedipine. Starch was able to decrease the water mobility more than MCC or MC; therefore, the crystallization rates were slower than those observed in the mixtures with MCC or MC. (21)

In our studies, humidity facilitated polymorphic transformation of III➔II. No other detectable polymorphs were present after milling or during storage based on ^{13}C ssNMR measurement. The magnitude of humidity effect in the presence of excipient was profound and altered by excipient type. One possible explanation is that the humidity effect on III➔II may be influenced by the ability of excipient to interfere with surface hydrogen bonding.

Conclusion

In Chapter III, the effects of excipient, temperature, and humidity on chemical degradation pathway of gabapentin (II and III) were described in qualitative terms. In this chapter, we have presented additional results that demonstrate the rate of polymorph III loss is also due to the transition of III➔II and indirectly due to the chemical loss of III. The rate of II concentration change was observed to be directly due to its formation from polymorph III and loss to lactam. The quantitative description of the interrelationship between these covalent and physical transitions requires a complex kinetic model that describes the sequential, parallel, and reversible processes and accounts for the differential effects of humidity, temperature and reaction composition on the rates of each individual process. The development of this kinetic model is the subject of Chapter V.

Chapter IV References

1. Hüttenrauch R, Fricke S, Zielke P. Mechanical Activation of Pharmaceutical Systems. Pharmaceutical Research. 1985;2(6):302-306.
2. Saleki-Gerhardt A, Ahlneck C, Zografi G. Assessment of disorder in crystalline solids. International Journal of Pharmaceutics. 1994;101(3):237-247.
3. Brittain HG. Effects of mechanical processing on phase composition. Journal of Pharmaceutical Sciences. 2002;91(7):1573-1580.
4. Takahashi Y, Nakashima K, Ishihara T, Nakagawa H, Sugimoto I. Polymorphism of Fostedil: Chracterization and Polymophic Change by Mechanical Treatments. Drug Development and Industrial Pharmacy. 1985;11(8):1543-1563.

5. Otsuka M, Kaneniwa N. Effect of seed crystals on solid-state transformation of polymorphs of chloramphenicol palmitate during grinding. Journal of Pharmaceutical Sciences. 1986;75(5):506-511.
6. Otsuka M, Otsuka K, Kaneniwa N. Relation between polymorphic transformation pathway during grinding and the physicochemical properties of bulk powders for pharmaceutical preparations. Drug Development and Industrial Pharmacy. 1994;20(9):1649-1660.
7. Bauer-Brandl A. Polymorphic transitions of cimetidine during manufacture of solid dosage forms. International Journal of Pharmaceutics 1996;140(2):195-206.
8. Zhang GGZ, Gu C, Zell MT, Burkhardt RT, Munson EJ, Grant DJW. Crystallization and transitions of sulfamerazine polymorphs. Journal of Pharmaceutical Sciences. 2002;91(4):1089-1100.
9. De Gusseme A, Neves C, Willart JF, Rameau A, Descamps M. Ordering and disordering of molecular solids upon mechanical milling: the case of fananserin. Journal of Pharmaceutical Sciences. 2008;97(11):5000-5012.
10. Matsuoka M, Hirata J, Yoshizawa S. Kinetics of solid-state polymorphic transition of glycine in mechano-chemical processing. Chemical Engineering Research and Design. 2010;88(9):1169-1173.
11. Shakhtshneider TP, Boldyrev VV. Phase transformations in sulfathiazole during mechanical activation. Drug Development and Industrial Pharmacy 1993;19(16):2055-2067.
12. Hu Y, Erxleben A, Hodnett BK, Li B, McArdle P, Rasmuson ÅC, Ryder AG. Solid-State Transformations of Sulfathiazole Polymorphs: The Effects of Milling and Humidity. Crystal Growth & Design. 2013;13(8):3404-3413.
13. Lin S-Y, Hsu C-H, Ke W-T. Solid-state transformation of different gabapentin polymorphs upon milling and co-milling. International Journal of Pharmaceutics. 2010;396(1–2):83-90.
14. Dempah K, Barich D, Kaushal A, Zong Z, Desai S, Suryanarayanan R, Kirsch L, Munson E. Investigating Gabapentin Polymorphism Using Solid-State NMR Spectroscopy. AAPS PharmSciTech. 2013;14(1):19-28.
15. Li H, Stowell JG, He X, Morris KR, Byrn SR. Investigations on solid-solid phase transformation of 5-methyl-2-[(4-methyl-2-nitrophenyl)amino]-3-thiophenecarbonitrile. Journal of Pharmaceutical Sciences. 2007;96(5):1079-1089.
16. Morris KR, Griesser UJ, Eckhardt CJ, Stowell JG. Theoretical approaches to physical transformations of active pharmaceutical ingredients during manufacturing processes. Advanced Drug Delivery Reviews. 2001;48(1):91-114.
17. Matsuda Y, Tatsumi E, Chiba E, Miwa Y. Kinetic study of the polymorphic transformations of phenylbutazone. Journal of Pharmaceutical Sciences. 1984;73(10):1453-1460.
18. Braga D, Grepioni F, Maini L, Rubini K, Polito M, Brescello R, Cotarca L, Duarte MT, Andre V, Piedade MFM. Polymorphic gabapentin: thermal behaviour, reactivity and interconversion of forms in solution and solid-state. New Journal of Chemistry. 2008;32(10):1788-1795.
19. Zong Z. Studies on the mechanisms of solid state and solution instability of drugs. The University of Iowa; 2011. p. 135.

20. Zografi G, Kontny MJ. The interactions of water with cellulose- and starch-derived pharmaceutical excipients. Pharmaceutical Research. 1986;3(4):187-194.
21. Aso Y, Yoshioka s, Kojima S. Relationship between water mobility, measured as nuclear magnetic relaxation time, and the crystallization rate of amorphous nifedipine in the presence of some pharmaceutical excipients. Chemical and Pharmaceutical Bulletin. 1996;44(5):1065-1067.

CHAPTER V

QUANTITATIVE KINETIC MODEL FOR SOLID-STATE DEGRADATION OF GABAPENTIN/EXCIPIENT MIXTURES

Introduction

Solid state drug degradation rates are generally complicated by the fact that molecules can exist in multiple states, including crystalline bulk, crystalline surface, crystal defect and amorphous. In each state, drug molecules are capable of undergoing covalent and/or non-covalent changes at distinct rates due to the differences in mobility and their environment; therefore, the overall degradation rate is potentially complex and difficult to use for elucidating mechanisms in those states. (1-3) In some cases, degradation pathways include formation of a metastable intermediate that can undergo degradation in secondary processes resulting in a lag phase in the appearance of the final degradation product. Moreover, degradation products may act as catalytic sites by creating disorder in which case the resultant kinetics as autocatalytic. (4)

A degradation mechanism describes the transformation of reactant to degradation product in a series of elementary steps. A process for mechanism elucidation is shown in Figure V-1. First, major degradation products and possible intermediates are identified. Then, reaction order for each step and initial conditions are determined. Next, a degradation scheme or model describing the relationships between reactants and degradation products is developed and shown to be consistent with kinetic data. The rate law that describes the quantitative relationship between the rate of reaction and the concentrations of reactants, intermediates and products present in the reaction mixture is determined. Finally, a mechanism for each process depicted in the degradation scheme is

devised. Each mechanism is a postulate that is consistent with kinetic data, structural characterizations of reaction components, and chemical intuition.

Figure V- 1. Process of mechanism elucidation.

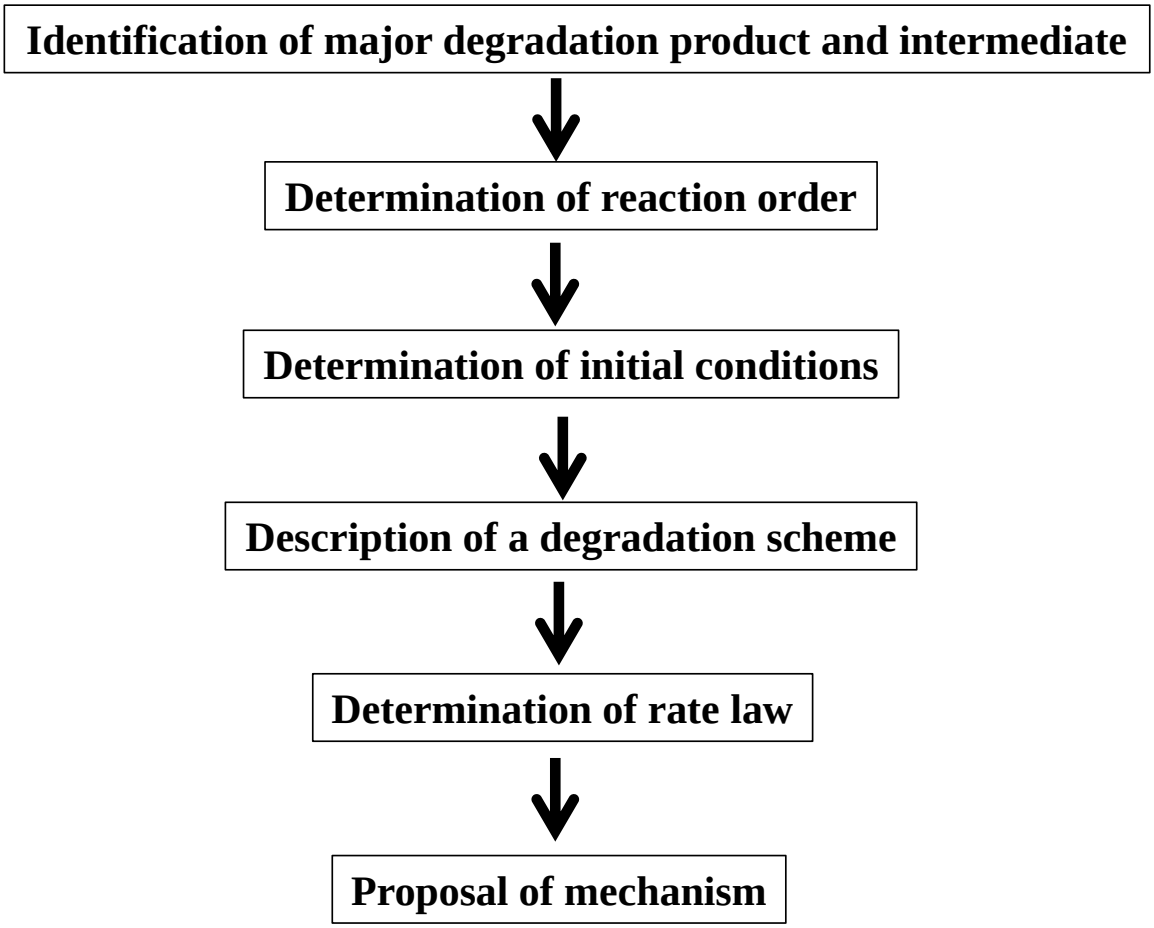

Solid State Drug Degradation Kinetics

Solid state degradation kinetics has been described using various models. (5) The Prout-Tompkins model is used to describe degradation of crystalline drugs. The initial reaction starts at crystal imperfection sites referred to as “nuclei”. The subsequent step is propagation whereby the reaction proceeds at the interface between substrate and product. This step is second order: proportional to the concentrations of substrate and product. The resultant concentration time profiles are sigmoid for loss of substrate or appearance of product. (4, 6, 7) The generalized Prout-Tompkins equation was modified

by Jacobs to account for rapid initial degradation due to the pre-existing concentrations of reactive nuclei. This modification was shown to fit experimental data over a broader range of circumstances than the original equation. (8)

A two-phase model was proposed to describe the solid state degradation of aspartame wherein the drug substance exists in two separate phases: intact crystalline and disorder state with higher molecular mobility and greater reactivity. These two states degraded in parallel by zero-order kinetics. (9) For the solid state degradation of tetraglycine methyl ester, Zografi and co-workers modified the two-phase model wherein parallel degradation occurs by first-order kinetics. (10)

The isoconversion model was proposed by Waterman. In this model, crystalline substrate degrades through the formation of a reactive intermediate (crystal defects) which can reversibly revert to intact crystalline or subsequently degrade to product. In the application of this model to the solid state degradations of ascorbic acid and aspirin tablets, each step was described by first-order kinetics. (11)

Typically, first-order or autocatalytic kinetic models have been generally used to describe the drug degradation in solids. For example, the degradation kinetic profiles of vitamin A palmitate in dry-slugged, mannitol-base, multivitamin chewable tablets were reported to follow first-order kinetics during storage in the presence of moisture. (12, 13) The first-order degradation of vitamin A, thiamine, and ascorbic acid in three multi-vitamin tablet formulations containing sucrose or mannitol as filler were observed after exposure to moisture (1-4 %) at room temperature for 38 months. (14, 15) The solid state degradation of ampicillin sodium salt under various thermal-stressed conditions was described by a model incorporating three sequential first-order processes. (16) The solid

state degradation of amoxicillin sodium salt was described by a serial reaction consisting of two first-order kinetics steps; however, amoxicillin trihydrate appeared to degrade in one step according to Prout-Tompkins (autocatalytic) kinetics. (17) The thermal-induced degradation profiles of penicillin G potassium salt in solid phase were successfully described by a Prout-Tompkins model. (18)

Gabapentin Solid State Degradation

A kinetic model has been recently published to describe the solid state degradation of milled gabapentin during storage under various controlled-temperature and humidity conditions by Zong et al. (19) Attempts were made to describe lactam formation profiles using the Prout-Tompkins model; however, this model failed to describe the initial rapid rate of lactamization. Similarly, the two-phase first-order models of Zografi and Waterman failed to describe the subsequent rate of lactamization. However, a combination of the two-phase Waterman model with Prout-Tompkins kinetics successfully described gabapentin lactamization.

The Zong model structure is shown in Figure V-2. No polymorphic forms other than II were observed in his experiments. Therefore, the Zong model was composed of II, II* and lactam. II* refers to a chemically-intact but physically-disordered state of II caused by milling. The inclusion of II* in the Zong model is consistent with the concept of "reactive" or "high-energy" phases included in Zografi, Waterman, and Skwierczynski models. (9-11)

Figure V- 2. Gabapentin solid state degradation model (Zong model (19)).

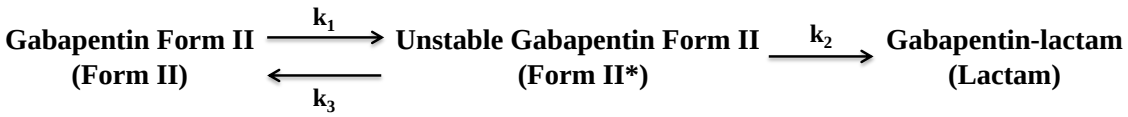

Effect of Milling on Crystalline Drug Substances

Milling-induced disorder of crystalline drug substances is typically described as "crystal defects" or "mechanical activation". This disorder may be localized at the surface and/or within the crystal lattice. The extent of disorder is not easily quantified by conventional techniques such as thermal analysis, electron microscopy and density determination. (20) A progressive accumulation of crystal defects beyond a critical defect concentration transforms a crystalline material to an amorphous state. The critical defect concentration is drug substance specific; therefore, some crystalline substances with severe defects may never become amorphous. (21)

Cryogenic milling has been used to generate the mechanically-activated drug substances for a number of model compounds including acetaminophen, aspirin, salicylamide, griseofulvin and felodipine.(22, 23) Several characterization methods were used to analyze cryogenically-milled materials including X-ray powder diffraction (XRPD), Raman spectroscopy and inverse gas chromatography (ICG). These methods were capable of distinguishing between intact crystals and defects or amorphous materials. (21, 23) For example, the presence of disorder in cryogenically-milled acetaminophen, aspirin and salicylamide resulted in decreased X-ray peak intensities. The lack of a diffuse halo pattern indicated the absence of amorphous state. ICG was used to demonstrate the relationship between mechanically-induced crystal surface energy increases and increased instability of ketoconazole and griseofulvin. However, the

method for quantifying intact crystals and defects in cryogenic-milled samples has not been identified. (24)

Arrhenius and Modified Arrhenius Equations

The Arrhenius equation has been used to describe the effect of temperature on solid state reaction rates and to predict appropriate temperature and shelf-life for drug products. (25-27) The natural logarithmic degradation rate constant (k) is plotted against the reciprocal of the absolute temperature $\left(\frac{1}{T}\right)$. As depicted in Equation V-1, A is the pre-exponential (frequency) factor; E_a is the activation energy, and R is the universal gas constant. (28)

To study the impact of humidity on drug degradation in solid state, the Arrhenius equation has been extended by adding a term composed of the product of a humidity constant (β) and storage humidity $(\%RH)$ [Equation V-2]. Reported β values are typically in the range from 0 to 0.2 where a value of 0 indicates no humidity influence on degradation rate constant. (11, 29-31)

$$\ln k = lnA - \frac{E_a}{R.T} \qquad \text{Equation V-1}$$

$$\ln k = lnA - \frac{E_a}{R.T} + \beta(\%RH) \qquad \text{Equation V-2}$$

The activation energy for gabapentin lactamization in solution (pH 6) was estimated to be 140-160 kJ/mol. (32) In the solid state, the temperature effect on lactamization of milled gabapentin has been reported. In accordance with Zong model [Figure V-2], the activation energy for lactam formation from disordered gabapentin (II*➔lactam) was estimated to be 69 kJ/mole, whereas the activation energy for the formation of disordered gabapentin (II➔II*) was estimated to be 89 kJ/mole. Additionally, the humidity was shown to primarily affect the conversion of II*➔II, and

the β value was estimated to be 0.2. The rapid conversion of II*➔II at higher humidity was responsible for an overall decrease in the rate of lactam formation. (19)

The Bayesian Approach and Markov Chain Monte Carlo Simulations

In the Bayesian approach, inferences about unknown parameters are a process of learning from data. In this process, prior information is incorporated, then observations are made, and the prior knowledge is updated to create posterior information. In contrast to obtaining point estimates from a nonlinear regression, Bayesian parameter estimation treats the model parameters as random variables and allows the modeler to discover the distribution that best describes them. Bayes' rule provides a mathematical framework to accomplish Bayesian parameter estimation [Equation V-3]. In this equation, $P_{Posterior}$ is the posterior probability and L is the likelihood function measuring how well the model predictions agree with the observation based on a probability distribution. The likelihood function (L) is defined by Equation V-4 where Y_i is observed data, $\hat{Y}_i(\theta)$ is predicted value for specific set of model parameters, n is the number observation and σ_i is standard deviation for the i^{th}data point. The prior probability distribution (P_{Prior}) represents the modeler's belief before experimentation. In the Bayesian approach, posterior information is a combination of both prior knowledge and experimental data. This results in the posterior distribution for a particular parameter that leverages both prior knowledge and experimental observation, thereby providing a narrower range of possible values for model parameter estimates. (33)

$$P_{Posterior} = \frac{L.P_{Prior}}{\int L.P_{Prior}} \qquad \text{Equation V-3}$$

$$L(\theta) = \prod_{i=1}^{n_{points}} \frac{1}{\sigma_i\sqrt{2\pi}} exp\left[-\frac{(Y_i-\hat{Y}_i(\theta))^2}{2\sigma_i^2}\right] \qquad \text{Equation V-4}$$

Multidimensional integrals contained in simple equations cannot be analytically solved for most models of interest. Markov Chain Monte Carlo (MCMC) provides a way to sample the posterior parameter distribution without knowing the multidimensional integral value. These posterior parameter distributions can then be used to make inferences about the properties of the system under study. (34) While the full historical development of MCMC is beyond the scope of this discussion, it is worth mentioning that the sampler used in this work is based on the well-known Metropolis-Hastings algorithm. (35, 36) This algorithm is adapted from a random walk that uses acceptance/rejection rules to converge to a specific target distribution. Model parameters are generally assigned initial values by random sampling from prior distribution. Thousands of samples are usually required. The MCMC inputs require experimental observations, a model, a likelihood function, prior distributions and initial values for model parameters. (37)

Methods

Degradation Model Building for Gabapentin/Excipient Mixtures

A schematic overview of the experimental approach used to quantitatively study the effects of compositional and environmental variations on the kinetics of chemical and physical gabapentin instability is depicted in Figure V-3. Reaction mixtures were generated by co-milling gabapentin Form II with various excipients including inorganic ($CaHPO_4$ and SiO_2) and organic (starch and HPC) compounds. After milling, these reaction mixtures contained gabapentin Form II, III and gabapentin-lactam (lactam) as measured by using ^{13}C ssNMR and HPLC. As summarized in Table V-1, the environmental effects were studied by storing reaction mixtures at 40, 50, 60 ^{o}C and 5,

10, 30, 50 %RH. The changes in polymorph and degradation product concentrations in the reaction mixtures were measured as a function of time. Degradation models that described the relationship between II, III and lactam in a series of sequential or parallel steps were developed based on analysis of the resultant concentration time profiles. Model parameters (including rate constants and humidity constants for individual pathways) were estimated by using the Bayesian approach.

In the Bayesian method, the model parameters were treated as random variables whose distributions were determined. Markov Chain Monte Carlo (MCMC) sampling was used by randomly sampling (Monte Carlo) parameter values (θ) from distributions and then adjusting the subsequent selections to achieve a better target for the posterior distribution via Markov chains. (33) The MCMC sampling method is more efficient than Monte Carlo methods but is still computationally challenging; therefore, nonlinear optimization was used to determine the initial estimates of model parameters for individual pathways. (38) These estimates were used as starting points for the MCMC sampling in the Bayesian estimation. The MCMC simulation using the Metropolis-Hastings algorithm was carried out to obtain posterior distributions for each parameter that described the likely values and associated uncertainty. A convergence assessment of Markov chain was diagnosed by observing a history plot which showed the paths of sampler output for each model parameter from every iterative step. The Markov chain converged when the sampled parameters were randomly distributed over sequential iterations and the sampling chain indicated no apparent trends. (34, 37)

The Advanced Modeling and Simulation Tool Kit (AMASTK, UI Copyright 2012) was used for nonlinear optimization, simulation and Bayesian estimation.

AMASTK was authored by Dr. Stephen Stamatis in R which is an open access programming language and software environment for data analysis and statistical applications. (39) An add-on package named *deSolve* in R was used to solve initial value problems in a system of ordinary differential equations (ODE) (40) that were constructed to describe time-dependent concentration changes in accordance with specific model structures. These model-specific ODE systems were numerically integrated using the *ode* function in the *deSolve* package. Another add-on package used was *FME* (41) which includes various functions to run complex model applications, such as sensitivity analyses and Monte Carlo analysis. Sensitivity analyses were used to investigate the influence of parameter variation on model outputs. *FME* was used to explore the effect of individual parameter variation on model output concentration as a function of time.

Figure V- 3. Schematic studies of solid state gabapentin degradation in the presence of excipient.

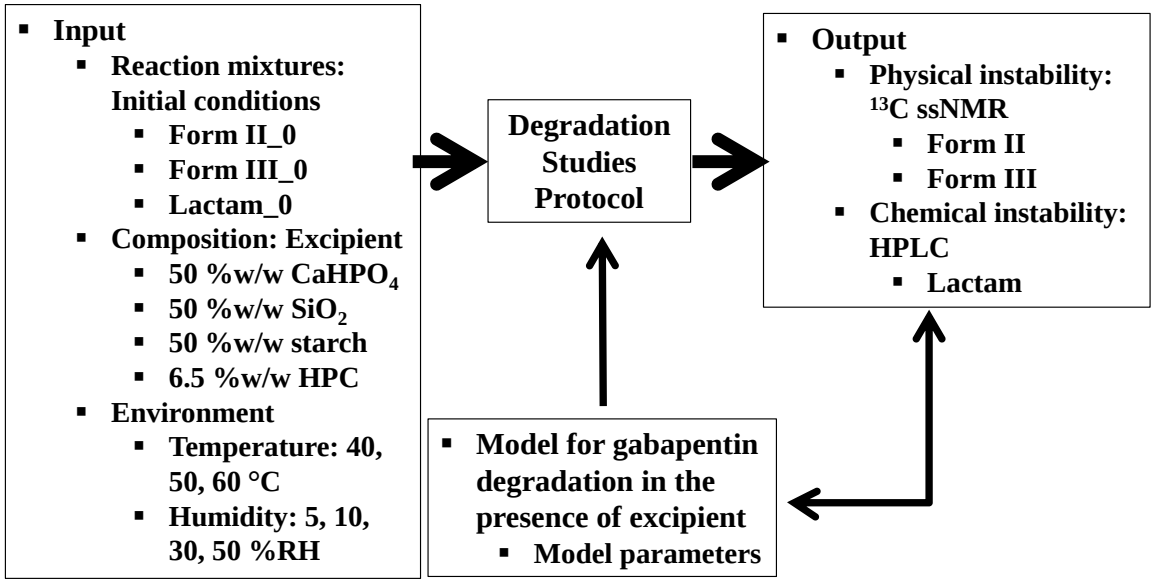

Table V- 1. Summary of composition, environment, and experimental data for studying degradation of co-milled gabapentin Form II/excipient mixtures.

Starting Polymorph (%w/w)	Composition (%w/w)	Environment		Analytical Method			
		°C	%RH	Chemical (HPLC)		Physical (^{13}C ssNMR)	
				Form (II+III)	Lactam	Form II	Form III
50 % Form II	50 % $CaHPO_4$ or 50 % SiO_2 or 50 % starch	40	5	X	X		
			12	X	X	X	X
			32	X	X		
			48	X	X	X	X
		50	5	X	X		
			11	X	X	X	X
93.5 % Form II	6.5 % HPC		29	X	X		
			47.5	X	X	X	X
		60	5	X	X		
			10	X	X	X	X
			27	X	X		
			44	X	X	X	X

Model building was conducted using the systematic approach depicted in Figure V-4. Various model structures were evaluated to describe the relationship between II, III and lactam as depicted in experimentally-obtained concentration time profiles. The degradation model proposed by Zong (19) to describe lactam formation (in the absence of excipients) was used as a starting point. Additional model structures were investigated to overcome the limitations of the Zong model. Secondly, the reaction order for individual pathways was considered. Thirdly, the initial concentrations of the various forms of gabapentin and its degradation product in the reaction mixtures were determined using ^{13}C ssNMR and HPLC or estimated based on kinetic analysis of experimental data generated under low moisture conditions. Next, the ability of the model to describe data was evaluated. The impact of model parameter variation on model outputs was investigated to determine the reliability of model parameter estimates. The mean values and the 95 % confidence limits for each model parameter were estimated using MCMC sampling from

the posterior distribution in Bayesian method. Finally, the effects of compositional and environmental variations on the kinetics of each pathway were determined.

Figure V- 4. Diagram of degradation model building for gabapentin/excipient mixtures.

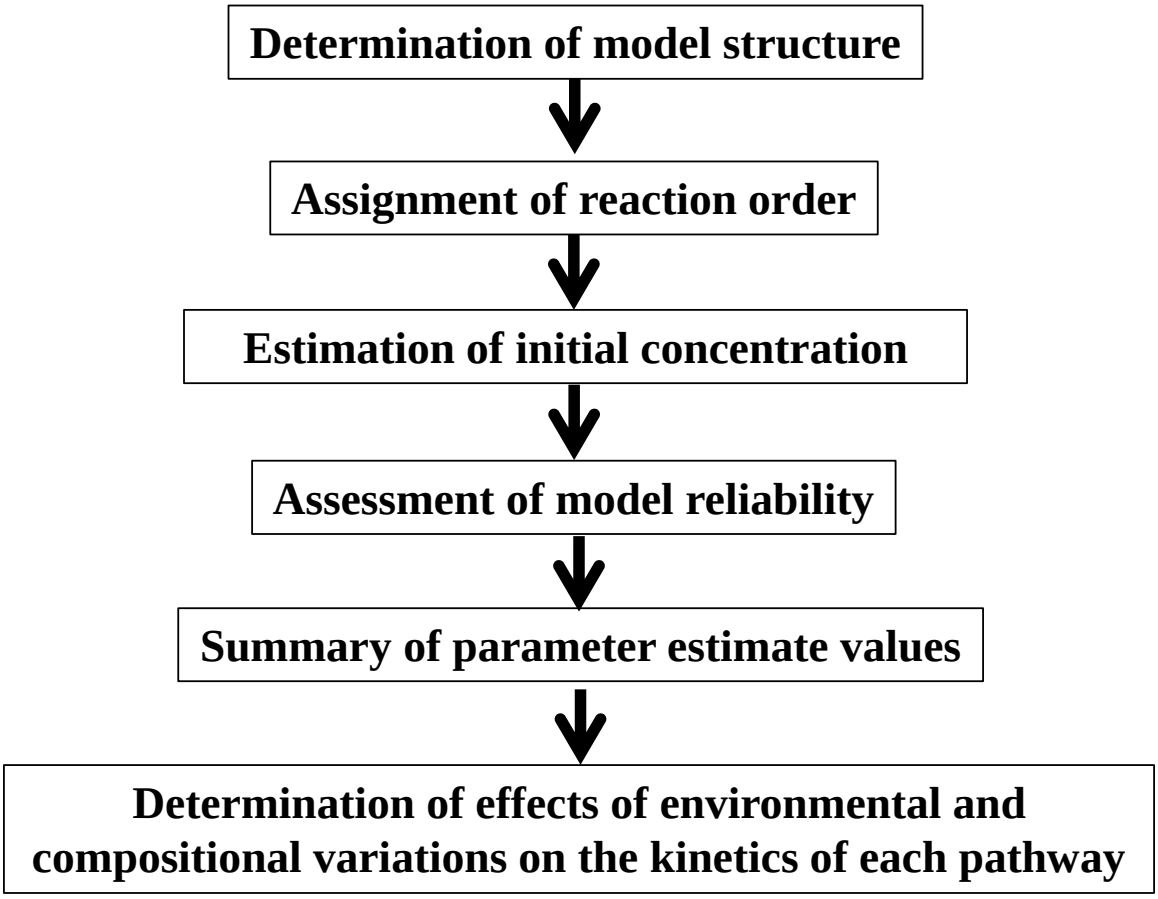

Results and Discussion

Determination of Model Structure

Prior Model

The Zong model [Figure V-2] was successfully used to describe the solid state degradation of milled gabapentin in the absence of excipients during storage under various controlled-temperature and humidity conditions. In his experiments, gabapentin (Form II) was subjected to milling for 60 minutes at speed setting 5. No polymorphic forms other than II were detected after milling. Therefore, the Zong model included II,

lactam and physically-disordered II (II*) which was hypothesized to be created during milling.

In the present study when gabapentin (Form II) was co-milled with excipients, Form III was also detected using ^{13}C ssNMR and XRPD. Therefore, the proposed model needed to describe the fates of II, II*, lactam and an additional polymorph, III. The concentrations of II, III and lactam were experimentally measured by using ^{13}C ssNMR and HPLC. Form II* could not be measured by ^{13}C ssNMR or XRPD; therefore, the initial concentration of II* was estimated using an initial rate method similar to the method developed by Zong. (19) The existence of II* is justified based on two pieces of empirical evidence. Firstly, the observed initial increase in lactam was not consistent with subsequent lower rates of formation, thereby suggesting the existence of an unstable fraction of substrate that contributed to initial lactam formation. An exemplary lactam profile is shown in Figure V-5. Secondly, the broadening of ^{13}C ssNMR spectra for Form II and the decreased proton relaxation times (^{1}H T_1) of co-milled gabapentin II pointed to the presence of some crystal disorder. Although the reaction mixture aliquots maintained crystal patterns that corresponded to II and III, some peak-broadening in ^{13}C ssNMR spectra were also found. Additionally, the proton relaxation times of the co-milled gabapentin samples were two orders of magnitude shorter than un-milled gabapentin. For example, the ^{1}H T_1 value of un-milled gabapentin was 134 s (42), whereas the ^{1}H T_1 values of co-milled gabapentin/HPC, starch, $CaHPO_4$, and SiO_2 were 8, 3, 2, and 1 s, respectively. According to the literature reports, the effects of milling crystalline drug can result in the creation of higher energy sites, reduced crystal integrity, and increasing

mobility in the crystal lattice that result in an overall reduction of proton relaxation times. (43, 44)

Figure V- 5. Lactamization profile of the reaction mixtures with SiO_2 (60 minutes at speed setting 7) stored at 40 ºC and 5 %RH.

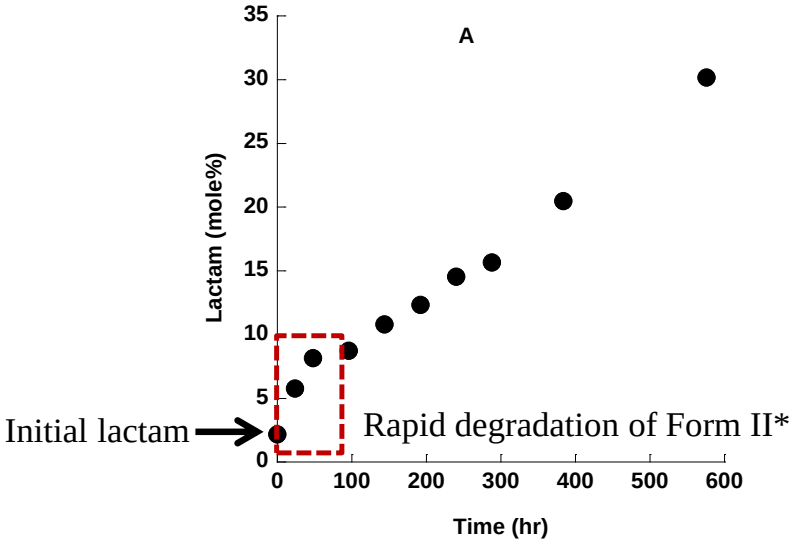

Current Models

Two additional model structures were evaluated to describe the connection between II, III, II*, and lactam in a series of elementary steps. The first model extended the Zong model to account for the presence of III [Figure V-6].

Figure V- 6. Extended Zong model

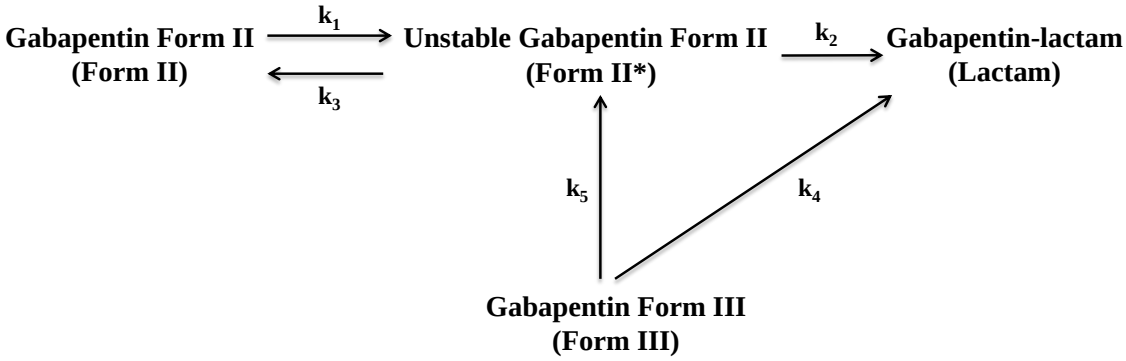

In this model, the connections between II, II* and lactam are consistent with the Zong model. Form III was included in the model by irreversible losses to II* and lactam.

This structure is consistent with the observation that under the conditions of storage, III converts to II, but II does not generate III (^{13}C ssNMR and XRPD). The conversion of III➔II has been previously reported .(45) And the lack of conversion of II➔III under identical storage conditions was confirmed in Zong's studies. The model is also consistent with the observation that the rate of lactam formation is greater than that which can be explained solely by its generation from II.

The model equations for the extended Zong model are described as follows.

$$\frac{d[Form\ II]}{dt} = -k_1[Form\ II]([Form\ II^*] + [Lactam]) + k_3[Form\ II^*][Form\ II]$$

Equation V-5

$$\frac{d[Form\ II^*]}{dt} =$$

$$k_1[Form\ II]([Form\ II^*] + [Lactam]) - k_2[Form\ II^*] - k_3[Form\ II^*][Form\ II] + k_5[Form\ III]$$

Equation V-6

$$\frac{d[Form\ III]}{dt} = -k_4[Form\ III][Lactam] - k_5[Form\ III]$$

Equation V-7

$$\frac{d[Lactam]}{dt} = k_2[Form\ II^*] + k_4[Form\ III][Lactam]$$

Equation V-8

This model was used to describe the concentration time profiles for II, III, and lactam. Nonlinear regression was used to estimate rate constants by simultaneously considering HPLC (lactam formation and gabapentin loss) and ^{13}C ssNMR data (II and III concentrations). The observed and model-predicted curves of II, III, and lactam for the reaction mixtures composed of gabapentin/$CaHPO_4$ stored at 60 °C and 10 %RH are shown in Figure V-7A, V-7B and V-7D. Overall, the model-predicted curves for II, III, and lactam showed good agreement with the observed data. However, the model-predicted profile for II* showed a substantial accumulation of II* [Figure V-7C].

Similarly, the model-predicted II* curves for other reaction mixtures stored under various conditions also showed the sizable accumulations of II*. For example, the II* curves of reaction mixtures containing SiO_2, HPC, and starch stored at 60 °C/10 %RH and 60 °C/44 %RH are shown in Figure V-8. The accumulated concentrations of II* varied from 70 to 95 mole % of the initial substrate concentration. These II* predictions may suggest that some changes in ^{13}C ssNMR should have been observed in reaction mixture aliquots; however, no such changes were observed. For example, the ^{13}C ssNMR spectra for the aliphatic region of co-milled II/$CaHPO_4$, SiO_2, starch, and HPC stored under 60 ºC/10 %RH at 0 and 96 hours are shown in Figure V-9 to V-12. The absence of major ^{13}C ssNMR changes suggested that either II* retained sufficient crystalline characteristics and thus ^{13}C ssNMR could not differentiate this material from intact Form II or II* did not accumulate to the extent predicted by the extended Zong model.

Figure V- 7. The observed (points) and model-predicted (curves) gabapentin Form II (A), gabapentin Form III (B), gabapentin Form II* (C), and lactam (D) of reaction mixtures with $CaHPO_4$ stored at 60 °C and 10 %RH. The curves were estimated by using extended Zong model.

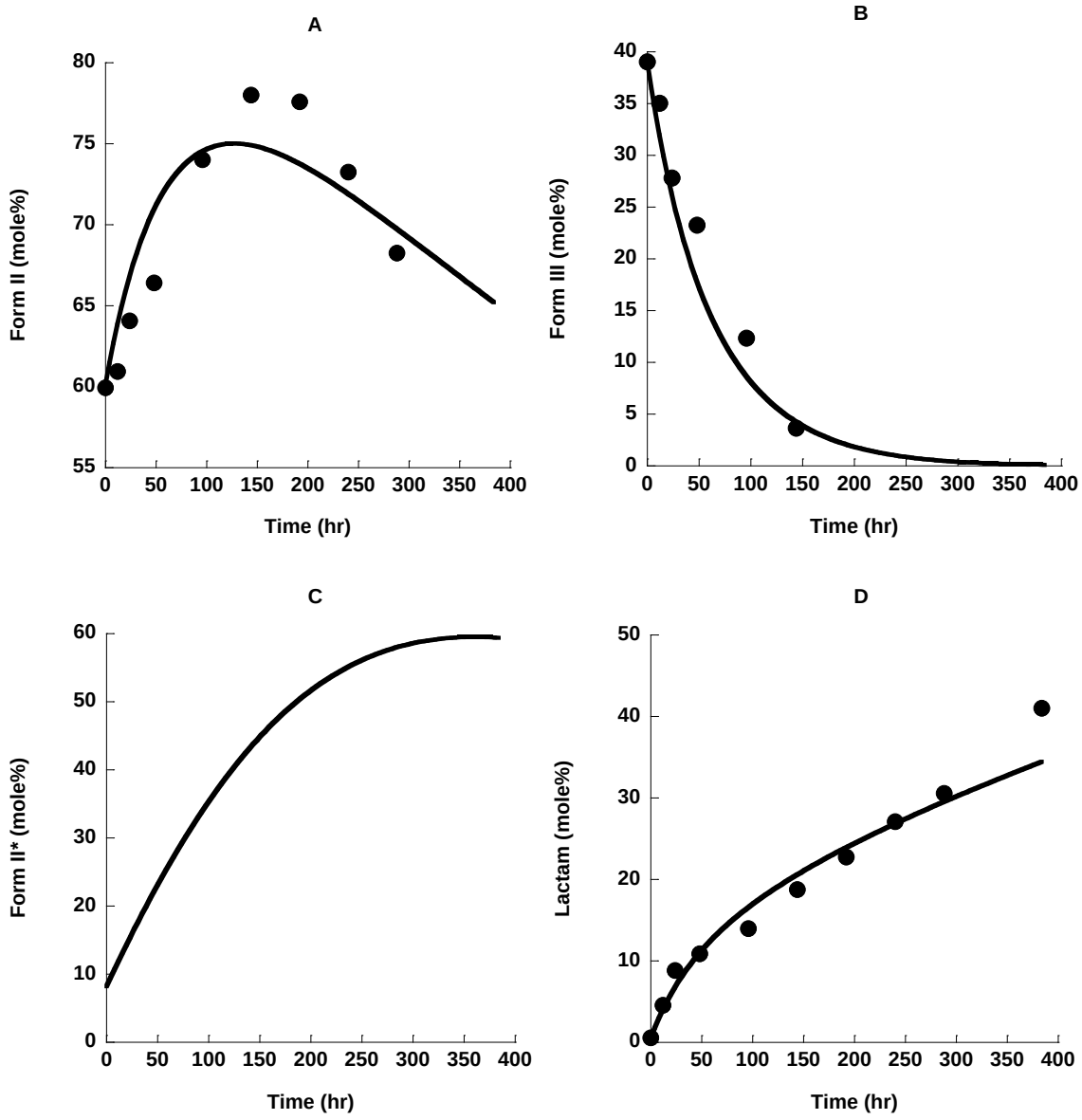

Figure V- 8. The model-predicted gabapentin Form II* of reaction mixtures with SiO_2, HPC, and starch stored at 60 °C/10 %RH and 60 °C/44 %RH. The curves were estimated by using extended Zong model.

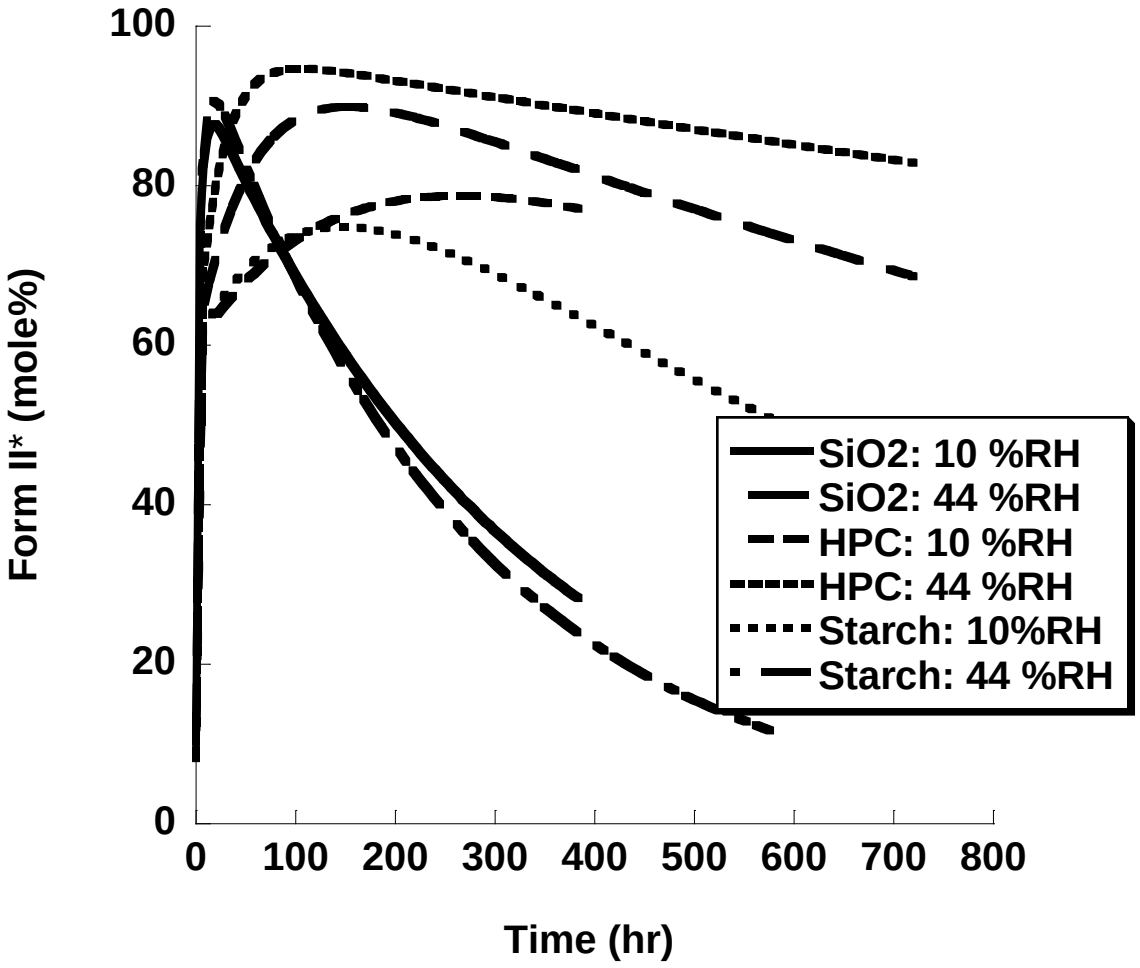

Figure V- 9. The representative ^{13}C ssNMR spectra for the aliphatic region of reaction mixtures with $CaHPO_4$ stored under 60 ºC/10 %RH at 0 and 96 hours. The ^{13}C ssNMR was operated under ambient conditions.

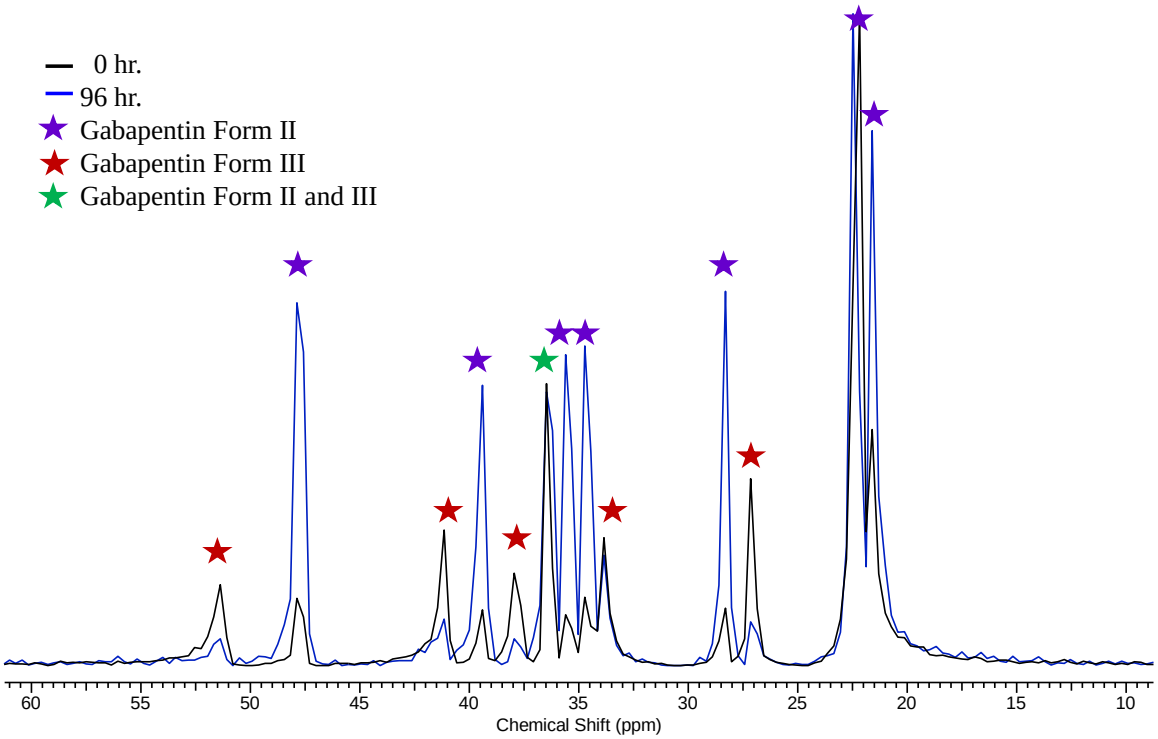

Figure V- 10. The representative ^{13}C ssNMR spectra for the aliphatic region of reaction mixtures with SiO_2 stored under 60 ºC/10 %RH at 0 and 96 hours. The ^{13}C ssNMR was operated under ambient conditions.

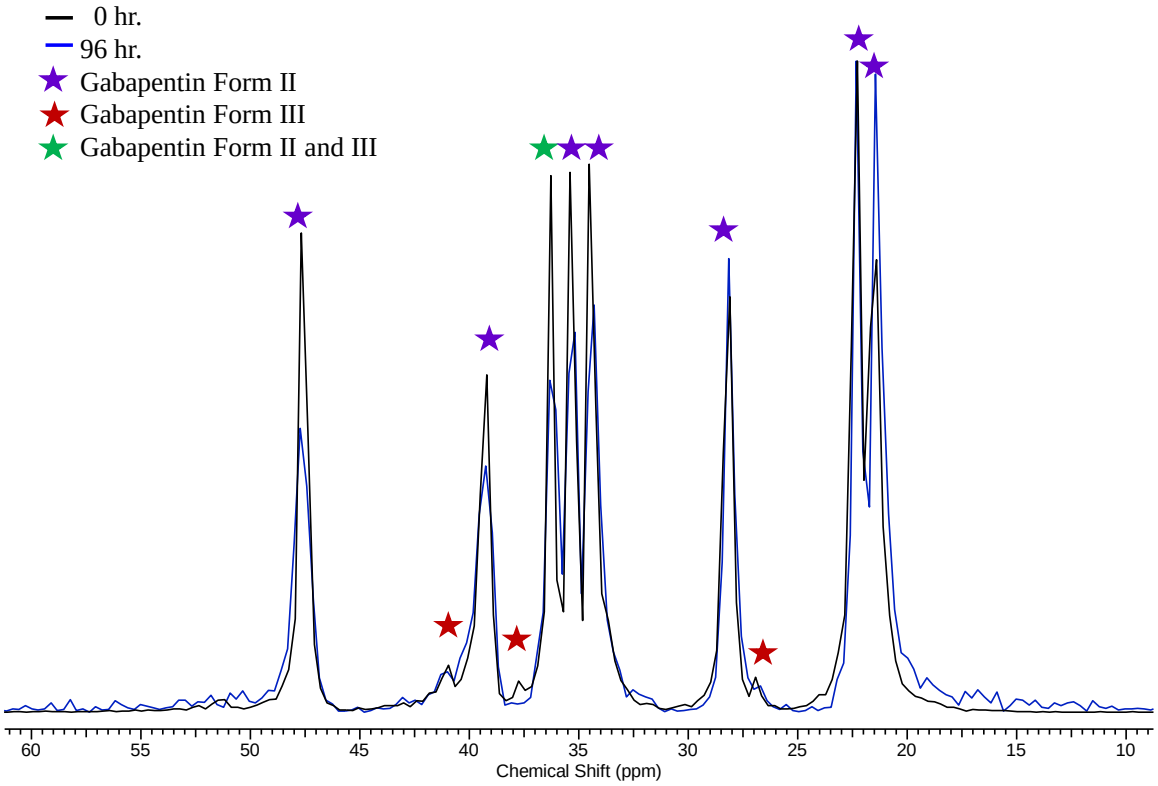

Figure V- 11. The representative ^{13}C ssNMR spectra for the aliphatic region of reaction mixtures with starch stored under 60 ºC/10 %RH at 0 and 96 hours. The ^{13}C ssNMR was operated under ambient conditions.

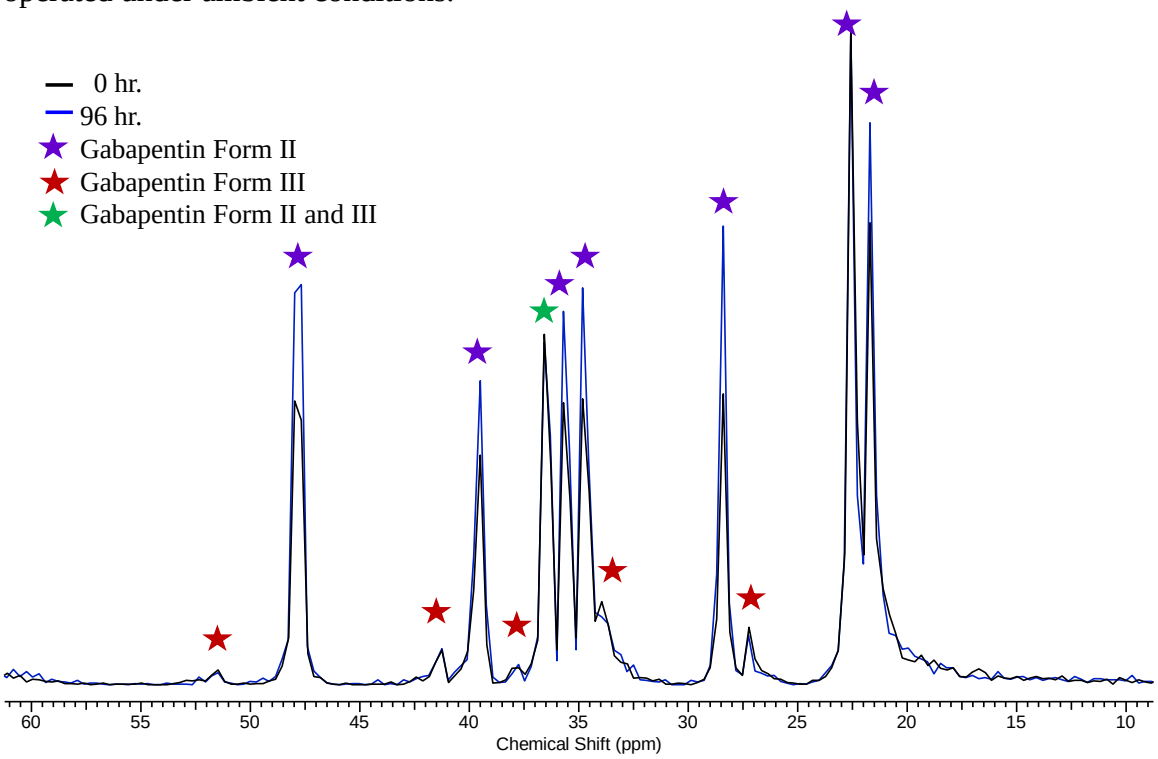

Figure V- 12. The representative ^{13}C ssNMR spectra for the aliphatic region of reaction mixtures with HPC stored under 60 ºC/10 %RH at 0 and 96 hours. The ^{13}C ssNMR was operated under ambient conditions.

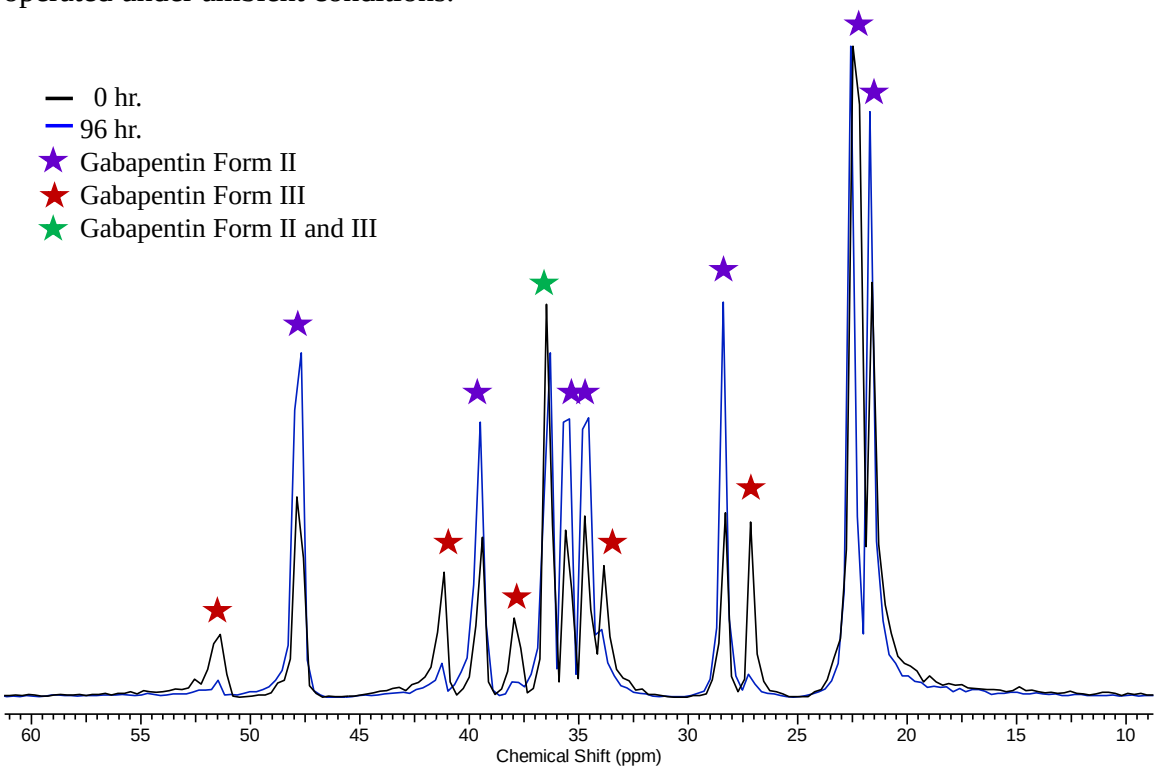

Another observation suggesting that II* may not be an intermediate as depicted in the extended Zong model [Figure V-6] is presented in Figure V-13. This study was one of a series of studies conducted by Dr. Eiji Ueyama in our laboratory. He conducted studies by milling gabapentin under mild condition, and then he stored reaction aliquots at 50 ºC/14 %RH and determined changes in lactam concentration over an extended time period (> 40 days). During the time period, no polymorphic transformations were observed. Lactam accumulated for about 16 days and then no further lactam was formed. In all the total lactam formation was about 1.2 mole % [Figure V-13]. Dr. Ueyama repeated these studies numerous times and the accumulation of lactam never exceed 2 mole %. These results strongly suggest that the accumulation of lactam from disordered Form II (II*) is not an intermediate in the pathway of conversion of intact Form II to lactam. Contrariwise, these results are consistent with a model wherein II* generated by mechanical stress during milling that is reversibly converted directly to lactam.

Figure V- 13. Lactamization profile of milled gabapentin Form II stored at 50 ºC and 14 %RH.

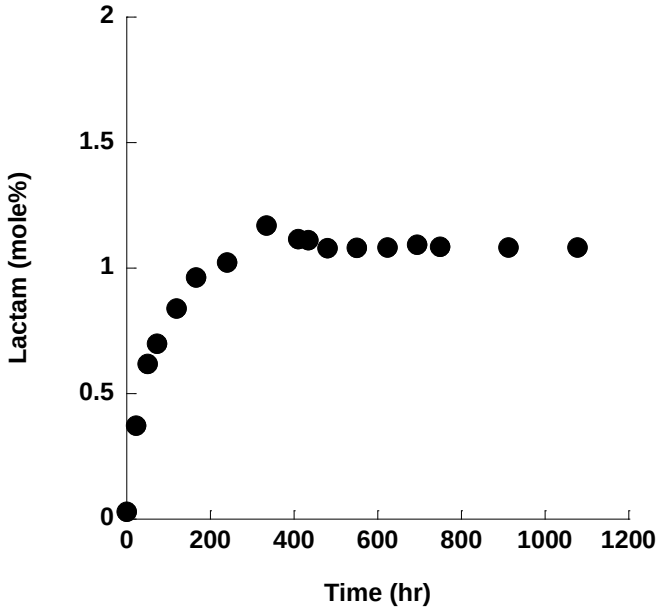

Based on Dr. Ueyama's experiments and the lack of any physical evidence for the predicted accumulation of II* (based on the extended Zong model), a second model [Figure V-14] was devised in which II* is a high-energy subpopulation of II that can be annealed to the more stable II or degrades directly to lactam.

Figure V- 14. New model

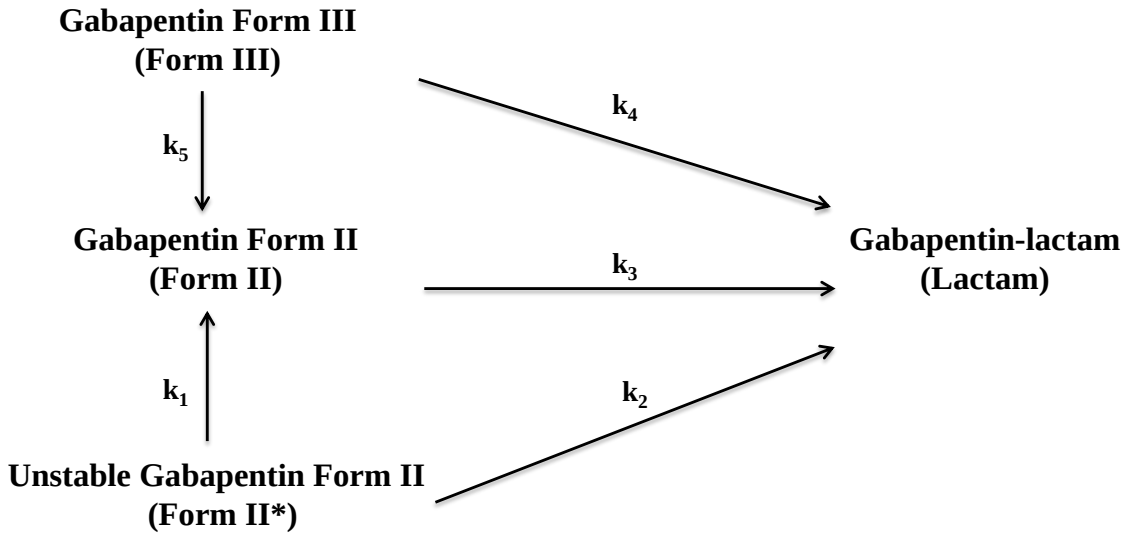

In this model, III converts to II or degrades to lactam, and II is capable of direct degradation to lactam. In the new model, the initial formation of lactam is primarily associated with the first-order degradation of II*➔lactam. After the initial phase of lactam formation, the degradation product profiles are typified by a small lag (which is not always observed) followed by accelerated rate of lactam formation. This type of degradation product plot is typical of autocatalytic kinetics, thus the conversion of II ➔lactam in the new model is described by Prout-Thompkins-type kinetics. For consistency, the formation of lactam from III is also depicted as autocatalytic. The differential equations that describe substrate and product concentrations time profiles are the following.

$$\frac{d[Form\ II]}{dt} = k_1[Form\ II^*] - k_3[Form\ II][Lactam] + k_5[Form\ III] \quad \text{Equation V-9}$$

$$\frac{d[Form\ II^*]}{dt} = -k_1[Form\ II^*] - k_2[Form\ II^*] \quad \text{Equation V-10}$$

$$\frac{d[Form\ III]}{dt} = -k_4[Form\ III][Lactam] - k_5[Form\ III] \quad \text{Equation V-11}$$

$$\frac{d[Lactam]}{dt} = k_2[Form\ II^*] + k_3[Form\ II][Lactam] + k_4[Form\ III][Lactam]$$

Equation V-12

The observed and model-predicted curves for II, III, and lactam generated from reaction mixtures containing $CaHPO_4$ stored at 60 °C and 10 %RH are shown in Figure V-15A, V-15B and V-15D. Overall, the model-predicted curves for II, III, and lactam obtained from new model were in good agreement with the observed data. Moreover, the model-predicted curve for II* showed no accumulation [Figure V-15C]. Similarly, the model-predicted II* curves for the reaction mixtures prepared with SiO_2, HPC, and starch stored at various conditions also showed no II* accumulation [Figure V-16]. In this respect, the new model agreed with the ^{13}C ssNMR results in that II* was never more than a minor component (< 10 mole %) in any of the reaction mixtures.

Figure V- 15. The observed (points) and model-predicted (curves) gabapentin Form II (A), gabapentin Form III (B), gabapentin Form II* (C), and lactam (D) of reaction mixtures with $CaHPO_4$ stored at 60 °C and 10 %RH. The curves were estimated by using new model.

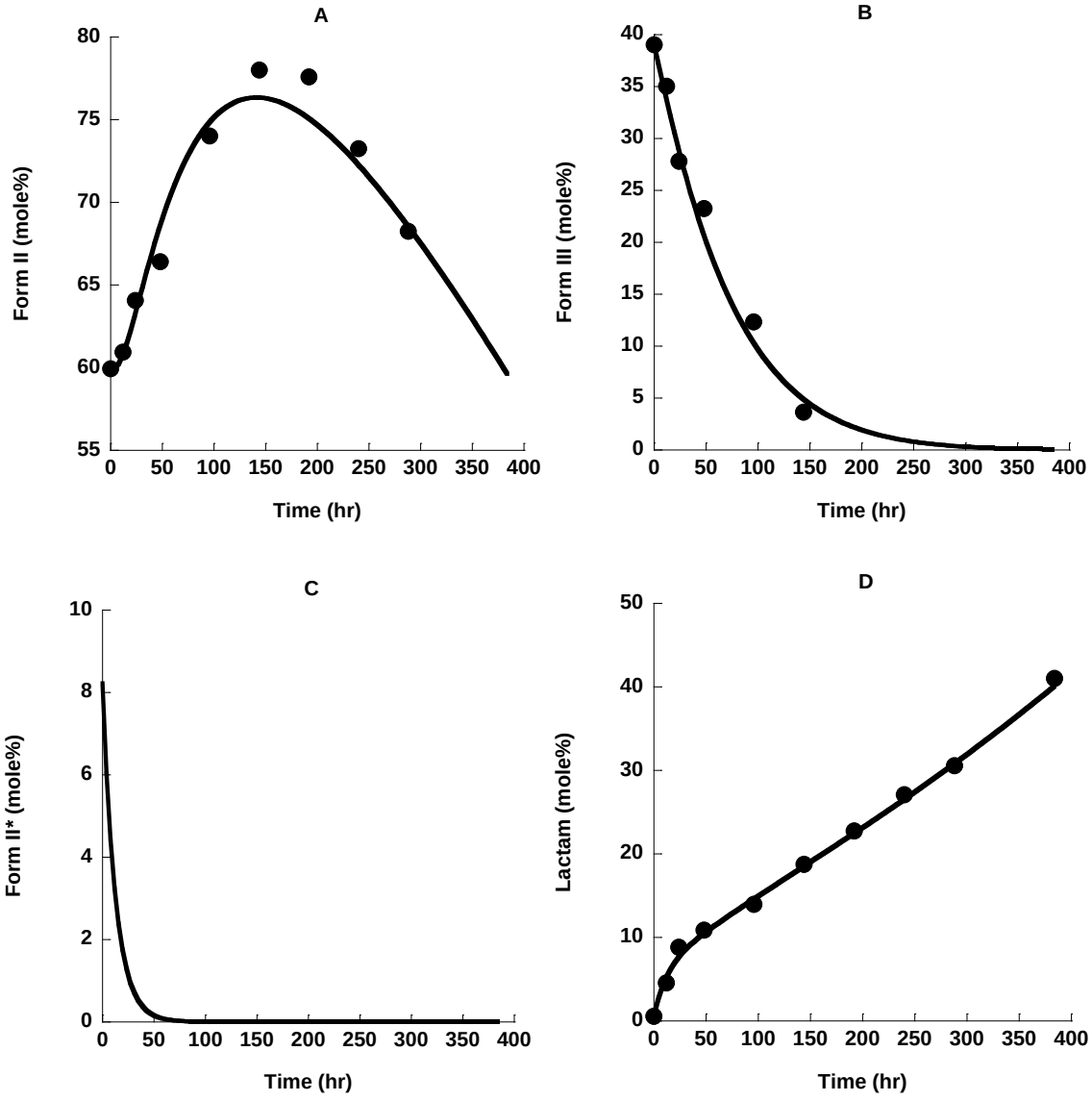

Figure V- 16. The model-predicted gabapentin Form II* of reaction mixtures with SiO_2, HPC, and starch at 60 °C/10 %RH and 60 °C/44 %RH estimated by using new model.

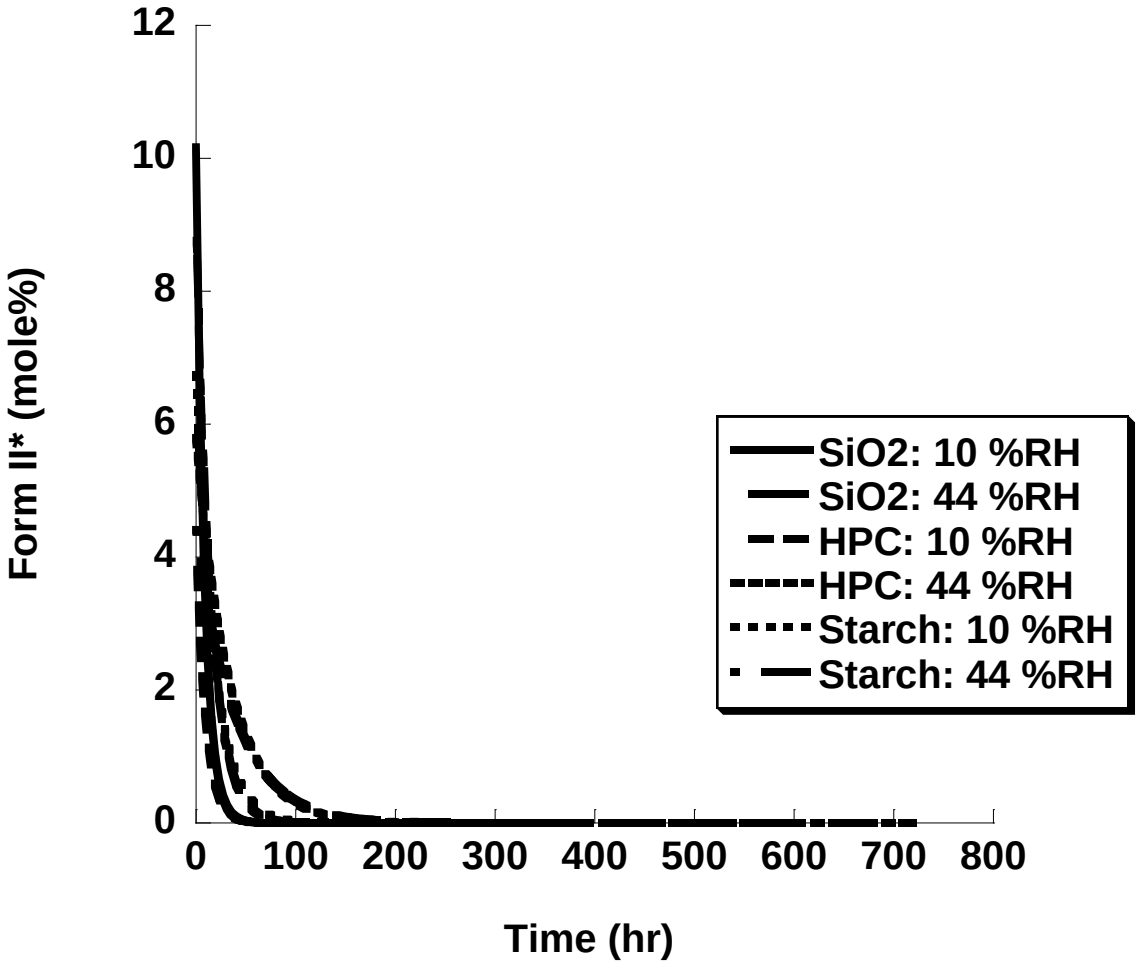

Assignment of Reaction Order

Reaction order for drug degradation in homogeneous systems (e.g. solution) can be difficult to define even under controlled (e.g. first-order) experimental conditions. The reaction order in heterogeneous systems (e.g. solid state and multiphase liquid states) can be very problematic to determine with certainty under any conditions. In our model, the reaction order for each individual pathway was assumed to be first-order unless a higher order could be empirically justified. First-order kinetics were assigned to the conversion of II* ➔ II (k_1), the rapid conversion of II* ➔ lactam (k_2) and the polymorphic transformation of III ➔ II (k_5). The assignment reflects the lack of any observation to indicate higher order kinetics. Contrariwise, the conversion of II➔lactam and III➔lactam did indicate higher order kinetics as described below.

Autocatalytic (Prout-Tompkins) kinetics are widely used to describe the solid state drug degradation. (6, 46) We conducted a study at 50 and 55 ºC using II or III as substrates after subjecting samples to a mild milling condition (5 minutes at speed setting 1). The mild condition was used to prevent III from converting to II and to suppress the formation of II* during milling. The reaction samples were then stored at 5 %RH to suppress the conversion of III to II during storage. Therefore, the primary degradation pathway in these experiments was substrate (either II or III) dehydration to lactam. The resultant lactam formation profiles are shown in Figure V-17 (A-B). The autocatalytic formation of lactam is a prominent feature for both substrates and particularly at the higher temperature. Therefore, the formation of lactam from both II (k_3) and III (k_4) appears to follow Prout-Tompkins (autocatalytic) kinetics.

Figure V- 17. Initial lactamization profiles of mildly-milled gabapentin Form II (A) and Form III (B) (5 minutes at speed setting 1) stored at 50 ºC/5 %RH and 55 ºC/5 %RH.

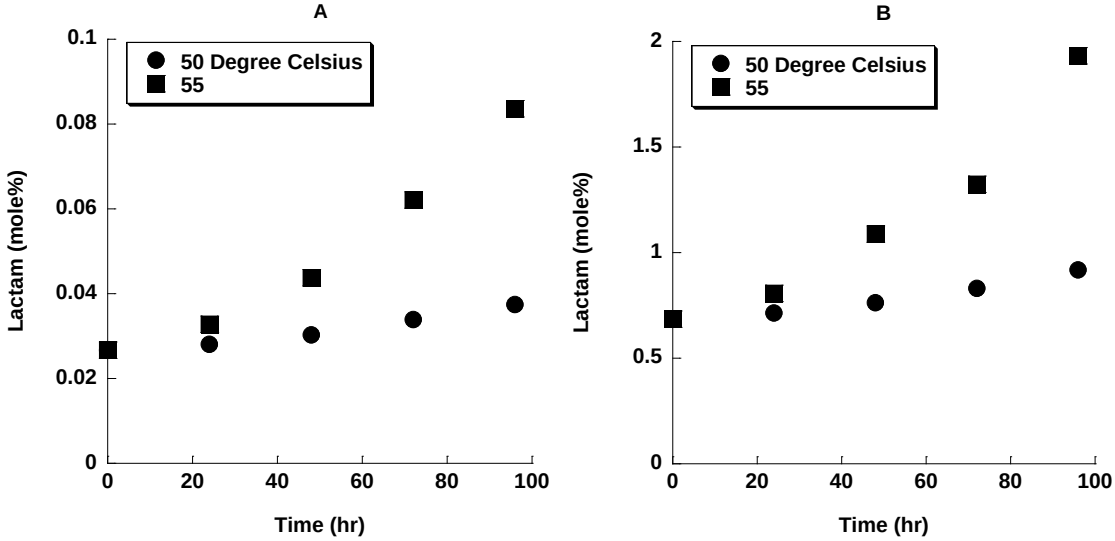

Estimation of Initial II* Concentration

Initial concentrations of II, III and lactam (II_0, III_0, and $lactam_0$) were experimentally measured with ^{13}C ssNMR and HPLC. However, the initial concentration of II* (II_0*) was estimated from lactam profiles obtained by a nonlinear optimization using the reaction mixtures for each excipient stored at 5 %RH and three temperatures (40, 50 and 60 ºC). The low humidity condition was used to estimate II_0* because previous studies have demonstrated that the conversions of III ➔ II and II*➔II are suppressed under this condition. Therefore, the predominant degradation events are the rapid initial formation of lactam from II* and its slower formation from II and III. Since the value of II_0* is unique for each excipient, but is the same for reactions conducted over a series of temperatures, the parameter optimization process was used to obtain a single estimate of II_0* for each excipient by simultaneously considering formation profiles generated at three different temperatures. A nonlinear optimization was used to determine the initial estimates of II_0* for each excipient mixture. These estimates were then used as starting points for the MCMC sampling in the Bayesian estimation. The 95% confidence

limits for II_0* in each excipient mixture are shown in Table V-2. These II_0* values for each excipient mixture were treated as fixed constants in further data analysis.

Table V- 2. Form II_0* estimates and 95% confidence lower (LB) and upper bounds (UB) of reaction mixtures with excipients stored at 5 %RH/40, 50, and 60 °C obtained from fitting new model to lactam curves via MCMC sampling.

Excipient	Estimate	95%LB	95%UB
50 %w/w CaHPO4	8.30	6.98	9.61
50 %w/w SiO2	8.80	7.03	10.58
50 %w/w starch	5.94	5.15	6.73
6.5 %w/w HPC	7.16	6.71	7.60

Assessment of Model Reliability

Our model for gabapentin instability in the presence of excipients is depicted in Figure V-14. The key features of the model are first-order physical state transitions of II* and III to II, first-order degradation of II* to lactam and autocatalytic lactamization of II and III. Initial concentrations of lactam, II and III were determined using a combination of HPLC to determine molar concentrations of lactam and gabapentin and ^{13}C ssNMR to determine the fractions of II and III. Kinetic analysis of low humidity lactam formation data at three storage temperatures was used to estimate the initial concentration of II* (II_0*).

Rate constants for each physical and chemical transition were estimated from combined HPLC and ^{13}C ssNMR data for each reaction mixture composed of co-milled gabapentin and excipient. The quality of the data, complexity of the model, and the relative rates of each transition determine the uncertainty of parameter estimation. The degree of uncertainty associated with each parameter estimate will vary and will affect the reliability of any conclusions or insights derived from the relationships between the effects of model input (e.g. environmental and compositional variations) and system response (e.g. instability kinetics). In order to evaluate parameter estimation uncertainty,

we have used five tools based on Bayesian methods: namely, global sensitivity analysis, local sensitivity analysis, pairwise plots, convergence assessment, and congruence of empirical concentration time profile data and confidence limits for the time-dependent, model-predicted concentrations.

Global sensitivity analysis was conducted by determining the relationship or dependency of overall model outputs (as measured by area under the curve for each measured reaction component) on the rate constant for each pathway. This analysis indicates our ability to estimate individual parameters from the available empirical data.

Local sensitivity analysis was conducted by determining the effect of concentration changes on parameter variability as a function of time for each concentration time profile. This analysis indicates what data from each time-dependent region is needed to estimate individual rate constants.

Pairwise plots were generated from pairs of local sensitivity analysis values for individual parameters. The existence of strong correlations between parameter sensitivity values indicates a lack of independence of parameter estimation.

Convergence assessment was conducted using history plots that depict the pattern or lack of pattern of sampled parameters as a function of sequential iterations using Markov Chain Monte Carlo (MCMC) sampling scheme. The lack of a sampling pattern indicates model parameter estimation convergence.

The final assessment of model and parameter reliability was a comparison of empirical data (i.e. reaction component concentration time profiles) to model-predicted values using MCMC sampling of parameter distributions to provide 95 % upper and lower bounds for each time-dependent concentration that reflect parameter estimation

uncertainty. Agreement between model-predicted and observed data was a prime determinant in model assessment.

The impact of model parameter variations on model outputs (concentration time profiles for II, III and lactam) were investigated to determine the reliability of model parameter estimates. Analyses were based on simulated model output associated with the reaction mixtures with $CaHPO_4$ stored at 40 °C/48 %RH and/or 60 °C/10 %RH. The simulated model output using sets of parameter estimates was made using MCMC scheme sampled from parameter probability density functions. (41, 47)

Global Sensitivity Analysis

For global sensitivity analysis, the effects of model parameter variations (k_1, k_2, k_3, k_4 and k_5) on area under the curves (AUC) of lactam, II, and III were evaluated by plotting AUC values as a function of parameter sampled value. The observation of a trend between a particular parameter value and resultant AUC value suggest that the output is sensitive to parameter variation. The plots depicting randomly scattered points suggest that the values of the parameter are not important determinants in the total concentration time profile.

The plots of simulated model outputs (AUC of lactam, II and III) versus each rate constant (k_1, k_2, k_3, k_4, and k_5) are shown in Figure V-18 (A-C). The patterns observed for the lactam AUC (A) versus k_2 and k_3 suggested that these model parameters affected the lactam concentration time profile. The lactam AUC and k_5 plot showed a random distribution indicating that this parameter played no role in determining lactam concentration. The relationship between the AUC of II (B) and k_3 indicated that k_3 value had the most impact on the concentration time profile of II. The relationship between the

AUC of III (C) versus k_4 and k_5 indicated that these parameters were predominant in defining III output. This analysis also suggested that some parameters, such as k_3 and k_4 could be estimated from multiple data sets, including profiles of lactam, II and III, whereas k_2 could be obtained only from lactam profiles. The estimated values of k_5 depended on the profile of III. Based on global sensitivity analysis, reliable estimates for k_1 were difficult to obtain with the available data. Clearly, a method of measuring the time-dependent changes of disordered II (II*) is needed to obtain k_1 estimates. However given the lack of XRPD or ^{13}C ssNMR changes associated with II* and its presence as a minor component (<10 %), accurate k_1 estimates were not possible.

Figure V- 18. The simulated model output-area under the curves in lactam (A), gabapentin Form II (B), and Form III (C) as a function of parameter values; k_1, k_2, k_3, k_4, and k_5. Analyses were based on simulated model outputs associated with the reaction mixtures with $CaHPO_4$ stored at 40 °C and 48 %RH.

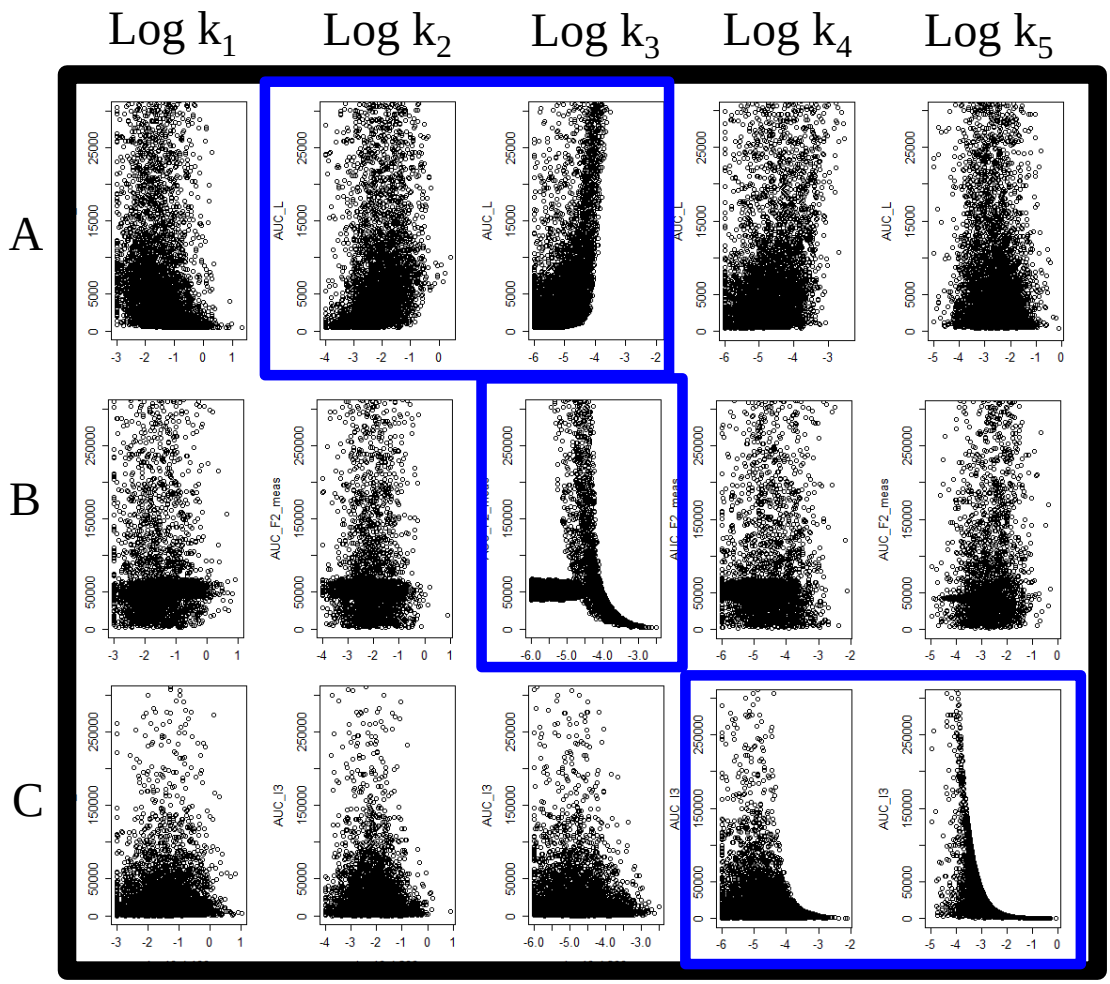

Local Sensitivity Analysis

An additional approach to identify the influence of individual parameter variation on model output concentration as a function of time was investigated using local sensitivity analysis. In this method, the derivatives of the model outputs (concentrations of lactam, II, and III) with respect to each parameter; k_1, k_2, k_3, k_4, and k_5 were estimated as a function of time. A dimensionless sensitivity value (S_{ij}) was calculated based on Equation V-13 where y_i is an output variable and Θ_j is a model parameter. ω_{yi} and $\omega_{\Theta j}$

are the scaling factors for output variables (y_i) and model parameters (Θ_j). The parameter sensitivity value (S_{ij}) for each model output was plotted as a function of time. This sensitivity plot indicates how impactful the parameter value is to the time-dependent model output. (41)

$$\frac{\partial y_i}{\partial \Theta_j} \cdot \frac{\omega_{\Theta j}}{\omega_{yi}}$$ Equation V-13

When the sensitivity value is near zero then the parameter value has no effect on that portion of the time-dependent model output. Contrariwise, when the absolute value of sensitivity is sufficiently greater than zero then the parameter is critical in determining model output. By plotting the sensitivity value as a function of time, it is possible to observe what time-dependent model output values are influenced by specific parameter values or, conversely, what output data is critical for the accurate estimation of specific model parameters.

The sensitivity plots for lactam, II, and III concentrations with respect to each of the five model rate constants (k_1, k_2, k_3, k_4, and k_5) as a function of time are shown in Figure V-19 (A-C). For the initial lactam concentrations [Figure V-19A], the values of k_1 and k_2 are the most important determinants (along with the separately estimated value of II_0*). Conversely, the lack of substantial "early-time" lactam data will significantly contribute to k_1 and k_2 uncertainty. Subsequent ("longer-time") lactam data [Figure V-19A] informs the estimated values for k_3 (II➔lactam) and k_4 (III➔lactam).

The profiles depicting loss of III [Figure V-19C] were dependent on k_5 estimates, although it should be noted that under conditions of lower humidity and higher temperature (i.e. 60 °C/10 %RH), k_4 values also were influential [Figure V-20]. The profiles of II [Figure V-19B] were primarily dependent on k_3 and k_5 values. Taken

together, this analysis demonstrated that lactam, II and III concentration time data are adequate to reliably estimate k_2, k_3, k_4, and k_5 rate constants assuming adequate samples been taken over the reaction time course and all three reaction component profiles are considered simultaneously. Once again, the sensitivity values for k_1 indicate an inability to reliably estimate its value.

Figure V- 19. The sensitivity plots of model output; lactam (A), gabapentin Form II (B), and gabapentin Form III (C) to parameters (k_1, k_2, k_3, k_4, and k_5) as a function of time. Analyses were based on simulated model outputs associated with the reaction mixtures with $CaHPO_4$ stored at 40 °C and 48 %RH.

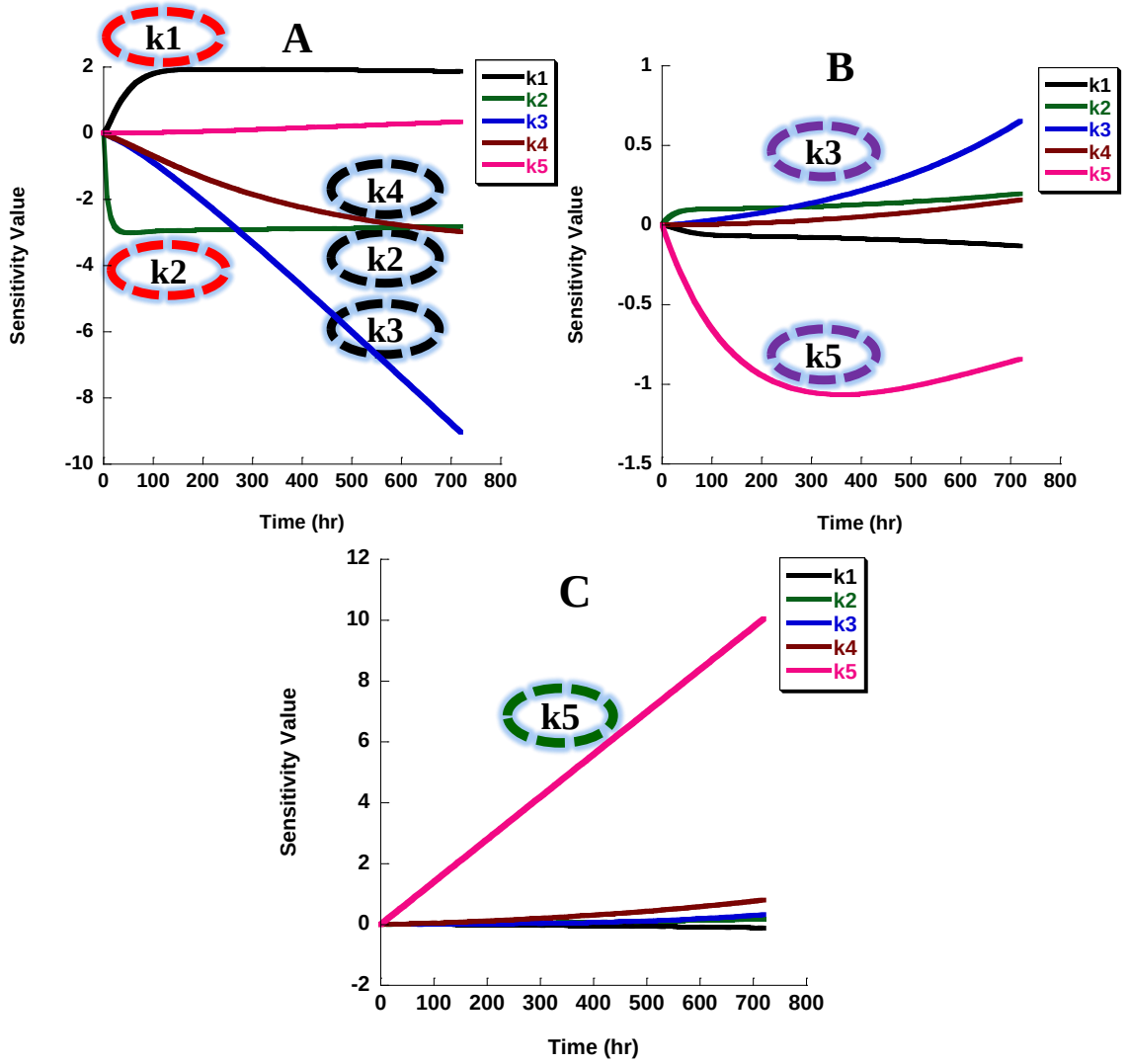

Figure V- 20. The sensitivity plots of model output; gabapentin Form III to parameters (k_1, k_2, k_3, k_4, and k_5) as a function of time. Analyses were based on simulated model outputs associated with the reaction mixtures with $CaHPO_4$ stored at 60 °C and 10 %RH.

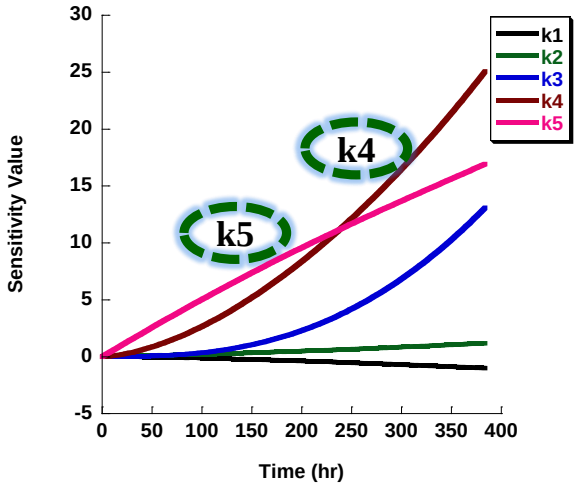

Pairwise Plots

Pairwise plots were created by plotting the local sensitivity values for each pair of parameters associated with concentration time profiles of lactam, II and III. The correlation between each pair was evaluated. Not surprisingly, the two pairs of rate constants that showed the strongest correlations were k_3 and k_4 with respect to lactam profiles [Figure V-21A] and k_4 and k_5 with respect to III profiles [Figure V-21B]. In the former case, these rate constants are associated with lactam formation pathways (II➔lactam and III➔lactam). In the latter case, the rate constants are associated with loss of III (III➔lactam and III➔II). Our parameter estimation procedure simultaneously considers both lactam formation and III loss; therefore, the estimates of k_3, k_4, and k_5 are expected to be a balance between independent empirical evidence. Therefore, these pairwise correlations were not considered to be problematic.

Another strong correlation between parameters is associated with the estimated values of II_0* and k_2. We have attempted to overcome this confounding correlation by separating the estimation of II_0* using a different set of data as described earlier.

Therefore, the estimation of k_2 was made without the confounding effects of II_0* estimation.

Figure V- 21. Pairwise plots of strongly-correlated parameters: k_3 versus k_4 for lactam (A) and k_4 versus k_5 for III (B). Analyses were based on simulated model outputs associated with the reaction mixtures with $CaHPO_4$ stored at 40 °C and 48 %RH.

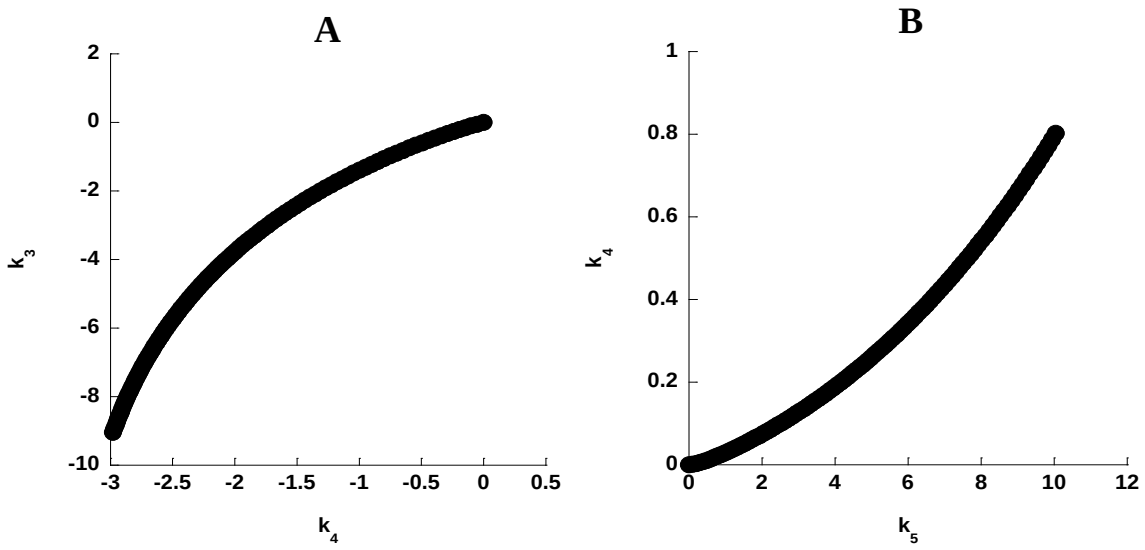

Convergence Assessment

A convergence assessment of Markov chain was conducted by observing a history plot that showed the paths of sampler output for each model parameter from every iterative step. The history plots for the reaction mixtures with $CaHPO_4$, SiO_2, starch, and HPC stored at 60 °C/10-44 %RH are shown in Figure V-22 (A-D). The MCMC sampler converged after 20,000 iterations. The sampled parameters were randomly distributed over sequential iterations and the sampling chain indicated no apparent trends.

Figure V- 22. The history plots of MCMC chain of seven parameters (k_1, k_2, k_3, k_4, k_5, β_1, and β_5) for the reaction mixtures with $CaHPO_4$ (A), SiO_2 (B), starch (C), and HPC (D) stored under 60 °C and 10, 27, and 44 %RH. The chains indicate the convergence by no apparent trends.

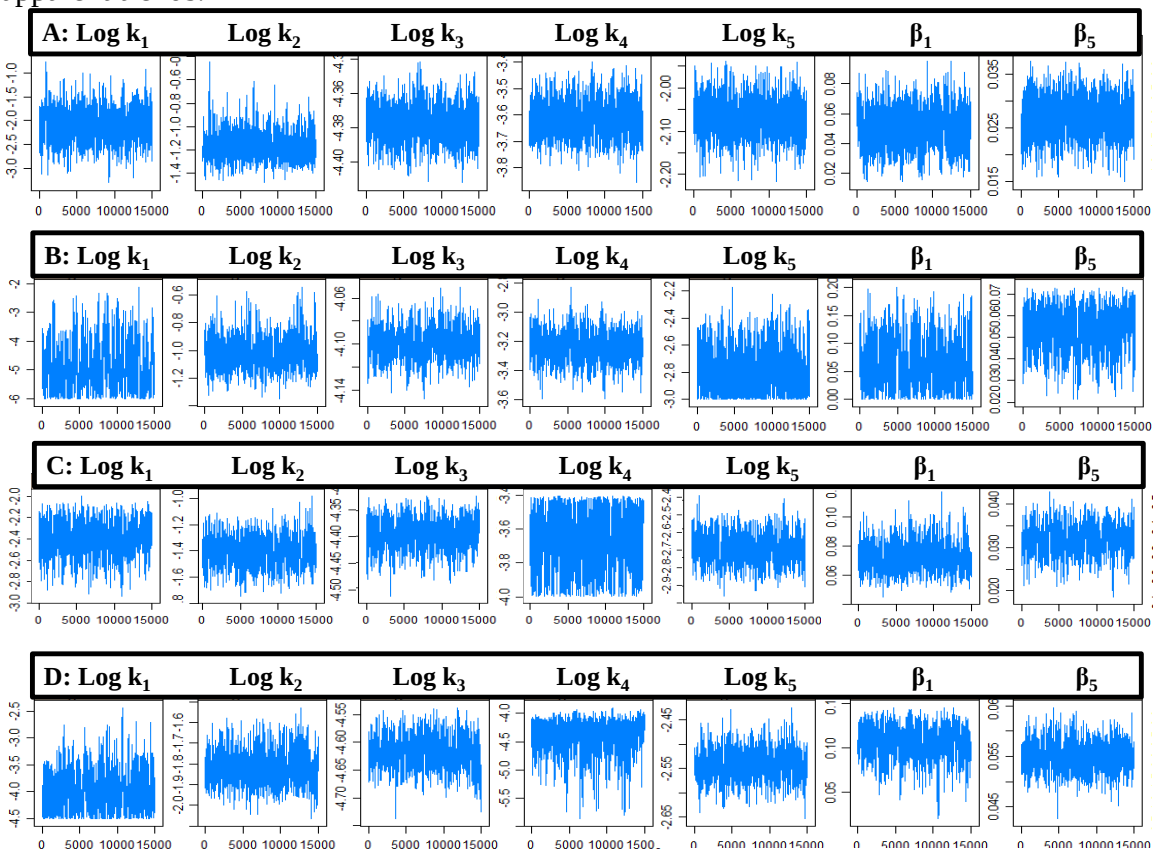

Comparison of Observed and Model Predicted Concentration Time Profiles

The mean predicted concentration time values of lactam, II, III and 95 % upper-lower bounds based on parameter distributions were generated by MCMC sampling. The experimentally-observed lactam, II and III of the reaction mixtures with $CaHPO_4$ [Figure V-23 to V-25 (A-C)], SiO_2 [Figure V-26 to V-28 (A-C)], starch [Figure V-29 to V-31 (A-C)], and HPC [Figure V-32 to V-34 (A-C)] stored at 40 °C/12- 48 %RH, 50 °C/11- 47.5 %RH, and 60 °C/10- 44 %RH were plotted with respect to times. The continuous curves represented the mean concentration time values and the dash lines represented the 95 % upper-lower bounds. Overall, our new model was useful for describing the relationship

between lactam, II and III. An agreement between model-predicted curves and experimentally-observed data was found. The range of predicted curves that represented the distributions of the model response as a function of the parameter values covered all but a few data points thus indicating the model was consistent with the observed data within the uncertainty of the estimated parameters. As described previously, the history plots indicated that the model converged and that the estimated model parameter distributions accurately reflected model uncertainty.

Figure V- 23. Concentration time profiles of lactam, gabapentin Form II and Form III. Points present the observed reaction mixtures with $CaHPO_4$ stored under 40 °C/12 %RH (A), 40 °C/32 %RH (B), and 40 °C/48 %RH (C). The solid and dash curves represent the mean, 95% upper and lower bounds of observed data predicted by MCMC sampling and new model.

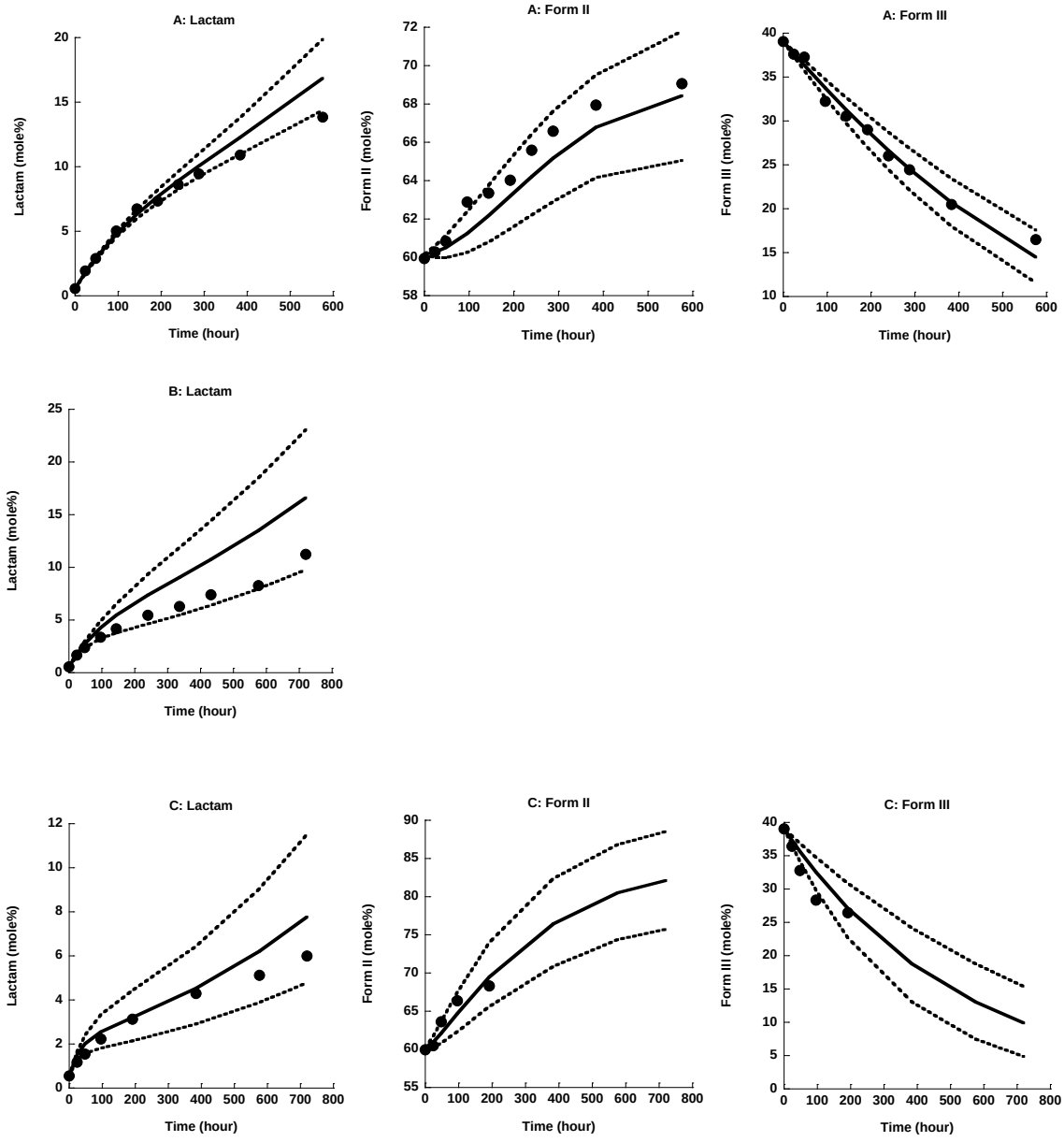

Figure V- 24. Concentration time profiles of lactam, gabapentin Form II and Form III. Points present the observed reaction mixtures with $CaHPO_4$ stored under 50 °C/11 %RH (A), 50 °C/29 %RH (B), and 50 °C/47.5 %RH (C). The solid and dash curves represent the mean, 95% upper and lower bounds of observed data predicted by MCMC sampling and new model.

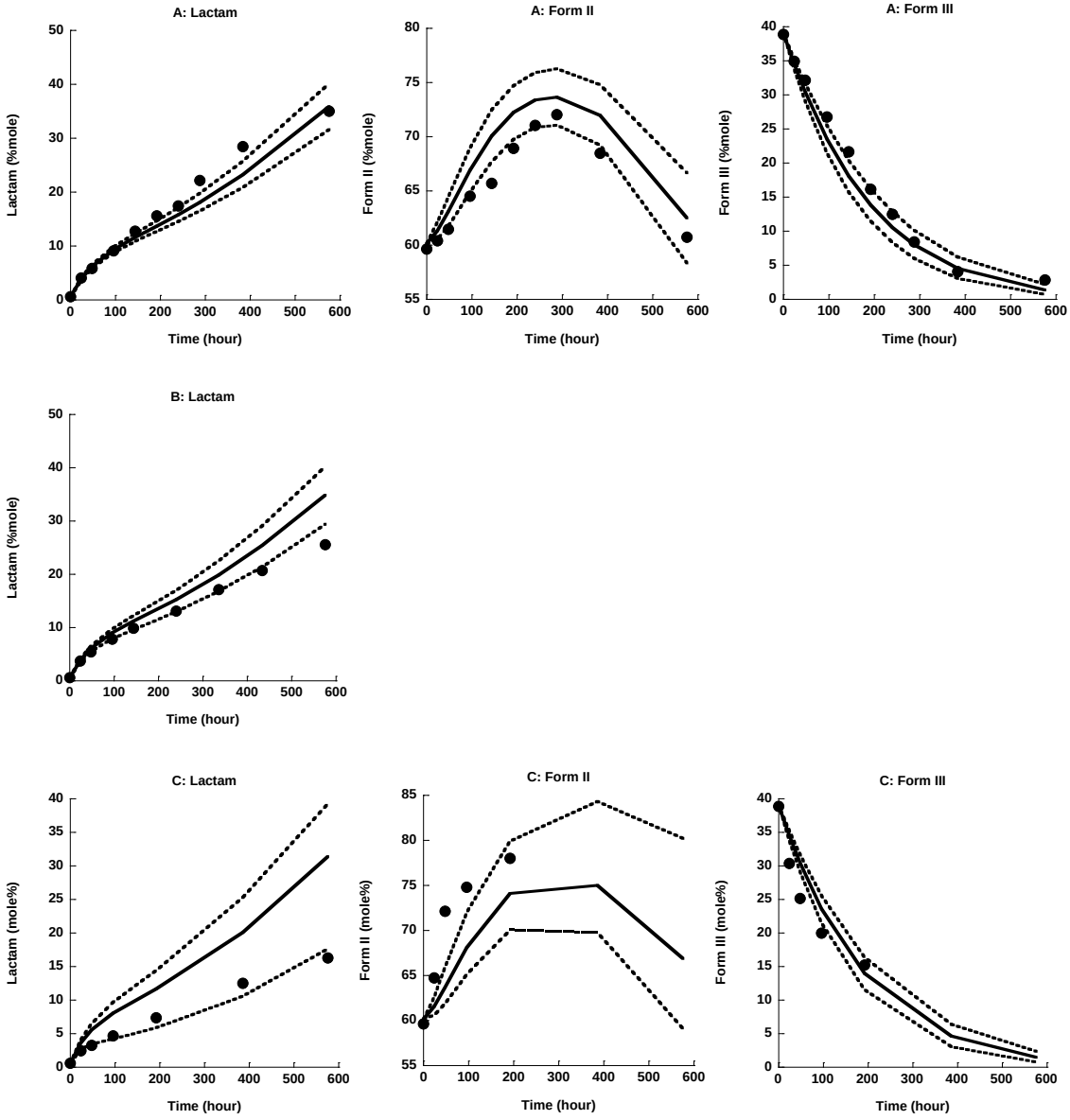

Figure V- 25. Concentration time profiles of lactam, gabapentin Form II and Form III. Points present the observed reaction mixtures with $CaHPO_4$ stored under 60 °C/10 %RH (A), 60 °C/27 %RH (B), and 60 °C/44 %RH (C). The solid and dash curves represent the mean, 95% upper and lower bounds of observed data predicted by MCMC sampling and new model.

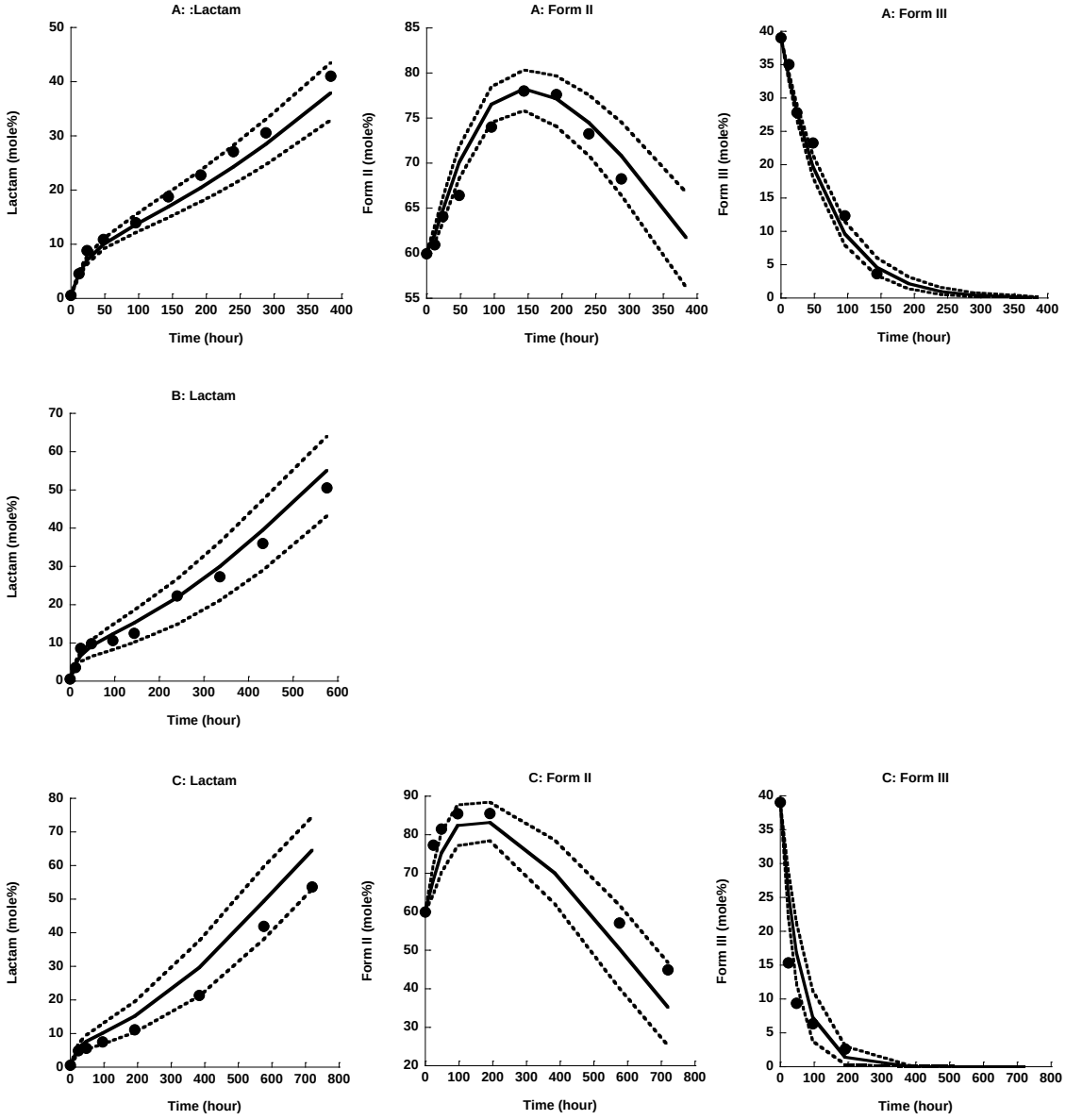

Figure V- 26. Concentration time profiles of lactam, gabapentin Form II and Form III. Points present the observed reaction mixtures with SiO_2 stored under 40 °C/12 %RH (A), 40 °C/32 %RH (B), and 40 °C/48 %RH (C). The solid and dash curves represent the mean, 95% upper and lower bounds of observed data predicted by MCMC sampling and new model.

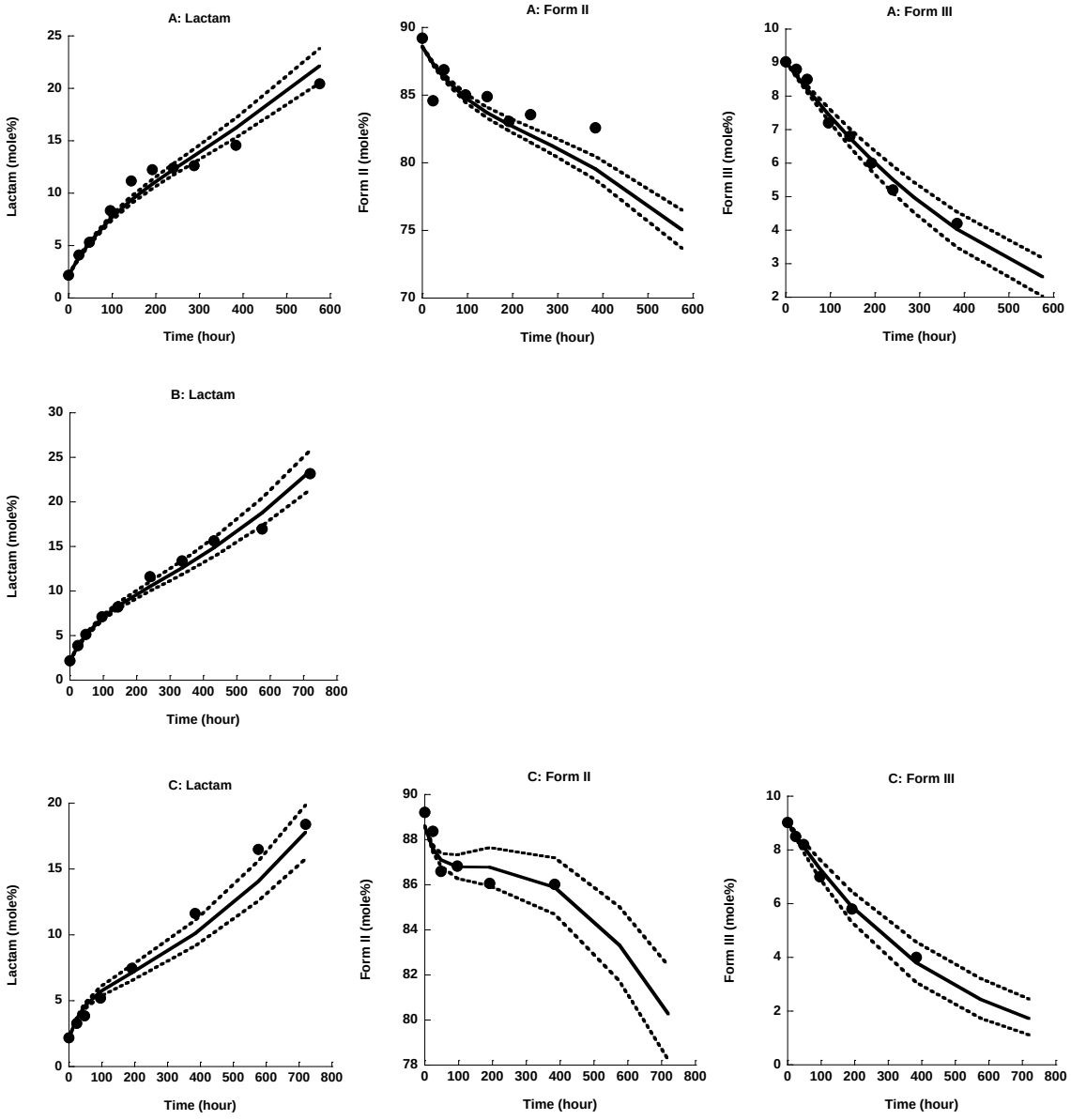

Figure V- 27. Concentration time profiles of lactam, gabapentin Form II and Form III. Points present the observed reaction mixtures with SiO_2 stored under 50 °C/11 %RH (A), 50 °C/29 %RH (B), and 50 °C/47.5 %RH (C). The solid and dash curves represent the mean, 95% upper and lower bounds of observed data predicted by MCMC sampling and new model.

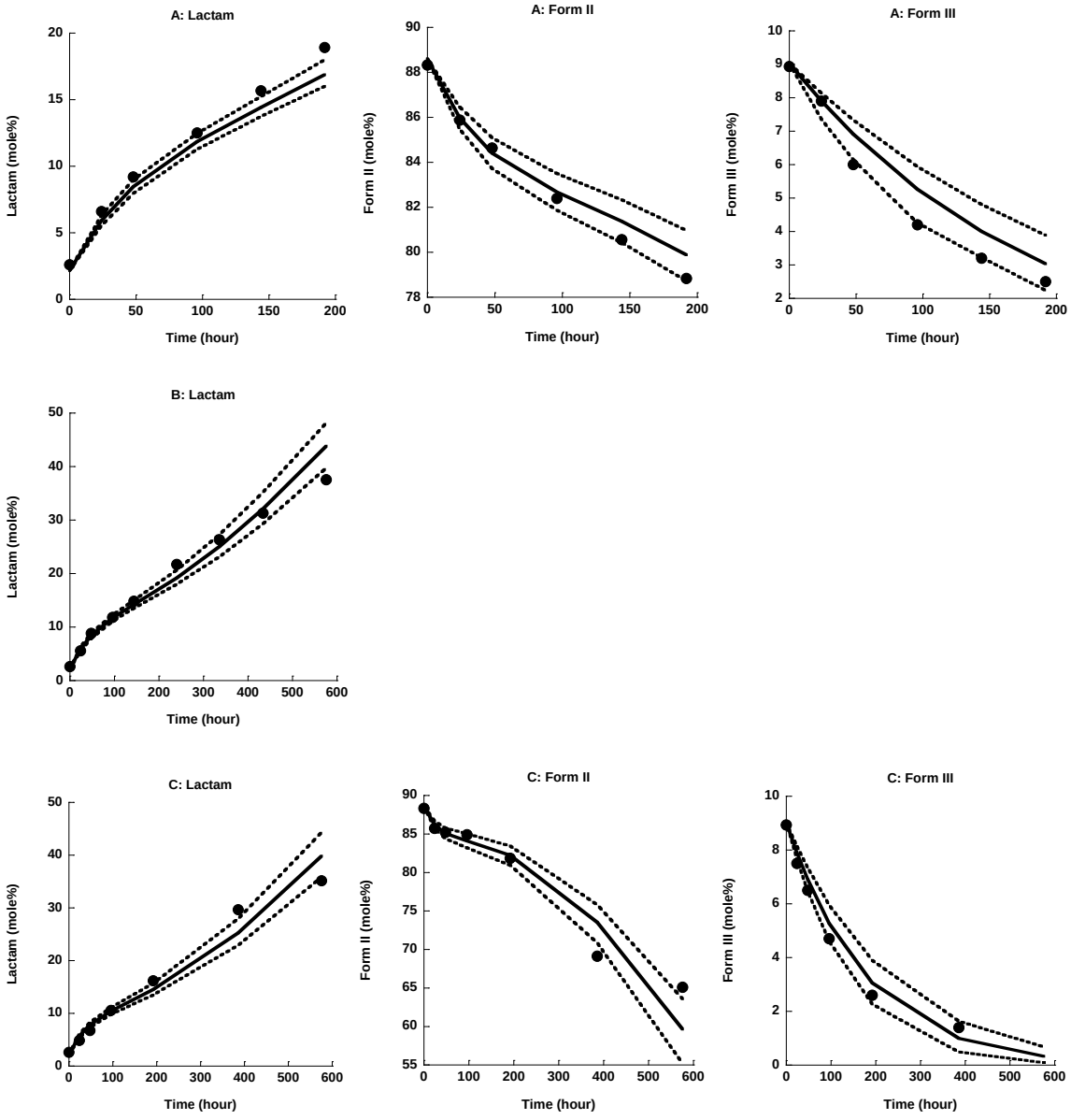

Figure V- 28. Concentration time profiles of lactam, gabapentin Form II and Form III. Points present the observed reaction mixtures with SiO_2 stored under 60 °C/10 %RH (A), 60 °C/27 %RH (B), and 60 °C/44 %RH (C). The solid and dash curves represent the mean, 95% upper and lower bounds of observed data predicted by MCMC sampling and new model.

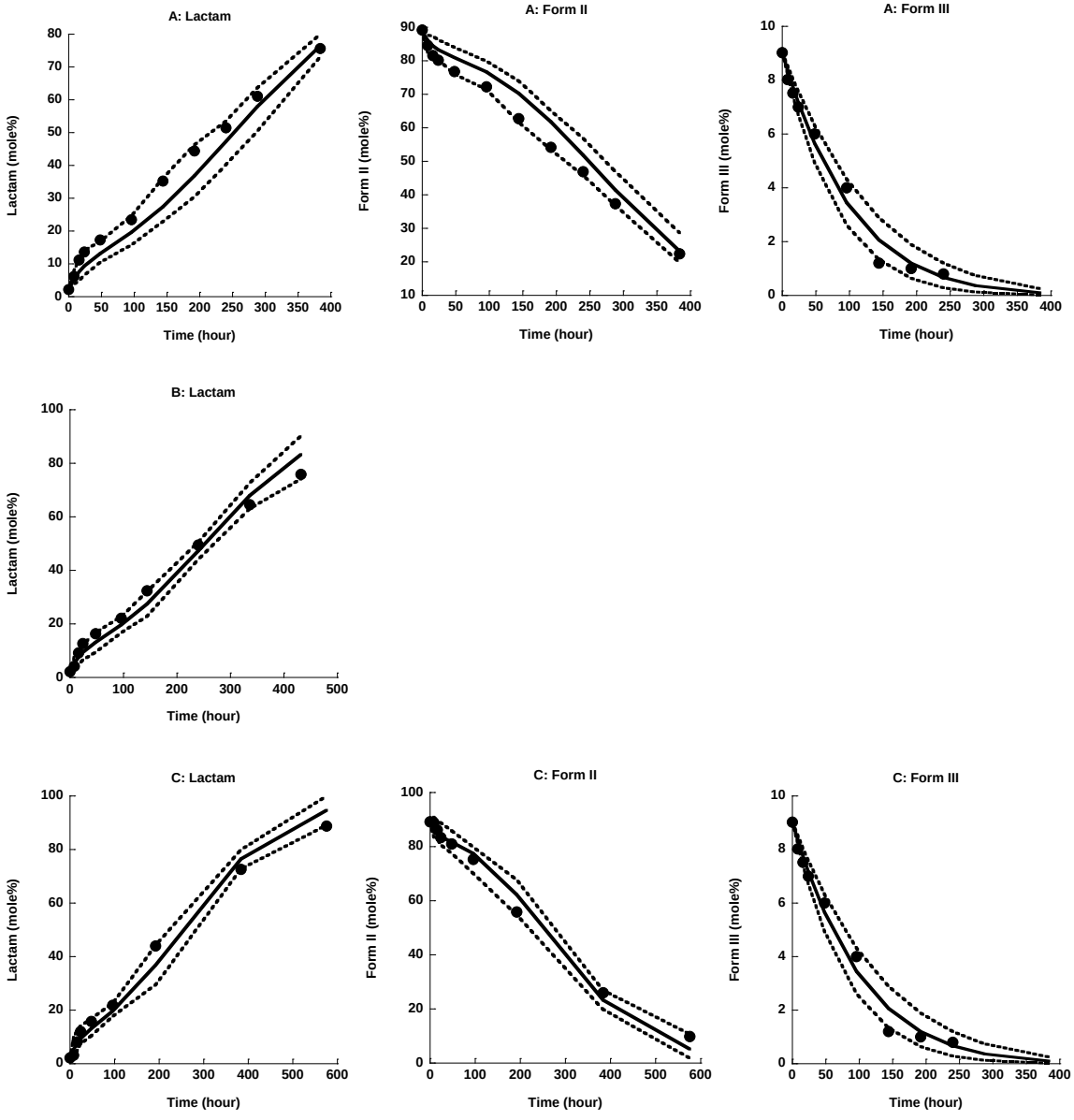

Figure V- 29. Concentration time profiles of lactam, gabapentin Form II and Form III. Points present the observed reaction mixtures with starch stored under 40 °C/12 %RH (A), 40 °C/32 %RH (B), and 40 °C/48 %RH (C). The solid and dash curves represent the mean, 95% upper and lower bounds of observed data predicted by MCMC sampling and new model.

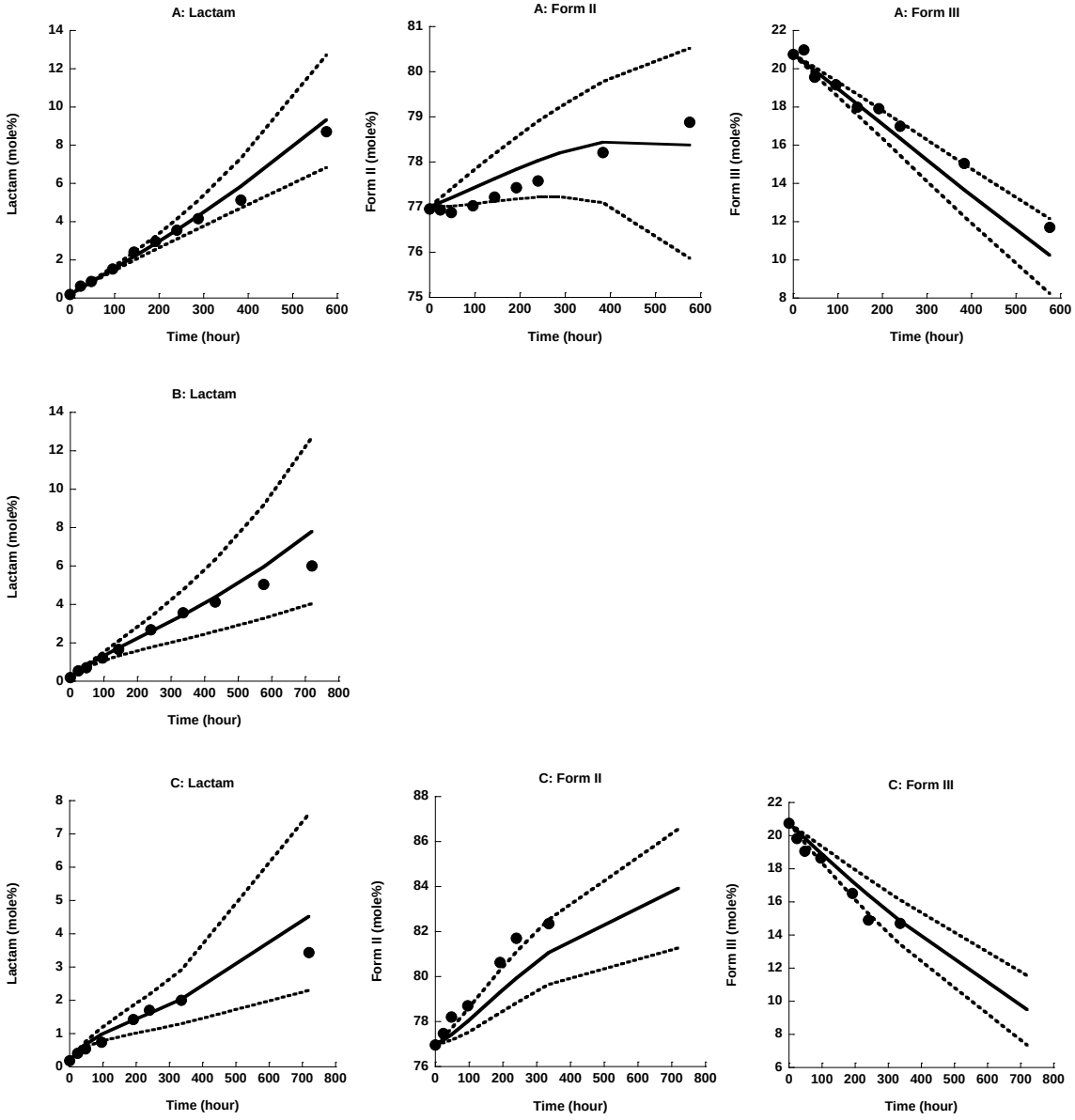

Figure V- 30. Concentration time profiles of lactam, gabapentin Form II and Form III. Points present the observed reaction mixtures with starch stored under 50 °C/11 %RH (A), 50 °C/29 %RH (B), and 50 °C/47.5 %RH (C). The solid and dash curves represent the mean, 95% upper and lower bounds of observed data predicted by MCMC sampling and new model.

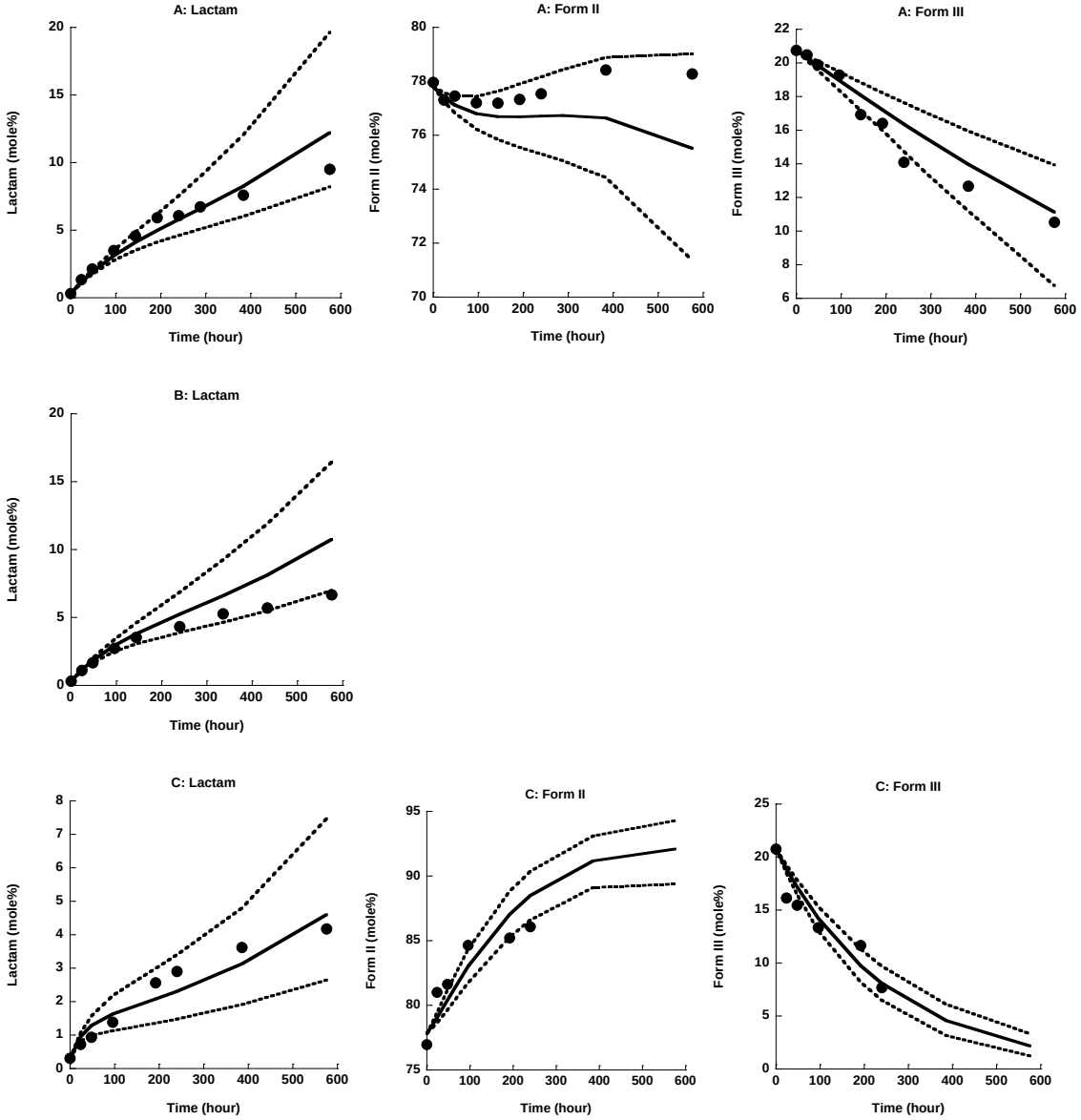

Figure V- 31. Concentration time profiles of lactam, gabapentin Form II and Form III. Points present the observed reaction mixtures with starch stored under 60 °C/10 %RH (A), 60 °C/27 %RH (B), and 60 °C/44 %RH (C). The solid and dash curves represent the mean, 95% upper and lower bounds of observed data predicted by MCMC sampling and new model.

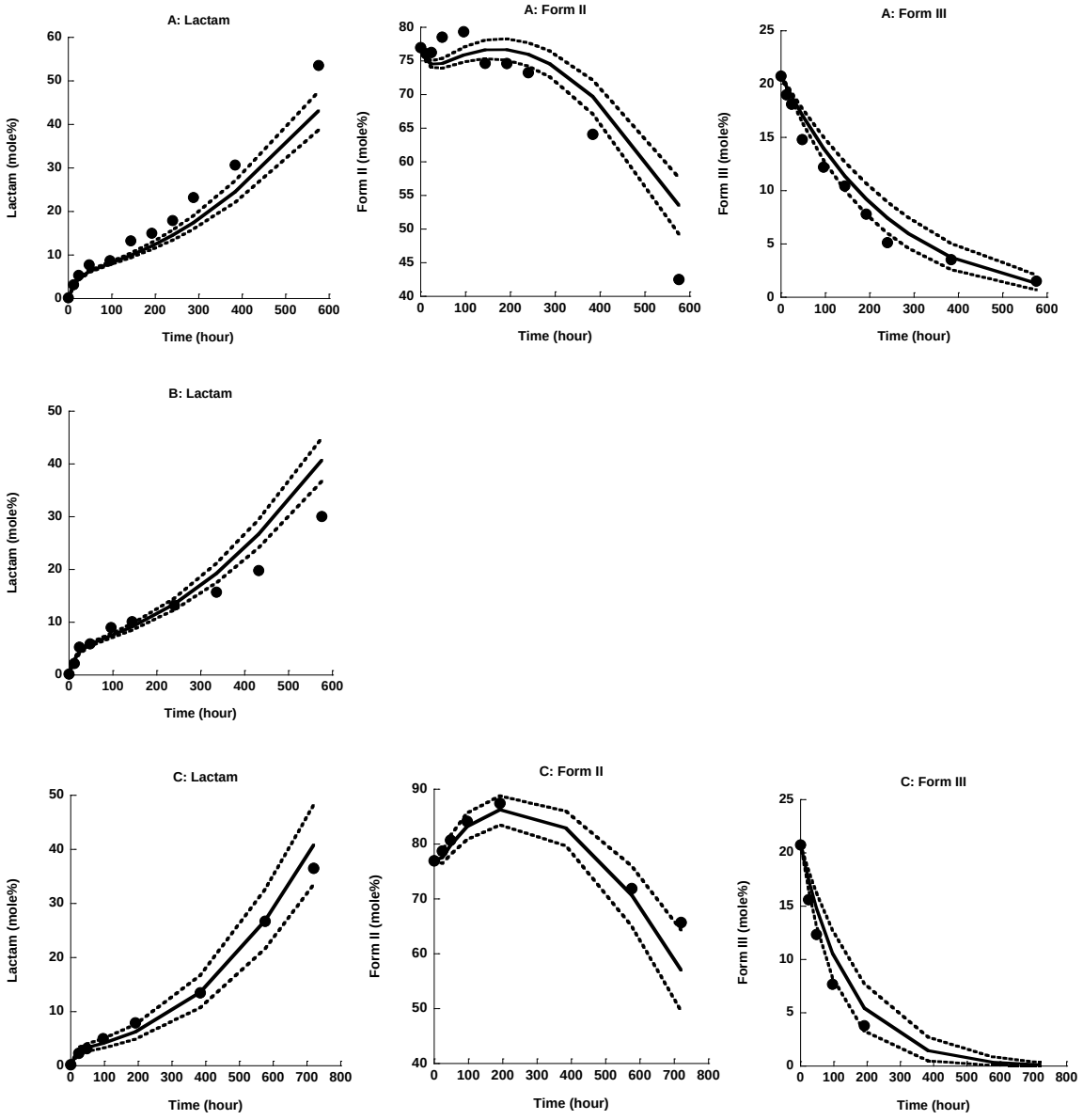

Figure V- 32. Concentration time profiles of lactam, gabapentin Form II and Form III. Points present the observed reaction mixtures with HPC stored under 40 °C/12 %RH (A), 40 °C/32 %RH (B), and 40 °C/48 %RH (C). The solid and dash curves represent the mean, 95% upper and lower bounds of observed data predicted by MCMC sampling and new model.

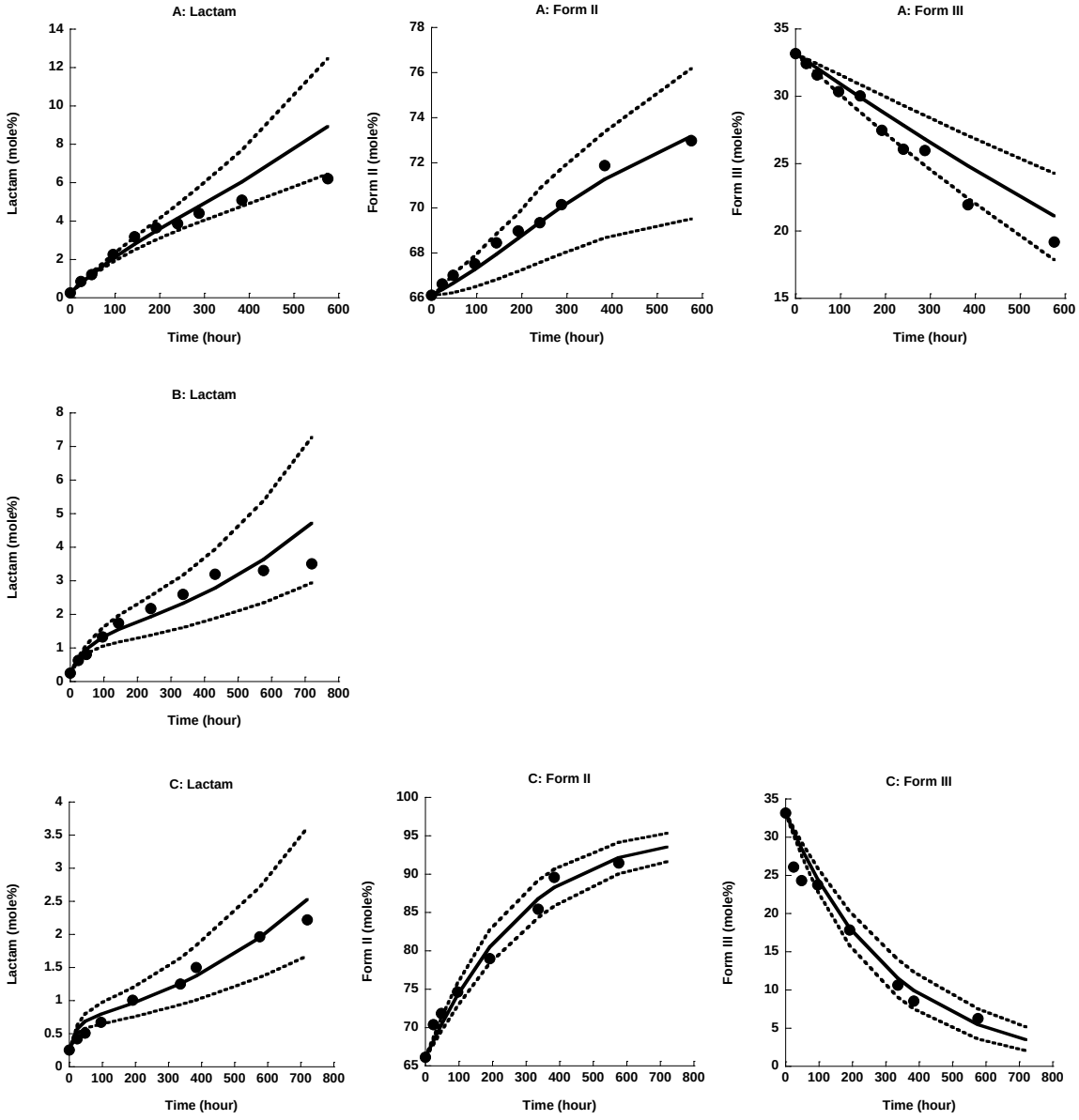

Figure V- 33. Concentration time profiles of lactam, gabapentin Form II and Form III. Points present the observed reaction mixtures with HPC stored under 50 °C/11 %RH (A), 50 °C/29 %RH (B), and 50 °C/47.5 %RH (C). The solid and dash curves represent the mean, 95% upper and lower bounds of observed data predicted by MCMC sampling and new model.

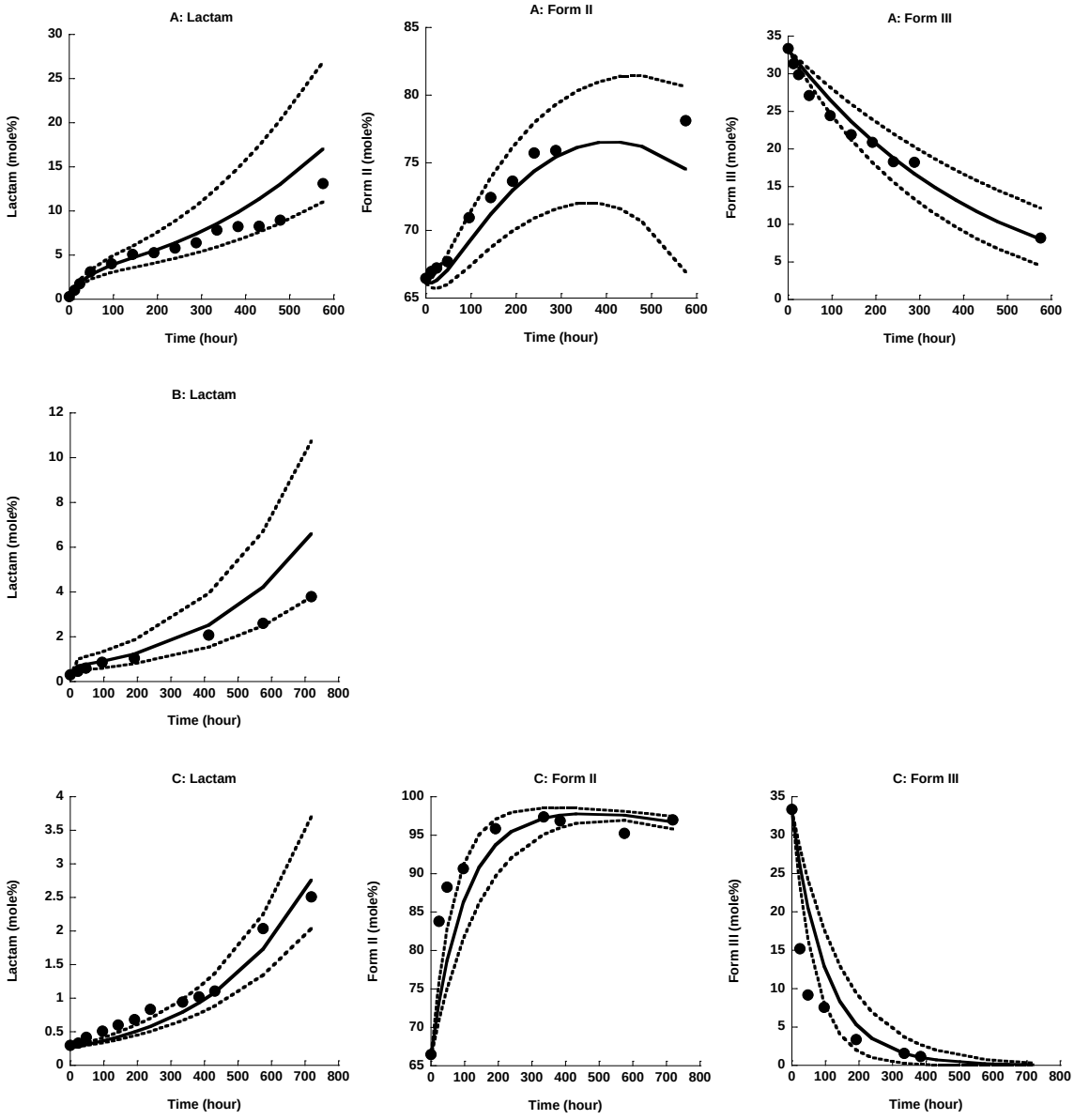

Figure V- 34. Concentration time profiles of lactam, gabapentin Form II and Form III. Points present the observed reaction mixtures with HPC stored under 60 °C/10 %RH (A), 60 °C/27 %RH (B), and 60 °C/44 %RH (C). The solid and dash curves represent the mean, 95% upper and lower bounds of observed data predicted by MCMC sampling and new model.

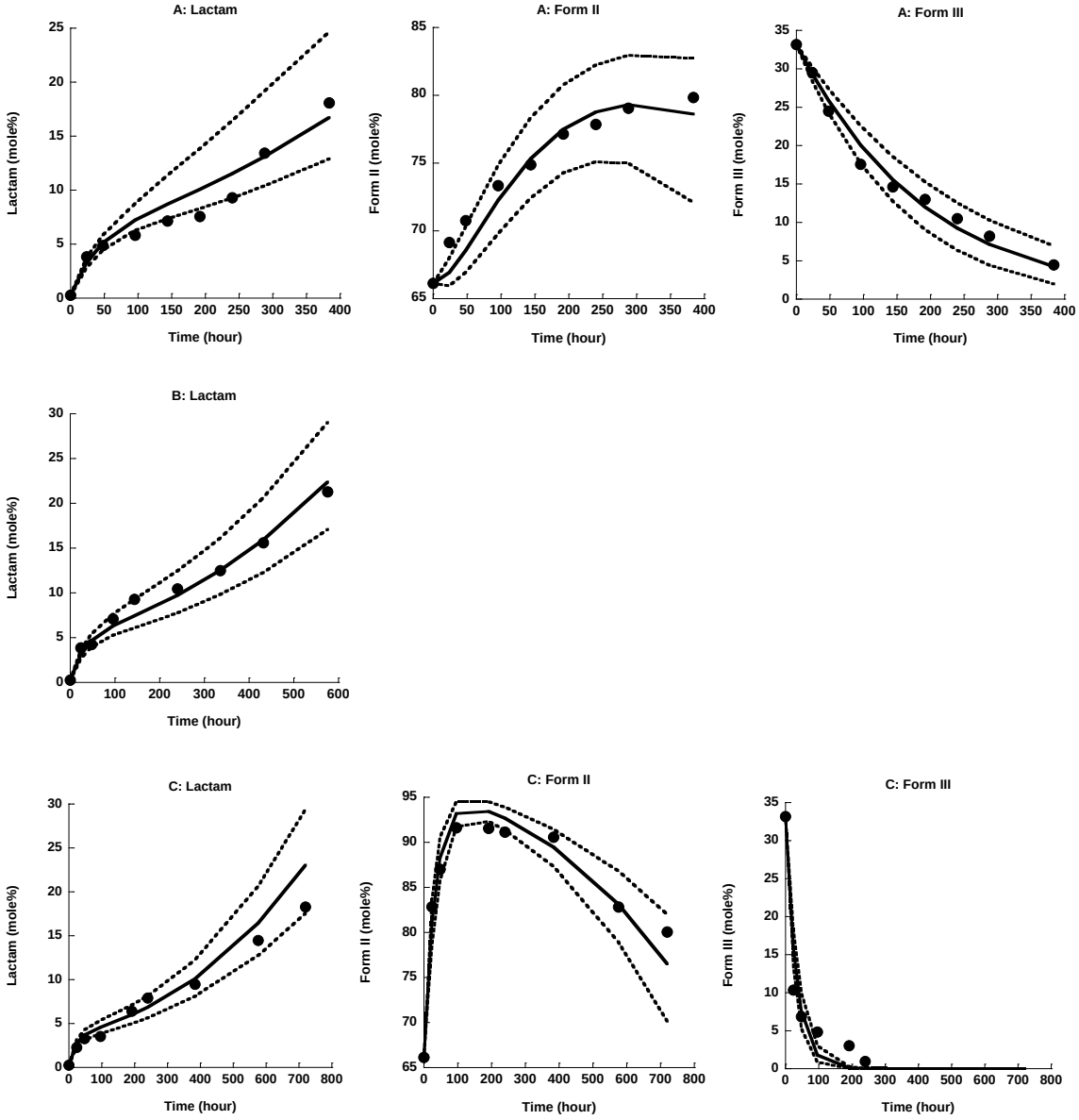

Summary of Parameter Estimate Values

We have demonstrated that our model [Figure V-14] was useful for describing the relationship between lactam, II and III. The concentration time profiles for each species were considered simultaneously to estimate model parameter distributions that accurately reflected model uncertainty. Rate constants for each physical and chemical transition: k_1 for the conversion of II*➔II, k_2 for the rapid conversion of II*➔lactam, k_3 for the conversion of II➔lactam, k_4 for the conversion of III➔lactam, and k_5 for the polymorphic transformation of III➔II were estimated.

A nonlinear optimization was used to simultaneously estimate five rate constants for each reaction mixture at each storage temperature (40, 50 and 60 °C). These estimates were used as starting points for the MCMC sampling in the Bayesian estimation. The MCMC simulation using the Metropolis-Hastings algorithm was carried out to obtain posterior distributions for each rate constant that described the likely-estimated values and the 95 % confidence limits for each rate constant.

The point estimates of rate constants (k_1) for the conversion of II*➔II at 40, 50, and 60 °C are shown in Table V-3. Based on global and local sensitivity analyses, the reliable estimates of k_1 were difficult to obtain with the available data. Accurate k_1 estimates require a method for measuring the time-dependent changes of II*; however, II* was a minor component (<10 %) in the reaction mixtures (XRPD and ^{13}C ssNMR), and no quantitative analytical method was found. Additionally, the lack of substantial "early-time" lactam data significantly contributed to k_1 uncertainty.

Table V- 3. The parameter point estimates (k_1) for the conversion of II*➔II. The estimates were obtained by simultaneously fitting lactam, II, and III concentration time profiles of the reaction mixtures with $CaHPO_4$, SiO_2, starch and HPC stored at 40, 50 and 60 °C.

k_1x10^3 (hr^{-1})	Excipient			
T (°C)	$CaHPO_4$	SiO_2	starch	HPC
40	1.06	0.0028	0.68	0.69
50	5.3	0.046	1.4	2.1
60	6.3	0.54	6.2	2.2

The estimated rate constants of k_2 (II*➔lactam), k_3 (II➔lactam), k_4 (III➔lactam) and k_5 (III➔II) for reaction mixtures stored at 40, 50, and 60 °C are shown in Table V-4, V-5, V-6 and V-7. Overall, reasonable estimates of k_2, k_3, k_4, and k_5 with relatively narrow 95% confidence limits were obtained. The global and local sensitivity analyses demonstrated that lactam, II and III concentration time data were adequate to reliably estimate these rate constants.

Table V- 4. The parameter estimates (k_2) for the rapid conversion of II*➔lactam. The estimates were obtained by simultaneously fitting lactam, II, and III concentration time profiles of the reaction mixtures with $CaHPO_4$, SiO_2, starch, and HPC stored at 40, 50 and 60 °C using the Bayesian estimation. The 95% confidence limits are shown parenthetically.

k_2x10^2 (hr^{-1})	Excipient			
T (°C)	$CaHPO_4$	SiO_2	starch	HPC
40	0.71 (0.66-0.89)	1.1 (1.0-1.3)	0.24 (0.21-0.27)	0.28 (0.23-0.45)
50	1.9 (1.4-6.5)	1.7 (1.2-2.5)	0.92 (0.67-1.0)	0.85 (0.12-2.1)
60	6.4 (4.6-13.9)	6.7 (6.4-16.8)	4.8 (2.6-9.7)	1.5 (1.1-2.2)

Table V- 5. The parameter estimates (k_3) for the conversion of II➔lactam. The estimates were obtained by simultaneously fitting lactam, II, and III concentration time profiles of the reaction mixtures with $CaHPO_4$, SiO_2, starch, and HPC stored at 40, 50 and 60 °C using the Bayesian estimation. The 95% confidence limits are shown parenthetically.

k_3x10^5 (hr.mole)$^{-1}$	Excipient			
T (°C)	$CaHPO_4$	SiO_2	starch	HPC
40	1.3 (0.68-1.9)	1.9 (1.6-2.1)	0.30 (0.17-0.70)	1.2 (0.56-1.7)
50	1.7 (1.2-1.9)	2.4 (2.1-2.8)	1.5 (1.2-2.0)	2.3 (2.1-2.7)
60	4.4 (4.0-4.4)	8.0 (7.5-8.4)	5.0 (3.6-5.1)	2.9 (2.6-3.3)

Table V- 6. The parameter estimates (k_4) for the conversion of III➔lactam. The estimates were obtained by simultaneously fitting lactam, II, and III concentration time profiles of the reaction mixtures with $CaHPO_4$, SiO_2, starch, and HPC stored at 40, 50 and 60 °C using the Bayesian estimation. The 95% confidence limits are shown parenthetically.

k_4x10^4 (hr.mole)$^{-1}$	Excipient			
T (°C)	$CaHPO_4$	SiO_2	starch	HPC
40	0.32 (0.065-0.52)	0.36 (0.11-0.50)	0.087 (0.052-0.25)	0.033 (0.011-0.17)
50	1.9 (1.6-2.6)	3.7 (1.5-5.4)	1.3 (0.98-1.6)	0.11 (0.011-0.33)
60	2.1 (1.9-3.3)	6.3 (3.9-8.5)	1.5 (1.3-3.3)	0.68 (0.081-0.87)

Table V- 7. The parameter estimates (k_5) for the polymorphic transformation of III➔II. The estimates were obtained by simultaneously fitting lactam, II, and III concentration time profiles of the reaction mixtures with $CaHPO_4$, SiO_2, starch, and HPC stored at 40, 50 and 60 °C using the Bayesian estimation. The 95% confidence limits are shown parenthetically.

k_5x10^3 (hr^{-1})	Excipient			
T (°C)	$CaHPO_4$	SiO_2	starch	HPC
40	1.3 (1.1-1.5)	2.1 (1.7-2.2)	0.44 (0.38-0.57)	0.61 (0.52-0.70)
50	2.4 (1.8-2.8)	3.0 (1.6-3.4)	0.83 (0.69-1.1)	1.2 (1.0-1.5)
60	8.1 (7.1-10.2)	10.0 (9.9-10.6)	2.7 (1.8-3.4)	2.7 (2.5-3.3)

Determination of Effects of Environmental and Compositional Variations on the Kinetics of Each Pathway

The effects of environmental (temperature and humidity) and compositional (excipient type) variations on each chemical and physical transition were investigated by determining the magnitude of activation energy (Ea) and humidity dependent term (β) by using the modified Arrhenius equation ($\ln k = lnA - \frac{E_a}{R.T} + \beta.\%RH$). Estimated rate constants k_2 (II*➔lactam), k_3 (II➔lactam) and k_4 (III➔lactam) for chemical transitions and k_1 (II*➔II) and k_5 (III➔II) for physical transitions of reaction mixtures with and without excipients were compared to determine compositional effects.

Environmental and Compositional Effects on Model Parameters for Chemical Transitions

Rapid Conversion of II➔lactam*

The effect of temperature on the rapid conversion of II*➔lactam was investigated by determining the magnitude of activation energy (Ea_2). The Ea_2 value for each excipient mixture [Figure V-35] was estimated using the Arrhenius equation [Equations V-14 to V-17]. The Ea_2 values ± standard errors of the reaction mixtures with $CaHPO_4$, SiO_2, starch, and HPC were calculated to be 95±7, 77±25, 130±10, and 73±12 kJ/mole, respectively. The Ea_2 values obtained from $CaHPO_4$, SiO_2, and HPC mixtures were similar. This suggested that the magnitude of temperature effect on the rapid conversion of II*➔lactam of these excipient mixtures was not different. The highest Ea_2 value was found for the starch mixture.

Figure V- 35. Natural logarithmic k_2 for rapid conversion of II*➔lactam of reaction mixtures with $CaHPO_4$, SiO_2, starch, and HPC versus the reciprocal of the absolute temperature. Error bars represent 95% confidence limits.

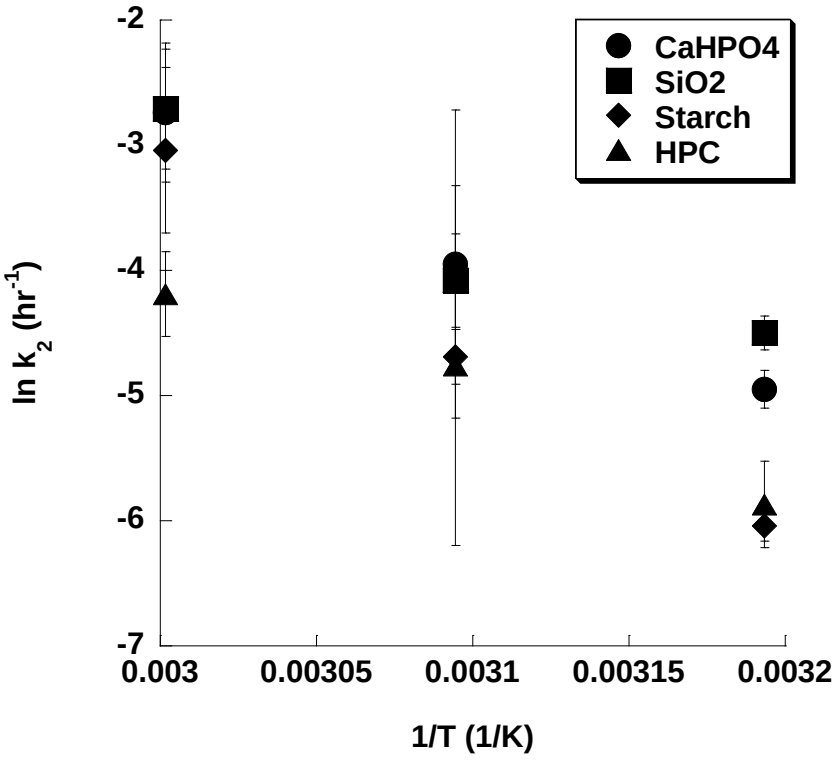

$$k_{2,CaHPO_4} = 5.56 \times 10^{13} \times \exp\left(\frac{-11475}{T}\right) \quad \text{Equation V-14}$$

$$k_{2,SiO_2} = 7.79 \times 10^{10} \times \exp\left(\frac{-9315}{T}\right) \quad \text{Equation V-15}$$

$$k_{2,starch} = 1.04 \times 10^{19} \times \exp\left(\frac{-15623}{T}\right) \quad \text{Equation V-16}$$

$$k_{2,HPC} = 4.34 \times 10^{9} \times \exp\left(\frac{-8762}{T}\right) \quad \text{Equation V-17}$$

The humidity dependence of chemical transition kinetics was evaluated by estimating β_2 in the modified Arrhenius equation using concentration time profiles for reaction mixtures stored at 10, 30 and 50 %RH in the temperature range 40 to 60 °C. The estimated β_2 values are displayed in Table V-8. In all cases, the estimated values were not different than zero thus indicating that these transitions were not humidity dependent.

Table V- 8. Humidity dependent term (β_2) for the rapid conversion of II*➔lactam of reaction mixtures with $CaHPO_4$, SiO_2, starch and HPC. The 95% confidence limits are shown parenthetically.

Excipient	Estimate
$CaHPO_4$	0 (0-0.004)
SiO_2	0 (0-0.001)
Starch	0 (0-0.003)
HPC	0 (0-0.001)

The effect of excipient on k_2 rate constants was determined by comparing the k_2 values of reaction mixtures with and without excipients. (19) The estimated k_2 values for mixtures with and without excipients ($CaHPO_4$, SiO_2, starch and HPC) stored at 40, 50 and 60 °C are shown in Figure V-36 (A-C). The k_2 estimates of all reaction mixtures (with and without excipients) were comparable, thereby demonstrating no apparent excipient effect on the rapid conversion of II*➔lactam.

Figure V- 36. Estimated rate constants (k_2) for the rapid conversion of II*➔lactam at 40 °C (A), 50 °C (B) and 60 °C (C). Error bars represent the 95% confidence limits. The k_2 rate constants were estimated by fitting concentration time profiles of the reaction mixtures with and without excipients ($CaHPO_4$, SiO_2, starch, and HPC) using the Bayesian estimation.

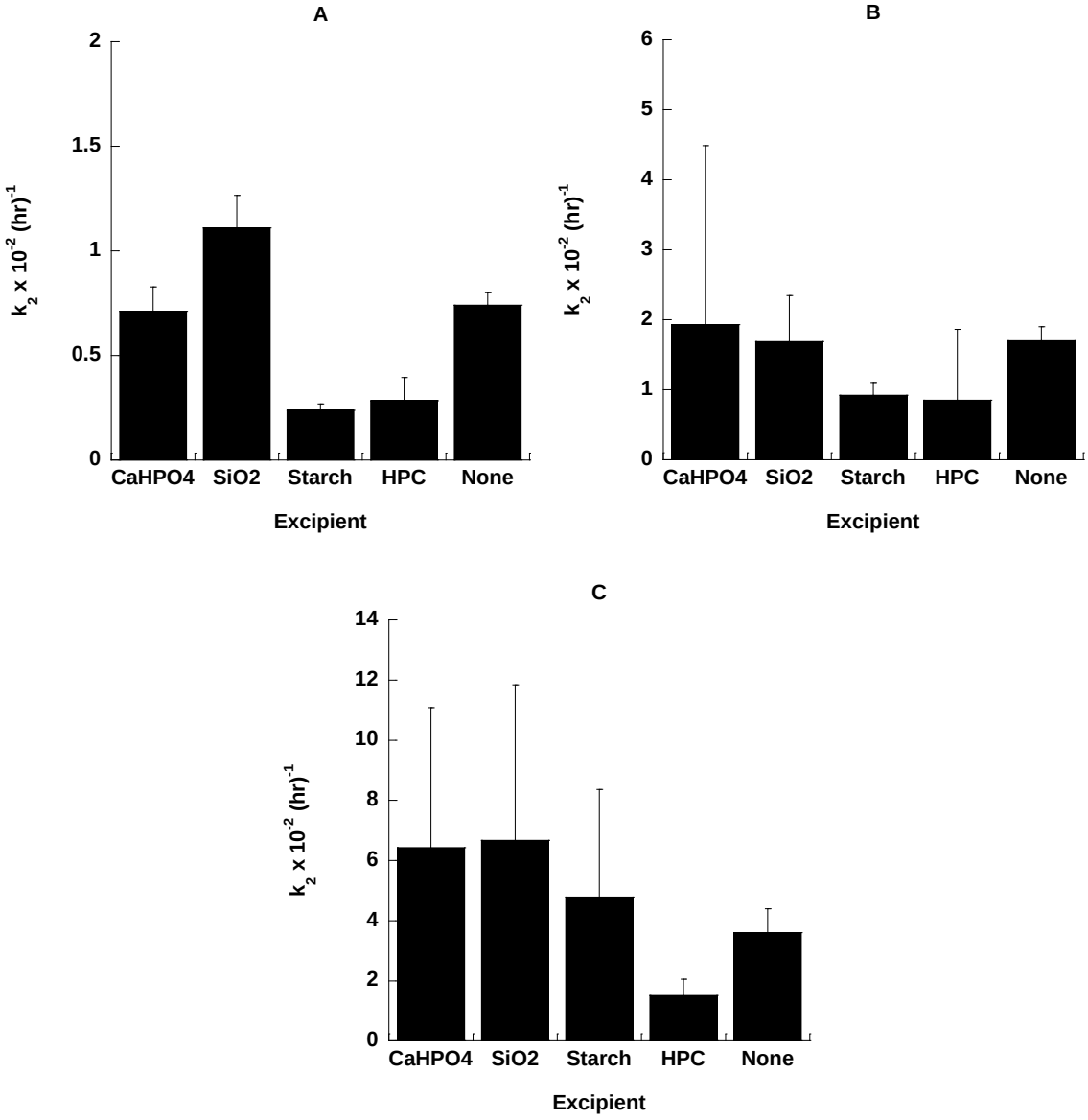

Conversion of II➔lactam

The effect of temperature on the conversion of II➔lactam was investigated by estimating the magnitude of activation energy (Ea_3) [Figure V-37 and Equations V-18 to V-21]. The Ea_3 values ± standard errors of the reaction mixtures with $CaHPO_4$, SiO_2, starch, and HPC were calculated to be 53±17, 63±25, 122±7, and 38±10 kJ/mole, respectively. The Ea_3 values of $CaHPO_4$, SiO_2, and HPC mixtures were similar. This suggested that the magnitude of temperature effect on the conversion of II➔lactam of these excipient mixtures was not different. The rate for the conversion of II➔lactam of starch mixture was the most sensitive to temperature, i.e. highest estimated Ea_3 value.

The significance of humidity dependent term (β_3) on the conversion of II➔lactam was estimated using the modified Arrhenius equation for concentration time profiles stored at different humidity conditions (10, 30 and 50 %RH). The estimated β_3 values for reaction mixtures with $CaHPO_4$, SiO_2, starch and HPC are illustrated in Table V-9. As observed in all excipient mixtures, no significant humidity effect on the conversion of II➔lactam was found. Therefore, the covalent transition appeared to be insensitive to humidity.

Figure V- 37. Natural logarithmic k_3 for conversion of II➔lactam of reaction mixtures with $CaHPO_4$, SiO_2, starch, and HPC versus the reciprocal of the absolute temperature. Error bars represent 95% confidence limits.

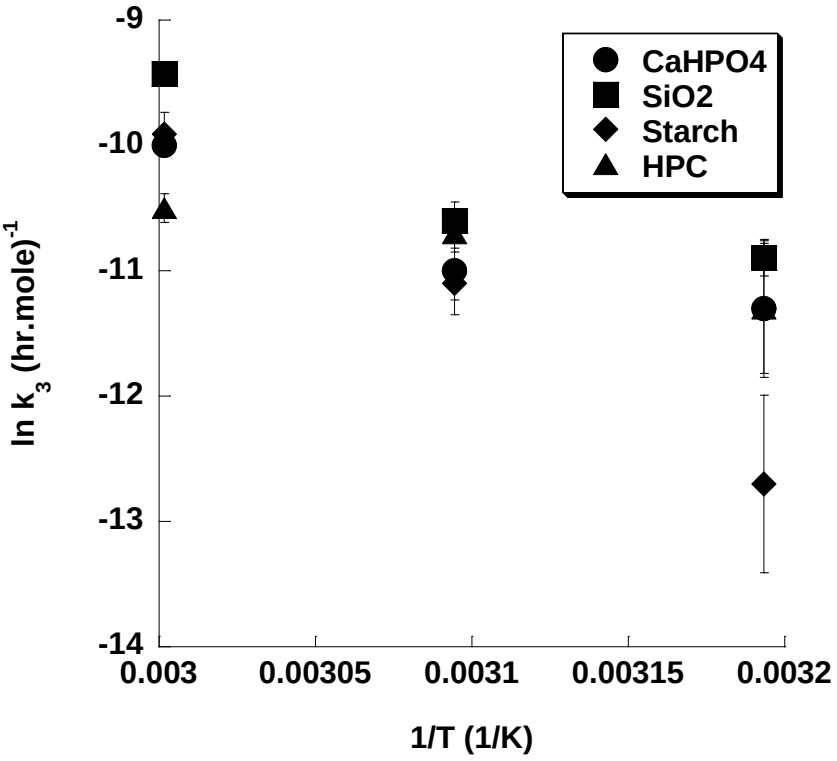

$$k_{3,CaHPO_4} = 8.60 \times 10^3 \times \exp\left(\frac{-6402}{T}\right)$$ Equation V-18

$$k_{3,SiO_2} = 4.56 \times 10^5 \times \exp\left(\frac{-7540}{T}\right)$$ Equation V-19

$$k_{3,starch} = 9.06 \times 10^{14} \times \exp\left(\frac{-14726}{T}\right)$$ Equation V-20

$$k_{3,HPC} = 3.00 \times 10^1 \times \exp\left(\frac{-4594}{T}\right)$$ Equation V-21

Table V- 9. Humidity dependent term (β_3) for the conversion of II➔lactam of reaction mixtures with $CaHPO_4$, SiO_2, starch and HPC. The 95% confidence limits are shown parenthetically.

Excipient	Estimate
$CaHPO_4$	0.002 (0-0.004)
SiO_2	0.002 (0-0.001)
Starch	0.001 (0-0.005)
HPC	0.001 (0-0.001)

The role of excipient on the lactam formation of Form II was investigated by comparing the k_3 values of reaction mixtures with and without excipients. For the reaction mixtures without excipient, the k_3 rate constants were estimated by using lactam formation data of mildly-milled II stored at 5 %RH/40, 50 and 60 °C. The mild milling condition was used to suppress the formation of II* and III during milling (XRPD and ^{13}C ssNMR). Therefore, the primary degradation pathway in these experiments was substrate II dehydration to lactam. The estimated k_3 rate constants of reaction mixtures with and without excipients ($CaHPO_4$, SiO_2, starch and HPC) stored at 40, 50 and 60 °C are shown in Figure V-38 (A-C). Excipients appeared to increase the rates for the conversion of II➔lactam.

Figure V- 38. Estimated rate constants (k_3) for the conversion of II➔lactam at 40 °C (A), 50 °C (B) and 60 °C (C). Error bars represent the 95% confidence limits. The k_3 rate constants were estimated by fitting concentration time profiles of the reaction mixtures with and without excipients ($CaHPO_4$, SiO_2, starch, and HPC) using the Bayesian estimation.

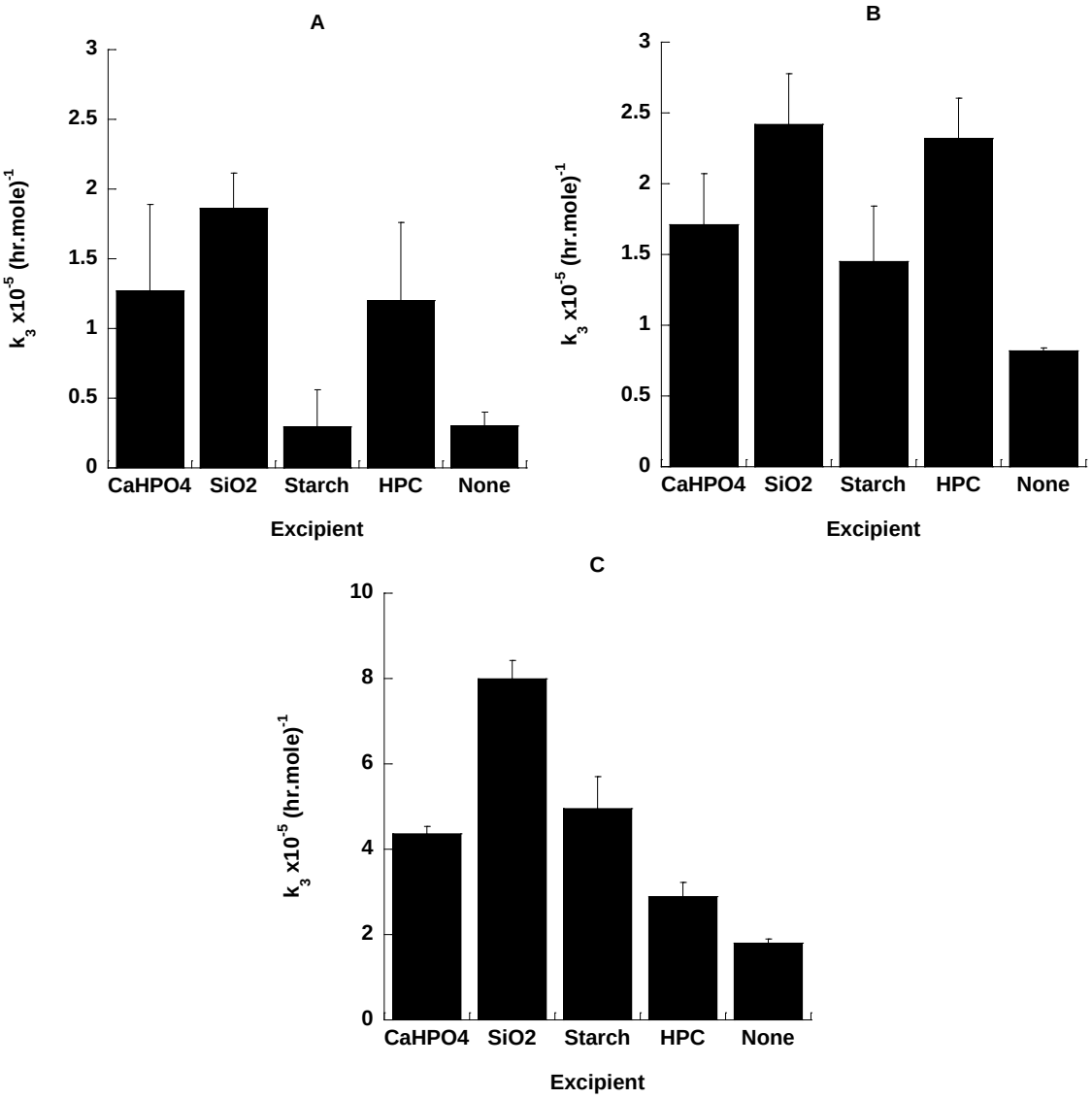

The effect of increasing excipient concentrations on the conversion of II➔lactam during storage was studied in our laboratory by Dr. Eiji Ueyama in parallel with the studies reported herein. Since his results have an important bearing on interpretation of my results, I am presenting a brief synopsis of his studies. Dr. Ueyama devised a protocol wherein he milled Form II under mild conditions and then stored reaction aliquots at 50 ºC/14 %RH for 400 hours. During this time period, II*(caused by milling) converted to lactam and reached a plateau [Figure V-39]. No polymorphic forms other than II (XRPD) were observed under this storage condition. After the 400-hour period, various concentrations of HPC (25, 50 and 75 %w/w) were gently blended with the pre-conditioned substrate (II) and the excipient/substrate mixtures were stored at 50 ºC/14 %RH. Since the conversion of II*(caused by milling) ➔lactam was completed during the first 400-hour of storage, the primary degradation pathway for substrate degradation in excipient mixtures was dehydration to lactam. The exemplary lactam formation profiles of reaction mixtures prepared with separately milled II and various concentrations of HPC stored at 50 ºC/14 %RH are shown in Figure V-39. These profiles clearly illustrate that HPC catalyzed the formation of lactam in a concentration-dependent fashion.

Figure V- 39. Lactamization profiles of reaction mixtures prepared with separately milled gabapentin and HPC (0, 25, 50 and 75 %w/w) stored at 50 ºC and 14 %RH.

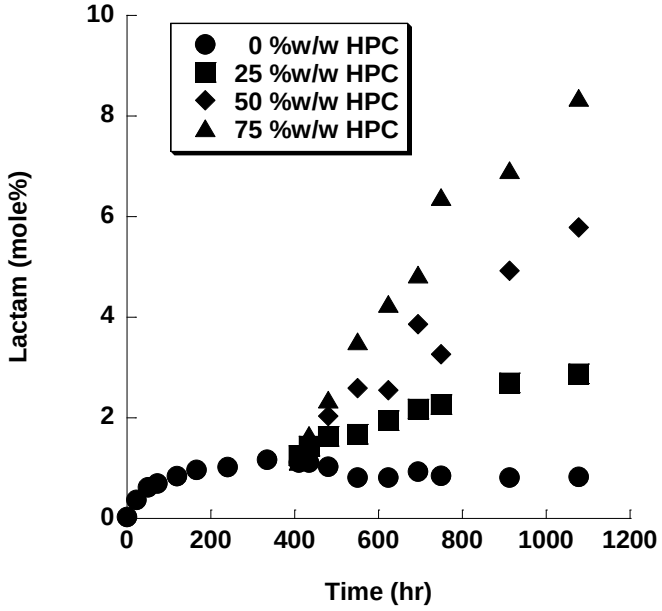

Conversion of III➔lactam

The effect of temperature on the conversion of III➔lactam was investigated by determining the magnitude of activation energy (Ea_4) [Figure V-40 and Equations V-22 to V-25]. The Ea_4 values ± standard errors of the reaction mixtures with $CaHPO_4$, SiO_2, starch, and HPC were calculated to be 82±41, 125±42, 127±60, and 130±16 kJ/mole, respectively. The Ea_4 values of all excipient mixtures appeared to be similar. The magnitude of temperature effect on the conversion of III➔lactam of all excipient mixtures did not appear to be different.

The effect of humidity on the conversion of III➔lactam was determined by the estimated values of β_4 according to the modified Arrhenius equation using concentration time profiles stored at different humidity conditions (10, 30 and 50 %RH). The results are listed in Table V-10. No humidity effects on the conversion of III➔lactam were found.

Figure V- 40. Natural logarithmic k_4 for conversion of III➔lactam of reaction mixtures with $CaHPO_4$, SiO_2, starch, and HPC versus the reciprocal of the absolute temperature. Error bars represent 95% confidence limits.

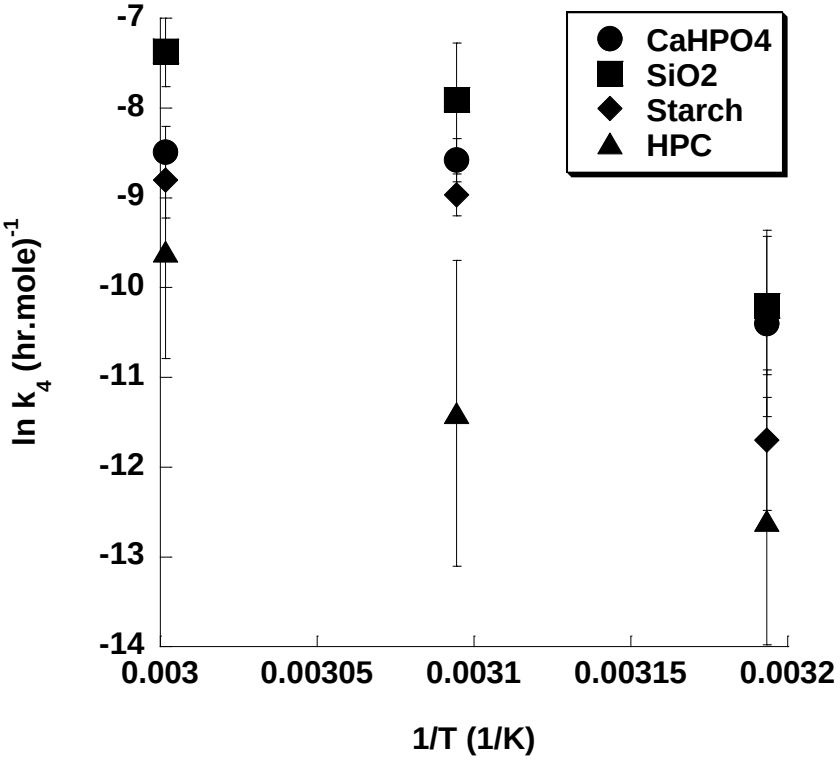

$$k_{4,CaHPO_4} = 2.09 \times 10^9 \times \exp\left(\frac{-9887}{T}\right)$$ Equation V-22

$$k_{4,SiO_2} = 3.45 \times 10^{16} \times \exp\left(\frac{-15046}{T}\right)$$ Equation V-23

$$k_{4,starch} = 8.26 \times 10^{15} \times \exp\left(\frac{-15006}{T}\right)$$ Equation V-24

$$k_{4,HPC} = 1.55 \times 10^{16} \times \exp\left(\frac{-15658}{T}\right)$$ Equation V-25

Table V- 10. Humidity dependent term (β_4) for the conversion of II➔lactam of reaction mixtures with $CaHPO_4$, SiO_2, starch and HPC. The 95% confidence limits are shown parenthetically.

Excipient	Estimate
$CaHPO_4$	0.001 (0-0.002)
SiO_2	0.001(0-0.001)
Starch	0.001(0-0.005)
HPC	0.001(0-0.002)

The effect of excipient variations on k_4 rate constants was investigated by comparing the k_4 values of reaction mixtures with and without excipients. For the reaction mixtures without excipient, the k_4 rate constants were estimated by using lactam formation data of mildly-milled III stored at 5 %RH/40, 50 and 60 °C. The mild milling condition was used to prevent III from converting to II and to suppress the formation of II* during milling. The reaction samples were then stored at 5 %RH to suppress the conversion of III to II during storage (XRPD and ^{13}C ssNMR). Therefore, the primary degradation pathway in these experiments was substrate III dehydration to lactam. The estimated k_4 rate constants of reaction mixtures with and without excipients ($CaHPO_4$, SiO_2, starch and HPC) stored at 40, 50 and 60 °C are shown in Figure V-41 (A-C). Excipients appeared to increase the rates for the conversion of III➔lactam.

Figure V- 41. Estimated rate constants (k_4) for the conversion of III➔lactam at 40 °C (A), 50 °C (B) and 60 °C (C). Error bars represent the 95% confidence limits. The k_4 rate constants were estimated by fitting concentration time profiles of the reaction mixtures with and without excipients ($CaHPO_4$, SiO_2, starch, and HPC) using the Bayesian estimation.

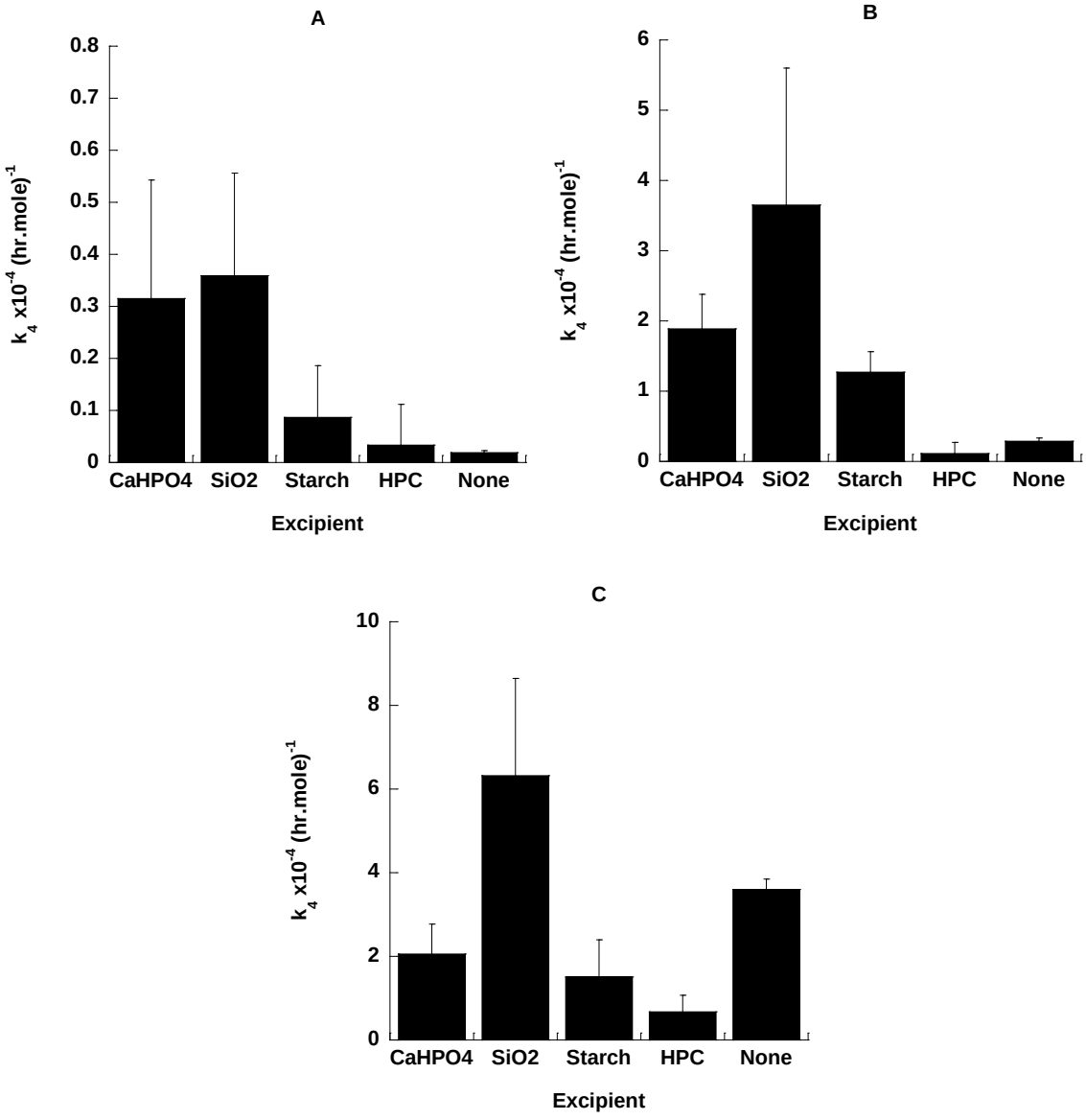

In summary, the chemical transitions were characterized by a lack of humidity effects but strong excipient effects that could be attributed to catalysis. According to the literature, the catalytic effects of excipients on solid state drug degradation typically occur at the interfacial area of contact between drug and excipient. (48-51) The crystal defects are more concentrated on the surface and increased surface energy may result in the increased susceptibility to drug degradation.

The effect of excipient properties on degradation of gabapentin during storage at 50 °C/5 %RH was studied by Akshata Nevrekar in Professor Buckner's laboratory at Duquesne University. These investigators devised a protocol to investigate the degree of contact between gabapentin and various excipients in (1:1) physical mixtures. Theoretically-calculated fraction of excipient surface area in contact with gabapentin *(f)* was estimated by considering size, shape, and density of excipient particles. True density was determined by helium pycnometry and volume of particles was calculated based on particle morphology and measuring dimensions (length/breadth) using optical microscopy. The apparent rate of lactam formation was found to be a function of the fraction of excipient surface area in contact with gabapentin. (52)

In another example, milled metoclopramide HCl was mixed with lactose and the Maillard-type degradation rates were measured. The increases in reactivity were proportional to the increased surface energy (due to the generation of crystal defects caused by milling), and increased contact area of drug/excipient. (53, 54)

In our studies, excipient appeared to influence the conversion rates of II and III to lactam [Figure V-38 (A-C) and V-41 (A-C)]. The catalytic effect was demonstrated by the concentration-dependent rates observed by Dr. Ueyama in our laboratory [Figure V-

39]. The magnitude of catalytic effects of excipients on the susceptibility of II and III to lactam was determined by comparing the rate constants k_3 and k_4 for each excipient mixture. The rate constants (k_3 and k_4) for the lactamization of II and III in excipient mixtures stored at 40, 50 and 60 °C are shown in Figure V-42 (A-C). Overall, the rates (k_4) for the conversion of III➔lactam appeared to be greater than the rates (k_3) for the conversion of II. The degradation rates in our heterogeneous system are complicated due to the differences in interfacial area of contacts (created by milling) between drug molecules (II or III) and excipient [Figure V-43]. Therefore, we have insufficient evidence to determine the relative magnitude of catalytic effects of excipients on the lactamization of III or II.

Figure V- 42. Estimated rate constants (k_3) for conversion of II➔lactam and k_4 for conversion of III➔lactam at 40 °C (A), 50 °C (B) and 60 °C (C). Error bars represent the 95% confidence limits. The k_3 and k_4 rate constants were estimated by fitting concentration time profiles of the reaction mixtures with $CaHPO_4$, SiO_2, starch, and HPC using the Bayesian estimation.

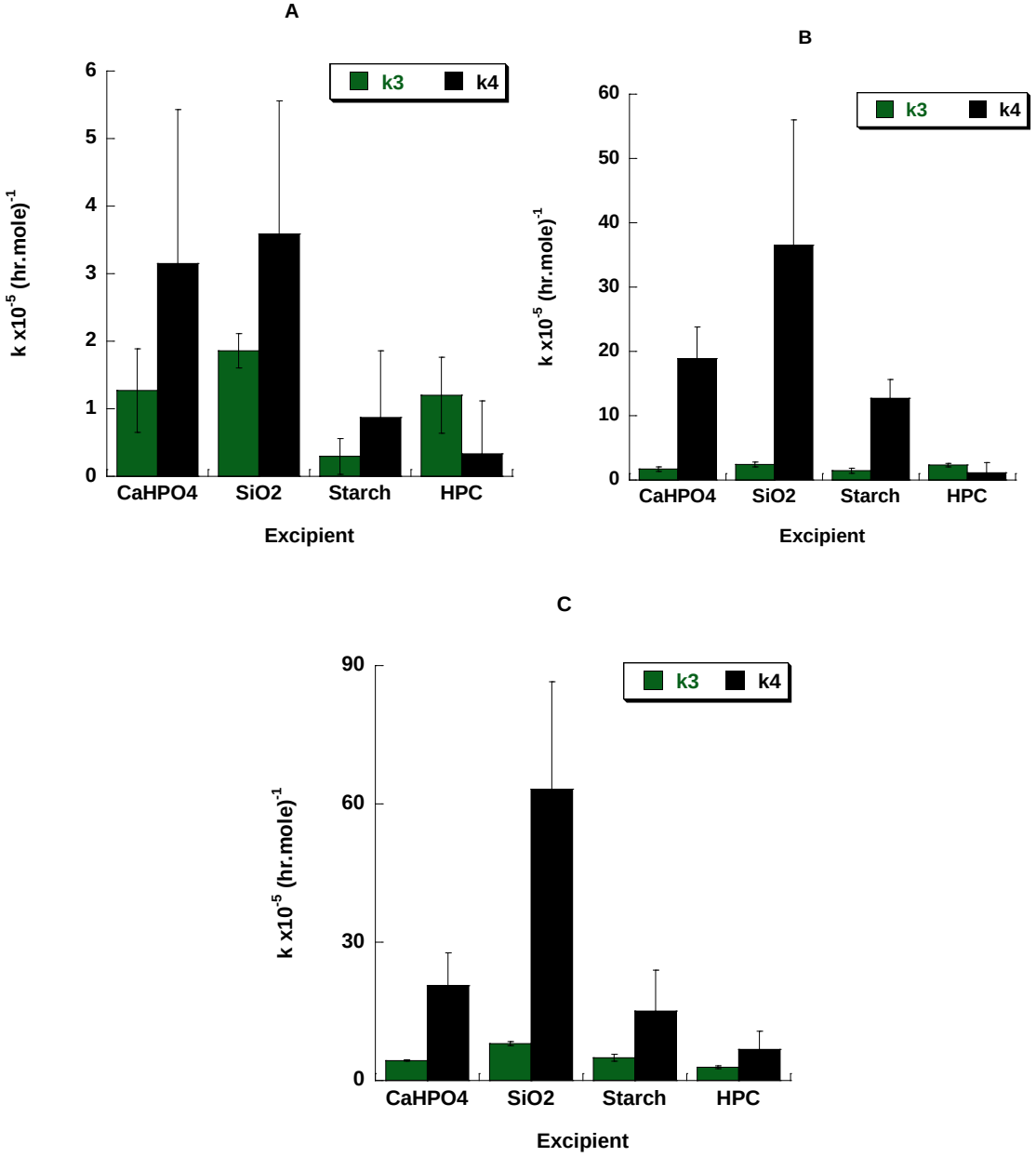

Figure V- 43. Graphical representation of the heterogeneous system in the solid state.

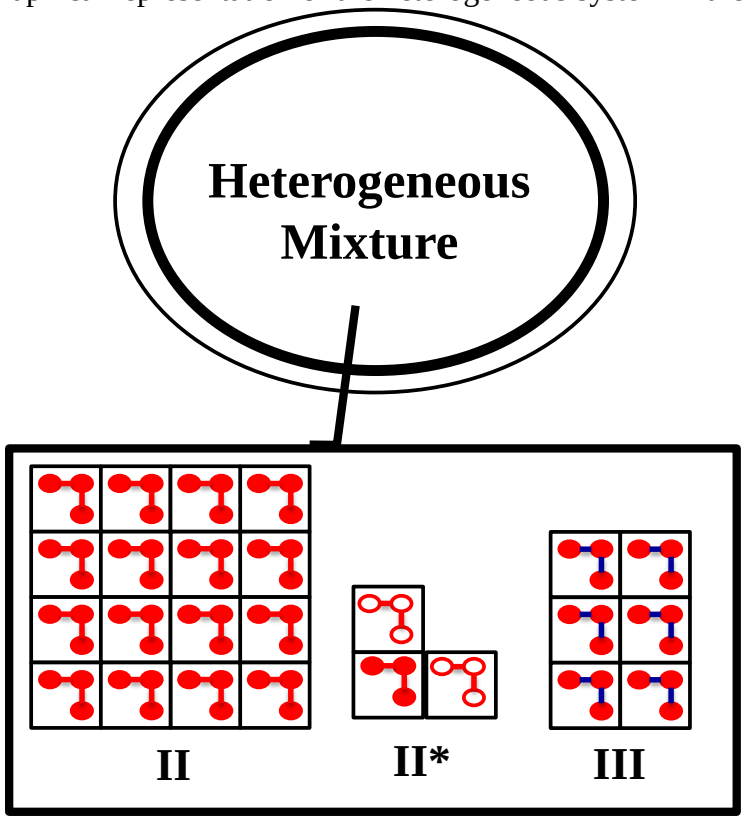

In the solid state, typical activation energy values for intramolecular cyclization or amine-carbonyl reaction of pharmaceutical compounds are in the range of 200-300 kJ/mole. For example, activation energy for cyclization of aspartylphenylalanine was reported to be 270 kJ/mol. This activation energy was much higher than that observed in typical solution reaction (70 kJ/mol), thereby suggesting high energy requirement for crystal lattice rearrangement. (55) The reported values of activation energy for thermally-induced solid state degradation of lisinopril were in the range of 170-300 kJ/mole. (56, 57) In another example, the activation energy of cyclization of enalapril maleate was reported to be 200 kJ/mol. (58, 59)

In our studies, the covalent transitions were characterized by a strong excipient effect. Reduction in activation energy of covalent transitions was observed [Table V-11]

and this was consistent with catalytic effect. One possible explanation is that excipients act as catalysts to increase the degradation rate of drug molecules by decreasing in activation energy without being consumed or changed at the end of reaction. (51, 60)

Table V- 11. Activation energy values of covalent transitions: conversion of II*to lactam (Ea_2), autocatalytic lactamization of II (Ea_3) and III (Ea_4) of reaction mixtures with $CaHPO_4$, SiO_2, starch, and HPC. SE represents standard error.

Reaction mixtures containing excipients	Ea_2±SE (kJ/mole)	Ea_3±SE (kJ/mole)	Ea_4±SE (kJ/mole)
$CaHPO_4$	95± 7	53±17	82±41
SiO_2	77±25	63±25	125±42
Starch	130±10	122±7	127±60
HPC	73±12	38±10	130±16

Environmental and Compositional Effects on Model Parameters for Physical Transitions

Polymorphic Transformation of III➔II

The effect of temperature on the polymorphic transformation of III➔II was investigated by determining the Ea_5 value for each excipient mixture by plotting the natural logarithmic k_5 rate constants versus the reciprocal of the absolute temperature [Figure V-44]. The Ea_5 values ± standard errors of the reaction mixtures with $CaHPO_4$, SiO_2, starch, and HPC were estimated to be 80±17, 68±23, 77±14, and 65±5 kJ/mole, respectively. The Ea_5 values of all excipient mixtures were indistinguishable from each other.

The humidity dependent term (β_5) for the polymorphic transformation of III➔II was estimated using the modified Arrhenius equation [Equation V-26 to V-29] for reaction mixtures with $CaHPO_4$, SiO_2, starch and HPC. The results are shown in Figure V-45. The values of β_5 were significantly greater than zero; thus this polymorphic transition is humidity dependent. The magnitude of humidity effect depended on excipient type. The β_5 values for organic excipient mixtures (HPC and starch) were

greater than inorganic excipient mixtures ($CaHPO_4$ and SiO_2). For example, the β_5 value for reaction mixtures containing HPC was 10 times greater than SiO_2 mixtures.

Figure V- 44. Natural logarithmic k_5 for polymorphic transformation of III➔II of reaction mixtures with $CaHPO_4$, SiO_2, starch, and HPC versus the reciprocal of the absolute temperature. Error bars represent 95% confidence limits.

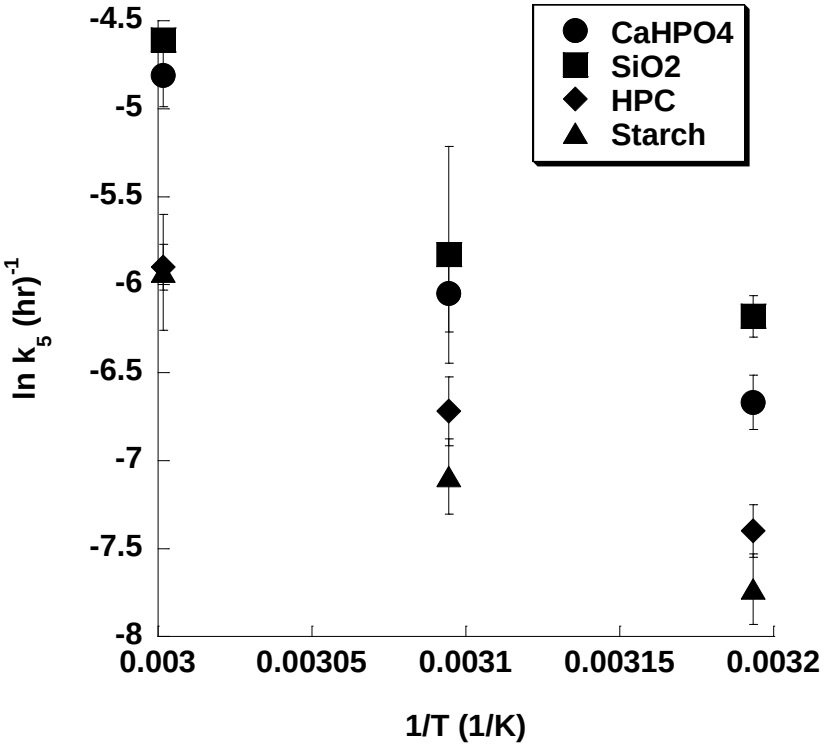

$$k_{5,CaHPO_4} = 2.62 \times 10^{10} \times \exp\left(\frac{-9634}{T}\right) \times \exp(0.020 \times \%RH) \quad \text{Equation V-26}$$

$$k_{5,SiO_2} = 3.52 \times 10^{8} \times \exp\left(\frac{-8147}{T}\right) \times \exp(0.005 \times \%RH) \quad \text{Equation V-27}$$

$$k_{5,starch} = 3.28 \times 10^{9} \times \exp\left(\frac{-9311}{T}\right) \times \exp(0.028 \times \%RH) \quad \text{Equation V-28}$$

$$k_{5,HPC} = 4.10 \times 10^{7} \times \exp\left(\frac{-7817}{T}\right) \times \exp(0.055 \times \%RH) \quad \text{Equation V-29}$$

Figure V- 45. Humidity dependent term (β_5) for the polymorphic transformation of III➔II of reaction mixtures with $CaHPO_4$, SiO_2, starch and HPC. Error bars represent the 95 % confidence limits.

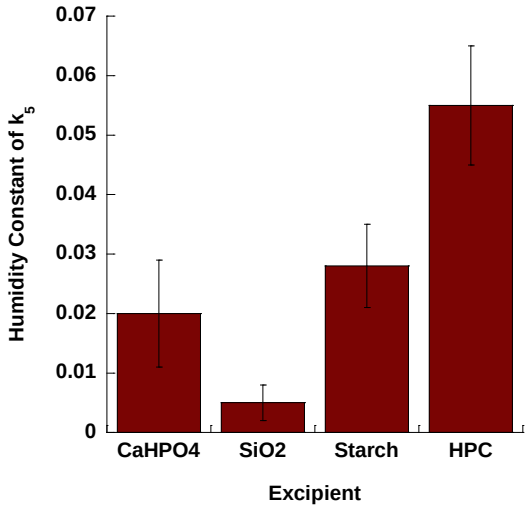

The effect of humidity on polymorphic transformation (III➔II) of gabapentin in the absence of excipient has been previously reported. Un-milled III was exposed to 50 %RH/room temperature and kinetic of polymorphic transformation of III➔II was determined. The transformation of III➔II was completed within 168 hours. (45) In another example, reaction mixtures were prepared by extensively milling II. The extensive milling condition was used to convert II➔III during milling. The resultant samples were stored at an elevated temperature (50 °C) and 29 %RH and the conversion of III➔II completed in less than ten hours. (61)

The effect of excipient-humidity interactions on k_5 rate constants was determined by comparing the k_5 values of reaction mixtures with and without excipients ($CaHPO_4$, SiO_2, starch and HPC) stored at 50 °C/29 %RH. The results are shown in Figure V-46. The estimated k_5 rate constants for the reaction mixtures with excipients were 60-185 times slower than that observed in the mixtures without excipients. This demonstrated that the humidity catalysis was substantially inhibited by excipients.

Figure V- 46. Estimated rate constants (k_5) for polymorphic transformation of III➔II at 50 °C/29 %RH. Error bars represent the 95% confidence limits. The k_5 rate constants were estimated by fitting concentration time profiles of the reaction mixtures with $CaHPO_4$, SiO_2, starch, and HPC using the Bayesian estimation. For the reaction mixture without excipient, the k_5 rate constant was reported by Zong. (61)

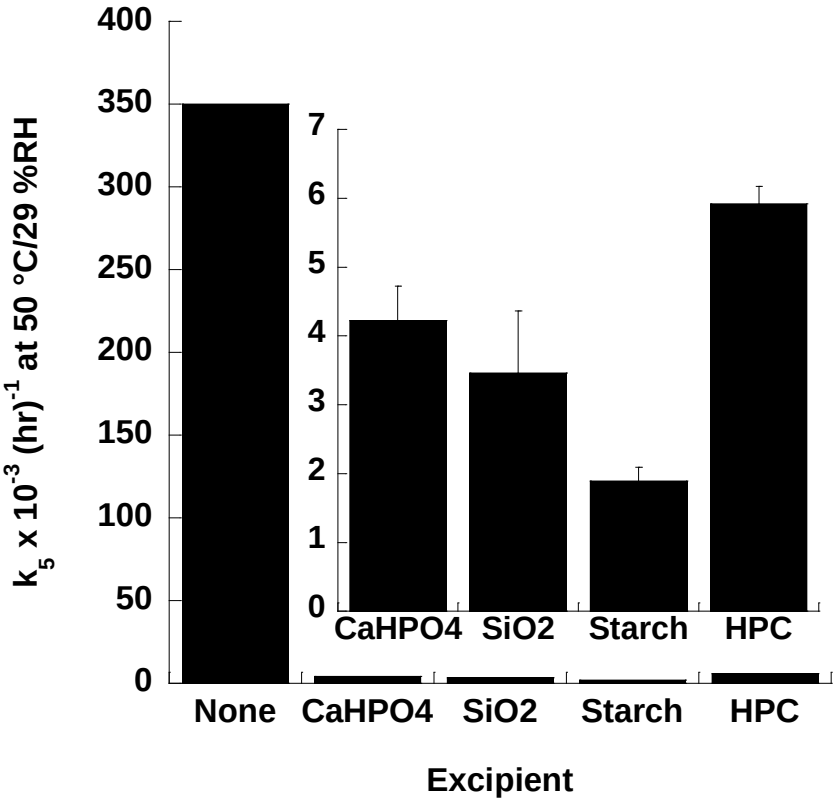

According to literature reports, the effect of humidity on polymorphic transformation is associated with the formation of hydrogen bonds on the substrate surface. (62, 63) For example, the humidity effect on polymorphic transformation of mannitol (δ ➔β) at 97 %RH/25 °C was studied. Based on scanning electron micrograph, water molecules assisted in forming hydrogen bonds of polymorphic β form on the surface, thereby facilitating the transformation of δ➔β. (64)

Microcrystalline cellulose, silicified microcrystalline cellulose, HPC and starch have been reported to decrease the hydration rates of piroxicam, theophylline and nitrofurantoin during wet granulation processes. Additionally, the ability to decrease the

hydration rates of piroxicam, theophylline and nitrofurantoin were dependent on the excipient-humidity interaction. For example, starch was able to hinder the formation of nitrofurantoin monohydrate during wet granulation more than silicified microcrystalline cellulose and HPC. (65-70)

In our studies, starch was able to decrease the rates for polymorphic transformation of III➔II more than other excipients [Figure V-46]. One possible explanation is that the humidity effect on polymorphic transformation may be influenced by the ability of starch to interfere with surface hydrogen bonding. Among excipients used in our studies, starch has a high affinity with water molecules due to the abundance of hydroxyl groups and an open conformation of glucose monomers. (71)

Another explanation is that the humidity effect may be influenced by the degree of contact between gabapentin and excipient. Theoretically-calculated fraction of excipient surface area in contact with gabapentin *(f)* has been previously reported by Nevrekar and Buckner who reported *f* values for starch, HPC and $CaHPO_4$ in contact with gabapentin to be 0.05, 0.06 and 0.001, respectively. (52) This suggested that the degree of contact with starch and HPC was greater than $CaHPO_4$. Even though the degree of contact with starch and HPC were comparable, the ability of starch to interact with water was higher than HPC. Based on our observations, starch was able to interfere with water and hinder the rates of polymorphic transformation (III➔II) more than HPC and $CaHPO_4$. This may be described by the degree of contact between starch and gabapentin and its ability to form hydrogen bond.

Inorganic excipients used in our studies ($CaHPO_4$ and SiO_2) appeared to hinder the rates of polymorphic transformation (III➔II), but to a lesser degree than starch. The

effects of $CaHPO_4$ and SiO_2 on solid-state kinetics transformation have been previously reported in other systems. For example, $CaHPO_4$ was shown to decrease the rate of indomethacin crystallization, although to a lesser extent compare to cellulose excipients such as MCC and HPMC. (72) Additionally, SiO_2 has been reported to decrease the rate of thiamine HCl hydrate transition at 40 °C/75 %RH. (63)

Conversion of II➔II*

We have demonstrated that reliable estimates of k_1 for conversion of II*➔II were difficult to obtain with the available data. Accurate k_1 estimates require a method for measuring the time-dependent changes of II*; however, II* was believed to be a minor component (<10 %) in the reaction mixtures and retained sufficient crystalline characteristics such that XRPD and ^{13}C ssNMR could not differentiate this material from intact Form II. Additionally, the lack of substantial "early-time" lactam data contributed to k_1 uncertainty. For these reasons, our ability to make inferences concerning the effects of environmental and compositional variation on II*➔II transition is limited.

Nonetheless, the humidity dependent term (β_1) associated with the conversion of II*➔II was significantly greater than zero. The estimated β_1 values for reaction mixtures with $CaHPO_4$, SiO_2, starch and HPC are shown in Figure V-47. The magnitude of humidity effect on the conversion of II*➔II depended on excipient type. The highest β_1 value was found for the HPC mixture, whereas the β_1 values of $CaHPO_4$, SiO_2, and starch mixtures were not different.

The effect of excipient-humidity interactions on β_1 values was determined by comparing the β_1 values of the reaction mixtures with and without excipients. The humidity parameter on the conversion of II*➔II in the absence of excipient has been

previously reported to be 0.2. (19) In our studies, the β_1 values of all excipient mixtures were less than that observed in the absence of excipients. This demonstrated that the interaction of humidity with excipients resulted in decreased magnitudes of humidity effect for the conversion of II*➔II. This observation is consistent with the effects of excipients on III➔II transformations.

Figure V- 47. Humidity dependent term (β_1) for the conversion of II*➔II of reaction mixtures with $CaHPO_4$, SiO_2, starch and HPC. Error bars represent the 95 % confidence limits.

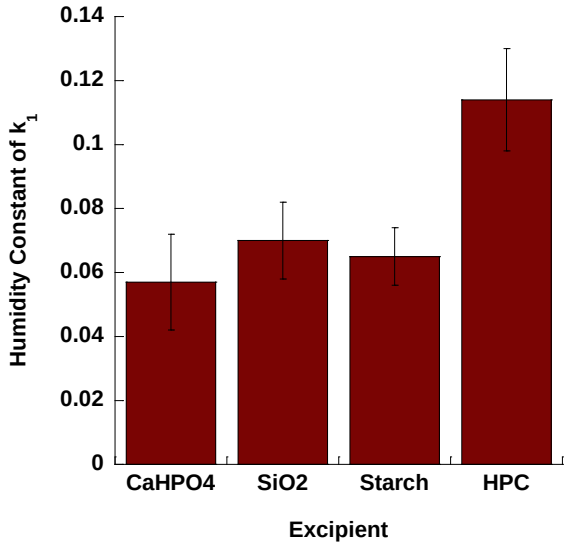

The effect of excipient-humidity interactions on k_1 rate constants was determined by comparing the point estimates (k_1) of reaction mixtures with and without excipients [Figure V-48]. The rate constants (k_1) obtained from reaction mixtures with excipients at 60 °C/ 44 %RH were 5-125 times lower than those estimated in the absence of excipients. Therefore, the interaction of humidity with excipient resulted in decreases in the catalytic humidity effect.

Overall, excipients modified the physical transitions of gabapentin by slowing down the polymorphic transformation of III➔II and conversion of II*➔II. This effect is

likely due to the ability of excipients to interfere with water at the surface and the degree of contact between drug and excipient.

Figure V- 48. Rate constant estimates (k_1) for conversion of II*➔II at 60 °C/44 %RH. The k_1 rate constants were estimated by fitting concentration time profiles of the reaction mixtures with and without excipients ($CaHPO_4$, SiO_2, starch, and HPC).

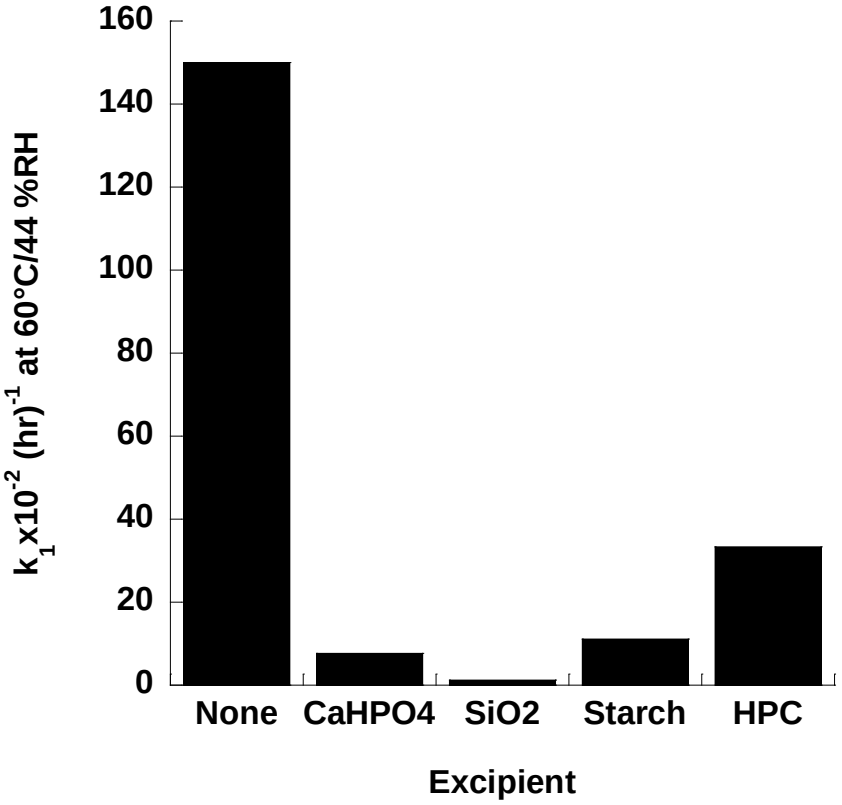

Conclusion

Mechanistic Considerations

Mechanism of gabapentin degradation in solution has been previously reported. The lactamization of gabapentin is pH-dependent with minimum rate at 5.5-6.2 and is buffer catalyzed. The Arrhenius activation energy for lactamization in solution (pH 6) was estimated to be 140-160 kJ/mol. (32) The reaction is favored when the amino group is un-protonated and carboxyl group is protonated. In acidic conditions, the mechanism involves with nucleophilic attack of nitrogen on carbonyl leading to a formation of

hydroxynium ion as an intermediate. The general acid catalysis may occur via the addition of a buffer proton to the leaving hydroxyl group. In basic conditions, the mechanism involves the free amine and carboxylate ion leading to formation of an anionic intermediate which eventually breaks down to form lactam. (73) These proposed mechanisms are similar to the typical mechanism of amide formation, i.e. lactam formation of 3-(2-aminophenyl) propionic acid and propionate in solution. (74, 75)

Elucidating reaction mechanisms in solid state, heterogeneous systems is difficult. Kinetics in solution may or may not be applicable to degradation in solid state. The crystal structure of Form II and, to a lesser extent, Form III depends on intermolecular hydrogen bonds between neighboring carboxylic acid and amine moieties in gabapentin. At crystal surfaces and crystal defects, this hydrogen bonding lattice is disrupted, thereby resulting in a greater opportunity for intramolecular dehydration to occur involving the amine and carboxylic acid moieties. The most likely explanation for the catalytic role of excipients is related to the excipients ability to competitively disrupt intermolecular and intramolecular hydrogen bonding. The result of the hydrogen bond disruption is to facilitate intramolecular nucleophilic attack of the amine on the carboxylic acid. In this scenario, the catalytic ability of the excipients would be determined by the combination of its ability to form hydrogen bond and the degree of contact between excipient and substrate.

The role of excipients in retarding polymorphic transformations is also likely to be due to competitive hydrogen bonding. However in this case, it is the ability of excipients to disrupt the catalyzing effects on water interactions with gabapentin that may explain the decreased humidity effects in the presence of excipients. Once again, the

relative excipient effects may be due to the compilation of surface area and hydrogen bonding ability.

In summary, our research goal was to develop a kinetic model to quantify the effects of environmental (temperature and humidity) and compositional (excipient type) variations on each physical and chemical transition of gabapentin. Our objective was accomplished by constructing the new model in which co-milling gabapentin with excipients determined three physically-initial concentrations (II_0*, II_0 and III_0) and one chemically-initial concentration ($lactam_0$). The key features of the model are first-order physical state transitions of II* and III to II, first-order degradation of II* to lactam and autocatalytic lactamization of II and III.

Our new model was shown to be robust to quantitatively account for the effects of temperature, humidity and excipient on rate constants associated with kinetics for each physical and chemical transition. For chemical transitions, no humidity effect was found and excipient appeared to influence the conversion of II and III➔lactam by catalyzing rate constants (k_3 and k_4). For physical transitions, excipient primarily influenced the physical state transitions of II* and III➔II through its ability to interact with humidity and the degree of contact between gabapentin/excipient. Additionally, the interaction of humidity-excipient resulted in the decreases in the magnitudes of humidity effect on the conversion of II*➔II and polymorphic transformation of III➔II. Therefore, this new model demonstrated to provide linkage between excipient, environmental storage condition, chemical and physical instability of gabapentin.

Chapter V References

1. Waterman KC. The Application of the Accelerated Stability Assessment Program (ASAP) to Quality by Design (QbD) for Drug Product Stability. AAPS PharmSciTech. 2011;12(3):932-937.
2. Waterman KC, Swanson JT, Lippold BL. A Scientific and Statistical Analysis of Accelerated Aging for Pharmaceuticals. Part 1: Accuracy of Fitting Methods. Journal of Pharmaceutical Sciences. 2014;103(10):3000-3006.
3. Byrn SR, Pfeiffer RR, Stephenson G, Grant DJW, Gleason WB. Solid-State Pharmaceutical Chemistry. Chemistry of Materials. 1994;6(8):1148-1158.
4. Brown ME, Glass BD. Pharmaceutical applications of the Prout-Tompkins rate equation. International Journal of Pharmaceutics. 1999;190(2):129-137.
5. Carstensen JT. Stability of solids and solid dosage forms. Journal of Pharmaceutical Sciences. 1974;63(1):1-14.
6. Prout EG, Tompkins FC. The thermal decomposition of potassium permanganate. Transactions of the Faraday Society. 1944;40(0):488-498.
7. Brown ME. The Prout-Tompkins rate equation in solid-state kinetics. Thermochimica Acta. 1997;300(1-2):93-106.
8. Jacobs PWM. Formation and Growth of Nuclei and the Growth of Interfaces in the Chemical Decomposition of Solids: New Insights. The Journal of Physical Chemistry B. 1997;101(48):10086-10093.
9. Skwierczynski RD. Disorder, molecular mobility, and solid-state kinetics: The two-environment model. Journal of Pharmaceutical Sciences. 1999;88(11):1234-1236.
10. Shalaev EY, Shalaeva M, Byrn SR, Zografi G. Effects of processing on the solid-state methyl transfer of tetraglycine methyl ester. International Journal of Pharmaceutics. 1997;152(1):75-88.
11. Waterman K, Carella A, Gumkowski M, Lukulay P, MacDonald B, Roy M, Shamblin S. Improved Protocol and Data Analysis for Accelerated Shelf-Life Estimation of Solid Dosage Forms. Pharmaceutical Research. 2007;24(4):780-790.
12. Carstensen JT. Stability patterns of vitamin A in various pharmaceutical dosage forms. Journal of Pharmaceutical Sciences. 1964;53(7):839-840.
13. Carstensen JT, Johnson JB, Valentine W, Vance JJ. Extrapolation of appearance of tablets and powders from accelerated storage tests. Journal of Pharmaceutical Sciences. 1964;53(9):1050-1054.
14. Tardif R. Reliability of accelerated storage tests to predict stability of vitamins (A, B1, C) in tablets. Journal of Pharmaceutical Sciences. 1965;54(2):281-284.
15. Carstensen JT, Osadca M, Rubin SH. Degradation mechanisms for water-soluble drugs in solid dosage forms. Journal of Pharmaceutical Sciences. 1969;58(5):549-553.
16. Pawelczyk E, Hermann T, Zajac M, Knitter B, Smilowski B. Kinetics of drug decomposition. Part 61. Kinetics of various ampicillin forms degradation in solid phase. Polish Journal of Pharmacology and Pharmacy. 1980;32(1):47-54.

17. Mendez R, Alemany MT, Jurado C, Martin J. Study on the rate of decomposition of amoxicillin in solid state using high-performance liquid chromatography. Drug Development and Industrial Pharmacy. 1989;15(8):1263-1274.
18. Pawelczyk E, Plotkowiak Z, Knitter K, Kozakiewicz-Wegner B. Kinetics of drug decomposition. Part 62. Kinetics of penicillin G potassium salt (PGP) thermal degradation in solid phase. Polish Journal of Pharmacology and Pharmacy. 1980;32(1):55-62.
19. Zong Z, Qiu J, Tinmanee R, Kirsch LE. Kinetic model for solid-state degradation of gabapentin. Journal of Pharmaceutical Sciences. 2012;101(6):2123-2133.
20. Qiu Z. Effect of pharmaceutical processing on the solid-state Maillard reaction between metoclopramide hydrochloride and lactose. Purdue University; 2002. p. 137.
21. Chamarthy SP, Pinal R. The nature of crystal disorder in milled pharmaceutical materials. Colloids and Surfaces A: Physicochemical and Engineering Aspects. 2008;331(1–2):68-75.
22. Wildfong PLD, Hancock BC, Moore MD, Morris KR. Towards an understanding of the structurally based potential for mechanically activated disordering of small molecule organic crystals. Journal of Pharmaceutical Sciences. 2006;95(12):2645-2656.
23. Feng T, Pinal R, Carvajal MT. Process induced disorder in crystalline materials: Differentiating defective crystals from the amorphous form of griseofulvin. Journal of Pharmaceutical Sciences. 2008;97(8):3207-3221.
24. Otte A, Carvajal MT. Assessment of milling-induced disorder of two pharmaceutical compounds. Journal of Pharmaceutical Sciences. 2011;100(5):1793-1804.
25. Šesták J, Berggren G. Study of the kinetics of the mechanism of solid-state reactions at increasing temperatures. Thermochimica Acta. 1971;3(1):1-12.
26. Málek J. The kinetic analysis of non-isothermal data. Thermochimica Acta. 1992;200(0):257-269.
27. Khawam A, Flanagan DR. Solid-State Kinetic Models: Basics and Mathematical Fundamentals. The Journal of Physical Chemistry B. 2006;110(35):17315-17328.
28. Alsante KM, Ando A, Brown R, Ensing J, Hatajik TD, Kong W, Tsuda Y. The role of degradant profiling in active pharmaceutical ingredients and drug products. Advanced Drug Delivery Reviews. 2007;59(1):29-37.
29. Genton D, Kesselring UW. Effect of temperature and relative humidity on nitrazepam stability in solid state. Journal of Pharmaceutical Sciences. 1977;66(5):676-680.
30. Waterman KC, Adami RC. Accelerated aging: Prediction of chemical stability of pharmaceuticals. International Journal of Pharmaceutics. 2005;293(1–2):101-125.
31. Waterman KC, Gerst P, MacDonald BC. Relative humidity hysteresis in solid-state chemical reactivity: A pharmaceutical case study. Journal of Pharmaceutical Sciences. 2012;101(2):610-615.
32. Zour E, Lodhi S, Nesbitt R, Silbering S, Chaturvedi P. Stability Studies of Gabapentin in Aqueous Solutions. Pharmaceutical Research. 1992;9(5):595-600.
33. Blau G, Lasinski M, Orcun S, Hsu S-H, Caruthers J, Delgass N, Venkatasubramanian V. High fidelity mathematical model building with

experimental data: A Bayesian approach. Computers & Chemical Engineering. 2008;32(4–5):971-989.
34. Gelman A, Carlin JB, Stern HS, Rubini DB. Bayesian Data Analysis. Chapman & Hall/CRC; 2003. p. 247-255, 285-310.
35. Metropolis N, Rosenbluth AW, Rosenbluth MN, Teller AH, Teller E. Equation of State Calculations by Fast Computing Machines. The Journal of Chemical Physics. 1953;21(6):1087-1092.
36. HASTINGS WK. Monte Carlo sampling methods using Markov chains and their applications. Biometrika. 1970;57(1):97-109.
37. Brooks SP. Bayesian computation: a statistical revolution. Philosophical Transactions of the Royal Society of London A: Mathematical, Physical and Engineering Sciences. 2003;361(1813):2681-2697.
38. Nash J. On Best Practice Optimization Methods in R. Journal of Statistical Software. 2014;60(2):1-14.
39. R Core Team. 2012. R: A language and environment for statistical computing.
40. Soetaert K, Petzoldt T, Setzer W. Solving Differential Equations in R: Package deSolve. Journal of Statistical Software. 2010;33(9):1-25.
41. Soetaert K, Petzoldt T. Inverse Modelling, Sensitivity and Monto Carlo Analysis in R Using Package FME. Journal of Statistical Software. 2010;33(3):1-28.
42. Dempah K, Barich D, Kaushal A, Zong Z, Desai S, Suryanarayanan R, Kirsch L, Munson E. Investigating Gabapentin Polymorphism Using Solid-State NMR Spectroscopy. AAPS PharmSciTech. 2013;14(1):19-28.
43. Lubach JW, Xu D, Segmuller BE, Munson EJ. Investigation of the effects of pharmaceutical processing upon solid-state NMR relaxation times and implications to solid-state formulation stability. Journal of Pharmaceutical Sciences. 2007;96(4):777-787.
44. Luisi BS, Medek A, Liu Z, Mudunuri P, Moulton B. Milling-induced disorder of pharmaceuticals: One-phase or two-phase system? Journal of Pharmaceutical Sciences. 2012;101(4):1475-1485.
45. Braga D, Grepioni F, Maini L, Rubini K, Polito M, Brescello R, Cotarca L, Duarte MT, Andre V, Piedade MFM. Polymorphic gabapentin: thermal behaviour, reactivity and interconversion of forms in solution and solid-state. New Journal of Chemistry. 2008;32(10):1788-1795.
46. Skrdla PJ. Use of Coupled Rate Equations To Describe Nucleation-and-Branching Rate-Limited Solid-State Processes. The Journal of Physical Chemistry A. 2004;108(32):6709-6712.
47. Soetaert K, deClippele V, Herman P. FEMME, a flexible environment for mathematically modelling the environment. Ecological Modelling. 2002;151(2–3):177-193.
48. Ahlneck C, Zografi G. The molecular basis of moisture effects on the physical and chemical stability of drugs in the solid state. International Journal of Pharmaceutics. 1990;62(2–3):87-95.
49. Hao YJ, Tanaka T. Role of the contact points between particles on the reactivity of solid. The Canadian Journal of Chemical Enginerring. 1988;66(5):761-766.

50. Waterman KC, Gerst P, Dai Z. A generalized relation for solid-state drug stability as a function of excipient dilution: Temperature-independent behavior. Journal of Pharmaceutical Sciences. 2012;101:4170-4177.
51. Narang A, Desai D, Badawy S. Impact of Excipient Interactions on Solid Dosage Form Stability. Pharmaceutical Research. 2012;29(10):2660-2683.
52. Nevrekar AA, Buckner IS. Expansion of a kinetic model for solid state degradation of gabapentin: Incorporating the effect of excipient properties. Unpublished manuscript, Mylan School of Pharmacy, Duquesne University. 2014.
53. Qiu Z, Stowell JG, Cao W, Morris KR, Byrn SR, Carvajal MT. Effect of milling and compression on the solid-state maillard reaction. Journal of Pharmaceutical Sciences. 2005;94(11):2568-2580.
54. Qiu Z, Stowell JG, Morris KR, Byrn SR, Pinal R. Kinetic study of the Maillard reaction between metoclopramide hydrochloride and lactose. International Journal of Pharmaceutics. 2005;303(1–2):20-30.
55. Leung SS, Grant DJW. Solid State Stability Studies of Model Dipeptides: Aspartame and Aspartylphenylalanine. Journal of Pharmaceutical Sciences. 1997;86:64-71.
56. Stanisz B. Kinetics of Lisinopril degradation in solid phase. Reaction Kinetics and Catalysis Letters. 2005;85(1):145-152.
57. Widjaja E, Tan WJ. Kinetics of Lisinopril Intramolecular Cyclization in Solid Phase Monitored by Fourier Transform Infrared Microscopy. Applied Spectroscopy. 2008;62(8):889-894.
58. Wang S-L, Lin S-Y, Chen T-F. Reaction Kinetics of Solid-state Cyclization of Enalapril Maleate Investigated by Isothermal FT-IR Microscopic System. Chemical and Pharmaceutical Bulletin. 2001;49(4):402-406.
59. Wang S-L, Lin S-Y, Chen T-F, Cheng W-T. Eudragit E Accelerated the Diketopiperazine Formation of Enalapril Maleate Determined by Thermal FTIR Microspectroscopic Technique. Pharmaceutical Research. 2004;21(11):2127-2132.
60. Byrn SR, Xu W, Newman AW. Chemical reactivity in solid-state pharmaceuticals: formulation implications. Advanced Drug Delivery Reviews. 2001;48(1):115-136.
61. Zong Z. Studies on the mechanisms of solid state and solution instability of drugs. The University of Iowa; 2011. p. 135.
62. Zografi G. States of water associated with solids. Drug Development and Industrial Pharmacy. 1988;14(14):1905-1926.
63. Thakral NK, Ragoonanan V, Suryanarayanan R. Quantification, Mechanism, and Mitigation of Active Ingredient Phase Transformation in Tablets. Molecular Pharmaceutics. 2013;10(8):3128-3136.
64. Yoshinari T, Forbes RT, York P, Kawashima Y. Moisture induced polymorphic transition of mannitol and its morphological transformation. International Journal of Pharmaceutics. 2002;247(1–2):69-77.
65. Airaksinen S, Karjalainen M, Kivikero N, Westermarck S, Shevchenko A, Rantanen J, Yliruusi J. Excipient selection can significantly affect solid-state phase transformation in formulation during wet granulation. AAPS PharmSciTech. 2005;6(2):E311-E322.

66. Christensen NPA, Cornett C, Rantanen J. Role of excipients on solid-state properties of piroxicam during processing. Journal of Pharmaceutical Sciences. 2012;101(3):1202-1211.
67. Wikstroem H, Carroll WJ, Taylor LS. Manipulating Theophylline Monohydrate Formation During High-Shear Wet Granulation Through Improved Understanding of the Role of Pharmaceutical Excipients. Pharmaceutical Research. 2008;25(4):923-935.
68. Airaksinen S, Karjalainen M, Shevchenko A, Westermarck S, Leppänen E, Rantanen J, Yliruusi J. Role of water in the physical stability of solid dosage formulations. Journal of Pharmaceutical Sciences. 2005;94(10):2147-2165.
69. Airaksinen S, Luukkonen P, Jørgensen A, Karjalainen M, Rantanen J, Yliruusi J. Effects of excipients on hydrate formation in wet masses containing theophylline. Journal of Pharmaceutical Sciences. 2003;92(3):516-528.
70. Jørgensen AC, Airaksinen S, Karjalainen M, Luukkonen P, Rantanen J, Yliruusi J. Role of excipients in hydrate formation kinetics of theophylline in wet masses studied by near-infrared spectroscopy. European Journal of Pharmaceutical Sciences. 2004;23(1):99-104.
71. Delwiche SR, Pitt RE, Norris KH. Examination of Starch-Water and Cellulose-Water Interactions With Near Infrared (NIR) Diffuse Reflectance Spectroscopy. Starch. 1991;43(11):415-422.
72. Schmidt AG, Wartewig S, Picker KM. Polyethylene oxides: protection potential against polymorphic transitions of drugs? Journal of Raman Spectroscopy. 2004;35(5):360-367.
73. Zambon E, Giovanetti R, Cotarca L, Pasquato L. Mechanistic investigation on 2-aza-spiro[4,5]decan-3-one formation from 1-(aminomethyl)cyclohexylacetic acid (gabapentin). Tetrahedron. 2008;64(28):6739-6743.
74. Camilleri P, Ellul R, Kirby AJ, Mujahid TG. The spontaneous formation of amides. The mechanism of lactam formation from 3-(2-aminophenyl)propionic acid. Journal of the Chemical Society, Perkin Transactions 2. 1979(12):1617-1620.
75. Kirby AJ, Mujahid TG, Camilleri P. Anilide formation from an aliphatic ester. The mechanism of cyclisation of methyl 3-(2-aminophenyl)propionate. Journal of the Chemical Society, Perkin Transactions 2. 1979(12):1610-1616.